Pd- and Ni-based catalysts for mild
C-S bond activation and formation

Dissertation

der Mathematisch-Naturwissenschaftlichen Fakultät

der Eberhard-Karls-Universität Tübingen

zur Erlangung des Grades eines

Doktors der Naturwissenschaften

(Dr. rer. nat.)

vorgelegt von

Paul Gehrtz

aus Wiesbaden

Tübingen

2018

Gedruckt mit Genehmigung der Mathematisch-Naturwissenschaftlichen Fakultät der Eberhard Karls Universität Tübingen.

Tag der mündlichen Qualifikation:	24.01.2019
Dekan:	Prof. Dr. Wolfgang Rosenstiel
1. Berichterstatter:	Jun.-Prof. Dr. Ivana Fleischer
2. Berichterstatter:	Prof. Dr. Martin E. Maier
3. Berichterstatter:	Prof. Dr. Olga Garcia-Mancheño

Table of Contents

1. Introduction

This thesis explores C-S bond scission and formation with homogeneous group 10 metal catalysts (Pd, Ni). To set the stage for the following chapters, the thiophilic interaction (section 1.1), differences between Ni and Pd catalysis (section 1.2) as well as current challenges in homogeneous catalysis (section 1.3) are discussed in short essays below.

1.1. The connection between homogeneous catalysis and the thiophilic interaction

The thiophilic interaction between organosulfur species and (late) transition metals or non-transition heavy metals can be classified as a Pearson soft-soft Lewis acid-base interaction. This interaction has been long recognized in the chemical history.[1] For example, mercaptide (meaning mercury capturing) is the historical name for a thiolate species. The Pearson Hard/Soft-Acid/Base (HSAB) concept allows a qualitative grouping of elements, ions and compounds as either soft, borderline cases or hard. A more quantitative scale of thiophilicity has been presented by Kepp.[2] The thiophilic interaction has been employed by nature in the human olfactory perception of thiols,[3] in material science and nanotechnology for the construction of self-assembled monolayers of alkanethiols on gold surfaces,[4] in the design of organic reactions, such as the Barton-McCombie-desoxygenation, the Raney-Nickel-mediated desulfurization reaction[5] or in homogeneous catalysis. The major problem associated with transition metal catalysis with thiol or thiolate actor ligands is deactivation, either by ligand displacement or energetic stabilization of transition metal organosulfides, hindering turnover.[6] Thus, choosing an appropriate ligand platform can prove decisive (e.g. by relying on a stabilizing chelate effect). Furthermore, organosulfur compounds are redox-active and do not conform to the octet rule, which opens a variety of competing processes and can complicate effective catalytic turnover.

Nature has long harnessed thiophilic interactions to stabilize late-transition metal containing enzymes using cysteine residues as spectator ligands. Man-made homogeneous catalysts often feature thiolates as actor ligands, but the thiophilic interaction can be employed to confer exquisite chemoselectivity in catalytic processes by providing a unique recognition motif for C-S bond activation. On the other hand, the intermediacy of thiols and thiolates as actor ligands in homogeneous catalysis also provides opportunities in C-S bond formation where traditional organic transformations fail or are impractical.

The catalytic C-S bond activation of thiols, thioesters, thiophenes, allyl-, benzyl-, (hetero)aryl- and alkenyl- sulfides has been reported using various low-valent transition metal complexes to give C_{sp2}-C_{sp2} cross-coupled products with organomagnesium, -zinc, -tin, and -boron reagents.[7] Due to the increased electron-withdrawing nature, the corresponding sulfoxides, sulfones, sulfoximines and

sulfonium salts represent more activated electrophiles than the sulfides. One recent advance has been the utilization of alkyl sulfones as electrophiles for desulfonylative C_{sp2}-C_{sp3} coupling using either Grignard reagents (Fe-catalyzed)[8] or organozinc reagents (Ni- or Co-catalyzed)[9]. Depending on the reaction conditions, classical cross-coupling mechanisms or radical-based mechanisms haven been proposed.

On the other hand, transition-metal catalyzed reactions, which target C-S bond formation usually benefit from two factors: 1. A potentially deactivating organosulfur species is incorporated into a more stable product and 2. Thiolates and thiols generally behave as nucleophilic species with stricter orbital control than ions.

1.2. Comparison of Ni and Pd homogeneous catalysis

To the outsider, the choice of catalytic metal for C-S bond formation or activation, or perhaps for any catalytic homogeneous reaction, may seem arbitrary. A range of cross-coupling reactions have been developed and are now routinely used in academic laboratories, drug discovery and process chemistry (Scheme 1.1). The Pd-catalyzed variants of these coupling reactions have proven themselves especially versatile, and due to high impact of this synthetic method, some of the key players in the field (Negishi, Suzuki, Heck) were awarded with the Nobel prize in Chemistry in 2010.
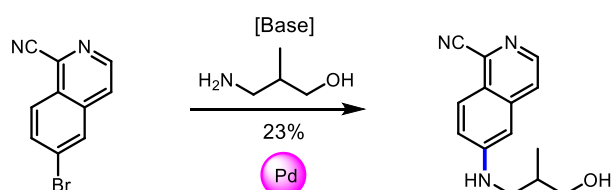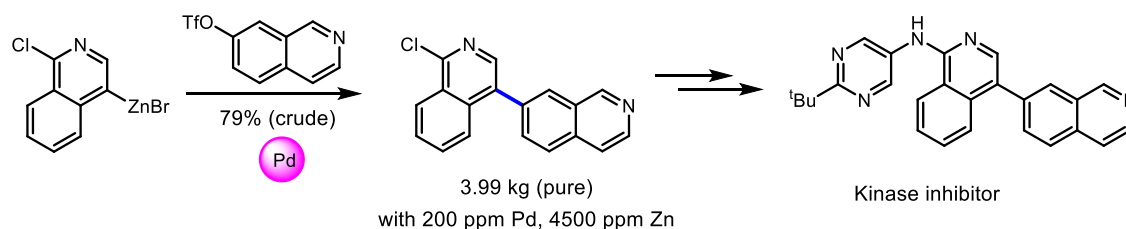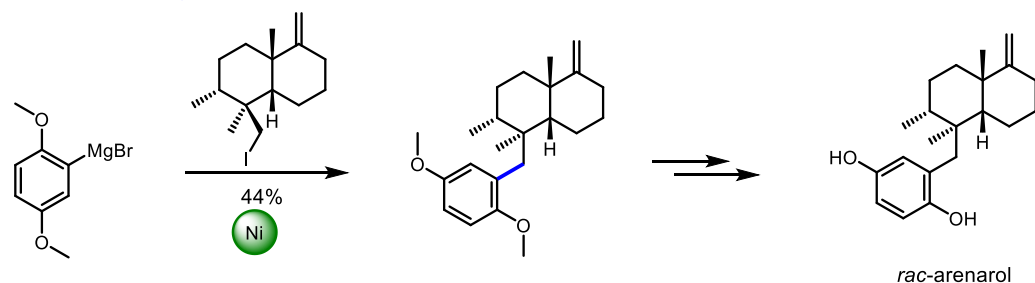
Scheme 1.1: Transition-metal catalyzed cross-coupling reactions are used in all branches of preparative organic chemistry. Reactions taken from cited references.[10]

Besides cross-coupling reactions, which are the most impactful, a great amount of research has been concerned with various C-X- and C-C-bond forming transition metal-catalyzed reactions to enable transformations, which are not possible with standard organic transformations, e.g. alkene/alkyne hydro- or difunctionalizations, C-H activation, and heterocycle formation. Palladium is often the metal of choice for a variety of transition-metal catalyzed reactions, and it is not limited to activity in cross-coupling chemistry. In contrast, other catalytic transition metals appear to have more specialized uses (e.g. Ru for metathesis, Rh for enantioselective alkene hydrogenations, etc.).

There are typically two arguments for the replacement of Pd with Ni in catalytic homogeneous reactions (Figure 1.1). The abundance of Ni in the earth crust is higher than that of Pd.[11] This fact is reflected in the current pricing of bulk metals, where Ni is available for a fraction of the cost of Pd. Obviously, such economic arguments have more weight in the process/production chemistry of fine chemicals. During a medicinal chemistry program or in the middle of a natural product synthesis, cost may be less of an issue whereas project progress is of importance. However, a holistic view of financial cost/benefits of transition metal catalysis in the process setting may be more realistic. For example, the cost of certain designer phosphines may exceed that of catalytic transition metals. In addition, purification of the products of TM-catalyzed reactions may become exceedingly costly and treatment of chemical waste rich in catalytic components could become challenging in order to comply with local environmental regulations.
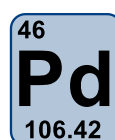
28 **Ni** **58.693**	**46** **Pd** **106.42**
10.53 € / 1 kg	**29350 € / 1 kg**
80 ppm of earth crust mass	0.0006 ppm of earth crust mass
$Ni(OAc)_2$ rat (oral) LD_{50} = 350 mg/kg	$Pd(acac)_2$ rat (oral) LD_{50} = >2000 mg/kg
atom radius 135 pm	atom radius 140 pm
harder	softer
electronegativity 1.91	electronegativity 2.20
oxidation states : -1, 0, 1, 2, 3, 4	oxidation states : 0, 1, 2, 3, 4
facile oxidative addition	facile reductive elimination
facile migratory insertion	facile β-hydride elimination
more accessible radical pathways	

Figure 1.1: Comparison of Ni vs Pd in transition metal-catalyzed chemistry. Adapted from a cited reference[11] and with changes made by I. Fleischer.

While the first perspective is certainly valid, Ni catalysis offers more than a cheap replacement of Pd catalysis. Ni (3d metal) is smaller than Pd (4d metal) and more electropositive. The most common oxidation states for Ni are 0, +I, +II, +III. For Pd, typical oxidation states are 0, +II, +IV. Going from Pd to Ni, the ligand field stabilization energy (LFSE) decreases. Therefore, the possibility of high-spin electron configurations and open-shell reaction pathways increases.

Secondly, reactivity of the metal increases,[12] as the LFSE is associated with the activation barrier for associative, dissociative and associative/dissociative reaction mechanisms. For example, the Ni-C bond

dissociation energy ranges from 159.0 – 213.8 kJ mol^{-1} whereas the Pd-C bond strength ranges from 202.1 - 231.0 kJ mol^{-1} (compared to the standard C-C BDE of 365.7 kJ mol^{-1}).[12] Similarly, activation energies for reductive elimination (from a C-Met-C complex) and oxidative addition (into a C-C-bond) are the lowest for Ni in the group 10 metals, but there appears to be less thermodynamic drive for reductive elimination compared to Pd. Due to slow formation of a β-agostic complex, β-hydride elimination is kinetically disfavoured in Ni complexes compared to Pd complexes.[13] Finally, Ni is also the strongest binder of alkene and alkyne fragments from the group 10 metals.[12] In summary, Ni complexes significantly ease the activation of challenging electrophiles in cross-coupling reactions, but reductive elimination becomes more unfavourable. Besides the increased reactivity, the other unique properties reviewed above allow for the design of new reactivity. The higher propensity for paramagnetic complexes can be used in radical cross-coupling approaches such as dual photoredox-Ni catalysis, cross electrophile couplings and thermal Ni-catalyzed radical cross-couplings. The high affinity for alkenes and alkynes can be employed for the reductive couplings of π-systems.

Although these behaviours allow for new reactivity, the development of new Ni-catalyzed methods targeting a single facet of the above reactivity also requires the possibility to shut down competing pathways, which can be accomplished by careful choice of reaction conditions and reaction partners.[14] A better choice to broaden substrate scope and condition space appears to be ancillary ligand choice or design.[15] For the reasons stated above, ligand frameworks successful in Pd-catalysis can not be generally transferred to Ni catalysis.

Because of these aspects, a 2017 literature survey showed that Ni-catalysts have not yet approached catalyst loadings comparable to Pd-catalysis, which limits their adoption.[16] A second issue is the perceived higher toxicity of Ni salts *versus* Pd salts.[17] While the average toxicity of various Ni salts across several test systems (cell cultures or organisms) is higher than that of Pd salts, the residual limits which are currently recommended in approved pharmaceuticals are quite similar (Ni: 20 ppm, Pd: 10 ppm, see Figure 1.2), based on animal study values, which were approximated to humans (ICH Q3D guideline for elemental impurities).

Therefore, in production, similar hurdles exist in stripping final products from group 10 residual metals, which can induce significant cost especially with chelating, Lewis-basic molecules. An approach of recycling of catalytic metal would however be more convenient and cost-efficient than stripping residual metals and adding them to the waste stream. However, this requires specialized techniques in catalyst design to allow for recycleable homogeneous catalysis. In small-scale discovery chemistry, potential users of Ni-based replacement catalysts are often concerned with lack of chemical predictability of newly reported methods from an academic environment.

With all these differences in mind, there are some common challenges in modern homogeneous catalysis. These are elaborated below with selected applied examples.
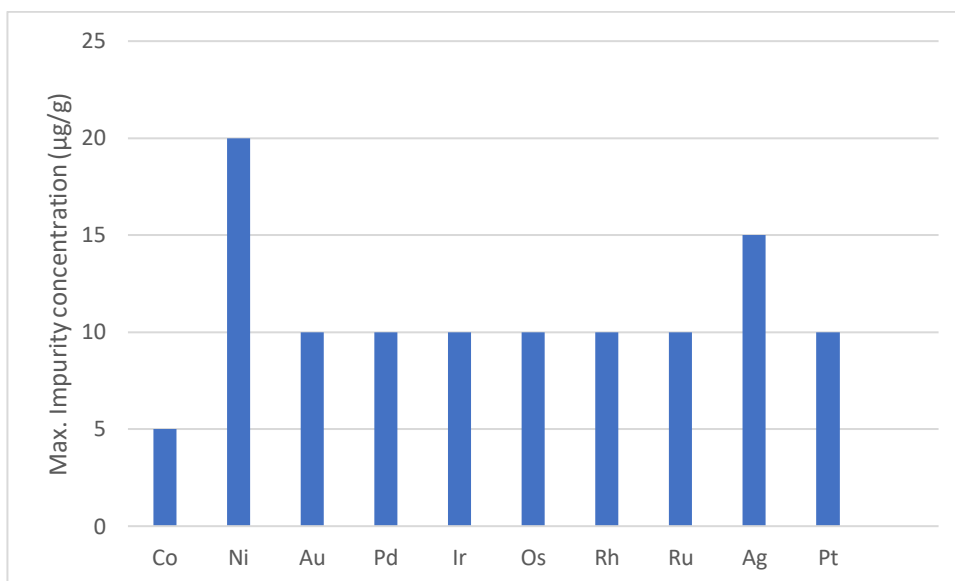

Figure 1.2: A selection of values for maximally allowed metal impurity concentrations in orally dosed pharmaceuticals (Data from ICH Q3D (Step 4) Guideline for elemental impurities). Cu (not shown) is listed with a max. impurity concentration of 300 µg/g. Fe is not listed due to its low toxicity.

1.3. Current challenges in homogeneous catalysis

In a recent perspective article,[18] the tolerance of a newly developed synthetic method towards heterocycles and polar functional groups, including polar protic functionality was identified as a key factor for uptake by industry users. These functional groups give compounds the important ability for directional intermolecular interactions and the desired physicochemical properties. In natural product synthesis, protecting group steps (which fall under the category of concession steps[19]) can be avoided by functional group-tolerant catalysis. However, such functionality is often detrimental for the activity of transition metal catalysts, either by protodemetalation of catalytic intermediates or Lewis-type interactions.

Various tests (classic scope evaluation, additive screening[20] and complex libraries[21]) have been proposed to search for incompatibilities in catalysis. While additive tests will certainly gain importance, standard evaluation of scope remains important and can reflect so-called aggregate behaviours such as solubility or chelating effects.

In some cases, incompatibilities are reaction-inherent, e.g. when highly basic Grignard reagents are employed in Kumada couplings. Thus, there is also an implicit drive towards milder reagents for organic synthesis. The popularity of boronic acid esters as synthetic intermediates is a testament to this fact. Increased robustness towards functional groups can also be achieved by lowering the reaction temperature, i.e. designing more effective catalysts. Faster reactions with the targeted functionality also mean less time available for catalyst deactivation processes.

Robustness also extends to the reproducibility of the reaction in untrained hands. Specialized techniques such as high-pressure reactions with reactive gases or photo-redox catalysis can produce a barrier to adoption by the non-specialist. In the best case, catalytic reactions should become kit-like where crude mixtures of reactions with 1:1 stoichiometry can be directly adsorbed on chromatographic media for purification and funneling material to the next synthetic step.

High-throughput experimentation for catalysis has become a common tool in the pharmaceutical industry to optimize problematic steps or allow for route re-design. For example, a Buchwald-Hartwig amination operant at room temperature in DMSO was found by evaluating all possible combinations of 6 bases with 16 precatalysts in a model reaction.[22] The screening was carried out in glass vials (manual dosing with multi-channel pipettes) or plasticware in well-plate format (robotic dosing, triplicate determination) located in a glovebox, and analysis was based on quantitative HPLC (Scheme 1.2). Naturally, automation of this type can be extended to data analysis and even feedback designs are possible. Large datasets generated from high-throughput screening (output) were recently used to train a machine learning model for the prediction of cross-coupling reactions, the input to the model

being various molecular descriptors from DFT calculations.[23] It should be noted that automatization and miniaturization of reaction setups is typically easier in a monophasic (liquid) system. At larger scales, for example in process development groups, metal loading, catalyst cost and metal contamination of final products become important, inextricably linked factors (see above).
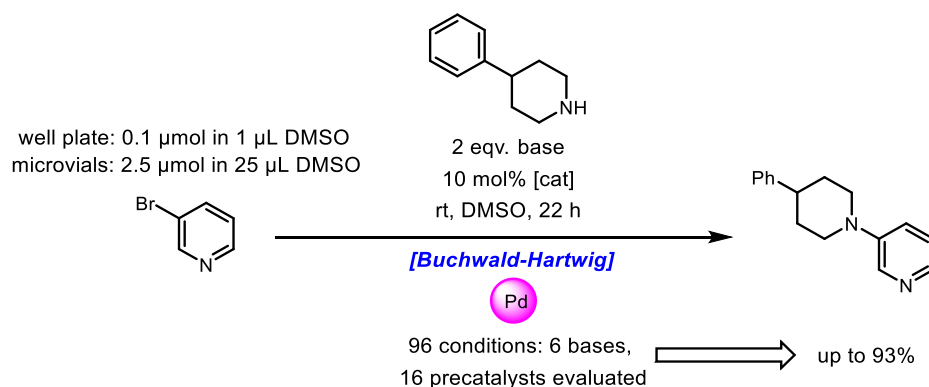
Scheme 1.2: Condition-driven optimization of a Buchwald-Hartwig coupling conducted in microvials and plastic well-plates using very little material.

In other circumstances, the desired transformation may not be feasible at all or unattractive from a cost-benefit standpoint. In a recent example from the literature (Scheme 1.3), the failure of an alkyl-alkenyl Suzuki-Miyaura coupling (20 documented, evaluated attempts) forced a re-evaluation of the synthetic plan towards a series of diterpenoid natural products then completed by an alternate strategy.[24]
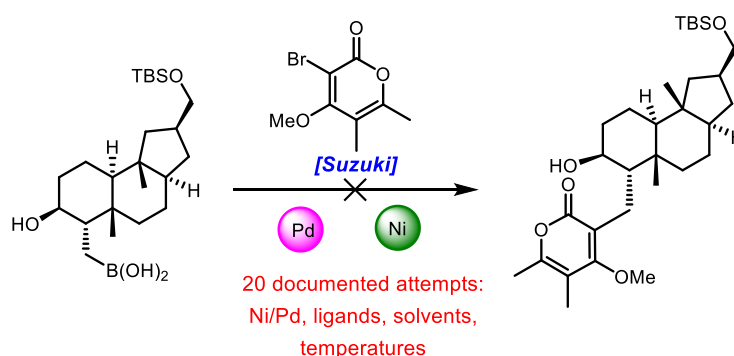
Scheme 1.3: Attempted sp^2-sp^3 Suzuki coupling in the synthesis of various pyrone-diterpenoid natural products.

Chemical literature steadily produces incremental advances in known catalytic methods, leading to a vast amount of successful conditions for often very specialized reactants. Dreher, Krska and co-workers have shown, through principal component analysis of raw data from cross-coupling reactions in the literature, that the chemical space examined in academic method development was often narrow and focused on low molecular weight, lipophilic, unfunctionalized examples compared to the chemical space populated by marketed drugs.[21] The comparison to the chemical space occupied by natural products would have been interesting but was not carried out by the industry-based researchers. This

fact may lead to the low predictability of group 10 TM-catalyzed reactions in a complex setting. At the same time, commercial providers aggressively market catalysts aimed at the production of fine chemicals. In the study cited above, the reaction of 24 structurally diverse, medicinal-chemistry like aryl boronic acid pinacol esters (ArBPin) with a bromoindole was carried out. Analysis of the obtained yields revealed that simple $Pd(dppf)Cl_2$ could be efficiently employed (average yield 59%) without the need for a specialized precatalyst containing a designer phosphine ligand. Another example is the Buchwald-Hartwig amination. Across a similar set of 18 aryl halides and piperidine as a coupling partner, various (pre)catalysts were examined which exhibited all-around disappointing performance (highest average yield 19%).

The Suzuki-Miyaura-, Sonogashira- and Buchwald-Hartwig-coupling are still the only cross-coupling methods routinely used in process chemistry,[25] underscoring the need for more predictable systems for other TM-catalyzed methods (Figure 1.4). Not surprisingly, all these couplings produce valuable C-C or C-heteroatom bonds with usually air-stable reagents and these reactions only require an inert gas purge to operate.
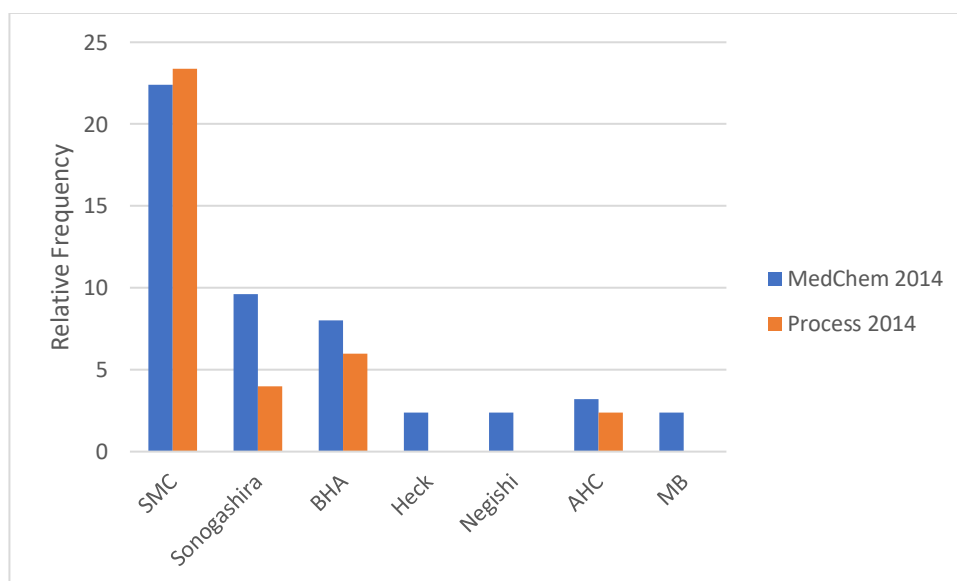
Figure 1.3: Relative frequency of transition metal catalyzed reactions in J. Med. Chem. (2014) subdivided into process (orange) and small-scale Medicinal Chemistry approaches (blue). SMC: Suzuki-Miyaura coupling, BHA: Buchwald-Hartwig amination, AHC: Aryl halide cyanation, MB: Miyaura borylation. Data taken from cited reference.[25]

In conclusion, current challenges in homogeneous catalysis are: 1. functional group tolerance of new methods, including polar protic groups and heterocycles; 2. User-friendliness (e.g. glovebox-free setup); 3. Scalability (e.g. to conduct both process-scale as well as miniaturized reactions).

1.4. Aims of this work

Of all the potential synthetic targets containing C-S bonds, thioesters are unique since they represent active intermediates for transfer of the acyl group, as inspired by nature where acyl coenzyme A species are employed to deliver this type of reactivity. Thus, the thioester is the central intermediate in this work (Scheme 1.4). The overall aim of these newly developed methods is to generate user-friendly protocols with broad substrate scope, which operate at relatively mild conditions (compared to competitive methods). All the developed methods herein utilize the thiophilic interaction with late transition metals.

These higher-energy bonds usually require a thermodynamic expenditure in the form of active ester intermediates (i.e. compared to the acid-catalyzed synthesis of oxoesters). Work leading up to the carbonylative Pd-catalyzed synthesis of thioesters from alkenes is presented in Chapter 2, which circumvents the use of active esters.

In the following two chapters, the facile activation of challenging electrophiles with Ni catalysis is leveraged. Acyl group transfer from thioesters was developed as a Ni-catalyzed process in Chapter 3. Finally, Chapter 4 shows that thiolates, either generated from a thioester or from the free thiol, can be transferred under similar conditions onto chloroarenes, under overall substitution, a process which is not readily found in nature.
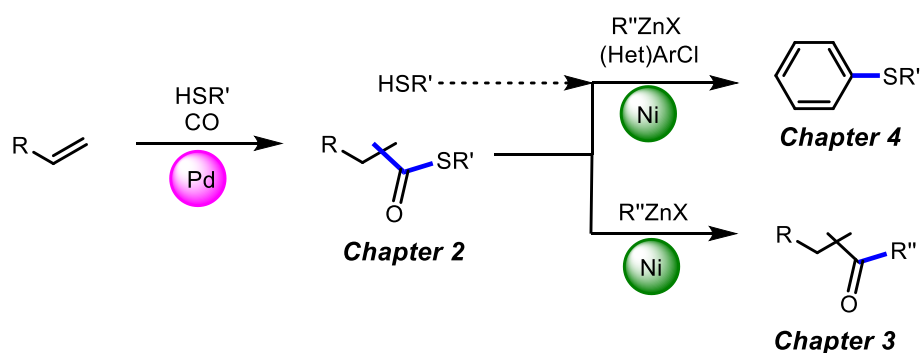
Scheme 1.4: Conceptual overview of the work on catalytic method development presented in this thesis. The thioester is the central intermediate from which both the acyl and thiyl moiety can be utilized depending on the exact reagents employed. The coloured circles represent the utilized catalytic metals and the blue bonds highlight newly formed bonds in a step.

1.5. References

[1]   T.-L. Ho, *Chemical Reviews* **1975**, *75*, 1-20.
[2]   K. P. Kepp, *Inorganic Chemistry* **2016**, *55*, 9461-9470.
[3]   S. Li, L. Ahmed, R. Zhang, Y. Pan, H. Matsunami, J. L. Burger, E. Block, V. S. Batista, H. Zhuang, *Journal of the American Chemical Society* **2016**, *138*, 13281-13288.
[4]   C. Vericat, M. E. Vela, G. Benitez, P. Carro, R. C. Salvarezza, *Chemical Society Reviews* **2010**, *39*, 1805-1834.
[5]   D. S. L. Teng-Kuei Yang, Julia Haas, in *Encyclopedia of Reagents for Organic Synthesis*, **2006**.
[6]   R. H. Crabtree, *Chemical Reviews* **2015**, *115*, 127-150.
[7]   S. Otsuka, K. Nogi, H. Yorimitsu, *Topics in Current Chemistry* **2018**, *376*, 13.
[8]   S. E. Denmark, A. J. Cresswell, *The Journal of Organic Chemistry* **2013**, *78*, 12593-12628.
[9]   a) R. R. Merchant, J. T. Edwards, T. Qin, M. M. Kruszyk, C. Bi, G. Che, D.-H. Bao, W. Qiao, L. Sun, M. R. Collins, O. O. Fadeyi, G. M. Gallego, J. J. Mousseau, P. Nuhant, P. S. Baran, *Science* **2018**; b) X.-G. Liu, C.-J. Zhou, E. Lin, X.-L. Han, S.-S. Zhang, Q. Li, H. Wang, *Angewandte Chemie International Edition* **2018**, *57*, 13096-13100.
[10]   a) A. T. Watson, K. Park, D. F. Wiemer, W. J. Scott, *The Journal of Organic Chemistry* **1995**, *60*, 5102-5106; b)D. Denni-Dischert, W. Marterer, M. Bänziger, N. Yusuff, D. Batt, T. Ramsey, P. Geng, W. Michael, R.-M. B. Wang, F. Taplin, R. Versace, D. Cesarz, L. B. Perez, *Organic Process Research & Development* **2006**, *10*, 70-77; c) J. B. Sperry, K. E. Price Wiglesworth, I. Edmonds, P. Fiore, D. C. Boyles, D. B. Damon, R. L. Dorow, E. L. Piatnitski Chekler, J. Langille, J. W. Coe, *Organic Process Research & Development* **2014**, *18*, 1752-1758.
[11]   S. Z. Tasker, E. A. Standley, T. F. Jamison, *Nature* **2014**, *509*, 299.
[12]   V. P. Ananikov, *ACS Catalysis* **2015**, *5*, 1964-1971.
[13]   Lin, L. Liu, Y. Fu, S.-W. Luo, Q. Chen, Q.-X. Guo, *Organometallics* **2004**, *23*, 2114-2123.
[14]   P.-A. Payard, L. A. Perego, I. Ciofini, L. Grimaud, *ACS Catalysis* **2018**, *8*, 4812-4823.
[15]   C. M. Lavoie, M. Stradiotto, *ACS Catalysis* **2018**, *8*, 7228-7250.
[16]   N. A. Weires, D. D. Caspi, N. K. Garg, *ACS Catalysis* **2017**, *7*, 4381-4385.
[17]   K. S. Egorova, V. P. Ananikov, *Organometallics* **2017**, *36*, 4071-4090.
[18]   D. C. Blakemore, L. Castro, I. Churcher, D. C. Rees, A. W. Thomas, D. M. Wilson, A. Wood, *Nature Chemistry* **2018**, *10*, 383-394.
[19]   T. Gaich, P. S. Baran, *The Journal of Organic Chemistry* **2010**, *75*, 4657-4673.
[20]   T. Gensch, M. Teders, F. Glorius, *The Journal of Organic Chemistry* **2017**, *82*, 9154-9159.
[21]   P. S. Kutchukian, J. F. Dropinski, K. D. Dykstra, B. Li, D. A. DiRocco, E. C. Streckfuss, L.-C. Campeau, T. Cernak, P. Vachal, I. W. Davies, S. W. Krska, S. D. Dreher, *Chemical Science* **2016**, *7*, 2604-2613.
[22]   A. Buitrago Santanilla, E. L. Regalado, T. Pereira, M. Shevlin, K. Bateman, L.-C. Campeau, J. Schneeweis, S. Berritt, Z.-C. Shi, P. Nantermet, Y. Liu, R. Helmy, C. J. Welch, P. Vachal, I. W. Davies, T. Cernak, S. D. Dreher, *Science* **2015**, *347*, 49-53.
[23]   D. T. Ahneman, J. G. Estrada, S. Lin, S. D. Dreher, A. G. Doyle, *Science* **2018**.
[24]   R. R. Merchant, K. M. Oberg, Y. Lin, A. J. E. Novak, J. Felding, P. S. Baran, *Journal of the American Chemical Society* **2018**, *140*, 7462-7465.
[25]   D. G. Brown, J. Boström, *Journal of Medicinal Chemistry* **2016**, *59*, 4443-4458.

Published, peer-reviewed work has been used to assemble four sections of this chapter.

Section 2.2.2. and the associated experimental data:

Author	Author position	Scientific ideas %	Data generation %	Analysis & Interpretation %	Paper writing %
P.H. Gehrtz	First	80%	80%	80%	90%
V. Hirschbeck	Second	20%	20%	20%	10%
I. Fleischer	Supervisor				
Title of paper:		A recyclable CO surrogate in regioselective alkoxycarbonylation of alkenes: indirect use of carbon dioxide *Chem. Commun.* **2015**, 51, 12574			
Status in publication process:		Published			

Section 2.2.3. and the associated experimental data:

Author	Author position	Scientific ideas %	Data generation %	Analysis & Interpretation %	Paper writing %
V. Hirschbeck	First	80%	80%	80%	90%
P.H. Gehrtz	Second	20%	20%	20%	10%
I. Fleischer	Supervisor				
Title of paper:		Regioselective Thiocarbonylation of Vinyl Arenes *J. Am. Chem. Soc.* **2016**, 138, 16794			
Status in publication process:		Published			

2. Pd-catalyzed hydro(thio)esterification of styrenes

2.1. Introduction

2.1.1. Carbonylative Hydrofunctionalizations

The *O,N,S*-nucleophile-terminated transition metal-catalyzed (TM-catalyzed) carbonylation of alkynes or alkenes to give carboxylic acid (derivatives) is informally known as Reppe chemistry,[1] named after the industrial researcher Walter Reppe (BASF), who discovered this class of reactions with acetylene and catalytic $Ni(CO)_4$.[2] Modern variants usually utilize catalytic Pd to give regioisomeric products (Scheme 2.1). As in hydroformylation, the typical challenge is to produce only one of the possible regioisomers.
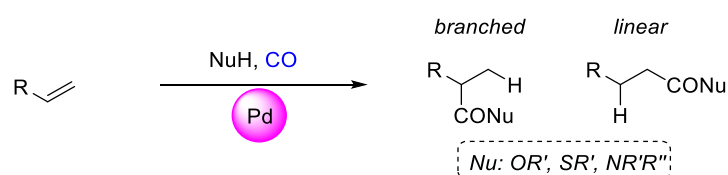
Scheme 2.1: Modern Reppe-type chemistry of alkenes giving both branched and linear carbonylated products.

One area of application of Reppe processes is in the manufacture of bulk chemicals, such as the production of methyl propionate (MeP). MeP is a precursor to methyl methacrylate (MMA), the monomer of Plexiglass (polymethylmethacrylate, polyMMA) as shown below (Scheme 2.2).[3]
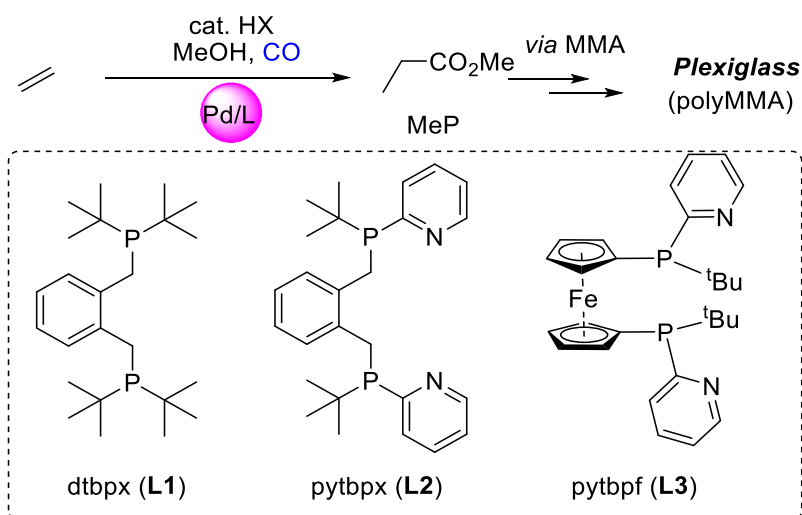
Scheme 2.2: Ethene methoxycarbonylation leads to the production of methyl propionate (MeP), an important upstream precursor of plexiglass polymers. The box shows industrially important ancillary ligands for ethene methoxycarbonylation.

The carbonylative route to MeP has been commercialized as the Lucite α-process, where methanol is reacted with ethene under a pressurized atmosphere of carbon monoxide (CO) using a homogeneous Pd catalyst in an acidic medium. An elaborate ancillary ligand design (such as in dtbpx, **L1**) is required to stabilize/destabilize key catalytic intermediates. This ligand was found in investigations of the perfectly alternating Pd-catalyzed CO/ethene co-polymerization. Newer ligand developments (**L2** – **L3**)

aim to accelerate the final elementary step in catalysis, namely the attack of the nucleophile on a Pd-acyl species.[4]

However, conditions and ligand designs aimed at bulk chemical (commodity chemical) production are not easily transferable to the synthesis of fine chemicals, where the requirements are different. First, environmental, health and safety (HSE) issues with carbon monoxide, which is a highly toxic and flammable gas, are usually adequately handled in the commodity chemical industry. The use of carbonylative processes to produce fine chemicals in process development or in small-scale academic laboratories (Figure 2.1) usually has an entry barrier in terms of technical requirements (for pressurized reactions) or poses a significant safety hazard (i.e. "balloon" chemistry).
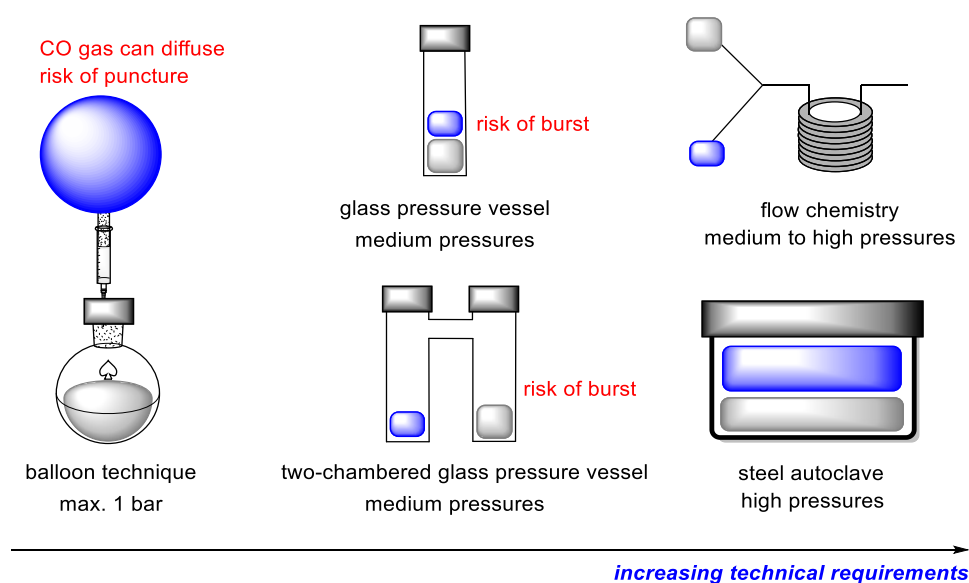
Figure 2.1: Comparison of reaction-ware to contain CO gas and in some cases, maintain a certain CO partial pressure in order of increasing technical requirements. The blue sphere denotes CO gas or a source thereof, whereas the grey sphere denotes the reactive liquid. The typically associated risks are highlighted in red. The safety level of the reaction vessels shown on the right depends heavily on the technical expertise in setting such systems up correctly.

A newer development is the utilization of flow chemistry in carbonylation chemistry. Pressure-resistant glass vessels can offer an alternative, if the reaction conditions allow the simultaneous generation and use of the CO gas from a CO surrogate (see section 2.1.2.).[5] In the Reppe-type reactions, an acidic environment is required, which is incompatible with the usually basic conditions required for CO release from various CO surrogates. Therefore, a compartmentalized reaction setup using a two-chambered (Chamber A: CO generation chamber, Chamber B: Reaction chamber) pressure-resistant glass vessel has been developed and commercialized by Skrydstrup.[6]

Second, the reactivity of polysubstituted alkenes is drastically lowered (in the order of ethene > terminal alkene > internal alkene > trisubstituted alkene > tetrasubstituted alkene), and side reactions such as non-carbonylative, acid-catalyzed hydrofunctionalization reactions become relevant.[4a] A similar influence of steric factors is found for the nucleophile.[7] Third, there is usually little control over

important selectivity issues, namely chemoselectivity (functional group tolerance), regioselectivity (branched vs. linear product ratio) and enantioselectivity (only for high-value products or intermediates). A recent advance in the area was described by the Beller group, which utilized a ligand design approach (**L2**) to achieve the successful alkoxycarbonylation of polysubstituted alkenes such as cholesterol, among many other examples. Despite the still harsh conditions (40 bar CO, 120 °C, 20 h), these overall excellent results showcase the power of ligand design in carbonylative reactions.[4a]

Reppe chemistry has also been exploited in natural product synthesis to effect Pd-catalyzed carbonylative lactonizations of allene-ols, for example in the racemic synthesis of stemoamide.[8] Finally, the carbonylation of styrenes is also a potential area of interest, since it can furnish derivatives of 2-arylpropionic acids. These compounds constitute a subclass of non-steroidal anti-inflammatory drugs. Some of these drugs have been marketed in enantiopure form, giving incremental pharmacokinetic benefits. The typical synthetic routes towards these pharmaceuticals generally use Friedel-Crafts acylation as the first step, followed by several other steps depending on the exact process employed. In principle, the carbonylative regio- and enantioselective access to 2-arylpropionic acids and esters thereof would significantly simplify the production of this pharmaceutical class. A few reports on enantioselective synthesis of this product class exist.[9] Obviously, the feasibility of this route heavily depends on the availability/pricing of the corresponding styrenic intermediates, which are also high-energy, unstable products. The regioselectivity issue of Reppe chemistry on styrenes is thus clearly focused on the production of the potentially high-value branched product. Due to the stabilization of benzylic Pd complexes by a possible η^3 coordination mode compared to the stabilization of purely aliphatic ligands, the regioselectivity is usually favoured towards the production of the branched product,[10] although the exact behavior is highly ligand-dependent.

In contrast to alkoxycarbonylations, the reaction with thiols was investigated with allenes,[11] conjugated dienes,[12] allylic alcohols[13] and vinyl cyclopropanes[14], but not styrenes. The reported examples generally require thermal conditions (> 100 °C), higher Pd loadings (3 – 5 mol%), and moderate CO pressure (up to 27 bar). Terminal alkenes with aliphatic appendages only appeared as substrates for hydrothioesterification in the patent literature.[15]

2.1.2. CO surrogates

Various CO surrogates have been developed to enable pressurized laboratory scale carbonylations, which can lower the entry barrier for small-scale chemistry groups to utilize such reactions in the appropriate glassware (Figure 1.2). A common point of comparison between these surrogates are their respective atom economies, i.e. the amount of CO transferred compared to the molecular weight of the surrogate. However, for small-scale laboratory scale reactions this might not be the most critical issue at hand. For example, the Wittig reaction produces considerable amounts of triphenyl phosphine oxide waste, which is also not easily reducible (and thus recyclable), yet it remains a standard laboratory reaction in organic chemistry. CO surrogates which have been employed with the Skrydstrup two-chamber system[6b] are shown below (Scheme 2.3).
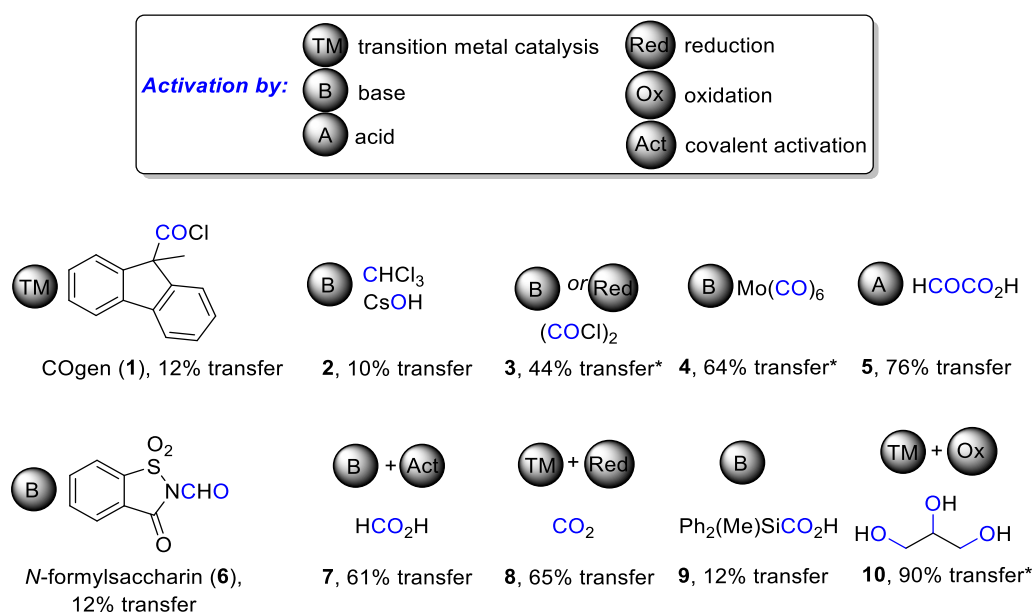
Scheme 2.3: *Comparison of CO surrogates which were successfully utilized in Skrydstrup's two chamber system. The activation triggers are depicted in black circles. The percentage numbers indicate how much CO is being transferred by the surrogate relative to its molecular weight. *: Assuming complete transfer of CO.*

Although various activation modes are possible (transition metal catalysis, oxidation/reduction, acid/base), the most commonly found activation mode involves treatment with a base. COgen (**1**) and the silacarboxylic acid **9** have been developed by Skrydstrup.[6b, 16] The same group also utilized glycerol (**10**) and CO_2 as a CO source for the first time in a two-chamber setup.[17] *N*-formylsaccharin (NFS, **6**), although employed in carbonylation reactions before, was first applied in a two-chamber system in this work. Larhed and co-workers applied **4** in the aminocarbonylation of aryl halides in the presence of challenging nitro functional groups.[18] Hull applied the base-mediated decomposition of chloroform (**2**) in another aminocarbonylation of aryl halides.[19] Gracza applied glyoxylic acid (**5**) as a CO surrogate in two-chamber reactions including aminocarbonylations, reductive formylations and carbonylative Heck/Suzuki/Sonogashira couplings of aryl halides.[20] Oxalyl chloride (**3**) can be employed as a CO surrogate either by reduction with Zn or treatment with base in a variety of transition-metal catalyzed

transformations.[21] Borggraeve reported the use of formic acid as a CO surrogate by formation of a mesylate ester, which undergoes decarbonylative decomposition upon treatment with base.[22]

2.1.3 Aims of the chapter

It was decided that for small scale reactions, a solid CO surrogate would be highly beneficial to allow for exact dosing. Furthermore, the decomposition products should be relatively easily recyclable and non-toxic. Thus, the choice fell on *N*-formylsaccharin (**6**) as the surrogate, which can be synthesized in one step from the widely available, non-expensive and non-toxic artificial sweetener saccharin and is also commercially available.[23]

In summary, carbonylative hydrofunctionalizations are interesting examples of multicomponent reactions with high atom economy, despite the high toxicity of CO gas. Thus, the usual entry barrier to adoption in laboratory scale are technical issues (pressure and safety). In this chapter, a strategy for the safe generation of CO gas (*ex situ*) in a two chambered pressure vessel using N-formylsaccharin **6** as a CO surrogate is to be developed and applied to the regioselective Pd-catalyzed hydro(thio)esterification of various vinyl arenes (styrenes), which is usually accomplished with much higher temperatures and CO partial pressures. The targeted products are oxo- and thio-esters of 2-arylpropionic acids. This moiety is found in important generic NSAIDs and it also constitutes an interesting motif for small molecule building blocks. In the latter category, the introduction of thioesters would enable higher reactivity towards a downstream C-C coupling than with oxo-esters (see Chapter 3).

2.2. Results and discussion

2.2.1. CO generation system

The first aim was the development of reproducible system for the release of carbon monoxide from NFS. A major problem was the batch-to-batch variation of NFS from commercial suppliers, leading to reproducibility issues in the carbonylation reactions. Some freshly opened commercial samples of NFS did not give satisfactory NMR spectra in comparison to literature reports for spectra of pure NFS. Considering the instability of NFS towards bases, this is not surprising and poses a significant safety hazard on scale. The unsuitability of commercial NFS was corroborated by a literature report.[24] Additionally, the synthesis of NFS (**6**) was initially problematic since mixtures of NFS and *N*-acetylsaccharin (NAS) were generated with the original procedure.[23] Based on a report detailing the successful formylation of an unrelated *N*-heterocycle,[25] it was however possible to successfully formylate saccharin without NAS impurities using a preformed solution of a mixed formic acid-acetic acid anhydride, which was added to a cooled basic solution of saccharin (**9**) in THF (up to 20 g isolated in a single batch, Scheme 2.4).
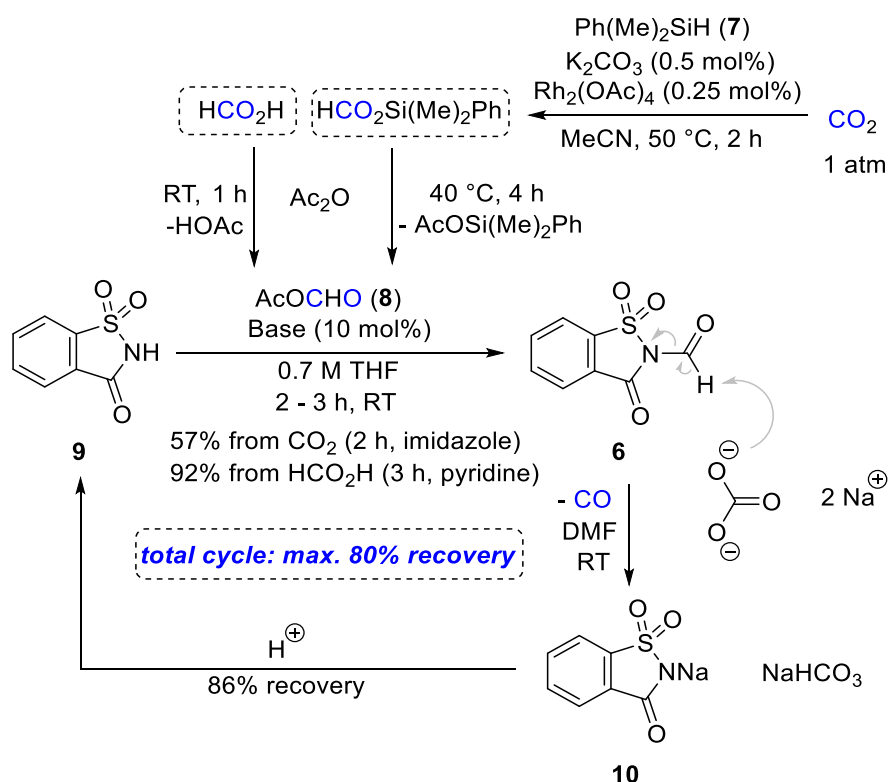
Scheme 2.4: N-formylsaccharin is a recyclable CO surrogate when applied with a two-chamber reaction setup. The mixed anhydride can be accessed either from CO₂ or formic acid.

The product was isolated by filtration and washing. NFS should be handled with caution and stored under an inert atmosphere. It was also possible to synthesize the mixed anhydride by Rh-catalyzed hydrosilylation of CO_2 using silane **7**,[26] followed by a transesterification of the resulting silyl formate with acetic anhydride. The transesterification reaction with the silyl formate required a slightly

elevated temperature (40 °C). Thus, CO_2 could be indirectly employed as a CO surrogate. However, a true tandem process would be more appealing in terms of overall efficiency and ease of handling since the isolation of the silyl formate required inert filtration technique.

While the decarbonylation of aliphatic aldehydes does not occur easily, it proceeds rapidly with NFS due to good stabilization of the resulting anion. The resulting saccharinate salt (**10**) could be recovered by acidic work-up and washing. The overall recovery efficiency of the cycle (Scheme 2.4) amounts to 80%.

In this work, this known decarbonylation reaction was employed in the two-chambered reaction setup to give hydrofunctionalized products from various styrenes (see Scheme 2.5). The generated CO gas (chamber A) then can pressurize the glass vessel to a desired set partial CO pressure (approximated using the ideal gas law) and the second chamber (chamber B) containing the catalytic components and reagents for the carbonylation then can consume the generated gas. Additionally, the compartmentalization ensures facile recyclability of the CO surrogate and inhibits off-reactions caused by the surrogate in the reaction chamber. *N*-formylsaccharin (NFS) is decarbonylated by an inorganic or organic base to yield CO gas and the saccharinate anion. Initially, Et_3N was used, but reproducibility issues were found. If Et_3N is inadvertently added to quickly, volatile amine (due to heat evolution) will enter the reaction chamber and quench the co-catalytic acid, thus inhibiting the reaction. A work-around was found by adding NFS and Na_2CO_3 to chamber A and finally adding solvent to start the decarbonylation reaction.
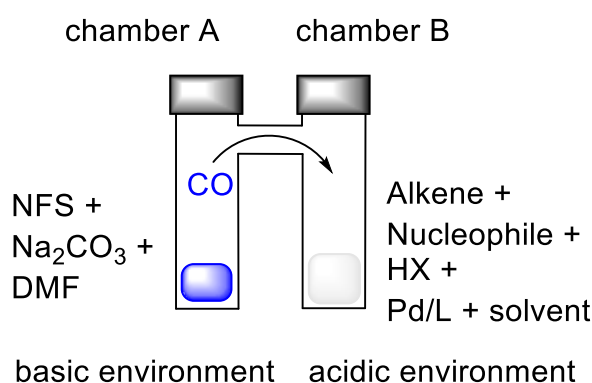
Scheme 2.5: CO generation system employed throughout this chapter. CO generation (max 2.5 bar): *6* (2.13 mmol, 449 mg), Na_2CO3 (3.19 mmol, 340 mg) in DMF (1 mL).

2.2.2. Hydroesterification of styrenes

The investigation started by the model reaction of styrene (**11**) with methanol (Table 2.1) to give the esters **13-b** (the desired regioisomer) and **13-l** (the undesired regioisomer) under a pressure of CO gas (generated as shown in Scheme 2.5). The industrial benchmark ligand dtbpx (**L1**) was employed

together with catalytic Pd(dba)$_2$ and various acids in dichloromethane. In technical chemistry applications of hydroesterification, the alcohol (methanol) acts both as a solvent and as a reactant.

Table 2.1: Optimization of the hydroesterification reaction of styrene and methanol under a CO atmosphere (2.5 bar) using various acids.
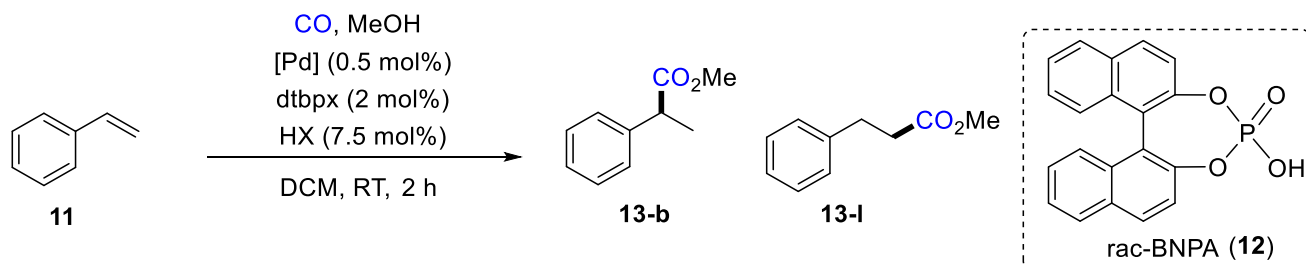
Entry	[Pd]	HX	pK_a (DMSO)	b:l[a]	Conv.[a]	Yield[a]
1	Pd(dba)$_2$	pTsOH	7.1	71:29	27%	9%
2	Pd(dba)$_2$	MsOH	1.6	51:49	28%	6%
3	Pd(dba)$_2$	PhCOOH	11.1	51:49	21%	2%
4	Pd(dba)$_2$	TFA	3.5	95:5	64%	38%
5	Pd(dba)$_2$	rac-BNPA	3.4	88:12	57%	56%
6	Pd(acac)$_2$	rac-BNPA	3.4	-	14%	0%
7	PdCl$_2$	rac-BNPA	3.4	-	18%	0%
8	Pd(PPh$_3$)$_4$	rac-BNPA	3.4	93:7	11%	1%
9	Pd(OAc)$_2$	rac-BNPA	3.4	92:8	16%	2%

[a]: Determined by quantitative GC-FID. BNPA: 1,1'-Binaphthyl-2,2'-diyl hydrogen phosphate. Reaction conditions: CO generation as in Scheme 2.5. styrene (1.00 mmol, 115 mL, 1 M solution), 1 : 3 MeOH : DCM (v/v), 0.5 mol% [Pd], 2 mol% dtbpx (20 mmol, 7.9 mg), 7.5 mol% HX, RT, 2 h.

The high concentration of the alcohol accelerates the catalytic reactions. To employ high-value alcohols, DCM was used as a replacement solvent and the reaction was carried out at room temperature to ensure user-friendliness. The typical acid co-catalysts exhibited unsatisfactory performance (entries 1 – 2). The use of a weak acid, such as benzoic acid, gave the expected negative outcome (entry 3). It was reasoned that an optimum acidity exists, which was found with the use of TFA (entry 4). The high activity of racemic BINOL-derived phosphoric acid (BNPA, **12**) with a similar pK_a value was encouraging (entry 5). Although a decreased selectivity for the wanted branched isomer was attained with BNPA, it was chosen for further studies because of more convenient reaction setup by

using solid over liquid acid. Other Pd^0 or Pd^{II} sources showed suboptimal performance (entries 6 – 9). Acid catalyzed etherification, a common side reaction in this type of chemistry, was not observed.

Using the optimal conditions (Table 2.1, entry 5) with longer reaction time to ensure full conversion (14 h), a scope evaluation of both the alkene and the alcohol components was carried out to reveal steric and electronic factors of the reaction and to test functional group tolerance, giving products **13**-**34** (Table 2.2).

Table 2.2: Scope evaluation of vinyl arene and alcohol components in the found hydroesterification reaction.
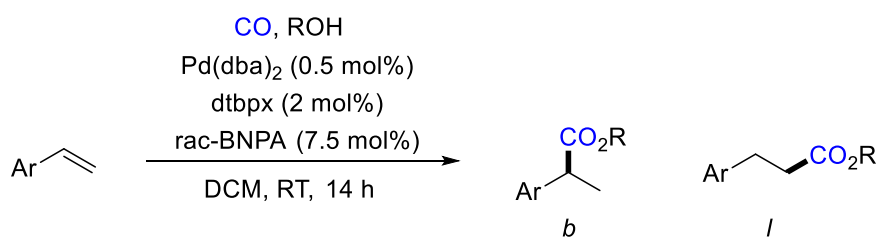
Entry	Compound	Ar	R	b:l[a]	Yield
1	**13**	Ph	Me	88:12	76%
2 [b]	**13**	Ph	Me	87:13	80%
3	**14**	Ph	Et	93:7	84%
4	**15**	Ph	^{i}Pr	90:10	15%
5	**16**	Ph	^{t}Bu	-	0%
6	**17**	Ph	Cy	93:7	21%
7	**18**	Ph	Bn	82:18	79%
8	**19**	3-Me-C_6H_4	Me	91:9	92%
9	**20**	3-OMe-C_6H_4	Me	89:11	76%
10	**21**	4-Me-C_6H_4	Me	91:9	55%
11[c]	**22**	4-^{t}Bu-C_6H_4	Me	94:6	89%
12,	**23**	4-OMe-C_6H_4	Me	93:7	97%
13[d]	**24**	4-COOH-C_6H_4	Me	77:23	21%
14	**25**	4-NO_2-C_6H_4	Me	-	0%

Entry	Compound	Ar	R	b:l[a]	Yield
15[c]	**26**	4-Cl-C$_6$H$_4$	Me	92:8	90%
16[c]	**27**	4-OAc-C$_6$H$_4$	Me	93:7	43%
17[c][e]	**28**	4-OAc-C$_6$H$_4$	Me	86:14	57%
18	**29**	2-OMe-C$_6$H$_4$	Me	64:56	66%
19[c]	**29**	2-OMe-C$_6$H$_4$	Me	41:59	60%
20	**30**	2-OAc-C$_6$H$_4$	Me	39:61	59%
21	**31**	2-Me-C$_6$H$_4$	Me	50:50	5%
22	**32**	2-CF$_3$-C$_6$H$_4$	Me	-	0%
23	**33**	2-HO-C$_6$H$_4$	Me	-	16%

[a]: Determined by GC-FID. [b]: DCE as solvent instead. [c]: Doubled Pd loading, the relative catalyst amounts of the other components remained unchanged. [d]: The diester was isolated. [e]: At 50 °C, the phenolic ester was isolated. Reaction conditions: CO generation as in Scheme 2.5. Styrene (1.00 mmol, 115 mL, 1 M solution), 1 : 3 ROH : DCM (v/v), Pd(dba)$_2$ (5.0 mmol, 2.9 mg), dtbpx (20 mmol, 7.9 mg), *rac*-BNPA (75 mmol, 26 mg), RT, 14 h.

Generally, the reaction was selective for the branched ester, typically with a b:l selectivity of 9:1. However, the products could not be isolated as pure regioisomers. The regioselectivity, determined by GC-FID was generally corroborated by peak ratios in ^{1}H-NMR of the isolated products. The activity of different alcohols in the carbonylations decreases in the order primary (giving esters **13**, **14**) > secondary (giving esters **15**, **17**) >> tertiary (giving no product **16**). The reaction is preparatively useful for primary alcohols. Less nucleophilic alcohols such as BnOH, gave similar yield such as aliphatic primary alcohols, but a decreased regioselectivity. Phenols were also inactive. The overall results point towards alcoholysis as the overall rate-determining step, which is in line with other experimental reports.[1] Alkyl, methoxy and chloro substituents in 3- or 4-position relative to the vinyl substituent were generally well-tolerated (giving products **19 – 23** and **26**). Benzoic acids (see Table 2.1, entry 13), which gave low yields and diester formation (**24**) and nitro-vinylarenes (giving no product) are difficult substrates (entries 13 – 14). The nitro functional group is notoriously problematic in Pd- and Ni catalysis due to its redox activity. Acetoxy substituents also had a negative influence on the yield (giving **27**). Using an elevated temperature with this substrate class (50 °C), acetoxy cleavage was observed, giving a phenolic ester **28** in moderate yield. Substituents in the 2-position were tolerated but gave 50:50 regioisomeric mixtures (on average, products **29**-**31**). Using 2-vinylphenol, a 5-membered lactone (**33**) was obtained, irrespective of the presence of MeOH. This type of reactivity (cyclocarbonylation) was explored in follow-up work by Hirschbeck and Fleischer.[27] In general, the activity decreased with

electron-withdrawing substituents on the arene, requiring higher catalyst loading. Combination of two challenging properties led to no conversion (e.g. hypothetical product **32**). Basic functional groups are not tolerated (not shown) since inhibition of the acid co-catalyst occurs.

Finally, the reactivity of non-styrenic olefins was also evaluated (Scheme 2.6) using either MeOH or BnOH as the nucleophile to allow for facile purification. The use of α-branched olefins (**34**, **44**) led to the formation of the corresponding linear esters. Similarly, internal alkenes without directing benzylic positions (**46**, **48**, **50**) also provided the linear esters selectively. The internal olefins (**48**, **50**) isomerized by hydride-chain walking mechanism to the terminal position. When a η^3-benzyl palladium(II) complex can be formed (**38**, **40**), the corresponding regioisomeric ester mixture is obtained, hinting at both factors (sterics and electronics) being influential. Vinyl acetate also appears to have directing group properties (alkene **36**), whereas no effect was observed in case of *N*-vinylphthalimide (**42**). The branched-selective methoxycarbonylation of **42** and analogues would be an interesting route to *C,N*-protected α-amino acids. The use of phenylacetylene (**52**) mainly gave an unknown polymer (perhaps poly(phenylacetylene) or the alternating CO/phenylacetylene copolymer) as the product, together with minor amounts of the cinnamic acid ester **53**.

Scheme 2.6: Hydroesterification of non-styrenic olefins with MeOH or BnOH (only the starting materials are shown, the product structures are implicated and can be found in the experimental part). alkene (1.00 mmol, 1 M solution), 1 : 3 MeOH : DCM (v/v), 0.5 mol% Pd(dba)2 (5.0 mmol, 2.9 mg), 2 mol% dtbpx (20 mmol, 7.9 mg), 7.5 mol% rac-BNPA (75 mmol, 26 mg), RT, 14 h. Isolated yields are shown and the bracketed ratio denotes b:l regioselectivity.

In summary, the introduction of an aryl group in an olefinic substrate gives a significant directing group effect towards the benzylic position (presumably by formation of a η^3-benzyl palladium(II) complex), which can compete with the usual selectivity of the Pd/dtbpx system towards the formation of linear esters. The latter type of selectivity is obtained with dtbpx under thermal conditions, probably due to

steric influence.[28] Branched selectivity in the case of styrenic substrates has also been documented by Tanaka (one synthetic example).[29] In cases where both driving forces can be found, synthetically less useful regioisomeric mixtures dominate. Hetero-atom directing groups produced mixed results but offer promising routes to high-value products such as amino acids.

2.2.3. Hydrothioesterification of styrenes

While the benzylic oxo-esters of the previous section are valuable products, the corresponding thio-esters should be easier to activate for follow-up transformations enabled by transition metal catalysis.[30] The initial attempts to transfer the previous system towards the hydrothioesterification of styrenes were met with mixed success. BINOL phosphoric acid (BNPA) of the previous section was replaced with diphenyl phosphoric acid in order to ensure full solubility of all components. With lighter thiols, reproducibility issues were encountered. It was hypothesized that more volatile thiols could enter the vessel headspace and be involved in an equilibrium over the two different liquid phases. In turn, the thiol concentration would vary over time, leading to the problematic reproducibility.

This problem was successfully addressed by Hirschbeck through the choice of a non-volatile thiol for further optimization. A second problem was the observed side reaction of hydrothiolation, which occurred with *anti*-Markovnikov selectivity. This reactivity was excluded by careful purification of all reagents and solvents involved and performing the desired reaction under strictly inert conditions. Control experiments revealed that this type of reactivity was most likely radical-based. The transformation proceeded generally without Pd-catalysis at elevated temperatures in a polar solvent in the presence of air (not under pure O_2 [thiol-olefin-cooxidation-conditions, TOCO] and not under N_2 or Ar). This hydrothiolation reaction (or thiol-ene reaction) has properties of a click reaction and has been reported with a variety of catalysts (including organic photo-redox catalysis[31], metal photo-redox catalysis[32]) whereas the original approach (alkene and thiol, neat or in acetic acid / sulfuric acid mixtures, RT) developed by Posner (1905 at the University of Greifswald) has received less attention although it is certainly preparatively useful and has been shown to work with a variety of alkenes.[33] It only requires oxygen as the radical initiator in concentrations as found in ambient air (Scheme 2.7).
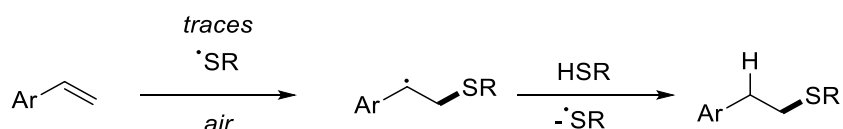
Scheme 2.7: Mechanism of the radical hydrothiolation of styrenes with thiols. Air contains a concentration of oxygen to initiate the reaction efficiently whereas under nitrogen no reaction occurs and pure oxygen gives an unclean product profile.

In fact, the practical advantage of the photocatalyzed versions of the thiol-ene reaction should be called into question in some cases (since the photocatalysts only provide a source of thiyl radicals). In fairness, at least one study by Stephenson concerned with photo-redox catalysis acknowledged "[...] a strong observed background reaction [...]"[32b] but there are certainly cases where better reaction kinetics can be obtained with photocatalysts.

In contrast to the previous section, a ligand screening in the hydrothioesterification of styrene with heptanethiol (**54**) to give the product **55** was conducted to highlight possible ligand structure-activity

relationship (Scheme 2.8). It was found that 1 mol% loading of the metal precursor was optimal for successful catalysis at room temperature. Interestingly, only the branched product could be detected in the hydrothioesterification reaction compared to the hydroesterification reaction using a variety of ligands (**L1**, **L4** – **L8**, **L12**).
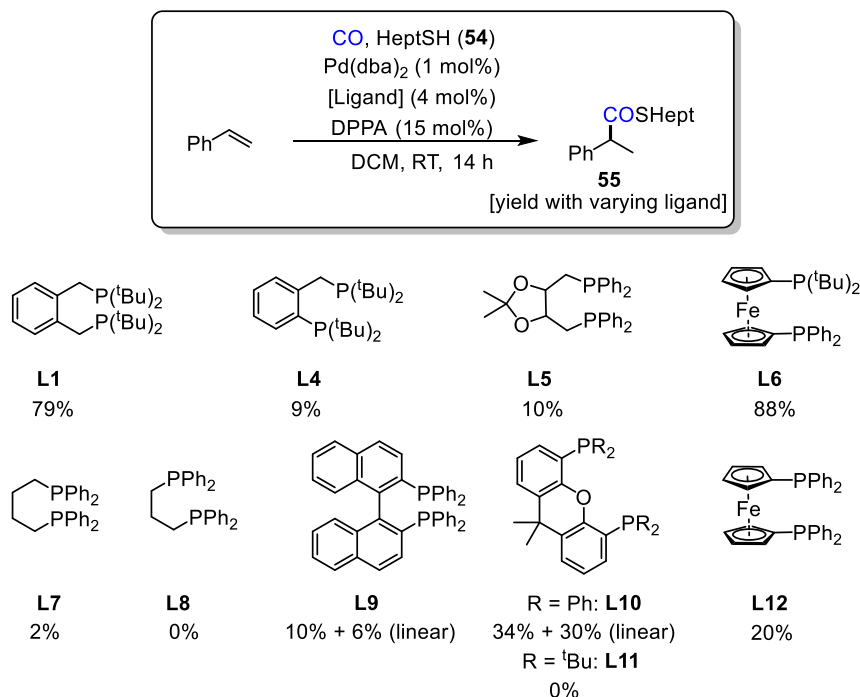
Scheme 2.8: Screening of P-based bidentate ligands in the hydrothioesterification of styrene with heptanethiol (**54**). The reaction was carried out in the autoclave (2.5 bar of CO). Condtions: styrene (115 µL, 1.0 mmol), 1 mol% Pd(dba)$_2$ (5.8 mg, 10 µmol), 4 mol% ligand (40 µmol), 15 mol% DPPA (38 mg, 150 µmol), HeptSH (210 µL, 177 mg, 1.3 mmol), 790 µL CH$_2$Cl$_2$, RT, 14 h. Yields were determined by quantitative NMR.

Bidentate ligands were chosen due to their similarity to the longtime benchmark ligand dtbpx (**L1**) and the ability to counter deactivation through the chelate effect. Overall, a strong bite angle effect was noticed (Figure 2.2), but also rigidity (**L5** vs. **L7**) and σ donor capability (**L6** vs. **L12**) play a role. In some cases (especially in **L6** vs **L12**), several ligand properties can be confounded, i.e. steric bulk of a di-tert-butylphosphino group is confounded with the strong basicity of the fragment. However, the observed regioselectivity effects (outliers **L9** and **L10**) could not be readily rationalized. Ligand **L11** is known to give *trans*-complexes, which explains the inactivity of this ligand in catalysis. Overall the ligand 1-di-*tert*-butylphosphino-1'-di-phenylphosphinoferrocene (dppdtbpf, **L6**), previously described by Holzapfel and Bredenkamp,[34] gave the best performance. **L6** exhibits the practical advantage of higher air stability (in the solid state) compared to **L1** combined with a relatively facile synthesis.
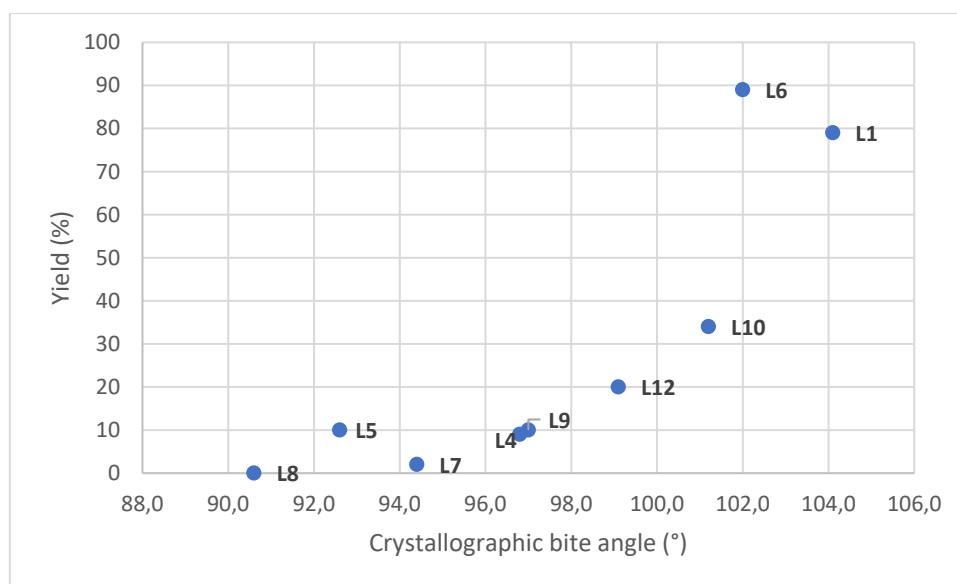
*Figure 2.2: The crystallographic bite angle of L_2PdCl_2 or L_2PtCl_2 model complexes correlates with the yield of a standard hydrothioesterification reaction under ligand screening conditions. The corresponding Cambridge Structural Database reference codes – **L1**: PEMCUH, **L4**: PEMDAO, **L5**: BICLOO, **L7**: KIBLUE, **L8**: DPPPDC, **L9**: GIBYOH, **L10**: ECOZEC, **L12**: PEMWIT. **L6**: own crystal structure.*

A screening of the acid co-catalyst revealed that a variety of acids were competent co-catalysts (MsOH, *p*TsOH) while TFA and benzoic acid were incompetent co-catalysts. Another source of Pd^0, $Pd(PPh_3)_4$ gave inferior results to $Pd(dba)_2$. Interestingly, most Pd^{II} precatalysts ($PdCl_2$, $Pd(OAc)_2$, $Pd(dppdtbpf)Cl_2$) failed to show the desired activity, but $Pd(acac)_2$ singularly showed some activity. This further strengthens the accepted position of precatalyst activation by protonation of a weak ligand to give dbaH or acacH respectively, which must be followed by ligand dissociation to enable the phosphine ligand coordination.

A survey of thiol nucleophiles revealed similar trends as in the previous section (Scheme 2.9): While primary thiols (giving products **55** - **57**) were efficiently converted, a secondary thiol reacted sluggishly (giving product **59**), and tertiary thiols were unreactive. An interesting synthetic example was the successful carbonylative installation of a cysteine thioester. The activity of thiophenol showed, by giving product **60**, that the previous explanation of precatalyst activation through β-hydride elimination of a Pd-bound alcohol or thiol could not be the only explanation in the thiocarbonylation reaction. However, linear product was also obtained in this case, making this reaction less preparatively useful. The underlying factors for the branched-linear regioselectivity remain unexplained but must be clearly connected to an electronic factor, i.e. the nucleophilicity of the thiol or alcohol. A competition experiment where both *n*-heptanol and *n*-heptanethiol were present in the reaction mixture gave selectively the styrene-derived thioester **55** over the corresponding oxo-ester.
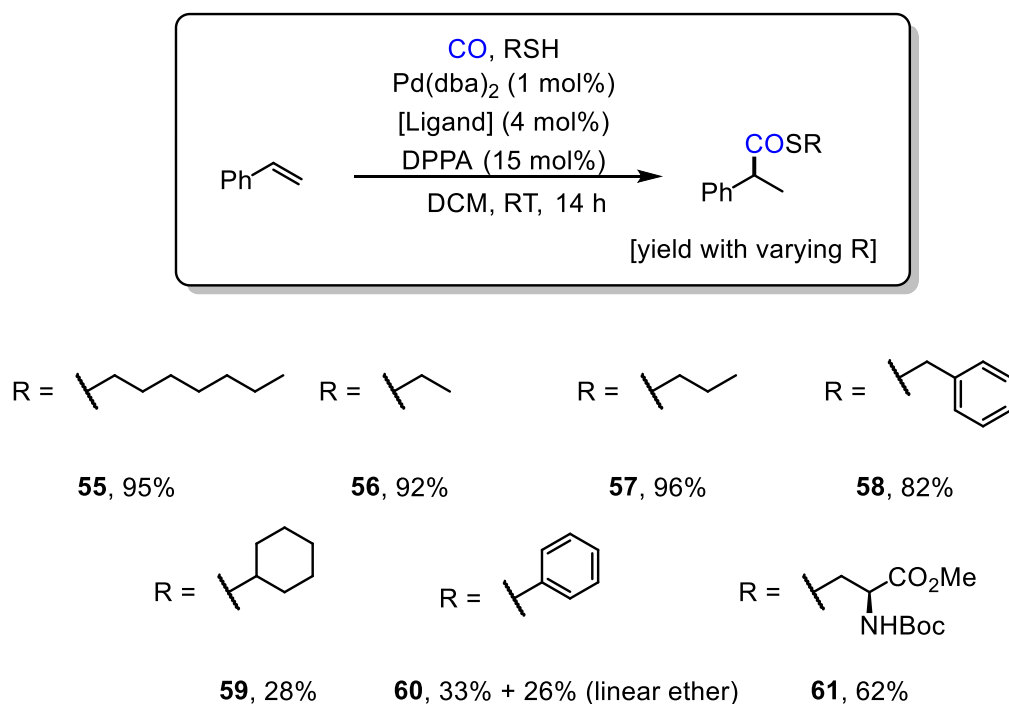
Scheme 2.9: Screening of thiol components in the hydrothioesterification of styrene. Reaction conditions: CO generation as in Scheme 2.5; styrene (115 µL, 1.0 mmol, 1 M solution), Pd(dba)$_2$ (5.8 mg, 10 µmol), **L6** (21 mg, 40 µmol), DPPA (38 mg, 150 µmol), RSH (1.3 mmol), 790 µL CH$_2$Cl$_2$, RT, 14 h.

A scope evaluation of the styrene component revealed that a variety of substituents were tolerated on the arene core in *ortho*- (products **76 – 79**), *meta*- (products **74** and **75**) or *para*-position (products **55 – 73**) without any detrimental effect to the regioselectivity. This is in strong contrast to the hydroesterification reaction of the previous section, where *ortho*-substituents led to a breakdown of regioselectivity (Scheme 2.10). Neither did the electronic nature of the substituents on the arene core influence the regioselectivity. However, the 4-CF$_3$-substituent induced a reduced yield (thioester **65**) and no observed product when placed in the 2-position. The corresponding thioesters were generally isolated in good to excellent yield after reaction at room temperature for 14 h under a pressure of CO in the apparatus previously described. In general, hydrogen-bond donors led to altered reactivity (such as cyclocarbonylation, giving product **76**) or lowered yields, whereas hydrogen-bond acceptors inhibit the catalytic activity due to their basicity (i.e. hypothetical product **70**). Pleasingly, halide substituents were generally tolerated (giving products **71** - **73**). A negative correlation to the ease of oxidative addition of a Pd^0 center into the respective halides was observed, which supports a mechanism involving zero-valent metal transition states or intermediates. Secondly, downstream cross-coupling chemistry is enabled by the found aryl halide tolerance.

$$\text{Ar}\diagdown \xrightarrow[\text{DCM, RT, 14 h}]{\substack{\text{CO, HeptSH} \\ \text{Pd(dba)}_2 \text{ (1 mol\%)} \\ \text{[Ligand] (4 mol\%)} \\ \text{DPPA (15 mol\%)}}} \text{Ar}\diagdown \text{COSHept}$$

[yield with varying Ar]

Ar =

R = H, **55**, 95%	R = OAc, **64**, 93%	R = NO₂, **67**, 0%	R = NH₂, **70**, 0%
R = Me, **62**, 99%	R = CF₃, **65**, 50%	R = OH, **68**, 49%	R = F, **71**, 91% R = Br, **73**, 72%
R = OMe, **63**, 99%	R = Ph, **66**, 86%	R = tBu, **69**, 95%	R = Cl, **72**, 81%

Ar =

R = Me, **74**, 99%
R = OMe, **75**, 99%

Ar =

R = OH, **76**, 55%[a]
R = OMe, **77**, 97%
R = OAc, **78**, 49%
R = Me, **79**, 89%

Ar =

80, 90%
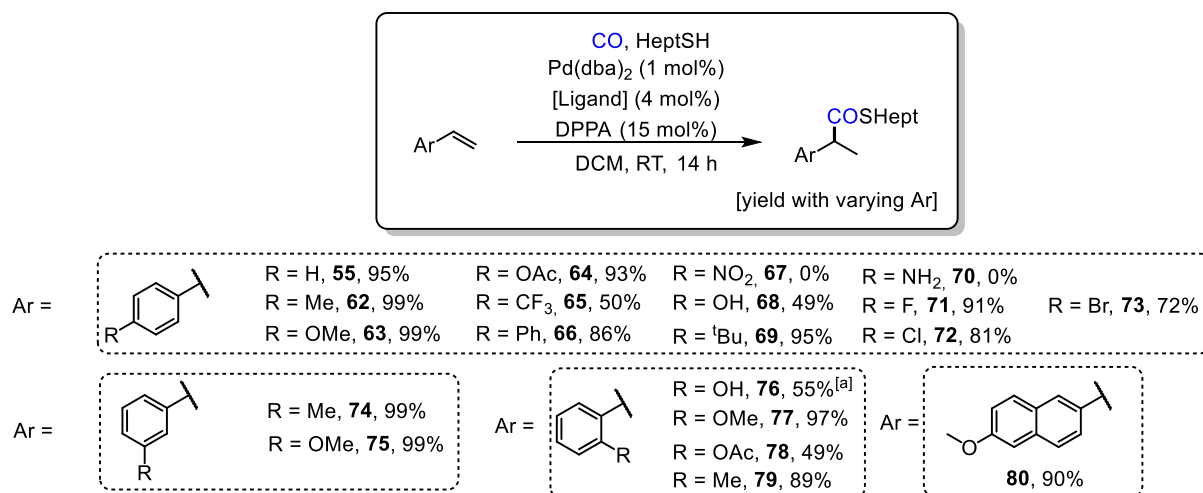
*Scheme 2.10: Screening of styrenic components in the hydrothioesterification reaction with heptanethiol. Reaction conditions: CO generation as in Scheme 2.5; vinyl arene (1.0 mmol), Pd(dba)₂ (5.8 mg, 10 μmol), **L6** (21 mg, 40 μmol), DPPA (38 mg, 150 μmol), HeptSH (210 μL, 177 mg, 1.3 mmol), 790 μL CH₂Cl₂, RT, 14 h. [a]: Cyclocarbonylation to the lactone was observed.*

In contrast to alkoxycarbonylation, no regioselectivity could be obtained in the hydrothioesterification of aliphatic alkenes, which provided regioisomeric mixtures. However, in the presence of a directing benzylic group, terminal olefins were selectively carbonylated in the benzylic position with the dppdtbpf/Pd system. Both aspects were investigated in more detail by Vera Hirschbeck.[35]

2.2.4. Mechanism

The currently widely accepted mechanism for the hydroesterification of olefins[36] is shown below ("hydride mechanism", Scheme 2.11) for the case of styrene substrates. A key factor for overall activity is the stability of the Pd hydride complex, which requires elaborate ligand design such as steric shielding. A suitable vinyl arene coordinates to the Pd hydride complex **A** and is subsequently hydropalladated to give complex **B**. As mentioned before, the regioselectivity of this step largely depends on two factors: 1. Minimization of steric strain, which is especially important for bulky phosphine ligands;[37] 2. Electronic stabilization such as the preferential formation of a benzylic complex due to two coordination modes being possible (η^3/ η^1).[10] All the complexes mentioned here exist both in their neutral or ion-pair form, depending on whether the acid counterion X$^-$ is coordinating or non-coordinating. In the extreme case of a highly coordinating counterion X$^-$, the reactivity is inhibited completely. For simplicity, the neutral form is used below.
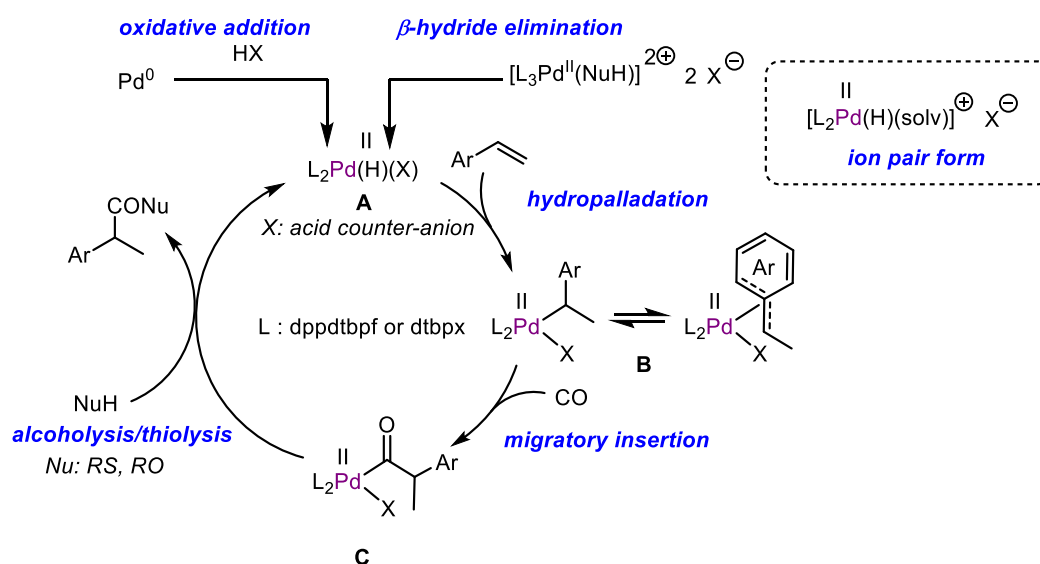
Scheme 2.11: Proposed simplified mechanism of the Pd-catalyzed carbonylative hydro(thio)esterification of vinyl arenes.

Next, CO first occupies a free coordination site, followed by migratory insertion of CO to form an acyl palladium(II) complex **C**, which undergoes alcoholysis to release the product and regenerate the starting palladium hydride complex **A**. It is unknown whether the alcoholysis proceeds intra- or intermolecularly. The transition state of the irreversible alcoholysis step exhibits Pd(0) character. The other elementary steps are assumed to be reversible. he acid co-catalyst has several roles. First, it activates the acyl palladium complex by protonation. Secondly, additional Lewis basic functionality (e.g. as in BNPA or DPPA) present in the acid co-catalyst can aid the activation of the Nu-H bond. Finally, the acid co-catalyst can furnish a Pd-hydride species through oxidative addition of a Pd^0 precursor into the HX bond.[38] Alternatively, the PdH species could be formed by β-hydride elimination from a suitable alcohol,[39] which would explain the inactivity of tertiary alcohols and phenols in the

hydroesterification reaction. In principle, the same mechanism could apply to the hydrothioesterification reaction, which shows better overall *b*-selectivity perhaps due to a kinetic effect of faster thiolysis than alcoholysis. In this reaction it was however found that thiophenol indeed gave product, which means that the activation of the Pd catalyst by oxidative addition is indeed occurring. To account for the high thiophilicity of Pd, it is not unreasonable to postulate an alternative mechanism for hydrothioesterification (Scheme 2.12). After oxidative addition of a Pd^0 intermediate **D** into a H-SR bond, a hydridopalladium(II) thiolate **E** is generated. The mechanism involves ligand hemilability, where the weaker diphenylphosphino σ-donor arm of dppdtbpf decoordinates (*via* **F**) allowing for transient alkene coordination, which undergoes rapid hydropalladation to give the preferred benzylpalladium(II) thiolate complex **G** with the phosphino arm recoordinated. Finally, CO coordination and migratory insertion, followed by reductive elimination would regenerate the Pd^0 complex **D**.
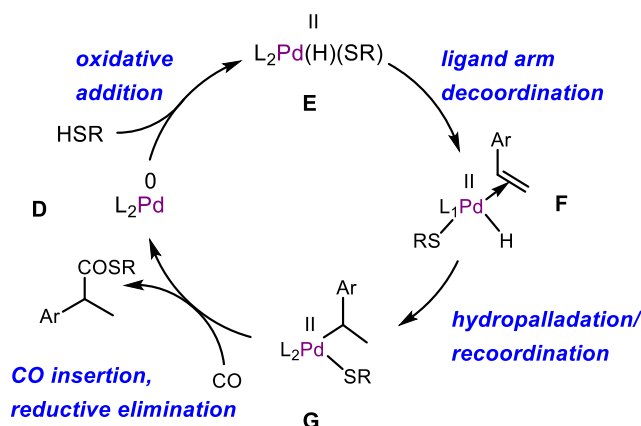
Scheme 2.12: Alternative mechanism for the Pd-catalyzed carbonylative hydrothioesterification of vinyl arenes involving ligand hemilability.

In this scenario, the acid co-catalyst would simply accelerate the final reductive elimination by protonating the acylpalladium(II) complex since it is known that the reaction does not proceed in the absence of an acid co-catalyst. Both postulated cycles could also co-exist and appear equally reasonable. To strengthen the second mechanistic hypothesis, stoichiometric organometallic experiments should be carried out. For example, the feasibility of the hydropalladation step using the hydrido palladium(II) thiolate species should be central to second mechanism.

2.3. Conclusion

In conclusion, highly active Pd-based systems for the regioselective (thio)esterification of vinyl arenes were developed using *ex situ* generation of CO. The reaction is performed in a simple two-chambered pressure vessel as originally devised by Skrydstrup, which significantly lowers the technical barrier to entry to this class of reactions. The introduction of a thioester moiety through carbonylative hydrofunctionalization of high-energy olefins bypasses the typical active ester route towards these functionalities, which enables facile downstream reactions (Chapter 3). There appear to be subtle mechanistic differences between hydroesterification and hydrothioesterification depending on the choice of the nucleophile, most likely through a strong thiophilic interaction in the case of thiol nucleophiles.

While aryl thioesters can be synthesized from aryl halides and benzylic thioesters (as shown here) from styrenes, an unresolved problem remains the selective synthesis of branched or linear aliphatic thioesters from simple olefins. The development of such reactions would complete the toolbox of carbonylative thioester synthesis. The second major unsolved problem is the non-compatibility of highly basic functional groups, which inhibit the acid co-catalyst.

2.4. Experimental part

2.4.1. General information

All chemicals were purchased from ABCR, Acros, Merck, TCI, Aldrich or Fluka. The ligand dppdtbpf (**L6**) was either commercially obtained from Sigma-Aldrich or synthesized according to Cullen et al.[S1] The ligand dtbpt (**L4**) was synthesized from 2-bromobenzyl-di-tert-butylphosphine[S2] according to a procedure by Mecking.[S3] When necessary, purification of chemicals was carried out with the standard methods. Furthermore, degassed and dry solvents were used where necessary; specifically dichloromethane, diethyl ether and tetrahydrofuran were obtained pre-dried from a Grubbs-type solvent purification system (MBraun, MB SPS-800). Pre-dried dichloromethane was refluxed over CaH_2, then distilled under nitrogen. Pre-dried diethyl ether and tetrahydrofuran were further dried with microwave-activated 3 Å molecular sieves (20% m/v, 3 days) and degassed when necessary by freeze-pump- thaw cycles (3x). Dry hexane was obtained by refluxing hexane (p.A. grade) over CaH_2, followed by distillation under N_2.

Unless otherwise noted, all reactions were carried out air- and moisture-free under an atmosphere of dry nitrogen by employing Schlenk techniques. The reaction glassware was freed from residual moisture by heating under vacuum and subsequent cooling under dry N_2 (3x); this treatment is called "flame-drying" below.

Column chromatography was carried out using normal- (60 Å) or flash-grade (40 Å) Silica gel (SiO_2) either using gravity flow or air overpressure flow conditions in a standard glass column setup with isocratic or gradient elution (composition of mobile phase noted in each experiment). Chromatography solvents were distilled prior to use.

For TLC analysis of reactions and purification processes, Kieselgel 60 F_{254} aluminium-backed plates were employed, visualization was carried out either by fluorescence quenching of UV active compounds or by dipping the developed plates in pre-made solutions of various TLC stains and heating the plate gently until maximum contrast occurred (used stain noted in each experiment).

Uncorrected melting points were determined on an Optimelt MPA100 apparatus from Stanford Research Systems (heating rate 2 °C/min) or a Büchi Melting Point B-545 aparatus (5 °C/min).

^{1}H- and ^{13}C-NMR spectra were recorded on *Bruker Avance 400* or *300 MHz* machines (400 or 300 MHz for ^{1}H experiments; 101 or 75 MHz for ^{13}C experiments) in commercially available deuterated solvents without TMS. ^{13}C-NMR experiments were recorded in proton-decoupled mode, and this is not explicitly noted below. The chemical shift is noted as δ (ppm) and referenced to the trace solvent signals; these signals and their relation to the 0 ppm TMS signal are available in the literature.[S4] Coupling constants across bonds are given as *J* (Hz). The nomenclature for spin multiplicities is as follows: s = singlet; d =

doublet; t = triplet; q = quartet; quin = quintet; sext = sextet; hept = heptet; m = multiplet. Usually, ^{13}C-NMR measurements were accompanied by a ^{13}C-DEPT135 experiment for further structural elucidation but are not noted explicitly in the experimental data. Occasionally, 2D-NMR experiments were carried out where assignments were ambiguous, but are not noted explicitly in the experimental data.

Infrared spectra were measured on a Excalibur FTS3000 MX FT-IR spectrometer from BioRad. The samples were applied neat on an ATR setup. Absorption bands are given in wave numbers $\tilde{v}$ (cm^{-1}) and peak intensities are abbreviated as follows: s - strong, m - medium, w - weak. Peak form descriptions are as follows: br - broad, sh - sharp.

For GC/MS analysis of crude mixtures, an Agilent 6890 N Network GC with an Agilent 5975 Inert Mass Selective Detector was employed. Carrier gas: Dry Hydrogen. The stationary phase was a column type BPX5 (30 m X 0.25 mm X 0.25 μm [film thickness]) from SGE. Program 50-300M: From 50 °C (2 min) by heating 25 °C/min towards 300 °C (5 min). Total time: 17 min; flow rate: 1.0 mL/min. HR-MS and GC/MS analysis for purified compounds was carried out by the Central Analytical Department, University of Regensburg on a Agilent Q-TOF 6540 UHD (APCI/ESI-HRMS) and Finnigan MAT SSQ 710 A (EI/CI-LR-GC/MS) machine respectively.

Gas chromatography (flame ionization detection) was carried out on a HP6890 GC-System with injector 7683B and Agilent 7820A System, carrier gas: Dry Hydrogen. Program 50-280M12: From 50 °C by heating towards 280 °C in 12 min after injection. In some cases, quantitative instrumental analysis was used to determine reaction yields and conversions by the *internal standard method*.

Autoclave reactions were performed in a high pressure vessel from Parr Instrument Company (model: 4774; volume: 0.16 L) with a metal inset for holding 6 septum-containing screw capped vials and controlled *via* a Parr reactor (model: 4838). Autoclave reactions with oven-dried screw-capped vials were set up under inert conditions by piercing the septum with a needle connected to a Schlenk line.

2.4.2. General procedures

General procedure **GP A** for hydroesterification

A two-chambered pressure vessel (COware 20 mL, SyTracks A/S, Sigma-Aldrich article #744077) equipped with stirring bars was charged with N-formylsaccharin (**6**) (450 mg, 2.13 mmol) and sodium carbonate (339 mg, 3.20 mmol) in chamber A [Figure S1, a)]; chamber B was charged with BNPA (**3**) (7.5 mol% up to 15 mol%, 15 eq. relative to Pd(dba)$_2$) [Figure S1, b)] and sealed with a septum-containing screw cap assembly (COware type, Sigma-Aldrich articles #743852 and #743968). Chamber A was fitted with a vacuum adapter screw cap and the reaction vessel was evacuated for 10 min [Figure S1, c)]. Under a N$_2$ backcurrent, Pd(dba)$_2$ (0.5 mol% up to 1.0 mol%, amounts specified below and referred to in each single experiment), dtbpx (**L1**) (2.0 mol% up to 4.0 mol%, 4 eq. relative to Pd(dba)$_2$) were added in chamber B [Figure S1, d)], the vessel was then subjected to evacuation/N$_2$-backfilling (3x).

Molar ratios	Pd(dba)$_2$	dtbpx	BNPA
1:4:15 (1 mmol starting material)	**0.5** mol%, 5 µmol, 2.9 mg	2.0 mol%, 20 µmol, 7.9 mg	7.5 mol%, 75 µmol, 26.1 mg
1:4:15 (1 mmol starting material)	**0.75** mol%, 7.5 µmol, 4.4 mg	3.0 mol%, 30 µmol, 11.9 mg	11.25 mol%, 11.3 µmol, 39.2 mg
1:4:15 (0.75 mmol starting material)	**0.75** mol%, 5.6 µmol, 3.3 mg	3.0 mol%, 22.5 µmol, 8.9 mg	11.25 mol%, 8.5 µmol, 29.4 mg
1:4:15 (1 mmol starting material)	**1.0** mol%, 10 µmol, 5.8 mg	4. mol%, 40 µmol, 15.8 mg.	15.0 mol%, 150 µmol, 52.2 mg

 Then, anhydrous DCM (750 µL) [Figure S1, e)], the alcohol (250 µL) [Figure S1, f)] and the olefin (1 mmol or 0.75 mmol, 100 mol%) were added to chamber B in exactly this order (solid olefins can be added at the beginning), resulting in a dark-red solution which was stirred at 750 rpm. The vacuum adapter screw cap of chamber A was exchanged to a septum-containing screw cap under positive N$_2$ pressure (using the septum inlet of chamber B) [Figure S1, g) and h)]. To start the decarbonylation, dry DMF (1 mL) was added to chamber A *via* septum addition [Figure S1, i)]. This resulted in a suspension in chamber A where gas evolution could be observed. Both reaction chambers were stirred at 750 rpm for 14 h at RT [Figure S1, j) after 14 h reaction time].

To stop the reaction, the screw caps were loosened in a well-ventilated enviroment (CO evolution may occur!). Excess NaHCO$_3$ in chamber A can be removed by addition of 1 M HCl, further addition of HCl

precipitates saccharin which can be recovered (340 mg, 1.83 mmol, 86%) by filtration, washing the filter cake with copious amounts of dist. H_2O to remove NaCl and DMF, and finally drying the solid *in vacuo*. The crude product can be subjected to GC analysis at this point, by adding a Pd metal scavenger (QuadraSil MP) and then filtering the crude solution through a cotton-plugged pasteur pipette filled with celite and basic aluminium oxide. Reaction mixtures giving non-volatile products can be adsorbed on Silica gel without further workup. Generally, special care must be taken to separate the products from catalyst components, which in the case of styrene derivatives as starting materials, often show retention behaviour similar the corresponding products. These impurities may give spectroscopically pure products a yellow appearance.
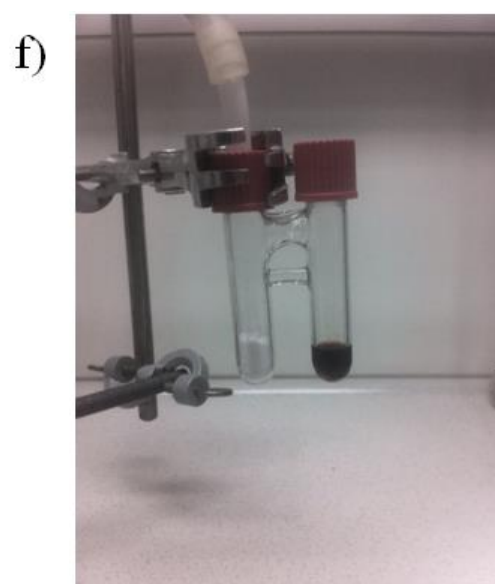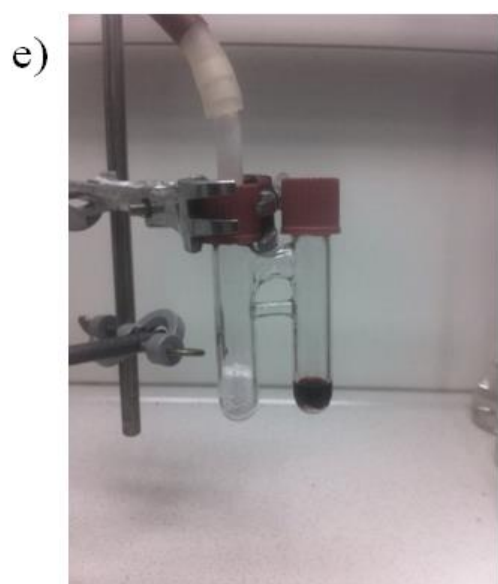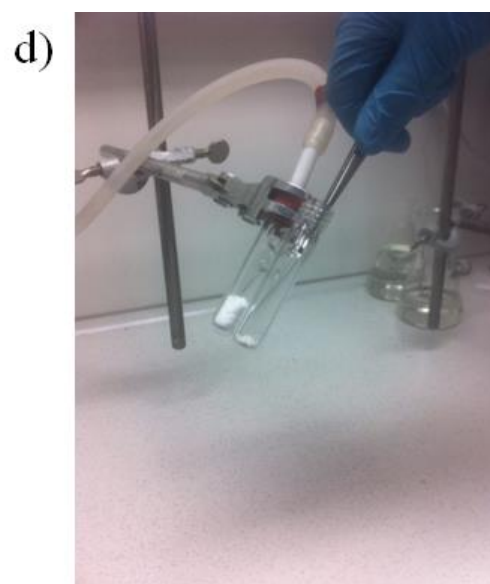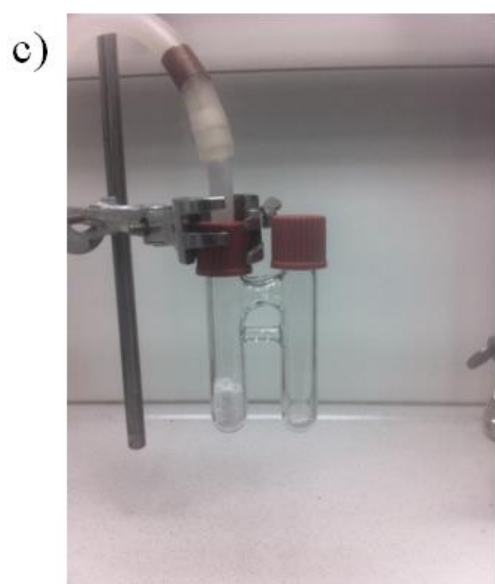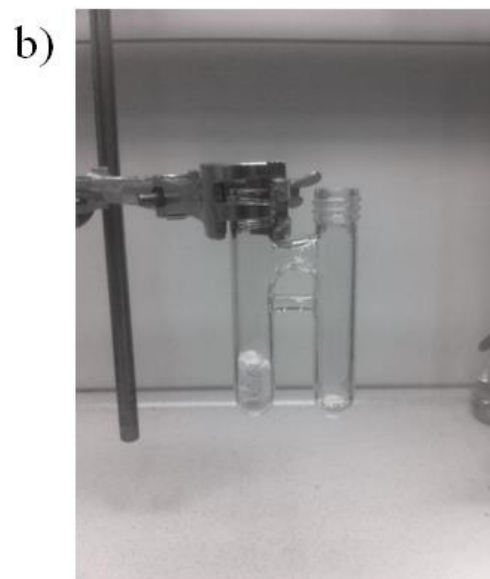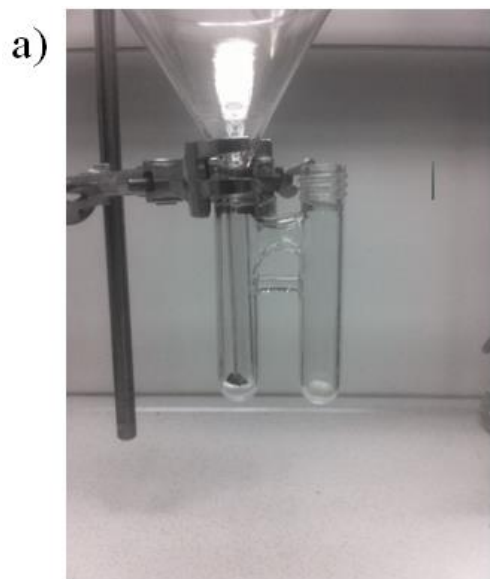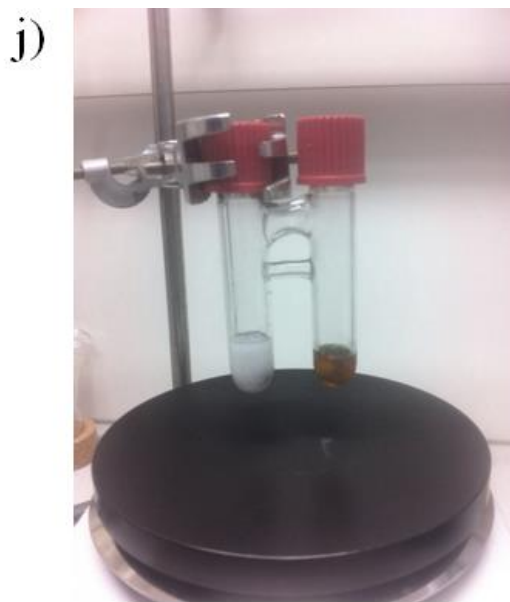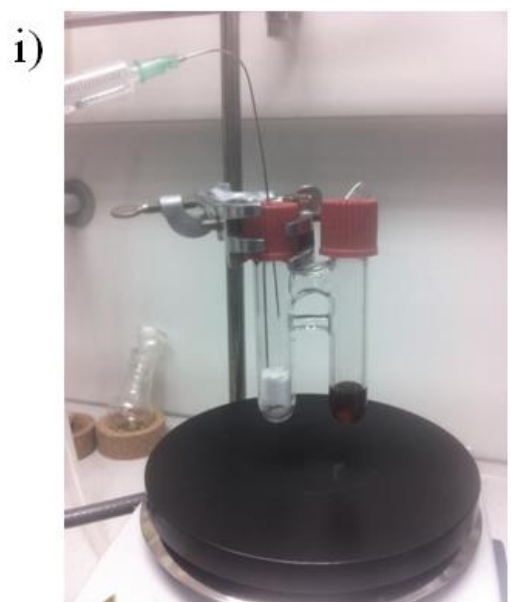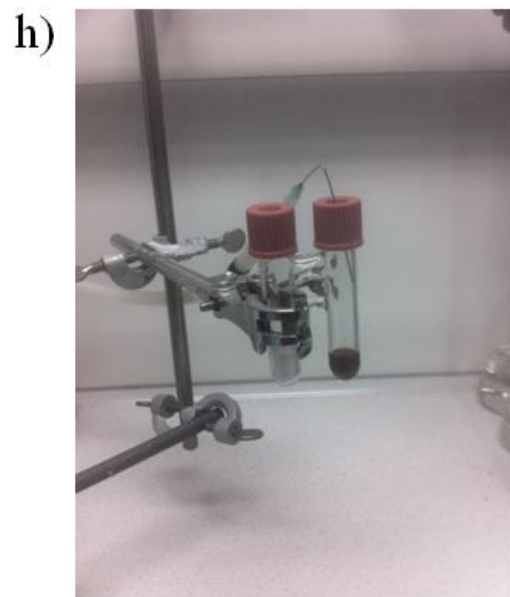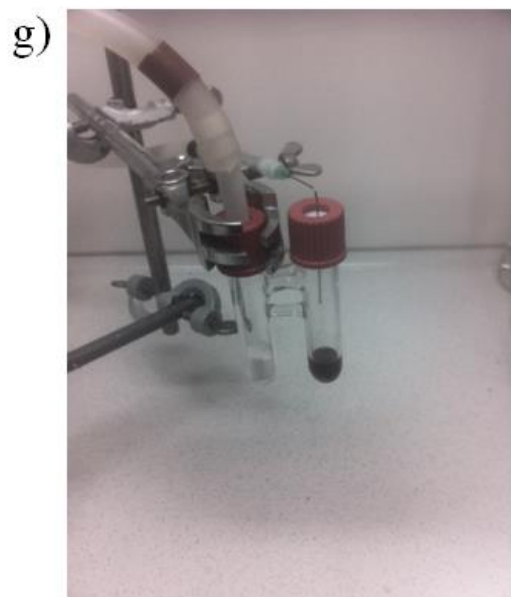
Figure S1: Setup of an alkoxycarbonylation reaction in a two-chambered vessel. See "General Procedure A" for steps a) – j).

General procedure **GP B** for Brønsted acid and Pd-precursor screening

General procedure **A** was followed using styrene as the olefin component and dist. MeOH as the alcohol, but with equimolar amounts of different acids or Pd precursors employed and 2 h reaction time. Solid acids (BNPA, pTsOH, PhCO$_2$H) were added at the start, while liquid acids (TFA, MsOH) were added via microsyringe to the olefin/MeOH/Pd(dba)$_2$/ligand DCM solution.

For quantitative GC-FID analysis of these catalytic carbonylation reactions, n-pentadecane (76.9 mg, 100 µL) was added to the crude reaction mixture with a 100 µL teflon microsyringe, the two-phase system vigorously stirred and diluted with DCM (2 mL) until a homogenous solution was obtained. A suitable Pd metal scavenger was added (QuadraSil MP) and the solution was then filtered through a cotton-plugged Pasteur pipette filled with celite and basic aluminium oxide and the sample in the GC vial was further diluted with DCM. The vial caps were sealed with parafilm to avoid evaporation of volatile components. Retention times under GC temperature program described above: t_R(styrene) = 2.99 min; t_R(n-pentadecane) = 6.00 min; t_R(methyl 2-phenylpropanoate **13**-b) = 4.99 min; t_R(methyl 3-phenylpropanoate **13**-l) = 5.32 min.

Response factors employed for yield calculations were $R_{Styrene}$ = 0.924 and $R_{Product}$ = 0.649 derived from calibration data by linear regression. b:l ratios were determined by comparison of the area integrals from the branched and linear product from the same GC-FID data.

General procedure **GP C** for hydrothioesterification in a two-chambered pressure vessel

A two-chambered pressure vessel (COware 20 mL, SyTracks A/S) equipped with stirring bars was charged with N-formylsaccharin (**6**) (450 mg, 2.13 mmol) and sodium carbonate (339 mg, 3.20 mmol) in chamber A; chamber B was charged with DPPA (15 mol%, 38 mg, 150 µmol) and sealed with a septum-containing screw cap assembly (COware type). Chamber A was fitted with a vacuum adapter screwcap and the reaction vessel was evacuated for 10 min. Under N$_2$ atmosphere, Pd(dba)$_2$ (1 mol%, 5.8 mg, 10 µmol), dppdtbpf (**L6**) (4 mol%, 21 mg, 40 µmol) were added to chamber B, the vessel was then subjected to evacuation/N$_2$-backfilling (3x).

Then, anhydrous dist. CH$_2$Cl$_2$ the thiol (1.34 eq) and the olefin (100 mol%, 1 mmol) were added to chamber A, resulting in a dark-red solution which was stirred at 750 rpm. The vacuum adapter screw cap of chamber A was exchanged to a septum containing screw cap under positive N$_2$ pressure (using the septum inlet of chamber B). To start the decarbonylation, dry DMF (1 mL) was added to chamber A via septum addition. Pictures of the two-chambered pressure vessel setup are available in the supporting information of our previous work.[4] Both reaction chambers were stirred at 750 rpm for 14 h at RT. The reaction was stopped by opening the reaction vessel. The crude product was purified by column chromatography. The exact amounts of thiols and CH$_2$Cl$_2$ are shown in Table 2.

Table 2: Exact amounts of thiol and CH_2Cl_2 for thiocarbonylation reaction.

Entry[a]	thiol	V(thiol)/ μL	V(CH_2Cl_2)/ μL
1	$^nC_7H_{15}SH$	210	790
2	^nPrSH	125	875
3	EtSH	100	900
4	BnSH	160	840
5	N-Boc-cysteine methyl ester	280	720
6	CySH	165	835
7	PhSH	140	860

2.4.3. Experimental procedures and analytical data

2.4.3.1. Synthesis of *N*-formylsaccharin

Dimethylphenylsilyl formate (quantitative ^{1}H-NMR analysis by conversion into formic acid)[S5]
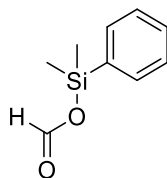
180.3 g/mol

A flame-dried 25 mL Schlenk tube with a stirring bar was charged with $Rh_2(OAc)_4$ (3.3 mg, 7.0 µmol, 0.25 mol%) and K_2CO_3 (2.1 mg, 14 µmol, 0.5 mol%) and then fitted with a rubber septum. The atmosphere in the reaction vessel was exchanged to CO_2 by triple evacuation and refilling with CO_2 (balloon reservoir). The solids were dissolved in dry MeCN (6 mL) by syringe addition under stirring, giving a purple solution. After dissolution of all solid components, the solution was heated to 50 °C and dimethylphenylsilane (460 µL, 3.00 mmol) was added *via* syringe (gas evolution occurs) and the reaction was further stirred at this temperature for 2 h.

After this time, the reaction was allowed to come to room temperature and the solvent was removed *in vacuo* (110 mbar, tepid water bath) without subjecting the intermediate silyl formate to atmospheric conditions in the process. The catalyst components were then precipitated under N_2 atmosphere by addition of dry hexane (3 mL) by syringe. The colourless solution was then transferred to a flame-dried 25 mL Schlenk tube by cannula filtration under inert conditions and the solvent subsequently removed again as described above, giving the silyl formate as a colourless to bronze liquid with slight turbidity. A qualitative analysis by ^{1}H-NMR [400 MHz, $CDCl_3$, δ (ppm): 8.12 (s, 1H, C<u>H</u>O), 7.50 (m, 5H, Ar<u>H</u>), 0.63 (s, 6H, Si(C<u>H</u>$_3$)$_2$] matched with the reported literature data[S6] but contained traces of acetonitrile and an unknown impurity, indicating decomposition that occurred while preparing the NMR sample.

For quantitative ^{1}H-NMR analysis, the silyl formate was treated with 2 mL of dist. H_2O for hydrolysis for 1 h at RT under stirring. As an internal standard, maleic acid (26 mg) was added. An aliquot of this mixture was taken up in D_2O.

For quantitative NMR data evaluation, all spectra were manually phase-corrected and the baseline automatically set. Chemical shifts of components used for evaluation in D_2O (ppm): Formic acid 8.16 (1H, s, <u>H</u>CO$_2$H); Maleic acid 6.34 (2H, s, HO$_2$C-C<u>H</u>=C<u>H</u>-CO$_2$H). Regression analysis of data points from calibration gave a response factor $R_{Formic\ acid}$ =1.01, and by using the obtained integral ratios for calculation, 150 mg (3.25 mmol, quant.) of formic acid was yielded after the hydrolysis.

_N_-Acetylsaccharin and _N_-Formylsaccharin **6**[S7]
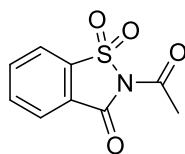
225.2 g/mol   211.2 g/mol
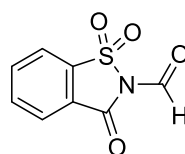
_N_-acetylsaccharin   **6**

A two-necked, flame-dried RBF equipped with a stirring bar and reflux condenser was charged with acetic anhydride (15.1 mL, 160 mmol, 4 Eqv.) and formic acid (7.80 mL, 208 mmol, 5.2 Eqv.) and heated to reflux for 5 h under stirring. Then, saccharin (7.33 g, 40.0 mmol, 1 Eqv.) was added to the solution and stirred at 60 °C overnight. Then, the reaction vessel was cooled to RT, diluted with dist. H_2O, the precipitate washed with dist. H_2O over a Buchner funnel and the resulting filter cake dried _in vacuo_ to afford a mixture of _N_-formyl- and _N_-acetylsaccharin as a colourless powder (5.10 g, 24 mmol, 60%).

Each component matches with the reported literature data.[S7, 8]

_R_f: Decomposition on normal-phase SiO_2.

¹H-NMR (300 MHz, CD_3CN): δ (ppm): 9.15 (s, 1H, HetArC<u>H</u>O), 8.31 – 7.72 (m, 4H, HetAr<u>H</u>); minor signals from _N_-acetylsaccharin: 8.31 – 7.72 (m, 4H, HetAr<u>H</u>),), 2.62 (s, 3H, N-COC<u>H</u>₃).

¹³C-NMR (75 MHz, CD_3CN) δ (ppm): 157.6 , 157.4, 137.8, 137.2, 136.7, 135.3, 135.0, 134.1, 126.0, 125.8, 124.6, 121.2, 120.7, 120.4, 25.1.

GC/MS (ESI**)**: t_R = 1.63 min (NFS), m/z = 212 (32, [MH⁺]), 184 (100, [MH⁺]-[CO]); t_R = 1.82 min (NAS), m/z = 226 (100, [MH⁺]).

_N_-Formylsaccharin **6** (from Formic acid)
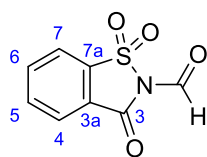
211.2 g/mol

6

Using a modified procedure by Goto,[S9] a two-necked, flame-dried 500 mL RBF with a N_2 inlet, rubber septum and stirring bar was charged with HCO_2H (98 mL, 2.6 mol, 24 Eqv.) and Ac_2O (113 mL, 1.2 mol, 12 Eqv.) and the resulting solution was stirred vigourosly for 1 h at RT (slightly exothermic). Meanwhile, a flame-dried assembly of a three-necked 500 mL Schlenk RBF with N_2 inlet, 100 mL dropping funnel and stirring bar and was charged with saccharin (18.3 g, 100 mmol, 1 Eqv.) and dissolved in dry THF (150 mL) under stirring. Upon the addition of pyridine (1.0 mL, 10 mmol, 10 mol%), the solution turned slightly cloudy and was further stirred. The formylating mixture prepared beforehand was then transferred _via_ cannula into the dropping funnel and then added to the stirred saccharin solution dropwise at a rate which keeps the stirred saccharin solution at room temperature. After complete addition, precipitation occurs, and the white suspension is further stirred at RT for 3 h. The precipitate was collected by vacuum filtration, washed with MeOH p.A. (150 mL), then H_2O (150 mL, caution: remaining AcOCHO decomposes exothermically in the filtrate under CO release), and the filter cake was dried _in vacuo_ to yield a colourless crystalline powder (19.4 g, 92.0 mmol, 92%). The analytical data matches with reported literature data.[S7]

R_f: Decomposition on normal-phase SiO_2.

Melting point: 227 °C (a change in crystallinity occurs between 120-150 °C, possibly due to decarbonylation).

FT-IR (ATR) $\tilde{v}$ (cm^{-1})**:** 1756 (s, sh), 1716 (s, sh), 1593 (m, sh), 1460 (m, sh), 1345 (s, sh), 1289 (s, sh), 1249 (s), 1175 (s, sh), 1159 (s, sh), 1104 (s, sh), 746 (s, sh), 672 (s, sh), 574 (s, sh).

^{1}H-NMR (400 MHz, CD_3CN) δ (ppm): 9.16 (s, 1H, N-C_HO), 8.19 (d, _J_ = 7.7 Hz, 1H, ArH), 8.14 – 8.07 (m, 2H, ArH), 8.04 – 8.00 (m, 1H, ArH).

^{13}C-NMR (101 MHz, CD_3CN) δ (ppm): 157.7 ($\underline{C}^3$), 157.4 (N-$\underline{C}$HO), 137.9 ($\underline{C}^{3a}$), 137.3 ($\underline{C}^6$), 135.3 ($\underline{C}^5$), 126.0 ($\underline{C}^7$), 124.6 ($\underline{C}^{7a}$), 121.2 ($\underline{C}^4$).

HR-MS (ESI)**:** [MH$^+$] m/z = calc. for $C_8H_6NO_4S$ 212.0012; found 212.0010.

N-Formylsaccharin **6** (from CO_2)
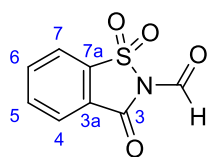
211.2 g/mol

6

A flame-dried 25 mL Schlenk tube with a stirring bar under N_2 atmosphere was charged with $Rh_2(OAc)_4$ (3.3 mg, 7.5 µmol, 0.25 mol%) and K_2CO_3 (2.1 mg, 15 µmol, 0.5 mol%) and then fitted with a rubber septum. The atmosphere in the reaction vessel was exchanged towards CO_2 by triple evacuation and refilling with CO_2 (balloon reservoir). The solids were dissolved in dry MeCN (6 mL) by syringe addition under stirring, giving a purple solution. After dissolution of all solid components, the solution was heated to 50 °C and dimethylphenylsilane (460 µL, 3.0 mmol) was added *via* syringe (gas evolution may occur) and the reaction was further stirred at this temperature for 2 h. After this time, the reaction was allowed to cool down to room temperature and the solvent was removed *in vacuo* (110 mbar, tepid water bath) without subjecting the intermediate silyl formate to atmospheric conditions in the process. The catalyst components were then precipitated under N_2 atmosphere by addition of dry hexane (6 mL) by syringe. The colourless solution was then transferred to a flame-dried 25 mL Schlenk tube by cannula filtration under inert conditions and the solvent subsequently removed again as described above, giving the silyl formate **9** as colourless to bronze liquid with slight turbidity.

To the neat silyl formate, Ac_2O (284 µL, 3.00 mmol) was added and stirred for 4 h at 40 °C to generate the formylating mixture. Meanwhile, an oven-dried 5 mL screw-capped glass vessel with septum inlet and stirring bar was filled with N_2, then charged with saccharin (0.30 mmol, 55 mg) and imidazole (10 mol%, 0.030 mmol, 2.0 mg). The solids were dissolved with dry THF (430 µL) under stirring. The formylating mixture was added dropwise under vigorous stirring *via* syringe. After complete addition, precipitation occurs, and the white suspension is further stirred at RT for 3 h. After the end of the reaction, the vessel contents were transferred to a Pasteur pipette plugged with cotton and filter paper. The resulting filter cake was washed with three pipette volumes of MeOH p.A., then three pipette volumes of cyclohexane, and the filtrate was discarded. The filter cake was then dissolved by addition of three pipette volumes MeCN, and the filtrate collected in a tared 5 mL RBF. The solvent was removed *in vacuo* to give the product as a colourless powder (36 mg, 0.17 mmol, 57% based on saccharin). Analytics as above.

2.4.3.2. Synthesis of oxoesters

Methyl 2-Phenylpropanoate (**13**-b) and Methyl 3-Phenylpropanoate (**13**-l)

164.2 g/mol

13-b   **13**-l
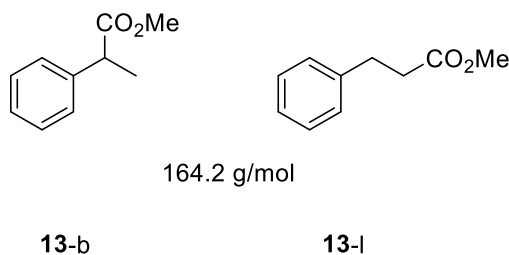
Using dist. styrene (115 µL, 104 mg, 1.00 mmol; long-term storage in the dark under N_2 at -20 °C) as the olefin component and dist. MeOH (250 µL, stored under N_2) as the alcohol component, **GP A** was employed using 0.5 mol% [Pd]. The b/l ratio of the crude product product was determined by GC-FID analysis to be 88:12. Purification by flash chromatography on SiO_2 (mobile phase: 95:5 CyH:EtOAc) gave the regioisomeric compounds as a colourless oil (124 mg, 0.76 mmol, 76%, b/l ratio 97:3 by NMR). The analytical data matches with reported literature data.[S10,11]

R_f: 0.35 (mobile phase 9:1 CyH:EtOAc, $KMnO_4$ stain)

Melting point: Ambient temperature.

^{1}H-NMR (400 MHz, $CDCl_3$) δ (ppm): 7.43 – 7.18 (m, 5H, ArH), 3.75 (q, J = 7.2 Hz, 1H, ArCH(CO$_2$Me)CH$_3$), 3.67 (s, 3H, R-CO$_2$CH$_3$), 1.52 (d, J = 7.2 Hz, 3H, ArCH(CO$_2$Me)CH$_3$); minor signals for linear regioisomer 2.99 (t, J = 7.8 Hz, 2H, ArCH$_2$CH$_2$CO$_2$Me), 2.66 (t, J = 7.8 Hz, 2H, ArCH$_2$CH$_2$CO$_2$Me).

^{13}C-NMR (101 MHz, $CDCl_3$) δ (ppm): 175.0 (R-CO$_2$CH$_3$), 140.6 (ArC), 128.7 (ArC), 127.5 (ArC), 127.2 (ArC), 52.0 (R-CO$_2$CH$_3$), 45.5 (ArCH(CO$_2$Me)CH$_3$), 18.6 (ArCH(CO$_2$Me)CH$_3$).

minor signals for linear regioisomer: 128.5 (ArC), 128.3 (ArC), 126.3 (ArC), 51.6 (R-CO$_2$CH$_3$), 35.7 (ArCH$_2$CH$_2$CO$_2$Me), 31.0 (ArCH$_2$CH$_2$CO$_2$Me).

GC-FID (50-280M12, from crude): t_R = 4.99 min (branched), t_R = 5.32 min (linear).

GC/MS (EI): t_R = 6.61 min (branched), m/z = 164 (35, [MH$^{+•}$]), 133 (1, [MH$^{+•}$]-[OMe$^•$]), 104 (100, [MH$^{+•}$]-[OMe$^•$]-[CO]), t_R = 7.37 min (linear), same m/z and intensity pattern.

Ethyl 2-phenylpropanoate (**14**-b) and Ethyl 3-phenylpropanoate (**14**-l)

178.2 g/mol

14-b   **14**-l
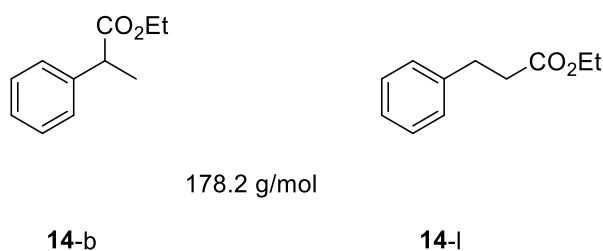
Using styrene (115 µL, 104 mg, 1.00 mmol) as the olefin component and dist. EtOH (250 µL, stored under N_2) as the alcohol component, **GP A** was employed using 0.5 mol% [Pd]. The b/l ratio of the crude product was determined by GC-FID analysis to be 93:7. Purification by column chromatography on SiO_2 (95:5 CyH:EtOAc) gave the regioisomeric compounds as a colourless oil (150 mg, 0.84 mmol, 84%, b/l ratio 97:3 by NMR). Analytical data matched with the reported literature data.[S12,13]

R_f: 0.44 (mobile phase 9:1 CyH:EtOAc), 0.34 (mobile phase 95:5 CyH:EtOAc), $KMnO_4$ stain.

Melting point: Ambient temperature.

^{1}H-NMR (400 MHz, $CDCl_3$) δ (ppm): 7.40 - 7.17 (m, 5H, Ar<u>H</u>), 4.20 – 4.06 (m, 2H, R-CO$_2$C<u>H$_2$</u>CH$_3$), 3.71 (q, J = 7.2 Hz, 1H, ArC<u>H</u>(CO$_2$Et)Me), 1.50 (d, J = 7.2 Hz, 3H, ArCH(CO$_2$Et)C<u>H$_3$</u>), 1.21 (t, J = 7.1 Hz, 3H, R-CO$_2$CH$_2$C<u>H$_3$</u>); minor signals from linear regioisomer: 2.96 (t, J = 8.0 Hz, 2H, ArC<u>H$_2$</u>CH$_2$CO$_2$Et), 2.63 (t, J = 8.0 Hz, 2H, ArCH$_2$C<u>H$_2$</u>CO$_2$Et).

^{13}C-NMR (101 MHz, $CDCl_3$) δ (ppm): 174.6 (<u>C</u>=O), 140.7 (Ar<u>C</u>), 128.6 (Ar<u>C</u>), 127.5 (Ar<u>C</u>), 127.1 (Ar<u>C</u>), 60.7 (CO$_2$<u>C</u>H$_2$CH$_3$), 45.6 (Ar<u>C</u>H(CO$_2$Et)Me), 18.6 (ArCH(CO$_2$Et)<u>C</u>H$_3$), 14.1 (CO$_2$CH$_2$<u>C</u>H$_3$), minor signals from linear regioisomer were not detected due to low concentration.

GC-FID (50-280M12): t_R = 5.16 min (branched), t_R = 5.55 min (linear).

GC/MS (EI): t_R = 7.30 min (branched), m/z = 178 (18, [M$^{+\bullet}$]), 105 (100, [C$_8$H$_9^+$]); t_R = 8.22 min (linear), m/z = 178 (18, [M$^{+\bullet}$]), 133 (100, [M$^{+\bullet}$]-[OEt$^\bullet$]).

Isopropyl 2-phenylpropanoate (**15**-b) and Isopropyl 3-phenylpropanoate (**15**-l)
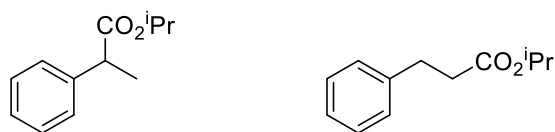
192.3 g/mol

15-b   **15**-l

Using styrene (115 µL, 104.2 mg, 1 mmol) at as the olefin component and dist. ^{i}PrOH (250 µL, stored under N_2) as the alcohol component, **GP A** was employed with 0.5 mol% [Pd]. The b/l ratio of the crude product was determined by GC-FID analysis to be 89:11. Purification by flash chromatography on SiO_2 (mobile phase: 95:5 CyH:EtOAc) gave the regioisomeric compounds as a colourless oil (90 mg, 0.47 mmol, 47%, b/l ratio 93:7 by NMR). Analytical data matched with the reported literature data. [S12,13]

R_f: 0.56 (mobile phase 9:1 CyH:EtOAc, $KMnO_4$ stain)

**Melting point**: Ambient temperature.

^{1}H-NMR (300 MHz, CDCl$_3$) δ (ppm): 7.40 – 7.18 (m, 5H, ArH), 5.01 (hept, J = 6.3 Hz, 1H, R-CO$_2$CH(Me)$_2$), 3.68 (q, J = 7.2 Hz, 1H, ArCH(CO$_2$^{i}Pr)Me), 1.50 (d, J = 7.2 Hz, 3H, ArCH(CO$_2$^{i}Pr)CH$_3$), 1.23 (d, J = 6.3 Hz, 3H, R-CO$_2$CH(CH$_3$)$_2$ diastereotopic), 1.14 (d, J = 6.3 Hz, 3H, R-CO$_2$CH(CH$_3$)$_2$ diastereotopic); minor signals from linear regioisomer: 2.96 (t, J = 7.9 Hz, 2H, ArCH$_2$CH$_2$CO$_2$^{i}Pr), 2.61 (t, J = 7.9 Hz, 2H, ArCH$_2$CH$_2$CO$_2$^{i}Pr).

^{13}C-NMR (75 MHz, CDCl$_3$) δ (ppm): 174.1 (C=O), 140.8 (ArC), 128.6 (ArC), 127.5 (ArC), 127.0 (ArC), 67.9 (R-CO$_2$CH(Me)$_2$), 45.8 (ArCH(CO$_2$^{i}Pr)CH$_3$), 21.8 (R-CO$_2$CH(CH$_3$)$_2$, 21.6 (R-CO$_2$CH(CH$_3$)$_2$, 18.6 (ArCH(CO$_2$^{i}Pr)CH$_3$); minor signals from linear regioisomer: 140.6 (ArC), 128.5 (ArC), 128.4 (ArC), 126.2 (ArC), 67.7 (R-CO$_2$CH(Me)$_2$), 36.3 (ArCH$_2$CH$_2$CO$_2$^{i}Pr), 31.1 (ArCH$_2$CH$_2$CO$_2$^{i}Pr).

GC-FID (50-280M12): t_R = 5.40 min (branched), t_R = 5.85 min (linear).

GC/MS (EI): t_R = 7.58 min (branched), m/z = 192 (25, [M$^{+\bullet}$]), 105 (100, [C$_8$H$_9$$^+$]); t_R = 8.59 min (linear), m/z = 192 (25, [M$^{+\bullet}$]).

Cyclohexyl 2-phenylpropanoate (**17**-b) and Cyclohexyl 3-phenylpropanoate (**17**-l)

232.3 g/mol

17-b   **17**-l

Using styrene (115 μL, 104 mg, 1.00 mmol) as the olefin component and cyclohexanol (250 μL) as the alcohol component, **GP A** was employed with 0.5 mol% [Pd]. The b/l ratio of the crude product was determined by GC-FID analysis to be 93:7. Purification by flash chromatography on SiO_2 (mobile phase: 95:5 CyH:EtOAc) gave the regioisomeric compounds as a colourless oil (48 mg, 0.21 mmol, 21%, b/l ratio 92:8 by NMR). The analytical data matches with reported literature data.[S14,15]

R_f: 0.47 (mobile phase 9:1 CyH:EtOAc, $KMnO_4$ stain)

Melting point: Ambient temperature.

^{1}H-NMR (300 MHz, $CDCl_3$) δ (ppm): 7.40 – 7.14 (m, 5H, Ar$\underline{H}$), 4.83 – 4.69 (m, 1H, Cyclohexyl-C$\underline{H}$), 3.69 (q, J = 7.2 Hz, 1H, ArC$\underline{H}$(CO_2Cy)CH$_3$), 1.88 – 1.54 (m, 5H Cyclohexyl-C$\underline{H}_2$), 1.49 (d, J = 7.2 Hz, 3H, ArCH(CO_2Cy)C$\underline{H}_3$), 1.43 – 1.17 (m, 5H, Cyclohexyl-C$\underline{H}_2$); minor signals from linear regioisomer: 2.95 (t, J = 7.8 Hz, 2H, ArC$\underline{H}_2$CH$_2$$CO_2$Cy), 2.61 (t, J = 7.8 Hz, 2H, ArCH$_2$C$\underline{H}_2$$CO_2$Cy).

^{13}C-NMR (75 MHz, $CDCl_3$) δ (ppm): 174.0 ($\underline{C}$=O), 140.9 (Ar$\underline{C}$), 128.5 (Ar$\underline{C}$), 127.5 (Ar$\underline{C}$), 127.0 (Ar$\underline{C}$), 72.7 (Cyclohexyl-$\underline{C}$H), 45.8 (Ar$\underline{C}$H(CO_2Cy)CH$_3$), 25.4 (Cyclohexyl-$\underline{C}$H$_2$), 23.6 (Cyclohexyl-$\underline{C}$H$_2$), 23.5 (Cyclohexyl-$\underline{C}$H$_2$), 18.5 (ArCH(CO_2Cy)$\underline{C}$H$_3$); minor signals from linear regioisomer: 128.5 (Ar$\underline{C}$), 128.3 Ar$\underline{C}$), 126.2 (Ar$\underline{C}$), 31.5 (ArCH$_2$$\underline{C}H_2$$CO_2$Cy), 31.2 (Ar$\underline{C}H_2CH_2$$CO_2$Cy).

GC-FID (50-280M12): t_R = 7.38 min (branched), t_R = 7.82 min (linear).

GC/MS (EI): t_R = 11.86 min (branched), m/z = 232 (4, [M$^{+•}$]); t_R = 12.79 min (linear), m/z = 232 (8, [M$^{+•}$]).

Benzyl 2-phenylpropanoate (**18**-b) and Benzyl 3-phenylpropanoate (**18**-l)
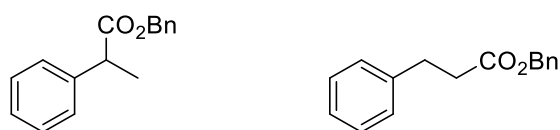
240.3 g/mol

18-b   **18**-l

Using styrene (115 μL, 104 mg, 1.00 mmol) as the olefin component and benzyl alcohol (250 μL) as the alcohol component, **GP A** was employed with 0.5 mol% [Pd]. The b/l ratio of the crude product was determined by GC-FID analysis to be 82:18. Purification by flash chromatography on SiO_2 (mobile phase: 95:5 CyH:EtOAc) gave the regioisomeric compounds as a colourless oil with a pleasant smell (191 mg, 0.80 mmol, 80%, b/l ratio 77:23 by NMR). The analytical data matches with reported literature data.[S10, 11]

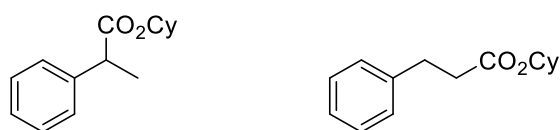R_f: 0.42 (mobile phase 9:1 CyH:EtOAc, $KMnO_4$ stain)

Melting point: Ambient temperature.

^{1}H NMR (300 MHz, $CDCl_3$) δ (ppm): 7.50 – 7.22 (m, 10H, Ar$\underline{H}$), 5.19 (ABq, $\Delta\delta_{AB}$ = 0.05, J = 12.9 Hz, 2H, C$\underline{H_2}$Ph), 3.86 (q, J = 7.2 Hz, 1H, ArC$\underline{H}$(CO$_2$CH$_2$Ph)Me), 1.61 (d, J = 7.2 Hz, 3H, ArCH(CO$_2$CH$_2$Ph)C$\underline{H_3}$); minor signals from linear regioisomer: 3.06 (t, J = 7.8 Hz, 2H, ArC$\underline{H_2}$CH$_2$CO$_2$Bn), 2.76 (t, J = 7.8 Hz, 2H, ArCH$_2$C$\underline{H_2}$CO$_2$Bn).

^{13}C NMR (75 MHz, $CDCl_3$) δ (ppm): 174.4 ($\underline{C}$=O), 140.5 (Ar$\underline{C}$), 136.1 (Ar$\underline{C}$), 128.7 (Ar$\underline{C}$), 128.7 (Ar$\underline{C}$), 128.6 (Ar$\underline{C}$), 128.4 (Ar$\underline{C}$), 128.3 (Ar$\underline{C}$), 128.2 (Ar$\underline{C}$), 128.0 (Ar$\underline{C}$), 127.7 (Ar$\underline{C}$), 127.3 (Ar$\underline{C}$), 126.4 (Ar$\underline{C}$), 66.5 (ArCH(CO$_2$$\underline{C}H_2$Ph)Me), 45.6 (Ar$\underline{C}$H(CO$_2CH_2$Ph)Me), 18.6 (ArCH(CO$_2CH_2$Ph)$\underline{C}H_3$); minor signals from linear regioisomer: 172.8 ($\underline{C}$=O), 136.1 (Ar$\underline{C}$), 66.4 (ArCH$_2$CH$_2$CO$_2$$\underline{C}H_2$Ph), 36.0 (ArCH$_2$$\underline{C}H_2CO_2$Bn), 31.1 (Ar$\underline{C}H_2CH_2CO_2$Bn).

GC-FID (50-280M12): t_R = 7.94 min (branched), t_R = 8.35 min (linear).

GC/MS (EI): t_R = 13.00 min (branched), m/z = 240 (12, [M$^{+•}$]), 105 (100, [C$_8$H$_9^+$]), 91 (75, [C$_7$H$_7^+$]); t_R = 13.91 min (linear), m/z = 240 (4, [M$^{+•}$]), 107 (100, [C$_7$H$_7$O$^+$]), 91 (100, [C$_7$H$_7^+$]).

Methyl 2-(m-tolyl)propanoate (**19**-b) and Methyl 3-(m-tolyl)propanoate (**19**-l)

178.2 g/mol

19-b   **19**-l

Using 3-methylstyrene (130 µL, 118 mg, 1.00 mmol) as the olefin component and dist. MeOH (250 µL, stored under N_2) as the alcohol component, **GP A** was employed with 0.5 mol% [Pd]. The b/l ratio of the crude product was determined by GC-FID analysis to be 91:9. Purification by flash chromatography on SiO_2 (mobile phase: 95:5 CyH:EtOAc) gave the regioisomeric compounds as a bright yellow oil (161 mg, 0.92 mmol, 92%, b/l ratio 91/9 by NMR).

R$_f$: 0.34 (mobile phase 95:5 CyH:EtOAc, $KMnO_4$ stain)

Melting point: Ambient temperature.

FT-IR (ATR) ν (cm^{-1}): 2981 (w, br), 2952 (w, br), 1734 (s, sh), 1608 (w, sh), 1455 (m, br), 1376 (m, br), 1335 (m, br), 1238 (m, br), 1196 (s, br), 1168 (s, br), 1067 (m, br).

^{1}H-NMR (300 MHz, CDCl$_3$) δ (ppm): 7.25 – 7.17 (m, 1H, Ar<u>H</u>), 7.12 – 6.99 (m, 3H, Ar<u>H</u>), 3.70 (q, *J* = 7.2 Hz, 1H, ArC<u>H</u>), 3.66 (s, 3H, OC<u>H</u>$_3$), 2.34 (s, 3H, ArC<u>H</u>$_3$), 1.49 (d, *J* = 7.2 Hz, 3H, ArCHC<u>H</u>$_3$); minor signals from linear regioisomer: 2.33 (s, 3H, ArC<u>H</u>$_3$), 2.92 (t, *J* = 7.5 Hz, 2H, ArC<u>H</u>$_2$CH$_2$CO$_2$Me), 2.62 (t, *J* = 7.5 Hz, 2H, ArCH$_2$C<u>H</u>$_2$CO$_2$Me).

^{13}C-NMR (101 MHz, CDCl$_3$) δ (ppm): 175.1 (<u>C</u>=O), 140.5 (Ar<u>C</u>), 138.3 (Ar<u>C</u>), 128.5 (Ar<u>C</u>), 128.2 (Ar<u>C</u>), 127.9 (Ar<u>C</u>), 124.5 (Ar<u>C</u>), 52.0 (ArCH(CO$_2$<u>C</u>H$_3$)Me), 45.4 (Ar<u>C</u>H(CO$_2$Me)Me), 21.4 (Ar<u>C</u>H$_3$), 18.6 (ArCH(CO$_2$Me)<u>C</u>H$_3$). Due to low concentration no signals from the linear regioisomer were observed.

GC-FID: (50-280M12): *t*$_R$ = 5.42 min (branched), *t*$_R$ = 5.75 min (linear).

GC-MS: *t*$_R$ = 6.03 min (branched), m/z = 178 (33, [M$^{+\bullet}$]), 119 (100, [M$^{+\bullet}$]-[$^\bullet$CO$_2$Me], 91 (28, [M$^{+\bullet}$]-[CO$_2$Me$^\bullet$]-[CH$_3$$^\bullet$]); *t*$_R$ = 6.77 min (linear), m/z = 178 (24, [M$^{+\bullet}$]), 147 (8, [M$^{+\bullet}$]-[OMe$^\bullet$]), 118 (100, [C$_9$H$_{10}$$^{+\bullet}$]), 105 (54, [M$^{+\bullet}$]-[CH$_2CO_2Me^\bullet$]).

HR-MS (APCI): m/z = [MH$^+$] calc. for C$_{11}$H$_{14}$O$_2$ 179.1067, found 179.1067.

Methyl 2-(3-methoxyphenyl)propanoate **(20**-b**)** and methyl 3-(3-methoxyphenyl)propanoate **(20**-l**)**

194.2 g/mol

20-b   **20**-l

Using 3-vinylanisole (140 µL, 134 mg, 1.00 mmol) as the olefin component and dist. MeOH (250 µL, stored under N_2) as the alcohol component, **GP A** was employed with 0.5 mol% [Pd]. The b/l ratio of the crude product was determined by GC-FID analysis to be 89:11. Purification by flash chromatography on SiO_2 (mobile phase: 95:5 CyH:EtOAc) gave the regioisomeric compounds as a bright yellow oil (148 mg, 762 µmol, 76%, b/l ratio 88/12 by NMR). The analytical data for the linear product matches with reported literature.[S16]

R_f: 0.21 (mobile phase 95:5 CyH:EtOAc, $KMnO_4$ stain)

Melting point: Ambient temperature.

^{1}H-NMR (400 MHz, $CDCl_3$) δ (ppm): 7.25 − 7.18 (m, 1H, Ar$\underline{H}$), 6.91 − 6.73 (m, 3H, Ar$\underline{H}$), 3.80 (s, 3H, ArOC$\underline{H}_3$), 3.70 (q, J = 7.2 Hz, 1H, ArC$\underline{H}$(CO$_2$Me)Me), 3.67 (s, 3H, RCO$_2$C$\underline{H}_3$), 1.49 (d, J = 7.2 Hz, 3H, ArCH(CO$_2$Me)C$\underline{H}_3$); minor signals from linear regioisomer: 3.79 (s, 3H, ArOC$\underline{H}_3$), 3.68 (s, 3H, ArCH$_2$CH$_2$COOC$\underline{H}_3$), 2.93 (t, J = 7.9 Hz, 2H, ArC$\underline{H}_2$CH$_2$CO$_2$Me), 2.63 (t, J = 7.9 Hz, 2H, ArCH$_2$C$\underline{H}_2$CO$_2$Me).

^{13}C-NMR (101 MHz, $CDCl_3$) δ (ppm): 174.9 ($\underline{C}$=O), 159.8 (Ar$\underline{C}$), 142.1 (Ar$\underline{C}$), 129.6 (Ar$\underline{C}$), 119.9 (Ar$\underline{C}$), 113.3 (Ar$\underline{C}$), 112.5 (Ar$\underline{C}$), 55.2 (ArO$\underline{C}$H$_3$), 52.1 (RCO$_2$$\underline{C}H_3$), 45.4 (Ar$\underline{C}$H(CO$_2$Me)Me), 18.6 (ArCH(CO$_2$Me)$\underline{C}H_3$); minor signals from linear regioisomer: 129.5 (Ar$\underline{C}$), 120.6 (Ar$\underline{C}$),114.1 (Ar$\underline{C}$), 111.6 (Ar$\underline{C}$), 51.6 (RCO$_2$$\underline{C}H_3$), 35.6 (ArCH$_2$$\underline{C}H_2CO_2$Me), 31.0 (Ar$\underline{C}H_2CH_2CO_2$Me).
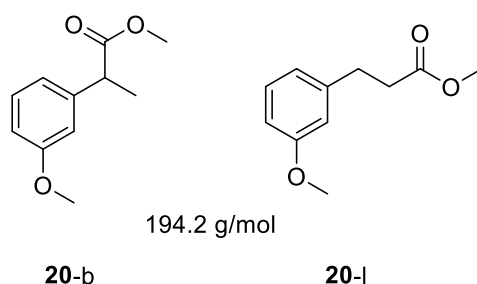
GC-FID: (50-280M12): t_R = 6.13 min (branched), t_R = 6.47 min (linear).

GC-MS: t_R = 7.56 min (branched), m/z = 194 (40, [M$^{+•}$]), 135 (100, [M$^{+•}$]-[$^•$CO$_2$Me]; t_R = 8.34 min (linear), m/z = 194 (46, [M$^{+•}$]), 163 (11, [M$^{+•}$]-[OMe$^•$]), 134 (100, [C$_9$H$_{10}$O$^{+•}$]).

Methyl 2-(p-tolyl)propanoate **(21**-b**)** and methyl 3-(p-tolyl)propanoate **(21**-l**)**

178.2 g/mol

5da-b   **5da**-l

Using 4-methylstyrene (130 µL, 118, 1.00 mmol) as the olefin component and dist. MeOH (250 µL, stored under N_2) as the alcohol component, **GP A** was employed with 0.5 mol% [Pd]. The b/l ratio of the crude product was determined by GC-FID analysis to be 90:10. Purification by flash chromatography on SiO_2 (mobile phase: 95:5 CyH:EtOAc) gave the regioisomeric compounds as a colorless oil (160 mg, 896 µmol, 91%, b/l ratio 91/9 by NMR). The analytical data for the branched product matches with reported literature. [S17]

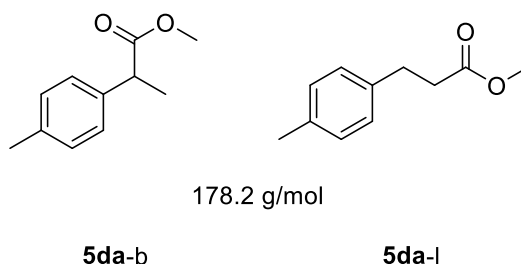**R$_f$:** 0.32 (mobile phase 95:5 CyH:EtOAc, $KMnO_4$ stain)

Melting point: Ambient temperature.

^{1}H-NMR (400 MHz, CDCl$_3$) δ (ppm): 7.19 (d, J = 8.1 Hz, 2H, Ar$\underline{H}$), 7.13 (d, J = 8.1 Hz, 2H, Ar$\underline{H}$), 3.69 (q, J = 7.2 Hz, 1H, ArC$\underline{H}$), 3.65 (s, 3H, ArCH(CO$_2$C$\underline{H}_3$)Me), 2.33 (s, 3H, ArC$\underline{H}_3$), 1.48 (d, J = 7.2 Hz, 3H, ArCH(CO$_2$Me)C$\underline{H}_3$); minor signals from linear regioisomer: 3.67 (s, 3H, ArCH$_2$CH$_2$CO$_2$C$\underline{H}_3$), 2.32 (s, 3H, ArC$\underline{H}_3$), 2.92 (t, J = 7.9 Hz, 2H, ArC$\underline{H}_2$CH$_2$CO$_2$Me), 2.61 (t, J = 7.9 Hz, 2H, ArCH$_2$C$\underline{H}_2$CO$_2$Me).

^{13}C-NMR (101 MHz, CDCl$_3$) δ (ppm): 175.2 ($\underline{C}$=O), 137.6 (Ar$\underline{C}$), 136.8 (Ar$\underline{C}$), 129.3 (Ar$\underline{C}$), 127.3 (Ar$\underline{C}$), 52.0 (RCO$_2$$\underline{C}H_3$), 45.0 (Ar$\underline{C}$H(CO$_2CH_3$)CH$_3$), 21.0 (Ar$\underline{C}H_3$), 18.6 (ArCH(CO$_2CH_3$)$\underline{C}H_3$); minor signals from linear regioisomer: 129.2 (Ar$\underline{C}$), 128.2 (Ar$\underline{C}$), 52.0 RCO$_2$$\underline{C}H_3$), 35.9 (ArCH$_2$$\underline{C}H_2CO_2$Me), 30.6 (Ar$\underline{C}H_2CH_2CO_2$Me).

GC-FID: (50-280M12): t_R = 5.47 min (branched), t_R = 5.79 min (linear).

GC-MS: t_R = 6.03 min (branched), m/z = 178 (17, [M$^{+•}$]), 119 (100, [M$^{+•}$]-[$^•$CO$_2$Me], 91 (19, [M$^{+•}$]-[CH$_2$CH$_2$CO$_2$Me$^•$]); t_R = 6.87 min (linear), m/z = 178 (25, [M$^{+•}$]), 118 (93, [C$_9$H$_{10}$$^{+•}$]), 105 (100, [M$^{+•}$]-[CH$_2CO_2Me^•$]).

Methyl 2-(4-(*tert*-butyl)phenyl)propanoate **(22**-b**)** and methyl 3-(4-(*tert*-butyl)phenyl) propanoate **(22**-l**)**

220.3 g/mol

22-b   **22**-l
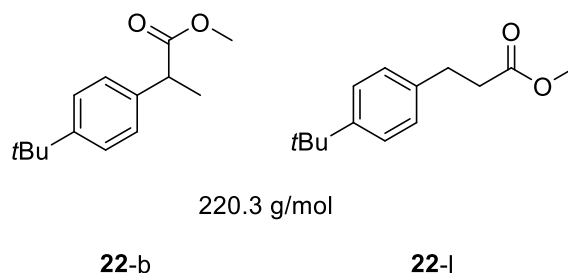
Using 4-*tert*-butylstyrene (200 µL, 163 mg, 1.00 mmol) as the olefin component and dist. MeOH (250 µL, stored under N_2) as the alcohol component, **GP A** was employed with 1.0 mol% [Pd]. The b/l ratio of the crude product was determined by GC-FID analysis to be 94:6. Purification by flash chromatography on SiO_2 (mobile phase: 95:5 CyH:EtOAc) gave the regioisomeric compounds as a colorless oil (199 mg, 902 µmol, 89%, b/l ratio 93/7 by NMR). The analytical data for the linear product matches with reported literature. [S16]

R$_f$: 0.32 (mobile phase 95:5 CyH:EtOAc, $KMnO_4$ stain)

Melting point: Ambient temperature.

^{1}H-NMR (400 MHz, $CDCl_3$) δ (ppm): 7.34 (d, *J* = 8.4 Hz, 2H, Ar$\underline{H}$), 7.23 (d, *J* = 8.4 Hz, 2H, Ar$\underline{H}$), 3.72 (q, *J* = 7.2 Hz, 1H, ArC$\underline{H}$(CO_2CH_3)Me), 3.66 (s, 3H, ArCH($CO_2C\underline{H}_3$)Me), 1.49 (d, *J* = 7.2 Hz, 3H, ArCH(CO_2Me)C$\underline{H}_3$), 1.31 (s, 9H, Ar-C(C$\underline{H}_3$)$_3$); minor signals from linear regioisomer: 3.68 (s, 2H, $RCO_2C\underline{H}_3$), 2.93 (t, *J* = 7.8 Hz, 2H, ArC$\underline{H}_2$$CH_2$$CO_2$Me), 2.63 (t, *J* = 7.8 Hz, 2H, $ArCH_2$C$\underline{H}_2$$CO_2$Me).

^{13}C-NMR (101MHz, $CDCl_3$) δ (ppm): 175.2 ($\underline{C}$=O), 150.00 (Ar$\underline{C}$), 137.5 (Ar$\underline{C}$), 127.1 (Ar$\underline{C}$), 125.6 (Ar$\underline{C}$), 52.0 ($RCO_2\underline{C}H_3$), 44.9 (Ar$\underline{C}$H(CO_2CH_3)Me), 34.5 (Ar-$\underline{C}$(CH_3)$_3$), 31.3 (Ar-C($\underline{C}H_3$)$_3$), 18.6 (ArCH(CO_2Me)$\underline{C}H_3$); due to low concentration, signals from the minor regioisomer were not detected.

GC-FID: (50-280M12): t_R = 6.53 min (branched), t_R = 6.84 min (linear).

GC-MS: t_R = 8.42 min (branched), m/z = 220 (25, [M$^{+\bullet}$]), 205 (100, [M$^{+\bullet}$]-[$CH_3^\bullet$]), 161 (75, [M$^{+\bullet}$]-[$^\bullet CO_2$Me]; t_R = 9.11 min (linear), m/z = 220 (21, [M$^{+\bullet}$]), 205 (100, [M$^{+\bullet}$]-[$CH_3^\bullet$]).

Methyl 2-(4-methoxyphenyl)propanoate (**23**-b) and Methyl 3-(4-ethoxyphenyl)propanoate (**23**-l)

194.2 g/mol

23-b   **23**-b

Using dist. 4-vinylanisole (135 μL, 134 mg, 1.00 mmol) as the olefin component and dist. MeOH (250 μL, stored under N_2) as the alcohol component, **GP A** was employed with 0.5 mol% [Pd]. The b/l ratio of the crude product was determined by GC-FID analysis to be 93:7. Purification by flash chromatography on SiO_2 (mobile phase: 95:5 CyH:EtOAc) gave the regioisomeric compounds as a colourless oil (193 mg, 0.97 mmol, 97%, b/l ratio 93:7 by NMR). The analytical data matches with reported literature data.[S18-20]

R_f: 0.31 (mobile phase 9:1 CyH:EtOAc, $KMnO_4$ stain)

Melting point: Ambient temperature.

^{1}H NMR (400 MHz, CDCl$_3$) δ (ppm): 7.25 – 7.20 (m, 2H, Ar<u>H</u>), 6.89 – 6.83 (m, 2H, Ar<u>H</u>), 3.78 (s, 3H, ArOC<u>H</u>$_3$), 3.69 (q, J = 7.2 Hz, 1H, ArC<u>H</u>(CO$_2$Me)Me), 3.65 (s, 3H, ArCH(CO$_2$C<u>H</u>$_3$)Me), 1.48 (d, J = 7.2 Hz, 3H, ArCH(CO$_2$Me)C<u>H</u>$_3$); minor signals for linear regioisomer: 2.90 (t, J = 7.8 Hz, 2H, ArC<u>H</u>$_2$CH$_2$CO$_2$Me), 2.60 (t, J = 7.8 Hz, 2H, ArCH$_2$C<u>H</u>$_2$CO$_2$Me).

^{13}C NMR (101 MHz, CDCl$_3$) δ (ppm): 175.3 (<u>C</u>=O), 158.7 (Ar<u>C</u>), 132.7 (Ar<u>C</u>), 128.5 (Ar<u>C</u>), 114.0 (Ar<u>C</u>), 55.2 (ArO<u>C</u>H$_3$), 51.9 (R-CO$_2$<u>C</u>H$_3$), 44.6 (Ar<u>C</u>H(CO$_2$Me)CH$_3$), 18.7 (ArCH(CO$_2$Me)<u>C</u>H$_3$); minor signals for linear regioisomer: 129.2 (Ar<u>C</u>), 113.9 (Ar<u>C</u>), 55.3 (ArO<u>C</u>H$_3$), 52.0 (RCO$_2$<u>C</u>H$_3$), 36.0 (ArCH$_2$<u>C</u>H$_2$CO$_2$Me), 30.9 (Ar<u>C</u>H$_2$CH$_2$CO$_2$Me).

GC-FID (50-280M12, from crude): t_R = 6.37 min (branched), t_R = 6.61 min (linear).

GC/MS (EI): t_R = 9.46 min (branched), m/z = 194 (18, [MH$^{+•}$]), 135 (100, [MH$^{+•}$]-[CO$_2$Me$^•$]); t_R = 10.14 min (linear), m/z = 194 (18, [MH$^{+•}$]), 121 (100, [MH$^{+•}$]-[CH$_2$CO$_2$Me$^•$]).

Methyl 4-(1-methoxy-1-oxopropan-2-yl)benzoate (**24**-b) and Methyl 4-(3-methoxy-3-oxopropyl)benzoate (**24**-l)

222.2 g/mol

24-b   **24**-l

Using 4-vinylbenzoic acid (148 mg, 1.00 mmol) as the olefin component and dist. MeOH (250 µL, stored under N_2) as the alcohol component, general procedure **A** was employed with 0.5 mol% [Pd]. The b/l ratio of the crude product was determined by GC-FID analysis to be 77:23. Purification by flash chromatography on SiO_2 (mobile phase: 90:10 DCM:MeOH) gave the regioisomeric compounds as a colourless solid paste (44 mg, 0.21 mmol, 21%, b/l ratio 91:9 by NMR). The analytical data matches with reported literature data.[S21, 22]

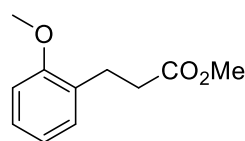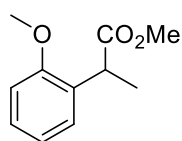R_f: 0.22 (mobile phase 8:2 DCM:MeOH, $KMnO_4$ stain)

^{1}H-NMR (300 MHz, $CDCl_3$) δ (ppm): 7.34 – 7.28 (m, 2H, Ar<u>H</u>), 7.07 – 7.01 (m, 2H, Ar<u>H</u>), 3.73 (q, J = 7.2 Hz, 1H, ArC<u>H</u>(CO$_2$Me)CH$_3$), 3.63 (s, 3H, ArCH(CO$_2$C<u>H$_3$</u>)CH$_3$), 2.29 (s, 3H, ArCO$_2$C<u>H$_3$</u>), 1.49 (d, J = 7.2 Hz, 3H, ArCH(CO$_2$CH$_3$)C<u>H$_3$</u>); minor signals from linear regioisomer: 3.65 (ArCH$_2$CH$_2$CO$_2$C<u>H$_3$</u>), 2.94 (t, J = 7.8 Hz, 2H, ArC<u>H$_2$</u>CH$_2$CO$_2$Me), 2.63 (t, J = 7.8 Hz, 2H, ArCH$_2$C<u>H$_2$</u>CO$_2$Me).

^{13}C-NMR (75 MHz, $CDCl_3$) δ (ppm): 174.8 (C=O), 169.6 (C=O), 149.7 (ArC), 138.0 (ArC), 129.3 (ArC), 128.6 (ArC), 121.7 (ArC), 121.6 (ArC), 52.1 (ArCH(CO$_2$<u>C</u>H$_3$)Me), 44.8 (Ar<u>C</u>H(CO$_2$CH$_3$)CH$_3$), 21.1 (Ar-CO$_2$<u>C</u>H$_3$), 18.6 (ArCH(CO$_2$CH$_3$)<u>C</u>H$_3$); minor signals from linear regioisomer: 51.7 (ArCH(CO$_2$<u>C</u>H$_3$)Me), 35.6 (ArCH$_2$<u>C</u>H$_2$CO$_2$Me), 30.3 (Ar<u>C</u>H$_2$CH$_2$CO$_2$Me).

GC-FID (50-280M12): t_R = 7.45 min (branched), t_R = 7.73 min (linear).

GC/MS (APCI)**:** t_R = 8.35 min (branched), m/z = 240.123 [M+NH$_4$$^+$]; t_R = 8.90 min (linear), m/z = 240.123 [M+NH$_4$$^+$].

HR-MS (APCI)**:** [MH$^+$] m/z = calc. for $C_{12}H_{14}O_4$ 223.0965; found 223.0968.

Methyl 2-(4-chlorophenyl)propanoate (**26**-b) and Methyl 3-(4-chlorophenyl)propanoate (**26**-l)

198.6 g/mol

26-b   **26**-l

Using 4-chlorostyrene (120 µL, 139 mg, 1.00 mmol) as the olefin component and dist. MeOH (250 µL, stored under N_2) as the alcohol component, general procedure **A** was employed using 1.0 mol% [Pd]. The b/l ratio of the crude product was determined by GC-FID analysis to be 92:8. Purification by chromatography on SiO_2 (mobile phase: 95:5 CyH:EtOAc) gave the regioisomeric compounds as a colourless oil (180 mg, 0.90 mmol, 90%, b/l ratio 96:4 by NMR). The analytical data matches with reported literature data.[S18, 23]
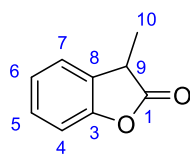
R_f: 0.29 (mobile phase 9:1 CyH:EtOAc, $KMnO_4$ stain) .

Melting point: Ambient temperature.

^{1}H-NMR (400 MHz, $CDCl_3$) δ (ppm): 7.31 – 7.27 (m, 2H, ArH), 7.25 – 7.21 (m, 2 H, ArH), 3.70 (q, J = 7.2 Hz, 1H, ArCH(CO_2Me)CH_3), 3.66 (s, 3H, ArCH(CO_2CH_3)CH_3), 1.48 (d, J = 7.2 Hz, 3H, ArCH(CO_2Me)CH_3); minor signals from linear regioisomer: 2.92 (t, J = 7.7 Hz, 2H, ArCH_2CH_2CO_2Me), 2.61 (t, J = 7.7 Hz, 2H, ArCH_2CH_2CO_2Me).

^{13}C-NMR (101 MHz, $CDCl_3$) δ (ppm): 174.6 (C=O), 138.97 (ArC), 133.0 (ArC), 128.9 (ArC), 128.8 (ArC), 52.1 (ArCH(CO_2CH_3)CH_3), 44.8 ArCH(CO_2Me)CH_3, 18.5 ArCH(CO_2Me)CH_3; minor signals from linear regioisomer: 173.0 (C=O), 132.1 (ArC), 129.7 (ArC), 128.6 (ArC) 51.7 (ArCH_2CH_2CO_2CH_3), 35.5 (ArCH_2CH_2CO_2Me), 30.3 (ArCH_2CH_2CO_2Me).

GC-FID (50-280M12, from crude): t_R = 5.99 min (branched), t_R = 6.31 min (linear).

GC/MS (EI): t_R = 8.73 min (branched), m/z = 198 (21, [MH$^{+•}$]), 139 (100, [MH$^{+•}$]-[CO_2Me$^•$]); t_R = 10.14 min (linear), m/z = 198 (21, [MH$^{+•}$]), 167 (17, [MH$^{+•}$]-[OMe$^•$]), 125 (80, [MH$^{+•}$]-[CH_2CO_2Me$^•$]).

Methyl 2-(4-acetoxyphenyl)propanoate (**27**-b) and Methyl 3-(4-acetoxyphenyl)propanoate (**27**-l)

222.2 g/mol

27-b   **27**-l

Using 4-vinylphenyl acetate (150 µL, 162 mg, 1.00 mmol) as the olefin component and dist. MeOH (stored under N_2) as the alcohol component, general procedure **A** was employed using 1.0 mol% [Pd]. Purification by flash chromatography on SiO_2 (mobile phase: 8:2 CyH:EtOAc) gave the regioisomeric compounds as a yellow oil (93 mg, 0.43 mmol, 43%) and the corresponding deacetylated byproducts (detected by NMR) as a yellow oil. The analytical data of the main product matches with reported literature data.[S24, 25]

R_f: 0.31 (mobile phase 8:2 DCM:MeOH, $KMnO_4$ stain).

^{1}H-NMR (300 MHz, $CDCl_3$) δ (ppm): 7.30 (d, *J* = 8.5 Hz, 2H, Ar$\underline{H}$), 7.02 (d, *J* = 8.6 Hz, 2H, Ar$\underline{H}$), 3.71 (q, *J* = 7.2 Hz, 1H, ArC$\underline{H}$(CO$_2$Me)CH$_3$), 3.63 (s, 3H, ArCH(CO$_2$C$\underline{H_3}$)CH$_3$), 2.26 (s, 3H, Acetyl-C$\underline{H_3}$), 1.47 (d, *J* = 7.2 Hz, 3H, ArCH(CO$_2$CH$_3$)C$\underline{H_3}$); minor signals from linear regioisomer: 2.93 (t, *J* = 7.8 Hz, 2H, ArC$\underline{H_2}$CH$_2$CO$_2$Me), 2.61 (t, *J* = 7.8 Hz, 2H, ArCH$_2$C$\underline{H_2}$CO$_2$Me).

^{13}C-NMR (75 MHz, $CDCl_3$) δ (ppm): 174.8 (methyl ester C=O), 169.5 (acetyl C=O), 149.7 Ar$\underline{C}$), 138.0 (Ar$\underline{C}$), 128.6 (Ar$\underline{C}$), 121.7 (Ar$\underline{C}$), 52.1 (R-CO$_2\underline{C}$H$_3$), 44.8 Ar$\underline{C}$H(CO$_2$Me)CH$_3$, 21.1 (acetyl $\underline{C}$H$_3$), 18.6 (ArCH(CO$_2$Me)$\underline{C}$H$_3$); minor signals from linear regioisomer: 35.6 (ArCH$_2\underline{C}$H$_2$CO$_2$Me), 30.3 (Ar$\underline{C}$H$_2$CH$_2$CO$_2$Me).

GC-FID (50-280M12, from crude): t_R = 6.80 min (branched), t_R = 7.10 min (linear).

GC/MS (EI): Main product - t_R = 10.82 min (branched), m/z = 222 (8, [MH$^{+•}$]), 180 (38, [MH$^{+•}$]-[CH$_2$CO]), 121 (100, [MH$^{+•}$]-[CH$_2$CO]-[CO$_2$Me$^•$]); t_R = 11.84 min (linear), m/z = 222 (8, [MH$^{+•}$]), 180 (65, [MH$^{+•}$]-[CH$_2$CO]), 107 (100, [MH$^{+•}$]-[CH$_2$CO]-[CH$_2$CO$_2$Me$^•$]). Deacetylated product - t_R = 10.01 min (branched), m/z = 180 (30, [MH$^{+•}$]), 121 (100, [MH$^{+•}$]-[CO$_2$Me$^•$]); t_R = 10.80 min (linear), m/z = 180 (30, [MH$^{+•}$]), 107 (100, [MH$^{+•}$]-[CH$_2$CO$_2$Me$^•$]).

Methyl 2-(4-hydroxyphenyl)propanoate (**28**-b) and Methyl 3-(4-hydroxyphenyl)propanoate (**28**-l)

180.2 g/mol

28-b   **28**-l

Using 4-vinylphenyl acetate (150 µL, 162 mg, 1.00 mmol) as the olefin component and dist. MeOH (250 µL, stored under N_2) as the alcohol component, general procedure **A** was employed using 1.0 mol% [Pd] at 50 °C. Purification by flash chromatography on SiO_2 (mobile phase: 8:2 CyH:EtOAc) gave the regioisomeric deacetylated compounds as a yellow oil (125 mg, 0.69 mmol, 69%) and the corresponding acetylated byproducts (27 mg, 0.12 mmol, 12%) as a yellow oil. The analytical data of the main product matches with reported literature data.[S24, 25]

R_f: 0.20 (mobile phase 8:2 DCM:MeOH, KMnO₄ stain).

1H-NMR (300 MHz, CDCl₃) δ (ppm): 7.30 (d, J = 8.5 Hz, 2H, Ar<u>H</u>), 7.02 (d, J = 8.6 Hz, 2H, Ar<u>H</u>), 3.71 (q, J = 7.2 Hz, 1H, ArC<u>H</u>(CO₂Me)CH₃), 3.63 (s, 3H, ArCH(CO₂C<u>H₃</u>)CH₃), 1.47 (d, J = 7.2 Hz, 3H, ArCH(CO₂CH₃)C<u>H₃</u>); minor signals from linear regioisomer: 2.93 (t, J = 7.8 Hz, 2H, ArC<u>H₂</u>CH₂CO₂Me), 2.61 (t, J = 7.8 Hz, 2H, ArCH₂C<u>H₂</u>CO₂Me).

13C-NMR (75 MHz, CDCl₃) δ (ppm): 174.8 (methyl ester <u>C</u>=O), 151.7 (Ar<u>C</u>), 138.0 (Ar<u>C</u>), 128.6 (Ar<u>C</u>), 121.7 (Ar<u>C</u>), 52.1 (R-CO₂<u>C</u>H₃), 44.8 Ar<u>C</u>H(CO₂Me)CH₃, 18.6 ArCH(CO₂Me)<u>C</u>H₃; minor signals from linear regioisomer: 35.6 (ArCH₂<u>C</u>H₂CO₂Me), 30.3 (Ar<u>C</u>H₂CH₂CO₂Me).

GC/MS (EI): t_R = 10.01 min (branched), m/z = 180 (30, [MH⁺•]), 121 (100, [MH⁺•]-[CO₂Me•]); t_R = 10.80 min (linear), m/z = 180 (30, [MH⁺•]), 107 (100, [MH⁺•]-[CH₂CO₂Me•]).

Methyl 2-(2-methoxyphenyl)propanoate (**29**-b) and Methyl 3-(2-methoxyphenyl)propanoate (**29**-l)

194.3 g/mol

29-b   **29**-l

Using 2-vinylanisole (135 µL, 134 mg, 1.00 mmol) as the olefin component and dist. MeOH (250 µL, stored under N_2) as the alcohol component, general procedure **A** was employed using 0.5 mol% [Pd]. The b/l ratio of the crude product was determined by GC-FID analysis to be 46:54. Purification by flash chromatography on SiO_2 (mobile phase: 95:5 CyH:EtOAc) gave the regioisomeric compounds as a colourless oil (126 mg, 0.66 mmol, 66%, b/l ratio 46:54 by NMR). The analytical data for the branched product matches with reported literature data.[S26]

R_f: 0.22 (mobile phase 95:5 CyH:EtOAc, $KMnO_4$ stain)

Melting point: Ambient temperature.

^{1}H-NMR (400 MHz, CDCl$_3$) δ (ppm): 7.29 – 7.11 (m, 2H, Ar$\underline{H}$), 6.99 – 6.82 (m, 2H, Ar$\underline{H}$), 4.08 (q, J = 7.2 Hz, 1H, ArC$\underline{H}$(CO$_2$Me)CH$_3$), 3.83 (s, 3H, R-CO$_2$C$\underline{H}_3$) 3.67 (s, 3H, ArOC$\underline{H}_3$), 1.48 (d, J = 7.2 Hz, 3H, ArCH(CO$_2$Me)C$\underline{H}_3$); signals from linear regioisomer: 3.68 (s, 3H, ArOC$\underline{H}_3$), 2.97 (t, J = 7.8 Hz, 2H, ArC$\underline{H}_2$CH$_2$CO$_2$Me), 2.64 (t, J = 7.8 Hz, 2H, ArCH$_2$C$\underline{H}_2$CO$_2$Me).

^{13}C-NMR (101 MHz, CDCl$_3$) δ (ppm): 174.5 ($\underline{C}$=O), 155.6 (Ar$\underline{C}$), 128.9 (Ar$\underline{C}$), 128.5 (Ar$\underline{C}$), 127.1 (Ar$\underline{C}$), 119.7 (Ar$\underline{C}$), 109.7 (Ar$\underline{C}$), 54.4 (ArO$\underline{C}$H$_3$), 50.8 (R-CO$_2$$\underline{C}H_3$), 38.1 (Ar$\underline{C}$H(CO$_2CH_3$)CH$_3$), 16.3 (ArCH(CO$_2$Me)$\underline{C}H_3$); signals from linear regioisomer: 172.2 ($\underline{C}$=O), 156.4 (Ar$\underline{C}$), 127.8 (Ar$\underline{C}$), 126.9 (Ar$\underline{C}$), 126.6 (Ar$\underline{C}$), 119.4 (Ar$\underline{C}$), 109.2 (Ar$\underline{C}$), 54.1 (ArO$\underline{C}$H$_3$), 50.4 (R-CO$_2$$\underline{C}H_3$), 33.0 (ArCH$_2$$\underline{C}H_2CO_2$Me), 25.1 (Ar$\underline{C}H_2CH_2CO_2$Me).

GC-FID (50-280M12, from crude): t_R = 5.92 min (branched), t_R = 6.27 min (linear).

GC/MS (EI): t_R = 8.88 min (branched), m/z = 194 (28, [M$^{+\bullet}$]), 135 (100, [M$^{+\bullet}$]-[$^\bullet$CO$_2$Me]); t_R = 9.67 min (linear), m/z = 194 (56, [M$^{+\bullet}$]), 163 (16, [M$^{+\bullet}$]-[OMe$^\bullet$]), 121 (100, [M$^{+\bullet}$]-[CH$_2$CO$_2$Me$^\bullet$]).

Methyl 2-(2-acetoxyphenyl)propanoate (**30**-b) and Methyl 3-(2-acetoxyphenyl)propanoate (**30**-l)

222.2 g/mol

30-b   **30**-l

Using 2-acetoxystyrene (117 mg, 720 µmol) as the olefin component and dist. MeOH (250 µL, stored under N_2) as the alcohol component, **GP A** was employed using 0.75 mol% [Pd]. The b/l ratio of the crude product was determined by GC-FID analysis to be 39:61. Purification by flash chromatography on SiO_2 (mobile phase: 80:20 CyH:EtOAc) gave the regioisomeric compounds as a bright yellow oil (94 mg, 0.42 mmol, 59 %, b/l ratio 36/64 by NMR).

R$_f$: 0.32 (mobile phase 80:20 CyH:EtOAc, $KMnO_4$ stain)

Melting point: Ambient temperature.

FT-IR (ATR) ṽ (cm^{-1}): 3062 (w, sh), 2990 (w, sh), 2953 (w, sh), 1806 (w, sh), 1763 (s, br), 1734 (s, br), 1585 (w, br), 1490 (m, sh), 1453 (m, sh), 1436 (m, sh), 1370 (m, sh), 1200 (s, br), 1170 (s, br), 1099 (m, sh), 1068 (w, sh), 1041 (m, sh), 1011 (m, sh), 913 (m, sh).

^{1}H-NMR (400 MHz, CDCl$_3$) δ (ppm): 7.37 – 7.27 (m, 1H, Ar<u>H</u>), 7.25 – 7.15 (m, 2H, Ar<u>H</u>), 7.09 – 7.01 (m, 1H, Ar<u>H</u>), 3.84 (q, *J* = 7.2 Hz, 1H, ArC<u>H</u>(CO₂Me)Me), 3.64 (s, 3H, ArCH(COOC<u>H₃</u>)Me), 2.31 (s, 3H, ArOCOC<u>H₃</u>), 1.47 (d, *J* = 7.2 Hz, 3H, ArCH(CO₂Me)C<u>H₃</u>); signals from linear regioisomer: 3.67 (s, 3H, ArCH₂CH₂CO₂C<u>H₃</u>), 2.89 – 2.84 (m, 2H, ArC<u>H₂</u>CH₂CO₂Me), 2.62 – 2.56 (m, 2H, ArCH₂C<u>H₂</u>CO₂Me), 2.34 (s, 3H, ArOCOC<u>H₃</u>).

^{13}C-NMR (101 MHz, CDCl$_3$) δ (ppm): 174.5 (methyl ester <u>C</u>=O), 169.3 (acetate C=O), 148.3 (Ar<u>C</u>), 132.3 (Ar<u>C</u>), 128.7 (Ar<u>C</u>), 128.1 (Ar<u>C</u>), 126.4 (Ar<u>C</u>), 122.8 (Ar<u>C</u>), 52.1 (ArCH(CO₂<u>C</u>H₃)Me), 39.9 (Ar<u>C</u>H(CO₂Me)Me), 20.8 (ArOCO<u>C</u>H₃), 17.2 (ArCH(CO₂Me)<u>C</u>H₃); signals from linear regioisomer: 173.3 (methyl ester C=O), 169.6 (acetate C=O), 149.0 (Ar<u>C</u>), 132.6 (Ar<u>C</u>), 130.1 (Ar<u>C</u>), 127.6 (Ar<u>C</u>), 126.3 (Ar<u>C</u>), 122.5 (Ar<u>C</u>), 51.7 (ArCH₂CH₂CO₂<u>C</u>H₃), 34.2 (ArCH₂<u>C</u>H₂CO₂CH₃), 25.5 (Ar<u>C</u>H₂CH₂CO₂CH₃), 20.9 (ArOCO<u>C</u>H₃).

GC-FID (50-280M12): t_R = 6.44 min (branched), t_R = 6.84 min (linear).

GC-MS: t_R = 7.54 min (branched), m/z = 223 (100, [MH$^+$]), 163 (20, [MH$^+$]-[$^\bullet$CO$_2$Me]), 149 (31, [MH$^+$]-[CO$_2$Me$^\bullet$]-[CH$_3$$^\bullet$]); t_R = 8.20 min (branched), m/z = 223 (100, [MH$^+$]), 163 (14, [MH$^+$]-[$^\bullet$CO$_2$Me]), 149 (64, [MH$^+$]-[CH$_2$CO$_2$Me$^\bullet$].

HR-MS (APCI): m/z = [MH$^+$] calc. for C$_{12}$H$_{14}$O$_4$ 223.0965, found 233.0967

Methyl 2-(*o*-tolyl)propanoate (**31**-b) and Methyl 2-(*o*-tolyl)propanoate (**31**-l)

178.2 g/mol

5na-b   **5na**-l

Using 2-methylstyrene (130 µL, 118 mg, 1.00 mmol) as the olefin component and dist. MeOH (250 µL, stored under N$_2$) as the alcohol component, **GP A** was employed using 0.5 mol% [Pd]. The b/l ratio of the crude product was determined by GC-FID analysis to be 50:50. Purification by flash chromatography on SiO$_2$ (mobile phase: 95:5 CyH:EtOAc) gave the regioisomeric compounds as a colourless oil (50 mg, 0.28 mmol, 28%, b/l ratio 20:80 by NMR). The analytical data matches with reported literature data.[S26, 27]

R_f: 0.28 (mobile phase 95:5 CyH:EtOAc, KMnO$_4$ stain)

Melting point: Ambient temperature.

^{1}H-NMR (400 MHz, CDCl$_3$) δ (ppm): 7.23 – 7.06 (m, 4H, Ar<u>H</u>), 3.96 (q, *J* = 7.1 Hz, 1H, ArC<u>H</u>(CO$_2$Me)Me), 3.66 (s, 3H, ArCH(CO$_2$C<u>H</u>$_3$)Me), 2.37 (s, 3H, ArC<u>H</u>$_3$), 1.48 (d, *J* = 7.1 Hz, 3H, ArCH(CO$_2$Me)C<u>H</u>$_3$); signals from linear regioisomer: 3.69 (s, 3H, ArCH$_2$CH$_2$CO$_2$C<u>H</u>$_3$), 2.95 (t, *J* = 8.1 Hz, 2H, ArC<u>H</u>$_2$CH$_2$CO$_2$Me), 2.60 (t, *J* = 8.1 Hz, 2H, ArCH$_2$C<u>H</u>$_2$CO$_2$Me), 2.33 (s, 3H, ArC<u>H</u>$_3$).

^{13}C-NMR (101 MHz, CDCl$_3$) δ (ppm): 175.3 (<u>C</u>=O), 139.2 (Ar<u>C</u>), 135.7 (Ar<u>C</u>), 130.5 (Ar<u>C</u>), 129.0 (Ar<u>C</u>), 127.0 (Ar<u>C</u>), 126.5 (Ar<u>C</u>), 52.0 (ArCH(CO$_2$<u>C</u>H$_3$)Me), 41.3 (Ar<u>C</u>H(CO$_2$CH$_3$)Me), 19.6 (Ar<u>C</u>H$_3$), 18.0 (ArCH(CO$_2$CH$_3$)<u>C</u>H$_3$); signals from linear regioisomer: 173.5 (<u>C</u>=O), 138.6 (Ar<u>C</u>), 136.0 (Ar<u>C</u>), 130.3 (Ar<u>C</u>), 128.5 (Ar<u>C</u>), 126.2 (Ar<u>C</u>), 51.7 (RCO$_2$<u>C</u>H$_3$), 34.4 (Ar<u>C</u>H$_2$CH$_2$CO$_2$Me), 28.4 (ArCH$_2$<u>C</u>H$_2$CO$_2$Me), 19.2 (Ar<u>C</u>H$_3$).

GC-FID (50-280M12): t_R = 4.58 min (branched), t_R = 4.81 min (linear).

GC/MS (EI): t_R = 7.68 min (branched), m/z = 178 (18, [M$^{+\bullet}$]), 119 (100, [M$^{+\bullet}$]-[CO$_2$Me$^\bullet$]); t_R = 8.56 min (linear), m/z = 178 (18, [M$^{+\bullet}$]), 105 (100, [M$^{+\bullet}$]-[CH$_2$CO$_2$Me$^\bullet$]).

3-Methylbenzofuran-2(3*H*)-one (**33**)

148.2 g/mol

33

Using freshly purified (column chromatography) 2-vinylphenol (115 µL, 120 mg, 1.00 mmol; storage at 6 °C) as the olefin component and dist. MeOH (50 µL; stored under N_2) as the alcohol component to dissolve the organophosphoric acid, general procedure **A** was employed using 0.5 mol% [Pd]. Purification by flash chromatography on SiO_2 (mobile phase: 95:5 CyH:EtOAc) gave the compound as a colourless oil (25 mg, 0.16 mmol, 16%). The analytical data matches with the reported literature data.[S28]

R_f: 0.36 (mobile phase 8:2 CyH:EtOAc, $KMnO_4$ stain)

Melting point: Ambient temperature.

^{1}H NMR (400 MHz, $CDCl_3$) δ (ppm): 7.35 – 7.23 (m, 2H, Ar<u>H</u>), 7.18 – 7.08 (m, 2H, Ar<u>H</u>), 3.73 (q, *J* = 7.6 Hz, 1H, C^9-<u>H</u>), 1.58 (d, *J* = 7.6 Hz, 3H, C<u>H$_3$</u>).

^{13}C NMR (101 MHz, $CDCl_3$) δ (ppm): 178.0 (<u>C</u>=O), 153.5 (Ar<u>C</u>) , 131.7 (Ar<u>C</u>), 128.8 (Ar<u>C</u>), 124.2 (Ar<u>C</u>), 123.9 (Ar<u>C</u>), 110.8 (Ar<u>C</u>), 38.4 (<u>C</u>^{9}), 15.9 (<u>C</u>^{10}).

GC/MS (EI): t_R = 7.11, m/z = 148 (100, [MH$^{+\bullet}$]), 120 (78, [MH$^{+\bullet}$]-[CO]), 91 (80, [$C_7H_7^+$]).

Dimethyl 2-methylsuccinate (**35**)

160.2 g/mol

35

Using methyl methacrylate (**34**) (105 μL, 100 mg, 1.00 mmol) as the alkene component and dist. MeOH (250 μL; stored under N_2) as the alcohol component, **GP A** was employed using 0.5 mol% [Pd]. Purification by flash column chromatography on SiO_2 (mobile phase: 9:1 CyH:EtOAc) gave the compound as a colourless liquid (74 mg, 0.46 mmol, 46%). The analytical data matches with the reported literature data.[S29]

R_f: 0.30 (mobile phase 9:1 CyH:EtOAc, $KMnO_4$ stain)

Melting point: Ambient temperature.

^{1}H NMR (400 MHz, $CDCl_3$) δ (ppm): 3.63 (s, 3H, $RC^1O_2C\underline{H}_3$), 3.61 (s, 3H, $R\text{-}C^4O_2C\underline{H}_3$), 2.94 – 2.78 (m, 1H, $\text{-}C^2\underline{H}(C^{2'}H_3)\text{-}$), 2.67 (m, 1H, diastereotopic $\text{-}C^3\underline{H}_2C^4O_2CH_3\text{-}$), 2.34 (m, 1H, diastereotopic $\text{-}C^3\underline{H}_2C^4O_2CH_3\text{-}$), 1.15 (d, J = 7.2 Hz, 3H, $\text{-}C^2H\text{-}C^{2'}\underline{H}_3$).

^{13}C NMR (101 MHz, $CDCl_3$) δ (ppm): 175.6 ($\underline{C}^1$), 172.2 ($\underline{C}^4$), 51.9 ($\underline{C}^1\text{-}OCH_3$), 51.6 ($\underline{C}^4\text{-}O\underline{C}H_3$), 37.4 ($\underline{C}^3$), 35.7 ($\underline{C}^2$), 16.9 ($C^2\text{-}\underline{C}H_3$).

GC/MS (EI): t_R = 4.78 min, m/z = 129 (50, $[M^{+\bullet}]\text{-}[OMe^\bullet]$), 128 (36, $[M^{+\bullet}]\text{-}[HOMe]$), 59 (100, $[CO_2Me^+]$).

<u>4-Benzyl 1-methyl 2-methylsuccinate (**35-Bn**)</u>

236.27 g/mol

35-Bn

Using methyl methacrylate (**11**) (155 µL, 146.0 mg, 1.5 mmol) as the alkene component and degassed BnOH (250 µL; stored under N_2) as the alcohol component, general procedure **A** was employed using 0.75 mol% [Pd]. Purification by flash column chromatography on SiO_2 (mobile phase: 95:5 CyH:EtOAc) gave the compound as a colourless liquid (176 mg, 0.75 mmol, 51%).

R_f: 0.10 (mobile phase 95:5 CyH:EtOAc, $KMnO_4$ stain)

Melting point: Ambient temperature.

^{1}H-NMR (400 MHz, CDCl$_3$) δ $_{(ppm)}$: 7.44 – 7.29 (m, 5H, Ar$\underline{H}$), 5.12 (ABq, Δδ$_{AB}$ = 0.02, J = 12.3 Hz, 2H, C$\underline{H_2}$Ph), 3.65 (s, 3H, RC^{1}O$_2$C$\underline{H_3}$), 2.95 (sext, J = 7.2 Hz, 1H, -C$^2\underline{H}$(C$^{2'}$H$_3$)-), 2.80 (m, 1H, diastereotopic C$^3\underline{H_2}$C^{4}O$_2$Bn-), 2.46 (m, 1H, diastereotopic C$^3\underline{H_2}$C^{4}O$_2$Bn-), 1.22 (d, J = 7.2 Hz, 3H, -C^{2}H-C$^{2'}\underline{H_3}$).

^{13}C-NMR (101 MHz, CDCl$_3$) δ (ppm): 175.7 ($\underline{C}^1$), 171.6 ($\underline{C}^4$), 135.8 (Ar$\underline{C}$), 128.6 (Ar$\underline{C}$), 128.3 (Ar$\underline{C}$), 128.3 (Ar$\underline{C}$), 66.5 (Ar$\underline{C}$H$_2$), 51.9 (C^1-O$\underline{C}$H$_3$), 37.7 ($\underline{C}^3$), 35.8 ($\underline{C}^2$), 17.0 (C^2-$\underline{C}$H$_3$).

FT-IR (ATR) v (cm^{-1}): 2953 (w, br), 1731 (s, sh), 1456 (m, sh), 1381 (m, sh), 1346 (m, sh), 1273 (m, br), 1159 (s, sh), 1057 (m, sh), 990 (m, br).

GC-MS: t_R = 8.98 min, m/z = 237 (77, [MH$^+$]), 129 (29, [MH$^+$]-[BnO$^•$]), 91 (100, [MH$^+$]-[C$_7$H$_7^•$]).

HR-MS (APCI): m/z = [MH$^+$] calc. for C$_{13}$H$_{16}$O$_4$ 237.1121, found 237.1126.

Benzyl 2-acetoxypropanoate (**37**)

222.4 g/mol

37

Using vinyl acetate (**36**) (90 μL, 86 mg, 1.00 mmol) as the alkene component and BnOH (250 μL) as the alcohol component, **GP A** was employed using either with 0.5 or 1.0 mol% [Pd]. Purification by flash column chromatography on SiO_2 (mobile phase: 95:5 CyH:EtOAc) gave the compound as a colourless liquid (69 mg, 0.32 mmol, 32% with 0.5 mol% [Pd] and 93 mg, 0.43 mmol, 43% with 1.0 mol% [Pd]). The analytical data matched the data reported in the literature.[S27]

R_f: 0.10 (mobile phase 95:5 CyH:EtOAc, $KMnO_4$ stain)

Melting point: Ambient temperature.

^{1}H NMR (400 MHz, $CDCl_3$) δ (ppm): 7.57 − 7.17 (m, 5H, Ar$\underline{H}$), 5.18 (ABq, $Δδ_{AB}$ = 0.03, J = 12.3 Hz, 2H, C$\underline{H_2}$Ph), 5.13 (q, J = 7.1 Hz, 1H, -C^{2}H-), 2.12 (s, 3H, Acetyl-C$\underline{H_3}$), 1.49 (d, J = 7.1 Hz, 3H,-C$^3\underline{H_3}$).

^{13}C NMR (101 MHz, $CDCl_3$) δ (ppm): 170.7 ($\underline{C}^1$), 170.4 (Acetyl $\underline{C}$=O), 135.4 (Ar$\underline{C}$), 128.6 (Ar$\underline{C}$), 128.4 (Ar$\underline{C}$), 128.1 (Ar$\underline{C}$), 68.6 ($\underline{C}^2$), 66.7 ($\underline{C}H_2$Ph), 20.7 (Acetyl-$\underline{C}H_3$), 16.0 ($\underline{C}^3$).

GC/MS (EI): t_R = 10.16 min, m/z = 162 (30, [M$^{+•}$]-[AcOH]), 91 (80, [$C_7H_7^+$]), 43 (100, [AcO$^+$]).

Methyl 2-Phenylbutanoate (**39**-b) and Methyl 4-Phenylbutanoate (**39**-l)

178.2 g/mol

39-b   **39**-l

Using β-methylstyrene (100 μL, 89 mg, 0.750 mmol) as the alkene component and dist. MeOH (250 μL; stored under N_2) as the alcohol component, general procedure **A** was employed using 1.0 mol% [Pd]. Purification by flash column chromatography on SiO_2 (mobile phase: 9:1 CyH:EtOAc) gave the regioisomeric compounds as a colourless oil with a pleasant smell (48 mg, 29.3 mmol, 39%, b/l ratio 53:47 by NMR^1). The analytical data matched the reported literature data.[S31-33]

R_f (linear isomer): 0.33 (mobile phase 9:1 CyH:EtOAc, $KMnO_4$ stain).

R_f (C^2-branched isomer): 0.42 (mobile phase 9:1 CyH:EtOAc, $KMnO_4$ stain).

Melting point: Ambient temperature.

^{1}H NMR (400 MHz, $CDCl_3$) δ (ppm): signals from linear isomer: 7.44 – 7.09 (m, 5H, Ar$\underline{H}$), 3.67 (s, 3H, R-$CO_2C\underline{H_3}$), 2.71 – 2.59 (m, 2H, ArCH$_2$CH$_2$C$\underline{H_2}$CO$_2$CH$_3$), 2.34 (t, J = 7.5 Hz, 2H, ArC$\underline{H_2}$CH$_2$CH$_2$CO$_2$CH$_3$), 2.02 – 1.88 (m, 2H, ArCH$_2$C$\underline{H_2}$CH$_2$CO$_2$CH$_3$); signals from C2-branched isomer: 3.47 (t, J = 7.7 Hz, 1H, ArC$\underline{H}$(CO$_2$Me)CH$_2$CH$_3$), 2.18 – 2.05 (m, 1H, diastereotopic ArCH(CO$_2$Me)C$\underline{H_2}$CH$_3$), 1.81 (m, 1H, diastereotopic ArCH(CO$_2$Me)C$\underline{H_2}$CH$_3$), 0.90 (t, J = 7.4 Hz, 3H, ArCH(CO$_2$Me)CH$_2$C$\underline{H_3}$).

^{13}C NMR (101 MHz, $CDCl_3$) δ (ppm): 174.0 ($\underline{C}$=O), 141.4 (Ar$\underline{C}$), 128.5 (Ar$\underline{C}$), 128.4 (Ar$\underline{C}$), 126.0 (Ar$\underline{C}$), 51.6 (R-CO$_2\underline{C}$H$_3$), 35.1 (ArCH$_2$CH$_2\underline{C}$H$_2$CO$_2$CH$_3$), 33.4 (Ar$\underline{C}$H$_2$CH$_2$CH$_2$CO$_2$CH$_3$), 26.5 (ArCH$_2\underline{C}$H$_2$CH$_2$CO$_2$CH$_3$); signals from C2-branched isomer: 174.6 ($\underline{C}$=O), 139.1 (Ar$\underline{C}$), 128.6 (Ar$\underline{C}$), 128.0 (Ar$\underline{C}$), 127.2 (Ar$\underline{C}$), 53.4 (R-CO$_2\underline{C}$H$_3$), 51.9 (Ar$\underline{C}$H(CO$_2$Me)CH$_2$CH$_3$), 26.5 (ArCH(CO$_2$Me)$\underline{C}$H$_2$CH$_3$), 12.2 (ArCH(CO$_2$Me)CH$_2\underline{C}$H$_3$)

GC/MS (EI): t_R = 7.41 min (C2-branched), m/z = 178 (20, [M$^{+•}$]), 163 (2, [M$^{+•}$]-[Me$^•$]), 150 (8, [M$^{+•}$]-[CO]-[OMe$^•$]); t_R = 8.58 min (linear), m/z = 178 (40, [M$^{+•}$]), 147 (40, [M$^{+•}$] -[OMe$^•$]), 146 (40, [M$^{+•}$]-[MeOH]).

---

^{1} The shown NMR spectra are not representative of the calculated regioselectivity by NMR due to differences in the regioisomeric composition of isolated product fractions.

Methyl 2-Phenylbutanoate (**39**-b) and Methyl 4-Phenylbutanoate (**39**-l) (from Allylbenzene)

178.2 g/mol

39-b   **39**-l

Using allylbenzene (130 µL, 118 mg, 0.750 mmol) as the alkene component and dist. MeOH (250 µL; stored under N$_2$) as the alcohol component, **GP A** was employed using 0.5 mol% [Pd]. Purification by flash column chromatography on SiO$_2$ (mobile phase: 95:5 CyH:EtOAc) gave the regioisomeric compounds as a colourless oil (41 mg, 29 mmol, 29%, b/l ratio 56:44 by NMR).

Analytical data as above.

Methyl 2-(1,3-dioxoisoindolin-2-yl)propanoate (**43**-b) and Methyl 2-(1,3-dioxoisoindolin-2-yl)propanoate (**43**-l)

233.2 g/mol

43-b   **43**-l

Using *N*-vinylphthalimide (**42**) (173 mg, 1.00 mmol) as the alkene component and dist. MeOH (250 µL; stored under N_2) as the alcohol component, **GP A** was employed using 0.5 or 1.0 mol% [Pd]. The b/l ratio of the crude product was determined by GC-FID analysis to be 44:56 (with both [Pd] loadings). Purification by flash column chromatography on SiO_2 (mobile phase: 9:1 CyH:EtOAc) gave the regioisomeric compounds as a brown solid (109 mg, 0.47 mmol, 47%, b/l ratio 85:15 by NMR with 0.5 mol% [Pd] and 192 mg, 0.82 mmol, 82%, b/l 45:55 by NMR with 1.0 mol% [Pd]). The analytical data matches with the reported literature data.[S34, 35]

*R*f: 0.39 (mobile phase 9:1 CyH:EtOAc, $KMnO_4$ stain)

Melting point: 60 °C.

^{1}H NMR (400 MHz, $CDCl_3$) δ (ppm): linear isomer: 7.80 – 7.72 (m, 2H, Ar<u>H</u>), 7.69 – 7.61 (m, 2H, <u>ArH</u>), 3.91 (t, *J* = 7.2 Hz, 2H, NC<u>H</u>$_2$CH$_2$CO$_2$CH$_3$), 3.60 (s, 3H, NCH$_2$CH$_2$CO$_2$C<u>H</u>$_3$), 2.65 (t, *J* = 7.2 Hz, 2H, NCH$_2$C<u>H</u>$_2$CO$_2$CH$_3$); minor signals from branched regioisomer: 4.97 (q, *J* = 7.3 Hz, 1H, NC<u>H</u>(CO$_2$Me)CH$_3$), 3.74 (s, 3H, NCH(CO$_2$C<u>H</u>$_3$)CH$_3$), 1.69 (d, *J* = 7.3 Hz, 3H, NCH(CO$_2$CH$_3$)C<u>H</u>$_3$).

^{13}C NMR (101 MHz, $CDCl_3$) δ (ppm): 171.2 (Ester <u>C</u>=O), 167.9 (Imide <u>C</u>=O), 134.0 (Ar<u>C</u>), 132.0 (Ar<u>C</u>), 123.3 (Ar<u>C</u>), 51.9 (NCH$_2$CH$_2$CO$_2$<u>C</u>H$_3$), 33.7 (N<u>C</u>H$_2$CH$_2$CO$_2$CH$_3$), 32.7 (NCH$_2$<u>C</u>H$_2$CO$_2$CH$_3$); minor signals from branched regioisomer: 170.2 (Ester <u>C</u>=O), 167.4 (Imide <u>C</u>=O), 134.2 (Ar<u>C</u>), 132.0 (Ar<u>C</u>), 123.5 (Ar<u>C</u>), 52.8 (NCH(CO$_2$<u>C</u>H$_3$)CH$_3$), 47.4 (NCH(CO$_2$CH$_3$)<u>C</u>H$_3$), 15.3 (NCH(CO$_2$CH$_3$)<u>C</u>H$_3$).

GC-FID (50-280M12, from crude): *t*$_R$ = 7.77 min (branched), *t*$_R$ = 8.12 (linear).

GC/MS (EI): *t*$_R$ = 12.56 min (branched), m/z = 233 (2, [M$^{+•}$]), 202 (1, [M$^{+•}$]-[OMe$^•$]), 174 (100, [M$^{+•}$]-[OMe$^•$]-[CO]), *t*$_R$ = 13.45 min (linear), m/z = 233 (15, [M$^{+•}$]), 202 (8, [M$^{+•}$]-[OMe$^•$]), 173 (100, [M$^{+•}$]-[OMe$^•$]-[CO]), 160 (100, [PhthalN$^+$=CH$_2$]).

Methyl 3-Phenylbutanoate (**45**) (from α-Methylstyrene)

178.2 g/mol

45

Using α-methylstyrene (100 µL, 0.75 mmol [0.75 mol% [Pd]] or 130 µL, 1 mmol [1.0 mol% [Pd]]) as the alkene component and dist. MeOH (250 µL; stored under N_2) as the alcohol component, **GP A** was employed at RT or 50 °C (in DCE), respectively. Purification by flash column chromatography on SiO_2 (mobile phase: 9:1 CyH:EtOAc) gave the compound as a colourless liquid (36 mg, 0.20 mmol, 20% with 0.75 mol% [Pd] and 60 mg, 0.34 mmol, 34% with 1.0 mol% [Pd]). The analytical data matched the data reported in the literature.[S36]

R$_f$: 0.48 (mobile phase 9:1 CyH:EtOAc, $KMnO_4$ stain)

Melting point: Ambient temperature.

1H NMR (400 MHz, $CDCl_3$) δ (ppm): 7.37 – 7.16 (m, 5H, Ar$\underline{H}$), 3.63 (s, 3H, R-CO$_2$C$\underline{H_3}$), 3.34 – 3.24 (m, 1H, ArC$\underline{H}$(Me)CH$_2$CO$_2$Me), 2.60 (m, 2H, ArCH(Me)C$\underline{H_2}$CO$_2$Me), 1.31 (d, *J* = 7.0 Hz, 3H, ArCH(C$\underline{H_3}$)CH$_2$CO$_2$Me).

13C NMR (101 MHz, $CDCl_3$) δ (ppm): 172.9 (ArCH(Me)CH$_2$$\underline{C}O_2$Me), 145.7 (Ar$\underline{C}$), 128.5 (Ar$\underline{C}$), 126.7 (Ar$\underline{C}$), 126.4 (Ar$\underline{C}$), 51.5 (ArCH(Me)CH$_2CO_2$$\underline{C}H_3$), 42.8 (ArCH(Me)$\underline{C}H_2CO_2$Me), 36.5 (Ar$\underline{C}$H(Me)CH$_2CO_2$Me), 21.8 (ArCH($\underline{C}H_3$)CH$_2CO_2$Me).

GC/MS (EI): *t*$_R$ = 7.80 min, m/z = 178 (20, [M$^{+\bullet}$]), 147 (5, [M$^{+\bullet}$]-[OMe$^{\bullet}$]), 105 (100, [C$_8$H$_9$$^+$]).
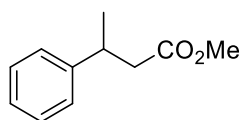
Methyl nonanoate (**47**) (from 1-octene **46**)
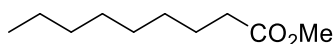
172.3 g/mol

47

Using 1-octene (160 µL, 114 mg, 1.00 mmol) as the alkene component and dist. MeOH (250 µL; stored under N_2) as the alcohol component, **GP A** was employed using 0.5 mol% [Pd]. Purification by flash column chromatography on SiO_2 (mobile phase: 95:5 CyH:EtOAc) gave the compound as a colourless liquid (91 mg, 0.53 mmol, 53%). The analytical data matches with the reported literature data.[S37]

R_f : 0.50 (mobile phase 9:1 CyH:EtOAc, $KMnO_4$ stain)

Melting point: Ambient temperature.

^{1}H NMR (300 MHz, $CDCl_3$) δ (ppm): 3.59 (s, 3H, RCO_2CH_3), 2.23 (t, J = 7.5 Hz, 2H, RCH_2-CO_2Me), 1.55 (sext, J = 7.5 Hz, 2H, R-CH_2-CH_2-CO_2Me), 1.20 (s br, 10H, Alkane-CH_2), 0.87 − 0.75 (t, J = 6 Hz, 3H, terminal CH_3).

^{13}C NMR (75 MHz, $CDCl_3$) δ (ppm): 174.3 (C1), 51.4 (R-CO_2CH_3), 34.1 (C2), 31.8 (C3), 29.2 (C4), 29.2 (C5), 29.1 (C6), 25.0 (C7), 22.6 (C8), 14.1 (C9).

GC/MS (EI): t_R = 6.70 min, m/z = 172 (2, $[M^{+\bullet}]$).

Methyl nonanoate (**47**) (from 2-octene **18**)
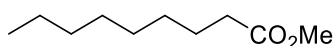
172.3 g/mol

47

Using 2-octene (155 µL, 111 mg, 1.00 mmol) as the alkene component and dist. MeOH (250 µL; stored under N_2) as the alcohol component, general procedure **A** was employed using 0.5 mol% [Pd]. Purification by flash column chromatography on SiO_2 (mobile phase: 95:5 CyH:EtOAc) gave the compound as a colourless liquid (67 mg, 0.39 mmol, 39%).

Analytical data as above.

Benzyl nonanoate (**47-Bn**) (from 1-octene)
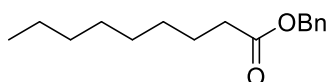
248.37 g/mol

47-Bn

Using 1-octene (160 µL, 113 mg, 1.00 mmol) as the alkene component and degassed BnOH (250 µL; stored under N_2) as the alcohol component, general procedure **C** was employed using 1 mol% [Pd] at 50 °C in DCE instead of DCM. Purification by flash column chromatography on SiO_2 (mobile phase: 95:5 CyH:EtOAc) gave the compound as a colourless liquid (229 mg, 0.91 mmol, 91%). The analytical data is in agreement with the reported literature.[S38]

R$_f$: 0.40 (mobile phase 95:5 CyH:EtOAc, $KMnO_4$ stain)

Melting point: Ambient temperature.

^{1}H-NMR (400 MHz, $CDCl_3$) δ $_{(ppm)}$: 7.41 – 7.29 (m, 5H, Ar$\underline{H}$), 5.12 (s, 2H, C$\underline{H}_2$Ph), 2.35 (t, J = 7.6 Hz, 2H, PhCH$_2$OCOC$\underline{H}_2$-R), 1.64 (quin, J = 7.6 Hz, 2H, ArCH$_2$OCOCH$_2$C$\underline{H}_2$-R), 1.36 – 1.19 (m, 10H, remaining C$\underline{H}_2$), 0.88 (t, J = 6.9 Hz, 3H, terminal C$\underline{H}_3$).

^{13}C-NMR (101 MHz, $CDCl_3$) δ $_{(ppm)}$: 173.7 ($\underline{C}$=O), 136.2 (Ar$\underline{C}$), 128.6 (Ar$\underline{C}$), 128.2 (Ar$\underline{C}$), 128.2 (Ar$\underline{C}$), 66.1 (R-$\underline{C}$H$_2$Ph), 34.4 ($\underline{C}$H$_2$), 31.8 ($\underline{C}$H$_2$), 29.2 ($\underline{C}$H$_2$), 29.2 ($\underline{C}$H$_2$), 29.1 ($\underline{C}$H$_2$), 25.0 ($\underline{C}$H$_2$), 22.7 ($\underline{C}$H$_2$), 14.1 (terminal $\underline{C}$H$_3$).

GC-MS: t_R = 9.16 min, m/z = 266 (60, [MNH$_4^+$]), 249 (17, [MH$^+$]), 91 (100, [MH$^+$]-[BnO$^\bullet$]).

Benzyl nonanoate (**47-Bn**) (from (*E*)-2-octene)
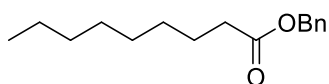
248.37 g/mol

47-Bn

Using 2-octene (155 μL, 111 mg, 1.00 mmol) as the alkene component and degassed BnOH (250 μL; stored under N_2) as the alcohol component, general procedure **A** was employed using 1 mol% [Pd] at 50 °C in DCE instead of DCM. Purification by flash column chromatography on SiO_2 (mobile phase: 95:5 CyH:EtOAc) gave the compound as a colourless liquid (225 mg, 0.89 mmol, 89%).

Analytical data as above.

Dimethyl nonadecanedioate (**51**)
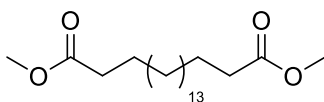
356.6 g/mol

51

Using methyl oleate (340 μL, 297 mg, 1.00 mmol) as the alkene component and dist. MeOH (250 μL; stored under N_2) as the alcohol component, **GP A** was employed using 0.5 mol% [Pd]. Purification by flash column chromatography on SiO_2 (mobile phase: 95:5 CyH:EtOAc) gave the compound bright yellow liquid (57 mg, 0.16 μmol, 16%).

R$_f$: 0.18 (CyH/ EtOAc 95:5)

m.p.: 58.5 °C (lit: 56-58°C)[36]

^{1}H-NMR (400 MHz, CDCl$_3$) δ (ppm): 3.66 (s, 6H, R-CO$_2$C$\underline{H}_3$), 2.30 (t, *J* = 7.3 Hz, 4H, MeO$_2$C-C$\underline{H}_2$-R), 1.67 – 1.56 (quin, *J* = 7.3 Hz, 4H, MeO$_2$C-CH$_2$C$\underline{H}_2$-R), 1.35 – 1.20 (m, 26H, remaining C$\underline{H}_2$).

^{13}C-NMR (75 MHz, CDCl3) δ (ppm): 174.4 (C=O), 51.5 (RCO$_2$$\underline{C}H_3$), 34.1 (CH$_2$), 29.7 (CH$_2$), 29.6 (CH$_2$), 29.5 (CH$_2$), 29.3 (CH$_2$), 29.2 (CH$_2$), 25.0 (CH$_2$).

FT-IR (ATR) v (cm^{-1}): 3024 (w, br), 2918 (s, sh), 2850 (m, sh), 1736 (s, sh), 1463 (w, br), 1437 (m, sh), 1419 (w, sh), 1381 (w, sh), 1343 (w, sh), 1269 (w, sh), 1231 (m, sh), 1215 (m, sh), 1200 (m, br), 1174 (m, br), 1117 (w, br), 1026 (w, br).

GC-FID: (50-280M12): t_R = 10.50 min.

GC-MS: t_R = 14.22 min, m/z = 357 (100, [MH$^+$]), 325 (22, [MH$^+$]-[$^•$OMe]), 279 (7, [MH$^+$]-[$^•$CO$_2$Me].

HR-MS (APCI): m/z = [MH$^+$] calc. for C$_{21}$H$_{40}$O$_4$ 357.2999, found 357.3004.

(*E*)-Methyl cinnamate (**53**)
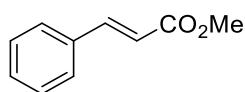
162.2 g/mol

53

Using ethinylbenzene (**52**) (80 µL, 102 mg, 0.750 mmol) as the alkyne component and dist. MeOH (250 µL; stored under N$_2$) as the alcohol component, **GP A** was employed using 0.75 mol% [Pd]. Upon addition of ethinylbenzene a highly exothermic process set in. During workup, an unknown yellow polymeric byproduct was noted. Purification by flash column chromatography on SiO$_2$ (mobile phase: 95:5 CyH:EtOAc) gave the compound as an off-white solid (13 mg, 0.08 mmol, 11%). The analytical data matches with the reported literature data.[S40]

R$_f$: 0.26 (mobile phase 8:2 CyH:EtOAc, KMnO$_4$ stain)

Melting point: 34 °C.

^{1}H NMR (400 MHz, CDCl$_3$) δ (ppm): 7.70 (d, *J* = 16.0 Hz, 1H, ArCHCHCO$_2$Me), 7.55 - 7.51 (m, 2H, ArH), 7.41 – 7.37 (m, 3H, ArH), 6.45 (d, *J* = 16.0 Hz, 1H, ArCHCHCO$_2$Me), 3.81 (s, 3H, ArCHCHCO$_2$CH$_3$).

^{13}C NMR (101 MHz, CDCl$_3$) δ (ppm): 167.5 (C=O), 144.9 (ArCHCHCO$_2$Me), 134.4 (*ipso*-ArC), 130.3 (*meta*-ArC), 128.9 (*ortho*-ArC), 128.1 (*para*-ArC), 117.8 (ArCHCHCO$_2$Me), 51.7 (ArCHCHCO$_2$CH$_3$).

GC/MS (EI): t_R = 8.60 min, m/z = 162 (49, [M$^{+•}$]), 131 (100, [M$^{+•}$]-[OMe$^•$]), 103 (61, [M$^{+•}$]-[OMe$^•$]-[CO]).

2.4.3.3. Synthesis of thioesters

S-Ethyl 2-phenylpropanethioate (**56**)

56
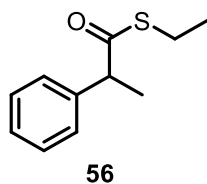
GP C was used to carbonylate dist. styrene (115 µL, 1.00 mmol) with 1.0 mol% catalyst and EtSH (100 µL, 1.35 eq) as the thiol component at RT. Purification by column chromatography (gradient CyH/ EtOAc 100:0 to 95:5) provided **56** as a bright yellow oil (186 mg, 957 µmol, 96%).

$C_{11}H_{14}OS$ (194.29 g/mol)

R_f: 0.43 (CyH/ EtOAc 95:5)

m.p.: Ambient temperature.

^{1}H-NMR (300 MHz, CDCl$_3$) δ_H/ppm: 7.38 – 7.27 (m, 5H, ArH), 3.88 (q, J = 7.1 Hz, 1H, ArCH), 2.89 – 2.78 (m, 2H, SCH$_2$), 1.54 (d, J = 7.1 Hz, 3H, ArCHCH$_3$), 1.21 (t, J = 7.4 Hz, 3H, SCH$_2$CH$_3$).

^{13}C-NMR (75 MHz, CDCl$_3$) δ_C/ppm: 201.3 (q), 140.0 (q), 128.7 (+), 127.9 (+), 127.4 (+), 54.2 (+), 23.5 (−), 18.4 (+), 14.5 (+).

FT-IR (ATR) $\tilde{v}$ (cm^{-1}): 3030 (w, sh), 2933 (m, sh), 2974 (m, sh), 2878 (w, sh), 1685 (s, sh), 1454 (m, sh), 1264 (m, sh), 947 (s, sh), 757 (s, sh).

GC-FID: (50-280M12): t_R = 6.19 min.

HR-MS (APCI): m/z = [MH$^+$] calc. for $C_{11}H_{15}OS$ 195.0838, found 195.0841.

S-Propyl 2-phenylpropanethioate (**57**)

57
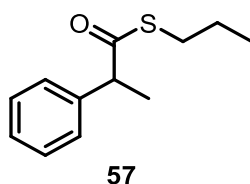
GP C was used to carbonylate dist. styrene (115 µL, 1.00 mmol) with 1.0 mol% catalyst and PrSH (125 µL, 1.35 eq) as a thiol component at RT. Purification by column chromatography (gradient CyH/ EtOAc 100:0 to 95:5) provided **57** as a bright yellow oil (191 mg, 918 µmol, 92%).

$C_{12}H_{16}OS$ (208.32 g/mol)

R_f: 0.50 (CyH/ EtOAc 95:5)

m.p.: Ambient temperature.

^{1}H-NMR (300 MHz, CDCl$_3$) δ_H/ppm: 7.38 – 7.26 (m, 5H, ArH), 3.89 (q, J = 7.1 Hz, 1H, ArCH), 2.90 – 2.74 (m, 2H, ArCHCOSCH$_2$), 1.49 – 1.59 (m, 2H, ArCHCOSCH$_2$CH$_2$), 1.54 (d, J = 7.1 Hz, 3H, ArCHCH$_3$), 0.92 (t, J = 7.3 Hz, 3H, ArCHCOSCH$_2$CH$_2$CH$_3$).

^{13}C-NMR (101 MHz, CDCl$_3$) δ_C/ppm: 201.3 (q), 140.1 (q), 128.7 (+), 128.5 (+), 128.4 (+), 127.9 (+), 127.4 (+), 54.3 (+), 31.0 (–), 22.9 (–), 18.5 (+), 13.3 (+).

FT-IR (ATR) $\tilde{v}$ (cm^{-1}): 2967 (m, sh), 2933 (m, sh), 2874 (w, sh), 1685 (s, sh), 1454 (m, sh), 995 (m, sh), 947 (s, sh).

HR-MS (APCI): m/z = [MH$^+$] calc. for $C_{12}H_{17}OS$ 209.0995, found 209.0995.

S-Heptyl 2-phenylpropanethioate (**55**)
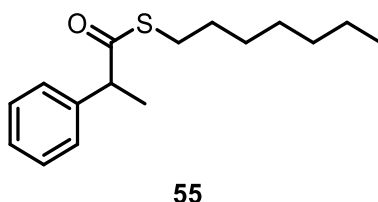
55

GP C was used to carbonylate dist. styrene (115 µL, 1.00 mmol) with 1.0 mol% catalyst and dist. HeptSH (210 µL, stored under N$_2$, 1.34 eq) as a thiol component at RT. Purification by column chromatography (gradient CyH → CyH/ EtOAc 95:5) provided **55** as a bright yellow oil (253 mg, 958 µmol, 95%).

$C_{16}H_{24}OS$ (264.43 g/mol)

R$_f$: 0.50 (CyH/ EtOAc 95:5)

m.p.: Ambient temperature.

^{1}H-NMR (300 MHz, CDCl$_3$) δ_H/ppm: 7.37 – 7.27 (m, 5H, ArH), 3.88 (q, J = 7.1 Hz, 1H, ArCH), 2.91 – 2.73 (m, 2H, ArCHCOSCH$_2$), 1.53 (d, J = 7.1 Hz, 3H, ArCHCH$_3$), 1.52 – 1.45 (m, 2H, SCH$_2$CH$_2$(CH$_2$)$_4$CH$_3$), 1.37 – 1.16 (m, 8H, SCH$_2$(CH$_2$)$_4$CH$_3$), 0.86 (t, J = 6.8 Hz, 3H, SCH$_2$(CH$_2$)$_5$CH$_3$).

^{13}C-NMR (101 MHz, CDCl$_3$) δ_C/ppm: 201.3 (q), 140.1 (q), 128.7 (+), 127.9 (+), 127.4 (+), 54.3 (+), 31.7 (–), 29.4 (–), 29.1 (–), 28.8 (–), 28.8 (–), 22.6 (–), 18.5 (+), 14.1 (+).

FT-IR (ATR) $\tilde{v}$ (cm^{-1}): 2930 (s, br), 2855 (m, sh), 1689 (s, sh), 1454 (m, sh), 995 (w, sh), 947 (s, sh), 701 (s, sh).

HR-MS (APCI): m/z = [MH$^+$] calc. for C$_{16}$H$_{25}$OS 265.1621, found 265.1624.

<u>S-Phenyl 2-phenylpropanethioate (**60-b**) and phenethyl(phenyl)sulfane (**60-l**)</u>

60   **60'**
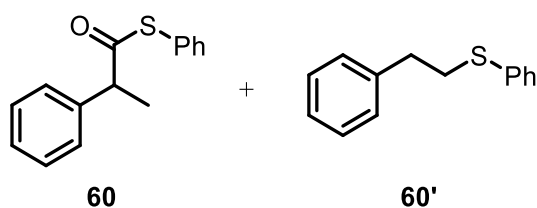
GP C was used to carbonylate dist. styrene (115 µL, 1.00 mmol) with 1.0 mol% catalyst and dist. PhSH (140 µL, stored under N$_2$, 1.37 eq) as a thiol component at RT. Purification by column chromatography (gradient <u>CyH</u> → CyH/ EtOAc 95:5) provided an inseparable mixture of **60** and **60'** as a bright yellow oil (135 mg, ether/ester = 41/59 → **60**: 80 mg, 329 µmol, 33%, **60'**: 55 mg, 259 µmol, 26%).

C$_{15}$H$_{14}$OS (242.34 g/mol) and C$_{14}$H$_{14}$S (214.33 g/mol)

R$_f$: 0.35, 0.20 (CyH/ EtOAc 95:5)

m.p.: Ambient temperature.

^{1}H-NMR (300 MHz, CDCl$_3$) δ_H/ppm: 7.42 – 7.27 (m, 14H, Ar<u>H</u>), 7.24 – 7.15 (m, 3H, Ar<u>H</u>), 4.01 (q, J = 7.1 Hz, 1H, ArC<u>H</u>), 3.24 – 3.12 (m, 2H, ArC<u>H$_2$</u>), 2.94 (dd, J = 9.3, 6.4 Hz, 2H, ArCH$_2$C<u>H$_2$</u>), 1.59 (d, J = 7.1 Hz, 3H, ArCHC<u>H$_3$</u>).

^{13}C-NMR (75 MHz, CDCl$_3$) δ_C/ppm: 199.1 (q), 140.2 (q), 139.6 (q), 136.4 (q), 134.5 (+), 129.3 (+), 129.2 (+), 129.1 (+), 129.0 (+), 128.8 (+), 128. 6 (+), 128.1 (+), 127.9 (q), 127.6 (+), 126.5 (+), 126.0 (+), 54.1 (+), 35.7 (–), 35.1 (–), 18.7 (+).

FT-IR (ATR) $\tilde{v}$ (cm^{-1}): 3027 (w, br), 2930 (w, br), 2974 (w, br), 1700 (s, sh), 1580 (m, sh), 1476 (s, sh), 1439 (s, sh), 932 (s, sh), 738 (s, sh), 690 (s, sh).

GC-MS (EI) **2ag**: 242 (2, [M+•]), 133 (10, [M+•]-[PhS•]), 105 (100, [M+•]-[PhSCO•]).

GC-MS (EI) **2ag'**: 214 (75, [M+•]), 123 (100, [M+•]-[PhCH$_2$•]), 105 (25, [M+•]-[PhS•]).

HR-MS (EI) **2ag**: m/z = [M+•] calc. for C$_{15}$H$_{14}$OS 242.0760, found 242.0767.

HR-MS (EI) **2ag'**: m/z = [M+•] calc. for C$_{14}$H$_{14}$S 214.0811, found 214.0814.

S-Benzyl 2-phenylpropanethioate (**58**)

58
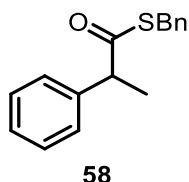
GP C was used to carbonylate dist. styrene (115 µL, 1.00 mmol) with 1.0 mol% catalyst and dist. BnSH (160 µL, 1.34 mmol, 1.34 eqv. stored under N$_2$) as the thiol component at RT. Purification by column chromatography (gradient CyH → CyH/ EtOAc 95:5) provided **58** as a colourless oil (210 mg, 820 µmol, 82%).

C$_{16}$H$_{16}$OS (256.36 g/mol)

R$_f$: 0.39 (CyH/ EtOAc 95:5)

m.p.: Ambient temperature.

^{1}H-NMR (300 MHz, CDCl$_3$) δ$_H$/ppm: 7.41 – 7.16 (m, 10H, Ar*H*), 4.09 (ABq, Δδ$_{AB}$ = 0.09, J_{AB} = 13 Hz, 2H, PhC*H$_2$*SR), 3.92 (q, *J* = 7.1 Hz, 1H, ArC*H*CH$_3$), 1.57 (d, *J* = 7.1 Hz, 3H, ArCHC*H$_3$*).

^{13}C-NMR (75 MHz, CDCl$_3$) δ$_C$/ppm: 200.6 (q), 139.7 (q), 137.4 (q), 128.9 (+), 128.7 (+), 128.6 (+), 128.0 (+), 127.6 (+), 127.3 (+), 54.1 (+), 33.5 (-), 18.5 (+).

FT-IR (ATR) $\tilde{\nu}$ (cm^{-1}): 3063 (w), 3030 (w), 2978 (w), 2933 (w), 1681 (s, sh), 1602 (m), 1494 (m, sh), 1453 (m, sh), 1099 (m, sh), 1069 (m, sh), 995 (m, sh), 939 (s, sh), 693 (s, sh).

HR-MS (APCI): m/z = [MH+] calc. for C$_{16}$H$_{17}$OS 257.0995, found 257.0995.

Methyl *N*-(*tert*-butoxycarbonyl)-*S*-(2-phenylpropanoyl)-L-cysteinate (**61**)
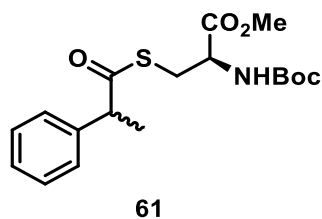
GP C was used to carbonylate dist. styrene (115 µL, 1.00 mmol) with 1.0 mol% catalyst and freshly opened *N*-Boc-L-cysteine methyl ester (205 µL, 1.00 mmol, 1 eqv., stored under N_2) as the thiol component at RT. The crude reaction mixture was treated with Et_3N (160 µL, 1.15 mmol) and stirred for 15 min at RT in order to remove the unreacted thiol. Purification by column chromatography (CyH/EtOAc 9:1) provided **61** as a colourless oil (227 mg, 620 µmol, 62%).

$C_{18}H_{25}NO_5S$ (367.46 g/mol)

R_f: 0.16 (CyH/ EtOAc 9:1)

m.p.: Ambient temperature.

¹H-NMR (400 MHz, $CDCl_3$) δ_H/ppm: 7.43 – 7.11 (m, 5H, Ar<u>H</u>), 5.23 (dd, *J* = 15.0, 8.1 Hz, 1H, N<u>H</u>), 4.47 (s br, 1H, RCOS-CH_2-C<u>H</u>(NHBoc)(CO_2Me)),), 3.87 (q, *J* = 7.1 Hz, 1H, Ph-C<u>H</u>(CH_3)(COS-cysteine)), 3.62 (2x s, 3H, RCOS-CH_2-CH(NHBoc)(CO_2C<u>H_3</u>)),), 3.36 – 3.19 (m, 2H, RCOS-C<u>H_2</u>-CH(NHBoc)(CO_2Me)), 1.50 (dd, *J* = 7.1, 2.2 Hz, 3H, Ph-CH(C<u>H_3</u>)(COS-cysteine)), 1.41 – 1.39 (2x s, 9H, C(C<u>H_3</u>)$_3$).

¹³C-NMR (101 MHz, $CDCl_3$) δ_C/ppm: 200.1 (q), 200.0 (q), 170.9 (q), 139.4 (q), 128.7 (+), 128.7 (+), 128.0 (+), 127.9 (+), 127.6 (q), 80.1 (q), 54.3 (+), 53.1 (+), 53.0 (+), 52.6 (+), 52.5 (+), 31.2 (-), 31.1 (-), 28.3 (+), 18.4 (+).

FT-IR (ATR) $\tilde{\nu}$ (cm^{-1}): 3373 (w, br), 2978 (w, sh), 2937 (w, sh), 1748 (m, sh), 1700 (s, sh), 1692 (s, sh), 1494 (m, sh), 1453 (m, sh), 1394 (w, sh), 1364 (m, sh), 1244 (m, sh), 1215 (m, sh), 1159 (s, sh), 1054 (m, sh), 1010 (m, sh), 943 (s, sh), 864 (m), 775 (m), 730 (m), 700 (s, sh).

HR-MS (ESI): m/z = [MNa+] calc. for $C_{18}H_{25}NNaO_5S$ 390.1346, found 390.1352.

S-Cyclohexyl 2-phenylpropanethioate (**59**)
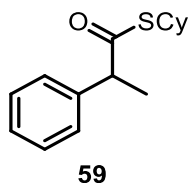
59

GP C was used to carbonylate dist. styrene (115 µL, 1.00 mmol) with 1.0 mol% catalyst and freshly opened cyclohexanethiol (165 µL, stored under N_2) as the thiol component at RT. Purification by column chromatography (gradient CyH → CyH/ EtOAc 95:5) provided **59** as a colourless oil (70 mg, 820 µmol, 28%).

$C_{15}H_{20}OS$ (248.38 g/mol)

R_f: 0.47 (CyH/ EtOAc 95:5)

m.p.: Ambient temperature.

^{1}H-NMR (300 MHz, $CDCl_3$) δ_H/ppm: 7.42 – 7.09 (m, 5H, Ar<u>H</u>), 3.86 (q, *J* = 7.1 Hz, 1H, ArC<u>H</u>(COSR)CH₃), 3.57 – 3.36 (m, 1H, cyclohexyl C<u>H</u>), 2.06 – 1.57 (m, 5H, cyclohexyl C<u>H₂</u>), 1.53 (d, *J* = 7.1 Hz, 3H, ArCH(COSR)C<u>H₃</u>), 1.48 – 1.08 (m, 5H, cyclohexyl C<u>H₂</u>).

^{13}C-NMR (75 MHz, $CDCl_3$) δ_C/ppm: 201.0 (q), 140.1 (q), 128.6 (+), 127.9 (+), 127.3 (+), 54.3 (+), 42.5 (+), 33.06 (-), 32.89 (-), 26.02 (-), 26.00 (-), 25.56 (-), 18.55 (+).

FT-IR (ATR) $\tilde{\nu}$ (cm^{-1}): 3030 (w, br), 2929 (s, sh), 2855 (m, sh), 1700 (s, sh), 1681 (s, sh), 1494 (w, sh), 1449 (m, sh), 1263 (w, sh), 995 (m, sh), 943 (s, sh), 730 (m, sh), 697 (s, sh).

HR-MS (APCI): m/z = [MH+] calc. for $C_{15}H_{21}OS$ 249.1308, found 249.1315.

S-Heptyl 2-(*o*-tolyl)propanethioate (**79**)

79
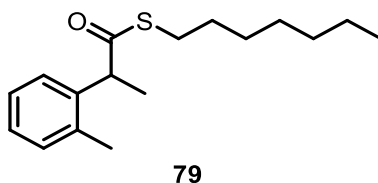
GP C was used to carbonylate dist. *ortho*-methylstyrene (130 µL, 1.00 mmol) with 1.0 mol% catalyst and dist. HeptSH (210 µL, stored under N_2, 1.34 eq) as a thiol component at RT.

Purification by column chromatography (gradient CyH → CyH/ EtOAc 95:5) provided **79** as a bright yellow oil (248.6 mg, 893 µmol, 89%).

$C_{17}H_{26}OS$ (278.45 g/mol)

R$_f$: 0.48 (CyH/ EtOAc 95:5)

m.p.: Ambient temperature.

^{1}H-NMR (300 MHz, CDCl$_3$) δ$_H$/ppm: 7.31 – 7.27 (m, 1H, ArH), 7.25 – 7.15 (m, 3H, ArH), 4.10 (q, J = 7.1 Hz, 1H, ArCH), 2.89 – 2.75 (m, 2H, SCH$_2$), 2.37 (s, 3H, ArCH$_3$), 1.51 (d, J = 7.1 Hz, 3H, ArCHCH$_3$), 1.56 – 1.47 (m, 2H, SCH$_2$CH$_2$(CH$_2$)$_4$CH$_3$), 1.34 – 1.17 (m, 8H, SCH$_2$CH$_2$(CH$_2$)$_4$CH$_3$), 0.86 (t, J = 6.8 Hz, 3H, SCH$_2$(CH$_2$)$_5$CH$_3$).

^{13}C-NMR (75 MHz, CDCl$_3$) δ$_C$/ppm: 201.8 (q), 138.3 (q), 136.2 (q), 130.5 (+), 127.3 (+), 127.2 (+), 126.4 (+), 50.1 (+), 31.7 (–), 29.5 (–), 29.1 (–), 28.78 (–), 28.77 (–), 22.6 (–), 19.9 (+), 18.1 (+), 14.1 (+).

FT-IR (ATR) $\tilde{v}$ (cm^{-1}): 2926 (s, sh), 2855 (m, sh), 1681 (s, sh), 1491 (w, sh), 1457 (m, sh), 999 (m, sh), 939 (s, sh), 738 (s, br).

GC-MS (EI): t$_R$ = 8.83 min, m/z = 119 (100, [M+•]-[•COSHept]), 91 (9, [M+•]-[•COSHept]-[CH3]), 250 (0.4, [M+•]-[CO]).

HR-MS (EI): m/z = [M+•] calc. for C$_{17}$H$_{26}$OS 278.1699, found 278.1702.

S-Heptyl 2-(*m*-tolyl)propanethioate (**74**)

74
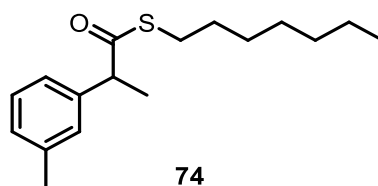
GP C was used to carbonylate dist. *meta*-methylstyrene (130 μL, 990 μmol) with 1.0 mol% catalyst and dist. HeptSH (210 μL, stored under N$_2$, 1.34 eq) as a thiol component at RT.

Purification by column chromatography (gradient CyH → CyH/ EtOAc 95:5) provided **74** as a bright yellow oil (274 mg, 984 μmol, 99%).

C$_{17}$H$_{26}$OS (278.45 g/mol)

R$_f$: 0.53 (CyH/ EtOAc 95:5)

m.p.: Ambient temperature.

^{1}H-NMR (300 MHz, CDCl$_3$) δ$_H$/ppm: 7.25 – 7.18 (m, 1H, ArH), 7.14 – 7.04 (m, 3H, ArH), 3.84 (q, J = 7.1 Hz, 1H, ArCH), 2.92 – 2.73 (m, 2H, SCH$_2$), 2.35 (s, 3H, ArCH$_3$), 1.51 (d, J = 7.1 Hz, 3H, ArCHCH$_3$), 1.57 – 1.47 (m, 2H, SCH$_2$CH$_2$(CH$_2$)$_4$CH$_3$), 1.36 – 1.15 (m, 8H, SCH$_2$CH$_2$(CH$_2$)$_4$CH$_3$)), 0.86 (t, J = 6.8 Hz, 3H, SCH$_2$(CH$_2$)$_5$CH$_3$).

^{13}C-NMR (75 MHz, CDCl$_3$) δ$_C$/ppm: 201.4 (q), 140.0 (q), 138.3 (q), 128.6 (+), 128.5 (+), 128.2 (+), 124.9 (+), 54.2 (+), 31.7 (–), 29.4 (–), 29.1 (–), 28.80 (–), 28.77 (–), 22.6 (–), 21.5 (+), 18.5 (+), 14.1 (+).

FT-IR (ATR) $\tilde{v}$ (cm^{-1}): 2926 (s, sh), 2855 (s, sh), 1684 (s, sh), 1607 (w, sh), 1454 (m, br), 947 (s, sh), 734 (m, br).

GC-MS (EI): t_R = 8.78 min, m/z = 119 (100, [M+•]-[•COSHept]), 91 (8, [M+•]-[•COSHept]-[CH3]), 250 (4, [M+•]-[CO]), 180 (3, [M+•]-[•Hept]).

HR-MS (EI): m/z = [M+•] calc. for $C_{17}H_{26}OS$ 278.1699, found 278.1702.

S-Heptyl 2-(*p*-tolyl)propanethioate (**62**)
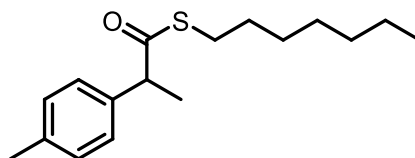
62

GP C was used to carbonylate dist. *para*-methylstyrene (130 µL, 990 µmol) with 1.0 mol% catalyst and dist. HeptSH (210 µL, stored under N_2, 1.34 eq) as a thiol component at RT.

Purification by column chromatography (gradient CyH → CyH/ EtOAc 95:5) provided **62** as a bright yellow oil (275 mg, 988 µmol, 99%).

$C_{17}H_{26}OS$ (278.45 g/mol)

R$_f$: 0.57 (CyH/ EtOAc 95:5)

m.p.: Ambient temperature.

^{1}H-NMR (300 MHz, CDCl$_3$) δ_H/ppm: 7.23 – 7.11 (m, 4H, ArH), 3.84 (q, J = 7.1 Hz, 1H, ArCH), 2.90 – 2.72 (m, 2H, SCH$_2$), 2.33 (s, 3H, ArCH$_3$), 1.51 (d, J = 7.1 Hz, 3H, ArCHCH$_3$), 1.57 – 1.47 (m, 2H, SCH$_2$CH$_2$(CH$_2$)$_4$CH$_3$), 1.38 – 1.17 (m, 8H, SCH$_2$CH$_2$(CH$_2$)$_4$CH$_3$), 0.86 (t, J = 6.8 Hz, 3H, SCH$_2$(CH$_2$)$_5$CH$_3$).

^{13}C-NMR (75 MHz, CDCl$_3$) δ_C/ppm: 201.6 (q), 137.10 (q), 137.07 (q), 129.4 (+), 127.8 (+), 53.9 (+), 31.7 (–), 29.4 (–), 29.1 (–), 28.8 (–), 28.8 (–), 22.6 (–), 21.1 (+), 18.5 (+), 14.1 (+).

FT-IR (ATR) $\tilde{v}$ (cm^{-1}): 2926 (s, sh), 2855 (m, sh), 1681 (s, sh), 1513 (m, sh), 1454 (m, sh), 1003 (m, sh), 943 (s, sh), 753 (m, sh).

GC-MS (EI): t_R = 8.871 min, m/z = 119 (100, [M+•]-[•COSHept]), 91 (7, [M+•]-[•COSHept]-[CH3]), 250 (2, [M+•]-[CO]).

HR-MS (EI): m/z = [M+•] calc. for $C_{17}H_{26}OS$ 278.1699, found 278.1699.

S-Heptyl 2-(2-methoxyphenyl)propanethioate (**77**)
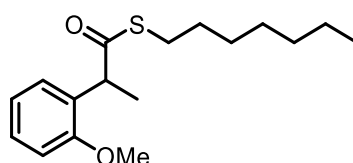
77

GP C was used to carbonylate dist. *ortho*-vinylanisole (135 µL, 1.01 mmol) with 1.0 mol% catalyst and dist. HeptSH (210 µL, stored under N_2, 1.34 eq) as a thiol component at RT.

Purification by column chromatography (gradient CyH → CyH/ EtOAc 95:5) provided **77** as a bright yellow oil (287 mg, 975 µmol, 97%).

$C_{17}H_{26}O_2S$ (294.45 g/mol)

R$_f$: 0.40 (CyH/ EtOAc 95:5)

m.p.: Ambient temperature.

^{1}H-NMR (300 MHz, CDCl$_3$) δ_H/ppm: 7.32 – 7.20 (m, 2H, Ar<u>H</u>), 7.03 – 6.82 (m, 2H, Ar<u>H</u>), 4.26 (q, J = 7.1 Hz, 1H, ArC<u>H</u>), 3.83 (s, 3H, ArOC<u>H</u>$_3$), 2.81 (t, J = 7.3 Hz, 2H, SC<u>H</u>$_2$), 1.54 – 1.44 (m, 2H, SCH$_2$C<u>H</u>$_2$(CH$_2$)$_4$CH$_3$), 1.48 (d, J = 7.1 Hz, 3H, ArCHC<u>H</u>$_3$), 1.34 – 1.18 (m, 8H, SCH$_2$CH$_2$(C<u>H</u>$_2$)$_4$CH$_3$), 0.86 (t, J = 6.8 Hz, 3H, SCH$_2$(CH$_2$)$_5$C<u>H</u>$_3$).

^{13}C-NMR (75 MHz, CDCl$_3$) δ_C/ppm: 202.2 (q), 157.0 (q), 128.6 (q), 128.5 (+), 128.4 (+), 120.7 (+), 110.7 (+), 55.5 (+), 47.3 (+), 31.7 (–), 29.6 (–), 28.9 (–), 28.81 (–), 28.80 (–), 22.6 (–), 17.3 (+), 14.1 (+).

FT-IR (ATR) $\tilde{v}$ (cm^{-1}): 2926 (s, br), 2855 (m, sh), 1685 (s, sh), 1599 (w, sh), 1491 (s, sh), 1461 (s, br), 1245 (s, sh), 1122 (m, br), 1029 (s, sh), 943 (s, sh), 753 (s, sh).

GC-MS (CI): t$_R$ = 9.207 min, m/z = 135 (100, [MH+]-[•COSHept], 295 (75, [MH+]), 163 (6, [MH+]-[•SHept).

HR-MS (APCI): m/z = [MH$^+$] calc. for $C_{17}H_{27}O_2S$ 295.1726, found 295.1737.

<u>S-Heptyl 2-(3-methoxyphenyl)propanethioate (**75**)</u>
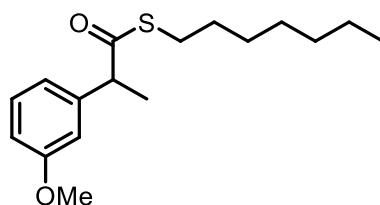
75

GP C was used to carbonylate dist. *meta*-vinylanisole (140 µL, 1.01 mmol) with 1.0 mol% catalyst and dist. HeptSH (210 µL, stored under N$_2$, 1.34 eq) as a thiol component at RT. Purification by column chromatography (gradient CyH → CyH/ EtOAc 95:5) provided **75** as a bright yellow oil (287 mg, 906 µmol, 90%).

$C_{17}H_{26}O_2S$ (294.45 g/mol)

R$_f$: 0.42 (CyH/ EtOAc 95:5)

m.p.: Ambient temperature.

^{1}H-NMR (300 MHz, CDCl$_3$) δ_H/ppm: 7.24 – 7.17 (m, 1H, Ar<u>H</u>), 6.88 – 6.73 (m, 3H, Ar<u>H</u>), 3.81 (q, J = 7.1 Hz, 1H, ArC<u>H</u>), 3.76 (s, 3H, ArOC<u>H</u>$_3$), 2.88 – 2.67 (m, 2H, SC<u>H</u>$_2$), 1.52 – 1.42 (m, 2H, SCH$_2$<u>CH</u>$_2$(CH$_2$)$_4$CH$_3$),

1.46 (d, J = 7.1 Hz, 3H, ArCHC$\underline{H_3}$), 1.33 − 1.11 (m, 8H, SCH$_2$CH$_2$(C$\underline{H_2)_4}$CH$_3$), 0.82 (t, J = 6.8 Hz, 3H, SCH$_2$(CH$_2$)$_5$C$\underline{H_3}$).

^{13}C-NMR (75 MHz, CDCl$_3$) δ$_C$/ppm: 201.2 (q), 159.7 (q), 141.6 (q), 129.6 (+), 120.3 (+), 113.6 (+), 112.7 (+), 55.2 (+), 54.3 (+), 31.7 (−), 29.4 (−), 29.1 (−), 28.80 (−), 28.77 (−), 22.6 (−), 18.4 (+), 14.1 (+).

FT-IR (ATR) $\tilde{v}$ (cm^{-1}): 2926 (s, sh), 2855 (m, sh), 1681 (s, sh), 1599 (s, sh), 1454 (s, sh), 1260 (s, br), 1044 (s, sh), 950 (s, sh), 753 (s, sh), 697 (s, sh).

GC-MS (EI): t$_R$ = 9.439 min, m/z = 135 (100, [M+•]-[•COSHept], 105 (9, [M+•]-[•COSHept]-[•OMe]), 296 (0.7, [M+•]).

HR-MS (EI): m/z = [M+•] calc. for C$_{17}$H$_{26}$O$_2$S 294.1648, found 294.1646.

<u>S-Heptyl 2-(4-methoxyphenyl)propanethioate (**63**)</u>
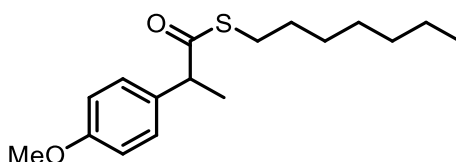
63

GP C was used to carbonylate dist. *para*-vinylanisole (140 μL, 1.01 mmol) with 1.0 mol% catalyst and dist. HeptSH (210 μL, stored under N$_2$, 1.34 eq) as a thiol component at RT. Purification by column chromatography (gradient CyH → CyH/ EtOAc 95:5) provided **63** as a bright yellow oil (295 mg, 1.00 μmol, 99%).

C$_{17}$H$_{26}$O$_2$S (294.45 g/mol)

R$_f$: 0.38 (CyH/ EtOAc 95:5)

m.p.: Ambient temperature.

^{1}H-NMR (300 MHz, CDCl$_3$) δ$_H$/ppm: 7.25 − 7.20 (m, 2H, Ar$\underline{H}$), 6.90 − 6.83 (m, 2H, Ar$\underline{H}$), 3.82 (q, J = 7.1 Hz, 1H, ArC$\underline{H}$), 3.80 (s, 3H, AroC$\underline{H_3}$) 2.91 − 2.70 (m, 2H, SC$\underline{H_2}$), 1.58 − 1.43 (m, 2H, SCH$_2$C$\underline{H_2}$(CH$_2$)$_4$CH$_3$), 1.50 (d, J = 7.1 Hz, 3H, ArCHC$\underline{H_3}$), 1.37 − 1.14 (m, 8H, SCH$_2$CH$_2$(C$\underline{H_2)_4}$CH$_3$), 0.86 (t, J = 6.7 Hz, 3H, SCH$_2$(CH$_2$)$_5$C$\underline{H_3}$).

^{13}C-NMR (75 MHz, CDCl$_3$) δ$_C$/ppm: 201.8 (q), 158.9 (q), 132.1 (q), 129.0 (+), 114.0 (+), 55.3 (+), 53.4 (+), 31.7 (−), 29.4 (−), 29.1 (−), 28.8 (−), 28.8 (−), 22.6 (−), 18.5 (+), 14.1 (+).

FT-IR (ATR) $\tilde{v}$ (cm^{-1}): 2926 (s, sh), 2855 (m, sh), 1677 (s, sh), 1610 (m, sh), 1513 (s, sh), 1461 (m, br), 1245 (s, sh), 1178 (s, sh), 943 (s, br), 831 (s, sh).

GC-MS (EI): t$_R$ = 9.589 min, m/z = 135 (100, [M+•]-[•COSHept], 105 (6, [M+•]-[•COSHept]-[•OMe]), 295 (0.4, [M+•]).

HR-MS (EI): m/z = [M+•] calc. for C$_{17}$H$_{26}$O$_2$S 294.1648, found 294.1646.

___

2-(1-(Heptylthio)-1-oxopropan-2-yl)phenyl acetate (**78**)

78
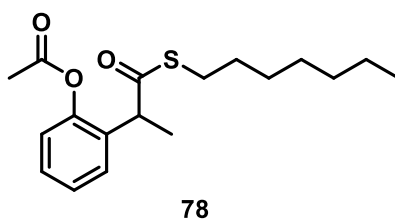
GP C was used to carbonylate dist. *ortho*-acetoxystyrene (162 mg, 1.00 mmol) with 1.0 mol% catalyst and dist. HeptSH (210 µL, stored under N_2, 1.34 eq) as a thiol component at RT.

Purification by column chromatography (gradient CyH → CyH/ EtOAc 95:5) provided **78** as a bright yellow oil (158 mg, 489 µmol, 49%).

$C_{18}H_{26}O_3S$ (322.46 g/mol)

R_f: 0.29 (CyH/ EtOAc 95:5)

m.p.: Ambient temperature.

^{1}H-NMR (300 MHz, CDCl$_3$) δ_H/ppm: 7.39 (dd, J = 7.5, 1.8 Hz, 1H, Ar<u>H</u>), 7.34 – 7.20 (m, 2H, Ar<u>H</u>), 7.09 (dd, J = 7.9, 1.5 Hz, 1H, Ar<u>H</u>), 4.02 (q, J = 7.1 Hz, 1H, ArC<u>H</u>), 2.96 – 2.72 (m, 2H, SC<u>H$_2$</u>), 2.34 (s, 3H, ArOCOC<u>H$_3$</u>), 1.61 – 1.45 (m, 2H, SCH$_2$C<u>H$_2$</u>(CH$_2$)$_4$CH$_3$), 1.50 (d, J = 7.1 Hz, ArCHC<u>H$_3$</u>), 1.26 (m, 8H, SCH$_2$CH$_2$(C<u>H$_2$</u>)$_4$CH$_3$), 0.87 (t, J = 7.0 Hz, 3H, SCH$_2$(CH$_2$)$_5$C<u>H$_3$</u>).

^{13}C-NMR (75 MHz, CDCl$_3$) δ_C/ppm: 200.7 (q), 169.2 (q), 148.5 (q), 131.9 (q), 128.7 (+), 128.4 (+), 126.4 (+), 122.7 (+), 47.9 (+), 31.7 (–), 29.4 (–), 29.1 (–), 28.8 (–), 22.6 (–), 21.0 (+), 17.5 (+), 14.1 (+).

FT-IR (ATR) $\tilde{\nu}$ (cm^{-1}): 2930 (m, sh), 2855 (w, sh), 1767 (s, sh), 1685 (s, sh), 1491 (w, sh), 1454 (w, br), 1372 (m, sh), 1193 (s, sh), 947 (s, sh), 910 (s, sh), 746 (s, br).

GC-MS (CI): t_R = 9.549 min, m/z = 149 (100, [MH+]-[•SHept]-[•CH$_3$CO]), 191 (18, [MH+]-[•SHept]), 323 (7, [MH+]), 263 (4, [MH+]-[•CH$_3$COO]).

HR-MS (APCI): m/z = [MH$^+$] calc. for $C_{18}H_{27}O_3S$ 323.1675, found 323.1682.

4-(1-(Heptylthio)-1-oxopropan-2-yl)phenyl acetate (**64**)

64
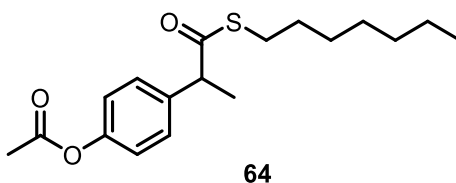
GP C was used to carbonylate dist. *para-acetoxy*styrene (155 µL, 1.01 mmol) with 1.0 mol% catalyst and dist. HeptSH (210 µL, stored under N_2, 1.34 eq) as a thiol component at RT.

Purification by column chromatography (gradient CyH → CyH/ EtOAc 95:5) provided **64** as a bright yellow oil (304 mg, 942 µmol, 93%).

___

$C_{18}H_{26}O_3S$ (322.46 g/mol)

R$_f$: 0.19 (CyH/ EtOAc 95:5)

m.p.: Ambient temperature.

^{1}H-NMR (300 MHz, CDCl$_3$) δ$_H$/ppm: 7.36 – 7.28 (m, 2H, Ar<u>H</u>), 7.08 – 7.00 (m, 2H, Ar<u>H</u>), 3.88 (q, J = 7.1 Hz, 1H, ArC<u>H</u>), 2.91 – 2.73 (m, 2H, SC<u>H</u>$_2$), 2.30 (s, 3H, ArOCOC<u>H</u>$_3$), 1.50 (d, J = 7.1 Hz, 3H, ArCHC<u>H</u>$_3$), 1.58 – 1.45 (m, 2H, SCH$_2$C<u>H</u>$_2$(CH$_2$)$_4$CH$_3$), 1.37 – 1.15 (m, 8H, SCH$_2$CH$_2$(C<u>H</u>$_2$)$_4$CH$_3$), 0.86 (t, J = 6.7 Hz, 3H, SCH$_2$(CH$_2$)$_5$C<u>H</u>$_3$).

^{13}C-NMR (75 MHz, CDCl$_3$) δ$_C$/ppm: 201.1 (q), 269.5 (q), 149.9 (q), 137.5 (q), 128.9 (+), 121.7 (+), 53.6 (+), 31.7 (−), 29.4 (−), 29.1 (−), 28.8 (−), 28.8 (−), 22.6 (−), 21.2 (+), 18.6 (+), 14.1 (+).

FT-IR (ATR) $\tilde{v}$ (cm^{-1}): 2930 (m, sh), 2855 (w, sh), 1763 (s, sh), 1681 (s, sh), 1506 (m, sh), 1368 (m, sh), 1193 (s, br), 947 (s, sh), 910 (s, sh).

GC-MS (EI): t$_R$ = 10.16 min, m/z = 121 (100, [M+•]-[•COSHept]-[•CH$_2$CO]), 163 (21, [M+•]-[•COSHept]), 280 (2, [M+•]-[•CH$_2$CO]), 322 (1, [M+•]).

HR-MS (EI): m/z = [M+•] calc. for $C_{18}H_{26}O_3S$ 322.1597, found 322.1591.

<u>S-Heptyl 2-(4-(trifluoromethyl)phenyl)propanethioate (**65**)</u>
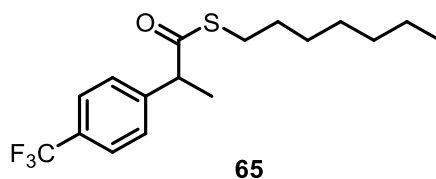
GP C was used to carbonylate dist. *para*-trifluoromethyl-styrene (150 µL, 1.02 mmol) with 1.0 mol% catalyst and dist. HeptSH (210 µL, stored under N$_2$, 1.34 eq) as a thiol component at RT. Purification by column chromatography (gradient CyH → CyH/ EtOAc 95:5) provided **65** as a bright yellow oil (168 mg, 504 µmol, 50%).

$C_{17}H_{23}F_3OS$ (332.43 g/mol)

R$_f$: 0.32 (CyH/ EtOAc 95:5)

m.p.: Ambient temperature.

^{1}H-NMR (400 MHz, CDCl$_3$) δ$_H$/ppm: 7.62 – 7.56 (m, 2H, Ar<u>H</u>), 7.46 – 7.41 (m, 2H, Ar<u>H</u>), 3.95 (q, J = 7.1 Hz, 1H, ArC<u>H</u>), 2.90 – 2.78 (m, 2H, SC<u>H</u>$_2$), 1.55 (d, J = 7.1 Hz, 3H, ArCHC<u>H</u>$_3$), 1.53 – 1.47 (m, 2H, SCH$_2$C<u>H</u>$_2$(CH$_2$)$_4$CH$_3$), 1.33 – 1.19 (m, 8H, SCH$_2$CH$_2$(C<u>H</u>$_2$)$_4$CH$_3$), 0.86 (t, J = 6.9 Hz, 3H, SCH$_2$(CH$_2$)$_5$C<u>H</u>$_3$).

^{13}C-NMR (101 MHz, CDCl$_3$) δ$_C$/ppm: 200.4 (q), 143.95 (q), 129.7 (quartet, J = 32.5 Hz, q), 128.2 (+), 125.6 (quartet, J = 3.8 Hz, +), 124.1 (quartet, J = 272.0 Hz, q), 54.0 (+), 31.7 (−), 29.4 (−), 29.2 (−), 28.7 (−), 28.7 (−), 22.6 (−), 18.5 (+), 14.0 (+).

^{19}F-NMR (282 MHz, CDCl$_3$) δ$_C$/ppm: - 62.9 (CF$_3$).

FT-IR (ATR) $\tilde{v}$ (cm^{-1}): 2929 (w, br), 2858 (w, sh), 1684 (m, sh), 1323 (s, sh), 1162 (m, sh), 1118 (s, sh), 1169 (m, sh), 946 (m, sh), 842 (m, sh).

HR-MS (APCI): m/z = [MH$^+$] calc. for $C_{17}H_{24}F_3OS$ 332.1494, found 332.1499.

S-Heptyl 2-([1,1'-biphenyl]-4-yl)propanethioate (**66**)

66
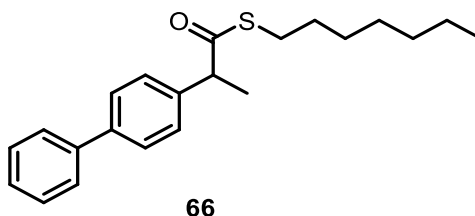
GP C was used to carbonylate dist. *para*-phenylstyrene (181 mg, 1.00 mmol) with 1.0 mol% catalyst and dist. HeptSH (210 µL, stored under N_2, 1.34 eq) as a thiol component at RT.

Purification by column chromatography (gradient CyH → CyH/ EtOAc 95:5) provided **66** as a bright yellow oil (293 mg, 860 µmol, 86%).

$C_{22}H_{28}OS$ (340.53 g/mol)

R$_f$: 0.51 (CyH/ EtOAc 95:5)

m.p.: Ambient temperature.

^{1}H-NMR (400 MHz, CDCl$_3$) δ_H/ppm: 7.61 – 7.54 (m, 4H, Ar$\underline{H}$), 7.46 – 7.31 (m, 5H, Ar$\underline{H}$), 3.93 (q, J = 7.1 Hz, 1H, ArC$\underline{H}$), 2.92 – 2.77 (m, 2H, SC$\underline{H_2}$), 1.57 (d, J = 7.1 Hz, 3H, ArCHC$\underline{H_3}$), 1.55 – 1.48 (m, 2H, SCH$_2$C$\underline{H_2}$(CH$_2$)$_4$CH$_3$), 1.35 – 1.19 (m, 8H, SCH$_2$CH$_2$(C$\underline{H_2}$)$_4$CH$_3$), 0.86 (t, J = 6.9 Hz, 3H, SCH$_2$(CH$_2$)$_5$C$\underline{H_3}$).

^{13}C-NMR (101 MHz, CDCl$_3$) δ_C/ppm: 201.3 (q), 140.8 (q), 140.3 (q), 139.1 (q), 128.8 (+), 128.3 (+), 127.4 (+), 127.3 (+), 127.1 (+), 54.0 (+), 31.7 (−), 29.4 (−), 29.2 (−), 28.8 (−), 28.8 (−), 22.6 (−), 18.5 (+), 14.1 (+).

FT-IR (ATR) $\tilde{v}$ (cm^{-1}): 2926 (m, br), 2855 (w, sh), 1685 (s, sh), 1454 (m, sh), 980 (m, sh), 812 (w, sh), 738 (s, sh), 697 (s, sh).

HR-MS (APCI): m/z = [MH$^+$] calc. for $C_{22}H_{29}OS$ 341.1934, found 341.1941.

S-Heptyl 2-(4-(tert-butyl)phenyl)propanethioate (**69**)

69
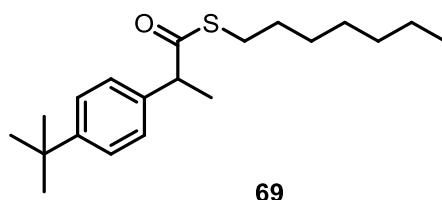
GP C was used to carbonylate dist. *para-tert*-butylstyrene (185 µL, 1.01 mmol) with 1.0 mol% catalyst and dist. HeptSH (210 µL, stored under N_2, 1.34 eq) as a thiol component at RT.

Purification by column chromatography (gradient CyH → CyH/ EtOAc 95:5) provided **69** as a bright yellow oil (307 mg, 957 µmol, 95%).

C$_{20}$H$_{32}$OS (320.54 g/mol)

R$_f$: 0.55 (CyH/ EtOAc 95:5)

m.p.: Ambient temperature.

^{1}H-NMR (300 MHz, CDCl$_3$) δ$_H$/ppm: 7.38 − 7.31 (m, 2H, Ar<u>H</u>), 7.25 − 7.21 (m, 2H, Ar<u>H</u>), 3.86 (q, J = 7.1 Hz, 1H, ArC<u>H</u>), 2.91 − 2.72 (m, 2H, SC<u>H</u>$_2$), 1.52 (d, J = 7.1 Hz, 3H, ArCHC<u>H</u>$_3$), 1.58 − 1.46 (m, 2H, SCH$_2$C<u>H</u>$_2$(CH$_2$)$_4$CH$_3$), 1.31 (s, 9H, ArC(C<u>H</u>$_3$)$_3$), 1.38 − 1.16 (m, 8H, SCH$_2$CH$_2$(C<u>H</u>$_2$)$_4$CH$_3$), 0.86 (t, J = 6.8 Hz, 3H, SCH$_2$(CH$_2$)$_5$C<u>H</u>$_3$).

^{13}C-NMR (75 MHz, CDCl$_3$) δ$_C$/ppm: 201.6 (q), 150.2 (q), 136.9 (q), 127.5 (+), 125.6 (+), 53.8 (+), 31.7 (−), 31.4 (+), 29.4 (−), 29.1 (−), 28.81 (−), 28.78 (−), 22.6 (−), 18.5 (+), 14.1 (+).

FT-IR (ATR) $\tilde{\nu}$ (cm^{-1}): 2960 (s, sh), 2930 (s, sh), 2855 (m, sh), 1685 (s, sh), 1461 (m, br), 1364 (m, sh), 999 (m, sh), 943 (s, sh), 835 (m, sh), 768 (m, sh).

GC-MS (EI): t$_R$ = 9.79 min, m/z = 161 (100, [M+•]-[•COSHept], 146 (10, [M+•]-[•COSHept]-[•CH$_3$]), 320 (1, [M+•]).

HR-MS (EI): m/z = [M+•] calc. for C$_{20}$H$_{32}$OS 320.2168, found 320.2160.

S-Heptyl 2-(4-hydroxyphenyl)propanethioate (**68**)
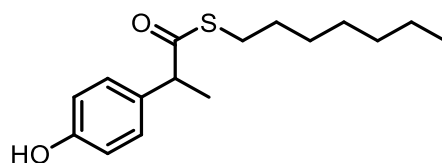
68

A flame dried RBF was treated with 4-acetoxysyrene (155 µL, 1.01 mmol, 1.0 eq.) which was dissolved in THF$_{dry}$ (2 mL) and was chilled in an ice bath. Afterwards, a degassed solution of sodium hydroxide (102 mg, 2.53 mmol, 2.5 eq) in water (0.5 mL) was added dropwise to the styrene solution and was stirred of 4 h. The reaction mixture was neutralized with HCl (2.5 mL, 1 M) and water (4 mL). The mixture was extracted with diethyl ether (2 x 5 mL). The combined organic phases were washed with brine (2 x 50 mL), dried over MgSO$_4$, DCE (790 µL) was added via syringe and diethyl ether and THF were removed under reduced pressure.

GP C was used to carbonylate 4-hydroxysyrene with 1.0 mol% catalyst and dist. HeptSH (210 µL, stored under N$_2$, 1.34 eq) as a thiol component at RT by adding the DCE/4-hydroxysyrene solution directly to chamber B. No further CH$_2$Cl$_2$ was used.

Purification by column chromatography (gradient CyH → CyH/ EtOAc 95:5) provided **68** as a bright yellow liquid (137 mg, 488 µmol, 48%)). Additionally, also the the acetylated product **64** was isolated as a bright yellow oil (91 mg, 283 µmol, 28%).

C$_{16}$H$_{24}$O$_2$S (280.43 g/mol)

R$_f$: 0.47 (CyH/ EtOAc 80:20)

m.p.: Ambient temperature.

^{1}H-NMR (300 MHz, CDCl3) δH/ppm: 7.17 – 7.09 (m, 2H, Ar<u>H</u>), 6.78 – 6.71 (m, 2H, Ar<u>H</u>), 4.85 (br, s, 1H, O<u>H</u>), 3.76 (q, J = 7.1 Hz, 1H, ArC<u>H</u>), 2.85 – 2.68 (m, 2H, SC<u>H$_2$</u>), 1.52 – 1.41 (m, 5H, ArCHC<u>H$_3$</u>, SCH$_2$C<u>H$_2$</u>(CH$_2$)$_4$CH$_3$), 1.31 – 1.10 (m, 8H, SCH$_2$CH$_2$(C<u>H$_2$</u>)$_4$CH$_3$), 0.82 (t, J = 6.8 Hz, 3H, SCH$_2$(CH$_2$)$_5$C<u>H$_3$</u>).

^{13}C-NMR (101 MHz, CDCl3) δC/ppm: 201.9 (q), 154.9 (q), 132.3 (q), 129.2 (+), 115.5 (+), 53.4 (+), 31.7 (–), 29.4 (–), 29.1 (–), 28.80 (–), 28.76 (–), 22.6 (–), 18.5 (+), 14.1 (+).

FT-IR (ATR) $\tilde{v}$ (cm^{-1}): 3399 (m, br), 2926 (s, br), 2855 (m, sh), 1655 (s, br), 1614 (m, sh), 1513 (s, sh), 1446 (m, sh), 1215 (s, br), 947 (s, sh), 835 (s, sh), 764 (m, sh).

GC-MS (CI): t$_R$ = 9.749 min, m/z = 281 (100, [MH+]), 121 (64, [MH+]-[•COSHept]).

HR-MS (APCI): m/z = [MH$^+$] calc. for C$_{16}$H$_{25}$O$_2$S 281.1570, found 281.1581.

<u>S-Heptyl 2-(4-fluorophenyl)propanethioate (**71**)</u>
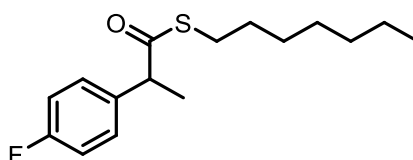
71

GP C was used to carbonylate dist. *para*-fluorostyrene (120 μL, 1.01 mmol) with 1.0 mol% catalyst and dist. HeptSH (210 μL, stored under N$_2$, 1.34 eq) as a thiol component at RT.

Purification by column chromatography (gradient CyH → CyH/ EtOAc 95:5) provided **71** as a bright yellow oil (257 mg, zz μmol, 91%).

C$_{16}$H$_{23}$FOS (282.42 g/mol)

R$_f$: 0.48 (CyH/ EtOAc 95:5)

m.p.: Ambient temperature.

^{1}H-NMR (300 MHz, CDCl$_3$) δ$_H$/ppm: 7.32 – 7.22 (m, 2H, Ar<u>H</u>), 7.07 – 6.96 (m, 2H, Ar<u>H</u>), 3.86 (q, J = 7.1 Hz, 1H, ArCHC<u>H$_3$</u>), 2.90 – 2.74 (m, 2H, SC<u>H$_2$</u>), 1.51 (d, J = 7.1 Hz, 3H, ArCHC<u>H$_3$</u>), 1.57 – 1.45 (m, 2H, SCH$_2$C<u>H$_2$</u>(CH$_2$)$_4$CH$_3$), 1.34 – 1.18 (m, 8H, SCH$_2$CH$_2$(C<u>H$_2$</u>)$_4$CH$_3$), 0.86 (t, J = 6.7 Hz, 3H, SCH$_2$(CH$_2$)$_5$C<u>H$_3$</u>).

^{13}C-NMR (75 MHz, CDCl$_3$) δ$_C$/ppm: 201.2 (q), 162.1 (doublet, J = 245.8 Hz, q), 135.7 (doublet, J = 3.3 Hz, q), 129.4 (doublet, J = 8.0 Hz, +), 115.5 (doublet, J = 21.4 Hz, +), 53.4 (+), 31.7 (–), 29.4 (–), 29.1 (–), 28.8 (–), 22.6 (–), 18.6 (+), 14.1 (+).

^{19}F-NMR (282 MHz, CDCl$_3$) δ$_C$/ppm: - 115.8 (CF).

FT-IR (ATR) $\tilde{v}$ (cm^{-1}): 2930 (s, br), 2855 (m, sh), 1681 (s, sh), 1603 (w, sh), 1510 (s, sh), 1457 (m, br), 1226 (s, sh), 1159 (m, sh), 999 (m, sh), 947 (s, sh), 835 (s, sh), 760 (s, sh).

GC-MS (EI): t_R = 8.347 min, m/z = 123 (100, [M+•]-[•COSHept], 184 (3, [M+•]-[•Hept]).

HR-MS (EI): m/z = [M+•] calc. for $C_{16}H_{23}FOS$ 282.1448, found 282.1444.

S-Heptyl 2-(4-chlorophenyl)propanethioate (**72**)
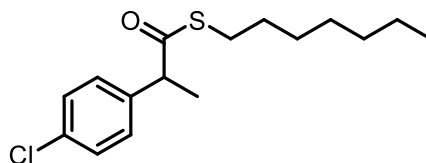
72

GP C was used to carbonylate dist. *para*-chlorostyrene (120 μL, 1.00 mmol) with 1.0 mol% catalyst and dist. HeptSH (210 μL, stored under N_2, 1.34 eq) as a thiol component at RT. Purification by column chromatography (gradient CyH → CyH/ EtOAc 95:5) provided **72** as a bright yellow oil (242 mg, 811 μmol, 81%).

$C_{16}H_{23}ClOS$ (298.87 g/mol)

R_f: 0.51 (CyH/ EtOAc 95:5)

m.p.: Ambient temperature.

¹H-NMR (300 MHz, $CDCl_3$) δ_H/ppm: 7.32 – 7.22 (m, 4H, ArH), 3.85 (q, J = 7.1 Hz, 1H, ArCH), 2.82 (m, 2H, SCH₂), 1.50 (d, J = 7.1 Hz, 3H, ArCHCH₃), 1.55 – 1.47 (m, 2H, SCH₂CH₂(CH₂)₄CH₃), 1.33 – 1.18 (m, 8H, SCH₂CH₂(CH₂)₄CH₃), 0.86 (t, J = 6.8 Hz, 3H, SCH₂(CH₂)₅CH₃).

¹³C-NMR (75 MHz, $CDCl_3$) δ_C/ppm: 200.9 (q), 138.5 (q), 133.3 (q), 129.2 (+), 128.8 (+), 53.6 (+), 31.7 (−), 29.4 (−), 29.2 (−), 28.8 (−), 22.6 (−), 18.5 (+), 14.1 (+).

FT-IR (ATR) $\tilde{v}$ (cm⁻¹): 2926 (s, sh), 2855 (m, sh), 1685 (s, sh), 1491 (s, sh), 1457 (m, br), 1092 (s, sh), 943 (s, br), 821 (s, sh), 757 (s, sh).

GC-MS (EI): t_R = 9.329 min, m/z = 139 (100, [M+•]-[•COSHept], 103 (24, [M+•]-[•COSHept]-[HCl]).

HR-MS (EI): m/z = [M+•] calc. for $C_{16}H_{23}ClOS$ 298.1153, found 298.1155.

S-Heptyl 2-(4-bromophenyl)propanethioate (**73**)
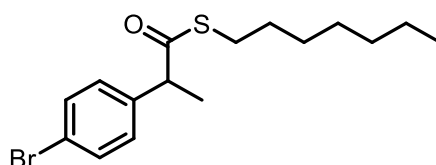
73

GP C was used to carbonylate dist. *para*-bromostyrene (130 μL, 1.00 mmol) with 1.0 mol% catalyst and dist. HeptSH (210 μL, stored under N_2, 1.34 eq) as a thiol component at RT.

Purification by column chromatography (gradient CyH → CyH/ EtOAc 95:5) provided **73** as a bright yellow oil (248 mg, 722 μmol, 72%).

$C_{16}H_{23}BrOS$ (343.32 g/mol)

R$_f$: 0.46 (CyH/ EtOAc 95:5)

m.p.: Ambient temperature.

^{1}H-NMR (300 MHz, CDCl$_3$) δ_H/ppm: 7.49 – 7.42 (m, 2H, Ar$\underline{H}$), 7.22 – 7.15 (m, 2H, Ar$\underline{H}$), 3.84 (q, J = 7.1 Hz, 1H, ArCHC$\underline{H_3}$), 2.81 (m, 2H, SC$\underline{H_2}$), 1.50 (d, J = 7.1 Hz, 3H, ArCHC$\underline{H_3}$), 1.55 – 1.46 (m, 2H, SCH$_2$C$\underline{H_2}$(CH$_2$)$_4$CH$_3$), 1.34 – 1.18 (m, 8H, SCH$_2$CH$_2$(C$\underline{H_2}$)$_4$CH$_3$), 0.86 (t, J = 6.8 Hz, 3H, SCH$_2$(CH$_2$)$_5$C$\underline{H_3}$).

^{13}C-NMR (75 MHz, CDCl$_3$) δ_C/ppm: 200.8 (q), 139.0 (q), 131.8 (+), 129.6 (+), 121.4 (q), 53.7 (+), 31.7 (–), 29.4 (–), 29.2 (–), 28.8 (–), 22.6 (–), 18.4 (+), 14.1 (+).

FT-IR (ATR) $\tilde{v}$ (cm^{-1}): 2926 (s, br), 2855 (m, sh), 1685 (s, sh), 1487 (s, sh), 1457 (m, sh), 1074 (s, sh), 1010 (s, br), 947 (s, sh), 828 (s, sh), 753 (s, sh).

GC-MS (CI): t$_R$ = 9.683 min, m/z = 343 (97, [MH+]), 183 (26, [MH+]-[•COSHept).

HR-MS (APCI): m/z = [MH$^+$] calc. for $C_{16}H_{24}BrOS$ 343.0726, found 343.0727.

S-Heptyl 2-(6-methoxynaphthalen-2-yl)propanethioate (**80**)
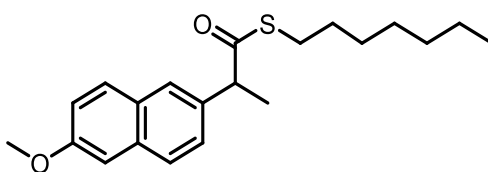
80

GP C was used to carbonylate 2-methoxy-6-vinylnaphthalene[35] (184 mg, 1.00 mmol) with 1.0 mol% catalyst and dist. HeptSH (210 μL, stored under N$_2$, 1.34 eq) as a thiol component at RT.
Purification by column chromatography (gradient CyH → CyH/ EtOAc 95:5) provided **80** as a as a white solid (317 mg, 919 μmol, 92%).

$C_{21}H_{28}O_2S$ (344.51 g/mol)

R$_f$: 0.32 (CyH/ EtOAc 95:5)

m.p.: Ambient temperature.

^{1}H-NMR (400 MHz, CDCl$_3$) δ_H/ppm: 7.74 – 7.66 (m, 3H, Ar$\underline{H}$), 7.40 (dd, J = 8.5, 1.8 Hz, 1H, Ar$\underline{H}$), 7.17 – 7.10 (m, 2H, Ar$\underline{H}$), 4.01 (q, J = 7.1 Hz, 1H, ArC$\underline{H}$), 3.92 (s, 3H, ArOC$\underline{H_3}$), 2.90 – 2.75 (m, 2H, SC$\underline{H_2}$), 1.60 (d, J = 7.1 Hz, 3H, ArCHC$\underline{H_3}$), 1.57 – 1.47 (m, 2H, SCH$_2$C$\underline{H_2}$(CH$_2$)$_4$CH$_3$), 1.35 – 1.15 (m, 8H, SCH$_2$CH$_2$(C$\underline{H_2}$)$_4$CH$_3$), 0.85 (t, J = 6.9 Hz, 3H, SCH$_2$(CH$_2$)$_5$C$\underline{H_3}$).

^{13}C-NMR (101 MHz, CDCl$_3$) δ_C/ppm: 201.5 (q), 157.8 (q), 135.2 (q), 133.9 (q), 129.4 (+), 129.0 (q), 127.2 (+), 126.6 (+), 126.5 (+), 119.0 (+), 105.7 (+), 55.3 (+), 54.3 (+), 31.7 (–), 29.4 (–), 29.2 (–), 28.80 (–), 28.77 (–), 22.6 (–), 18.5 (+), 14.1 (+).

FT-IR (ATR) $\tilde{v}$ (cm^{-1}): 2926 (m, br), 2855 (w, sh), 1681 (s, sh), 1607 (m, sh), 1461 (m, sh), 1390 (m, sh), 1267 (s, sh), 1033 (m, sh), 947 (s, sh), 850 (m, sh).

HR-MS (APCI): m/z = [MH$^+$] calc. for $C_{21}H_{29}O_2S$ 345.1883, found 345.1891.

<u>3-Methylbenzofuran-2(3H)-one (**76**)</u>
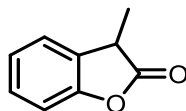
76

GP C was used to carbonylate dist. *ortho*-vinylphenol (121 mg, 1.00 mmol) with 1.0 mol% catalyst and dist. HeptSH (210 µL, stored under N$_2$, 1.34 eq) as a thiol component at RT.

Purification by column chromatography (gradient CyH → CyH/ EtOAc 95:5) provided **76** as a bright yellow oil (82.3 mg, 556 µmol, 56%).

$C_9H_8O_2$ (148.16 g/mol)

R$_f$: 0.18 (CyH/ EtOAc 95:5)

m.p.: Ambient temperature.

^{1}H-NMR (300 MHz, CDCl$_3$) δ_H/ppm: 7.35 – 7.23 (m, 2H, Ar<u>H</u>), 7.19 – 7.06 (m, 2H, Ar<u>H</u>), 3.74 (q, J = 7.6 Hz, 1H, ArC<u>H</u>), 1.58 (d, J = 7.6 Hz, 3H, ArCHC<u>H</u>$_3$).

^{13}C-NMR (75 MHz, CDCl$_3$) δ_C/ppm: 178.0 (q), 153.5 (q), 128.8 (q), 128.8 (+) 124.2 (+), 123.9 (+), 110.8 (+), 38.4 (+), 15.9 (+).

2.4.3.4. Hydrothiolation control experiments

Under inert conditions with a dtbpx/Pd/DPPA system, the presence of only one or two catalyst components usually gives a decreased yield (Table 4, entries 2-7) whereas if no catalyst components are present thioether is obtained in low yield (Table 4, entry 1), possibly due to the presence of trace oxygen brought in during reaction set-up. If all the catalytic components are present under strictly inert conditions, no thioether is formed (Table 4, entry 8). The same applies to the dppdtbpf (**L2**)/Pd/DPPA system (Table 4, entries 9-10). We never found the corresponding branched thioether, which hints at the classical hydrothiolation pathway *via* a stabilized benzyl radical intermediate.

We additionally screened for metal-catalyzed hydrothiolation activity in air by using inhibitor-containing styrene (Sigma-Aldrich reagent grade plus) which slows down any radical chain mechanism. We obtained only a low yield of the thioether using our standard hydrothioesterification conditions (however in air in a pressure tube) when no catalyst was present (Table 4, entry 11).   A higher yield was obtained when all catalyst components were present (Table 4, entry 12). A ligand screening (not shown) did not give any improved results. We found that the same result could be obtained with palladium acetate (Table 4, entry 13). A solvent screening revealed that polar solvents increased the yield (not shown), the best being alcoholic solvents. At higher temperatures, the yield further increased (Table 4, entry 13), however it seems that the background reaction without any catalyst component is fast enough at this temperature (Table 4, entry 14) and becomes preparatively useful at 80 °C (Table 4, entry 15). We interpret this as follows: A metal-catalyzed hydrothiolation pathway might be operative at lower temperatures with oxygen concentrations found in air whereas trace oxygen as found under "inert" conditions (even with inhibitor-free styrene) is not sufficient for such a reaction. At higher temperatures, the oxygen-initiated radical-chain hydrothiolation pathway is sufficiently fast enough to outcompete any metal-catalyzed hydrothiolation even in the presence of inhibitor. We did not exclude the possibility of other trace metals found in commercial palladium acetate or Pd(dba)$_2$ being responsible for hydrothiolation activity.

Supplementary Table 1: Hydrothiolation of styrene with heptanethiol under different conditions as shown below.

$$HS(CH_2)_6CH_3 \xrightarrow{\text{[conditions]}} C_6H_5CH_2CH_2S(CH_2)_6CH_3$$
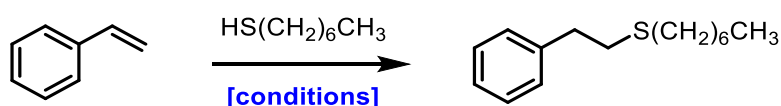
	[Pd]	L	HX	T (°C)	Solv.	t (h)	eqv. RSH	c. (%)[a]	y. (%)[a]	remarks
1	-	-	-	RT	DCM	24	1.0	54	**8**	dist Styrene, dist HeptSH, dry CH$_2$Cl$_2$
2	-	-	7.5 mol% DPPA	RT	CH$_2$Cl$_2$	24	1.0	52	**3**	dist Styrene, dist HeptSH, dry CH$_2$Cl$_2$
3	-	2 mol % (**L1**)	-	RT	CH$_2$Cl$_2$	24	1.0	53	**7**	dist Styrene, dist HeptSH, dry CH$_2$Cl$_2$
4	0.5 mol% Pd(dba)$_2$	-	-	RT	CH$_2$Cl$_2$	24	1.0	63	**6**	dist Styrene, dist HeptSH, dry CH$_2$Cl$_2$
5	-	2 mol % (**L1**)	7.5 mol% DPPA	RT	CH$_2$Cl$_2$	24	1.0	57	**3**	dist Styrene, dist HeptSH, dry CH$_2$Cl$_2$
6	0.5 mol% Pd(dba)$_2$	2 mol % (**L1**)	-	RT	CH$_2$Cl$_2$	24	1.0	56	**9**	dist Styrene, dist HeptSH, dry CH$_2$Cl$_2$
7	0.5 mol% Pd(dba)$_2$	-	7.5 mol% DPPA	RT	CH$_2$Cl$_2$	24	1.0	48	**2**	dist Styrene, dist HeptSH, dry CH$_2$Cl$_2$
8	0.5 mol% Pd(dba)$_2$	2 mol	7.5 mol% DPPA	RT	CH$_2$Cl$_2$	24	1.0	46	**0**	dist Styrene, dist HeptSH, dry CH$_2$Cl$_2$

	[Pd]	L	HX	T (°C)	Solv.	t (h)	eqv. RSH	c. (%)[a]	y. (%)[a]	remarks
		% (L1)								
9[b]	1.0 mol% Pd(dba)$_2$	4 mol % (L2)	15 mol% DPPA	RT	CH$_2$Cl$_2$	18	1.34	41	**0**	dist Styrene, dist HeptSH, dry CH$_2$Cl$_2$
10[b]	1.0 mol% Pd(dba)$_2$	4 mol % (L2)	-	RT	CH$_2$Cl$_2$	18	1.34	37	**1**	dist Styrene, dist HeptSH, dry CH$_2$Cl$_2$
11[c]	-	-	-	RT	CH$_2$Cl$_2$	18	1.34	19	**2**	Styrene + inhibitor, undist. HeptSH, "wet" CH$_2$Cl$_2$
12[c]	0.5 mol% Pd(dba)$_2$	2 mol % (L2)	7.5 mol% DPPA	RT	CH$_2$Cl$_2$	18	1.34	31	**10**	Styrene + inhibitor, undist. HeptSH, "wet" CH$_2$Cl$_2$
13[c]	0.5 mol% Pd(OAc)$_2$	2 mol % (L2)	7.5 mol% DPPA	RT	CH$_2$Cl$_2$	18	1.34	33	**10**	Styrene + inhibitor, undist. HeptSH, "wet" CH$_2$Cl$_2$
14[c]	0.5 mol% Pd(OAc)$_2$	2 mol % (L2)	7.5 mol% DPPA	50	iPrOH	18	1.34	57	**48**	Styrene + inhibitor, undist. HeptSH, "wet" iPrOH
15[c]	-	-	-	50	iPrOH	18	1.34	58	**49**	Styrene + inhibitor,

	[Pd]	L	HX	T (°C)	Solv.	t (h)	eqv. RSH	c. (%)[a]	y. (%)[a]	remarks
										undist. HeptSH, "wet" iPrOH
16[c]	-	-	-	80	iPrOH	18	1.34	95	**79**	Styrene + inhibitor, undist. HeptSH, "wet" iPrOH

Unless otherwise noted, reactions were carried out in argon-filled septum-capped vials using 1 mmol of styrene. Solid catalyst components were placed into the glass vials and then dissolved in CH$_2$Cl$_2$ (to give a 1 M solution of the styrene) and stirred for 2 min. Then, styrene and heptanethiol were added under Argon via the septum. Inhibitor means 4-*tert*-butyl catechol in the levels present in a bottle from Sigma-Aldrich (Reagent plus grade, >99%). [a]: Determined by quantitative GC-FID analysis. [b]: Carried out with Schlenk technique under argon. [c]: Carried out under air in a pressure tube.

2.5. References

[1]   G. Kiss, *Chemical Reviews* **2001**, *101*, 3435-3456.

[2]   W. Reppe, *Justus Liebigs Annalen der Chemie* **1953**, *582*, 1-37.

[3]   G. Cavinato, L. Toniolo, *Molecules* **2014**, *19*, 15116.

[4]   a) K. Dong, X. Fang, S. Gülak, R. Franke, A. Spannenberg, H. Neumann, R. Jackstell, M. Beller, *Nature Communications* **2017**, *8*, 14117; b) K. Dong, R. Sang, X. Fang, R. Franke, A. Spannenberg, H. Neumann, R. Jackstell, M. Beller, *Angewandte Chemie* **2017**, *129*, 5351-5355.

[5]   a) T. Ueda, H. Konishi, K. Manabe, *Angewandte Chemie International Edition* **2013**, *52*, 8611-8615; b) T. Ueda, H. Konishi, K. Manabe, *Organic Letters* **2013**, *15*, 5370-5373; c) P. Gautam, P. Kathe, B. M. Bhanage, *Green Chemistry* **2017**, *19*, 823-830.

[6]   a) S. D. Friis, A. T. Lindhardt, T. Skrydstrup, *Accounts of Chemical Research* **2016**, *49*, 594-605; b) P. Hermange, A. T. Lindhardt, R. H. Taaning, K. Bjerglund, D. Lupp, T. Skrydstrup, *Journal of the American Chemical Society* **2011**, *133*, 6061-6071.

[7]   K. Dong, R. Sang, J. Liu, R. Razzaq, R. Franke, R. Jackstell, M. Beller, *Angewandte Chemie International Edition* **2017**, *56*, 6203-6207.

[8]   Y. Wang, L. Zhu, Y. Zhang, R. Hong, *Angewandte Chemie International Edition* **2011**, *50*, 2787-2790.

[9]   a)G. J. Harkness, M. L. Clarke, *European Journal of Organic Chemistry* **2017**, *2017*, 4859-4863; b) T. M. Konrad, J. A. Fuentes, A. M. Z. Slawin, M. L. Clarke, *Angewandte Chemie International Edition* **2010**, *49*, 9197-9200.

[10]   B. M. Trost, L. C. Czabaniuk, *Angewandte Chemie International Edition* **2014**, *53*, 2826-2851.

[11]   W.-J. Xiao, G. Vasapollo, H. Alper, *The Journal of Organic Chemistry* **1998**, *63*, 2609-2612.

[12]   a) W.-J. Xiao, G. Vasapollo, H. Alper, *The Journal of Organic Chemistry* **2000**, *65*, 4138-4144; b) W.-J. Xiao, H. Alper, *The Journal of Organic Chemistry* **2001**, *66*, 6229-6233.

[13]   W.-J. Xiao, H. Alper, *The Journal of Organic Chemistry* **1998**, *63*, 7939-7944.

[14]   C.-F. Li, W.-J. Xiao, H. Alper, *The Journal of Organic Chemistry* **2009**, *74*, 888-890.

[15]   a) P. Foley, **1983**; b) E. Drent, **1990**.

[16]   S. D. Friis, R. H. Taaning, A. T. Lindhardt, T. Skrydstrup, *Journal of the American Chemical Society* **2011**, *133*, 18114-18117.

[17]   a) D. B. Nielsen, B. A. Wahlqvist, D. U. Nielsen, K. Daasbjerg, T. Skrydstrup, *ACS Catalysis* **2017**, *7*, 6089-6093; b) C. Lescot, D. U. Nielsen, I. S. Makarov, A. T. Lindhardt, K. Daasbjerg, T. Skrydstrup, *Journal of the American Chemical Society* **2014**, *136*, 6142-6147.

[18]   P. Nordeman, L. R. Odell, M. Larhed, *The Journal of Organic Chemistry* **2012**, *77*, 11393-11398.

[19]   S. N. Gockel, K. L. Hull, *Organic Letters* **2015**, *17*, 3236-3239.

[20]   M. Markovič, P. Lopatka, P. Koóš , T. Gracza, *ChemistrySelect* **2016**, *1*, 2454-2457.

[21]   a) S. V. F. Hansen, T. Ulven, *Organic Letters* **2015**, *17*, 2832-2835; b) M. Markovič, P. Lopatka, P. Koóš, T. Gracza, *Organic Letters* **2015**, *17*, 5618-5621.

[22]   C. Veryser, S. Van Mileghem, B. Egle, P. Gilles, W. M. De Borggraeve, *Reaction Chemistry & Engineering* **2016**, *1*, 142-146.

[23]   T. Cochet, V. Bellosta, A. Greiner, D. Roche, J. Cossy, *Synlett* **2011**, *2011*, 1920-1922.

[24]   M. F. Hideyuki Konishi, Tsuyoshi Ueda, Kei Manabe, Jordan C. Beck, Sarah E. Reisman, *Organic Synthesis* **2017**, *94*, 66-76.

[25]   H. Yazawa, S. Goto, *Tetrahedron Letters* **1985**, *26*, 3703-3706.

[26]   S. Itagaki, K. Yamaguchi, N. Mizuno, *Journal of Molecular Catalysis A: Chemical* **2013**, *366*, 347-352.

[27]   V. Hirschbeck, I. Fleischer, *Chemistry − A European Journal* **2018**, *24*, 2854-2857.

[28]   a) I. Fleischer, R. Jennerjahn, D. Cozzula, R. Jackstell, R. Franke , M. Beller, *ChemSusChem* **2013**, *6*, 417-420; b) Q. Liu, K. Yuan, P.-B. Arockiam, R. Franke, H. Doucet, R. Jackstell, M. Beller, *Angewandte Chemie International Edition* **2015**, *54*, 4493-4497.

[29]   H. Ooka, T. Inoue, S. Itsuno, M. Tanaka, *Chemical Communications* **2005**, 1173-1175.

[30]   V. Hirschbeck, P. H. Gehrtz, I. Fleischer, *Chemistry − A European Journal* **2018**, *24*, 7092-7107.

[31]   S. Kaur, G. Zhao, E. Busch, T. Wang, *Organic & Biomolecular Chemistry* **2018**.

[32]   a) E. L. Tyson, M. S. Ament, T. P. Yoon, *The Journal of Organic Chemistry* **2013**, *78*, 2046-2050;
         b) M. H. Keylor, J. E. Park, C.-J. Wallentin, C. R. J. Stephenson, *Tetrahedron* **2014**, *70*, 4264-
         4269; c) H. Liu, H. Chung, *ACS Sustainable Chemistry & Engineering* **2017**, *5*, 9160-9168; dM.
         Teders, C. Henkel, L. Anhäuser, F. Strieth-Kalthoff, A. Gómez-Suárez, R. Kleinmans, A. Kahnt, A.
         Rentmeister, D. Guldi, F. Glorius, *Nature Chemistry* **2018**, *10*, 981-988.

[33]   T. Posner, *Berichte der deutschen chemischen Gesellschaft* **1905**, *38*, 646-657.

[34]   C. Holzapfel, T. Bredenkamp, *ChemCatChem* **2015**, *7*, 2598-2606.

[35]   V. Hirschbeck, University of Regensburg (Regensburg), **2018**.

[36]   a) G. R. Eastham, B. T. Heaton, J. A. Iggo, R. P. Tooze, R. Whyman, S. Zacchini, *Chemical
         Communications* **2000**, 609-610; b) G. R. Eastham, R. P. Tooze, M. Kilner, D. F. Foster, D. J. Cole-
         Hamilton, *Journal of the Chemical Society, Dalton Transactions* **2002**, 1613-1617; c) R. P. Tooze,
         K. Whiston, A. P. Malyan, M. J. Taylor, N. W. Wilson, *Journal of the Chemical Society, Dalton
         Transactions* **2000**, 3441-3444.

[37]   P. Roesle, L. Caporaso, M. Schnitte, V. Goldbach, L. Cavallo, S. Mecking, *Journal of the American
         Chemical Society* **2014**, *136*, 16871-16881.

[38]   B. M. Trost, *Chemistry – A European Journal* **1998**, *4*, 2405-2412.

[39]   W. Clegg, G. R. Eastham, M. R. J. Elsegood, B. T. Heaton, J. A. Iggo, R. P. Tooze, R. Whyman, S.
         Zacchini, *Journal of the Chemical Society, Dalton Transactions* **2002**, 3300-3308.

[S1]   I. R. Butler, W. R. Cullen, T. J. Kim, S. J. Rettig, J. Trotter, *Organometallics* **1985**, *4*, 972-980.

[S2]   T. Fanjul, G. Eastham, J. Floure, S. J. K. Forrest, M. F. Haddow, A. Hamilton, P. G. Pringle, A. G.
         Orpen, M. Waugh, *Dalton Trans.* **2013**, *42*, 100-115.

[S3]   J. T. Christl, P. Roesle, F. Stempfle, P. Wucher, I. Göttker-Schnetmann, G. Müller, S. Mecking,
         Chemistry - A European Journal **2013**, *19*, 17131-17140.

[S4]   G. R. Fulmer, A. J. M. Miller, N. H. Sherden, H. E. Gottlieb, A. Nudelman, B. M. Stoltz, J. E.
         Bercaw and K. I. Goldberg, *Organometallics*, 2010, **29**, 2176-2179.

[S5]   S. Itagaki, K. Yamaguchi and N. Mizuno, *J. Mol. Catal. A: Chem.*, 2013, **366**, 347-352.

[S6]   A. Jansen and S. Pitter, *J. Mol. Catal. A: Chem.*, 2004, **217**, 41-45.

[S7]   T. Cochet, V. Bellosta, A. Greiner, D. Roche and J. Cossy, *Synlett*, 2011, DOI: DOI 10.1055/s-
         0030-1260951, 1920-1922.

[S8]   S.-Y. Choi, S.-G. Lee, Y.-J. Yoon and K.-W. Kim, *J. Heterocycl. Chem.*, 1989, **26**, 1073-1076.

[S9]   H. Yazawa and S. Goto, *Tetrahedron Lett.*, 1985, **26**, 3703-3706.

[S10]   P. J. Black, M. G. Edwards and J. M. J. Williams, *Eur. J. Org. Chem.*, 2006, **2006**, 4367-4378.

[S11]   C. Kuhakarn, W. Panchan, S. Chiampanichayakul, N. Samakkanad, M. Pohmakotr, V. Reutrakul
         and T. Jaipetch, *Synthesis*, 2009, **2009**, 929-934.

[S12]   J. A. Fuentes, A. M. Z. Slawin and M. L. Clarke, *Catal. Sci. Tech.*, 2012, **2**, 715.

[S13]   M. Hayashi, H. Kawabata, K. Yoshimoto and T. Tanaka, *Phosphorus Sulfur Silicon Relat. Elem.*,
         2007, **182**, 433-445.

[S14]   I. Shiina, K. Nakata, K. Ono, Y.-s. Onda and M. Itagaki, *J. Am. Chem. Soc.*, 2010, **132**, 11629-
         11641.

[S15]   T. Ohshima, T. Iwasaki, Y. Maegawa, A. Yoshiyama and K. Mashima, *J. Am. Chem. Soc.*, 2008,
         130, 2944-2945.

[S16]   T. O. Vieira, M. J. Green and H. Alper, *Organic Letters*, 2006 **8**, 6143-6145.

[S17]   I. Masataka, M. Katsuhiko and T. Hideo, *Tetrahedron*, 2013 **69**, 2961-2970.

[S18]   M. Noji, H. Sunahara, K.-i. Tsuchiya, T. Mukai, A. Komasaka and K. Ishii, *Synthesis*, 2008, **2008**,
         3835-3845.

[S19]   M. L. Kantam, R. Chakravarti, V. R. Chintareddy, B. Sreedhar and S. Bhargava, *Adv. Synth. Catal.*,
         2008, **350**, 2544-2550.

[S20]   P. L. Smith, J. M. Keane, S. E. Shankman, M. D. Chordia and W. D. Harman, *J. Am. Chem. Soc.*,
         2004, **126**, 15543-15551.

[S21]   M. Amatore, C. Gosmini and J. Périchon, *J. Org. Chem.*, 2006, **71**, 6130-6134.

[S22]   C. M. Williams, J. B. Johnson and T. Rovis, *J. Am. Chem. Soc.*, 2008, **130**, 14936-14937.

[S23]   J. Louie, C. W. Bielawski and R. H. Grubbs, *J. Am. Chem. Soc.*, 2001, **123**, 11312-11313.

[S24]   J. M. Clough, R. V. H. Jones, H. McCann, D. J. Morris and M. Wills, *Org. Biomol. Chem.*, 2003, **1**, 1486-1497.

[S25]   K. Hino, H. Nakamure, S. Kato, A. Irie, Y. Nagai and H. Uno, *Chem. Pharm. Bull.*, 1988, **36**, 3462-3467.

[S25]   K. Kobayashi, Y. Yamamoto and N. Miyaura, *Organometallics*, 2011, **30**, 6323-6327.

[S26]   T. O. Vieira, M. J. Green and H. Alper, *Org. Lett.*, 2006, **8**, 6143-6145.

[S27]   U. Azzena, L. Pisano and M. Pittalis, *Appl. Organomet. Chem.*, 2008, **22**, 523-528.

[S28]   J. D. Hargrave, J. Herbert, G. Bish and C. G. Frost, *Org. Biomol. Chem.*, 2006, **4**, 3235-3241.

[S29]   A. Rioz-Martínez, A. Cuetos, C. Rodríguez, G. De Gonzalo, I. Lavandera, M. W. Fraaije and V. Gotor, *Angew. Chem. Int. Ed. Engl.*, 2011, **50**, 8387-8390.

[S30]   S. Karlsson, A. Hallberg and S. Gronowitz, *Journal*, 1991, **403**, 133-144.

[S31]   L. Demange, D. Boeglin, A. Moulin, D. Mousseaux, J. Ryan, G. Bergé, D. Gagne, A. Heitz, D. Perrissoud, V. Locatelli, A. Torsello, J. C. Galleyrand, J. A. Fehrentz and J. Martinez, *J. Med. Chem.*, 2007, **50**, 1939-1957.

[S32]   A. H. Mermerian and G. C. Fu, *J. Am. Chem. Soc.*, 2005, **127**, 5604-5607.

[S33]   D. Marosvölgyi-Haskó, A. Petz, A. Takács and L. Kollár, *Tetrahedron*, 2011, **67**, 9122-9128.

[S34]   B. C. Zhu and X. Z. Jiang, *Appl. Organomet. Chem.*, 2006, **20**, 277-282.

[S35]   N. Kakusawa, S. Yasuike and J. Kurita, *Heterocycles*, 2009, **77**, 1269-1283.

[S36]   F. Zimmermann, E. Meux, J.-L. Mieloszynski, J.-M. Lecuire and N. Oget, *Tetrahedron Lett.*, 2005, **46**, 3201-3203.

[S37]   I. Fleischer, R. Jennerjahn, D. Cozzula, R. Jackstell, R. Franke and M. Beller, *ChemSusChem*, 2013, **6**, 417-420.

[S38]   R. Toubiana and J. Asselineau, *Ann. Chim. (Paris)*, 1962, **7**, 593-642.

[S39]   Z. Zhang, Z. Zha, C. Gan, C. Pan, Y. Zhou, Z. Wang and M. M. Zhou, *J. Org. Chem.*, 2006, **71**, 4339-4342.

[S40]   E. Alacid, C. Nájera, *J. Org. Chem.* **2008**, *73*, 2315-2322.

Published, peer-reviewed work has been used to assemble this chapter.

Section 3.1.2. is an extract of a review – the extracted part presented here:

Author	Author position	Scientific ideas %	Data generation %	Analysis & Interpretation %	Paper writing %
P.H. Gehrtz	Second	100% (of part)	Not applicable (review article)	100% (of part)	100% (of part)
V. Hirschbeck	First	0% (of part)	Not applicable (review article)	0% (of part)	0% (of part)
I. Fleischer	Supervisor				
Title of paper:		Metal-Catalyzed Synthesis and Use of Thioesters: Recent Developments (Section 3.1 was extracted) *Chem. Eur. J.* **2018**, 24, 7092			
Status in publication process:		Published			

The other sections (except for section 3.1.1., original work) are based on a research article:

Author	Author position	Scientific ideas %	Data generation %	Analysis & Interpretation %	Paper writing %
P.H. Gehrtz	First	95%	80%	80%	95%
P. Kathe	Second	5%	20%	20%	5%
I. Fleischer	Supervisor				
Title of paper:		Nickel-Catalyzed Coupling of Arylzinc Halides with Thioesters *Chem. Eur. J.* **2018**, 24, 8774			
Status in publication process:		Published			

3. Nickel-catalyzed coupling of aryl zinc halides with thioesters

3.1. Introduction

3.1.1. Properties and uses of thioesters

Thioesters are carboxylic acid derivatives, which are more reactive towards addition-elimination reactions than oxo-esters. Thus, the order of reactivity of carbonyl compounds towards nucleophiles is: amides < esters = carboxylic acids < thioesters < ketones < aldehydes < anhydrides < carboxylic acid halides. Along this reactivity order, the corresponding wavenumber of the C=O stretching IR-induced vibration increases as delocalization of C=O bond π electrons into the appended group decreases. Similarly, decreased delocalization strengthens the C=O bond by lesser donation of electrons from the appended group into the antibonding $\pi^*_{C=O}$ orbital. The problem with the delocalization argument is that oxygen atoms are more electronegative than sulfur atoms, giving the latter more power for delocalization and thus C-O bond weakening, which is not observed experimentally (Scheme 3.1, top).
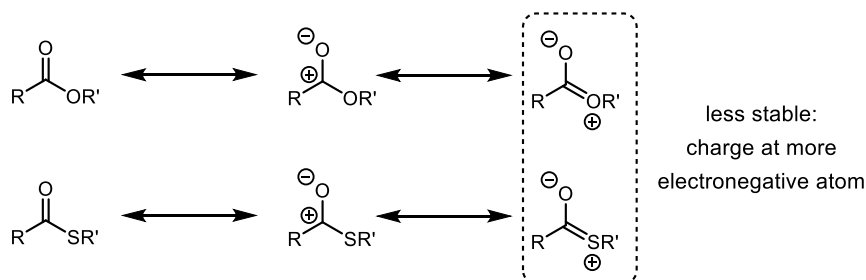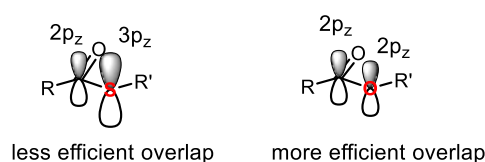
Scheme 3.1: Using a combination of mesomeric structures and electronegativity arguments, one arrives at a prediction of reactivity that is contradicted by experimental results (top). Using the hybrid orbital approach (and remaining non-hybridized atomic orbitals) the increased reactivity of thioesters relative to oxoesters is explained by a partially disrupted delocalization due to orbital size differences (bottom). In terms of mesomeric structure arguments, the right-hand side structure becomes less important in the thioester case.

For carboxylic acid derivatives, which react by addition-elimination (as opposed to simpler addition reactions of aldehydes and ketones), the leaving group ability of the attached group is also a decisive factor. The leaving group ability of anions is often judged by the acid strength of the conjugate acid, i.e. a strong acid will have a conjugate base of excellent leaving group ability. In fact, thiols are stronger acids than alcohols (when the organic appendages are the same). On a molecular level, the relatively better leaving group ability of the thiolate anion could be explained by better delocalization of a negative charge on the larger sulfur atom (compared to the oxygen atom).

A similar reasoning and conclusion is found in a purely orbital-based analysis (Scheme 3.1, bottom), based on the interaction of the sp^2-hybrid orbital of the carbonyl C-atom with the interaction of the sp^2-hybrid orbital of the appended group heteroatom. Since hybrid orbitals are linear combinations of atomic orbitals, both 3s- and 3p-type atomic orbitals are employed for the construction of the *S*-atom centered sp^2-hybrid orbital, whereas 2s- and 2p-type atomic orbitals are used for the construction of the *O*-atom centered sp^2-hybrid orbital. The latter sort of atomic orbital is smaller than the former type (i.e. in 90% density isosurface) and has one more node. Thus, the C-S sp^2-sp^2 hybrid orbital overlap will be less efficient than the C-O sp^2-sp^2 hybrid orbital overlap. The same applies to the overlap of the remaining p_z-orbitals of carbon and sulfur, which results in the decreased π-character of the C-S bond. This explains both the better leaving group ability of the thiolate (due to negative charge stabilization on the larger sp^3-hybrid orbital centered on the heteroatom, compared to the alkoxide) and the higher electrophilicity of the thioester (due to disrupted delocalization, compared to the ester). A $2p_z$ (on carbon) to 3d (on sulfur) interaction could also weaken the C=O bond, but such an interaction would have to rely on the correct orbital alignment as well as a favorable, small energetic difference between the 2p and 3d orbital, which is commonly thought to be not the case.

The disrupted delocalization also causes an increased acidity of the α-anions of thioesters, which can aid in the so-called soft-enolization of thioesters, which can also be exploited in the laboratory.[1] This property is used by the enzyme citrate synthase, where a catalytic histidine residue causes soft enolization of acetyl-S-CoA (coenzyme A) to trigger aldol chemistry. The final, irreversible hydrolysis (around 31.4 kJ mol^{-1} in acetyl-S-CoA) of the high energy C-S bond drives the equilibrium aldol reaction to the product side. The high energy associated with thioester hydrolysis, which is comparable in exergonicity to ATP hydrolysis, has led to theories, which implicate thioesters in the emergence of early life and/or prebiotic self-replicators. In short,[2] thioester formation would occur near hot (to overcome the endergonicity of the reaction) deep sea vents rich in H_2S (to facilitate thiol production). The reductive power necessary to explain the formation of H_2S could then be explained by an inorganic process, namely the oxidation of Fe^{2+} to Fe^{3+} (resulting in large deposits of iron oxides found today). In this way, the thioester world elegantly link to the so-called iron-sulfur world.[3] The so-formed thioesters could then have acted as precursors for the formation of esters, amides and polymers thereof (giving a possibility for abiotic protein synthesis), which is known to occur experimentally. More speculatively, acyl phosphates and aldehydes have been proposed as prebiotic products of thioesters by de Duve.[2] In this world-view of life emergence, thioesters are ancient relics in metabolic processes, much like the ribonucleic component in the ribosome is put forward by proponents of the RNA world.[4] However, due to lack of clear evidence pointing in only one direction, the thioester world and competing theories are under constant scrutiny and proponents of these theories engage in heated debates.

The comparison of such theories is beyond the scope of this thesis. It is however interesting to note, that many of the (pre)biotic reactions of thioesters have emerged as immensely useful laboratory reactions when catalyzed by transition metals (see sections below).[5] Thus, it is tempting to speculate that, should the thioester world theory be right, these reactions were likely catalyzed by transition metals, which would give an early prebiotic-chemical evolutionary advantage for faster (catalyzed) thioester-forming and breaking reactions. Besides utilization of thioesters in biological and synthetic aldol chemistry (both as nucleophiles and electrophiles), the transition-metal catalyzed activation of thioesters (leading to organometallic intermediates) in nature is not too common. In this context, it should be noted that a recent (2016) genetic analysis concluded that the last universal common ancestor likely utilized CO_2 (carbon source) and H_2 (reductant) in the established Wood-Ljungdahl pathway to generate acetyl-S-CoA by Nickel catalysis (acyl CoA synthase, coupled with CO dehydrogenase, see Scheme 3.2).[6] The reverse pathway is utilized by methanogenic bacteria, which then must include cleavage of the thioester bond by this Ni-containing enzyme.[7]

Acetyl CoA synthase (ACS) is a tetrameric protein with a total mass of 310 kDa.[7] The organometallic active site is called the A-cluster. It is a protein-complexed (through the backbone atoms and cysteine residues) assembly of a cubane-type $[Fe_4S_4]$-cluster, linked by a bridging thiolate (from a Cys residue) to the proximal Ni atom (termed Ni_p), which is in turn connected via bridging thiolates (again from Cys residues) to a distal Ni atom (termed Ni_d). Only Ni_p is catalytically active. Both diamagnetic ($Ni^{0/II}$ redox cycles) and paramagnetic ($Ni^{I/II/III}$) catalytic mechanisms are under discussion, but Ni(0) states are suspected to be improbable under physiological conditions and near other electropositive metal centers in the cluster.[7] The paramagnetic mechanism is depicted (Scheme 3.2). The A-cluster is initially reduced at the proximal site from Ni(II) to Ni(I) (complex **A**), followed by recombination with an acetyl radical, which is generated from reductive cleavage of acetyl-S-CoA to regenerate a Ni(II) acetyl species **B**. This undergoes migratory deinsertion to give a Ni(II) methyl carbonyl species **C**, which is able to deliver the electron necessary for initial thioester reduction (internal SET), giving a Ni(III) methyl carbonyl intermediate (not shown). This intermediate undergoes a redox reaction with a Co(I) species (found in the corrinoid iron-sulfur protein, CFeSP) to give a Co(III) methyl species and a Ni(I) carbonyl species **D**. The Ni(I) carbonyl must undergo thermodynamically unfavourable ligand loss to restart the cycle.
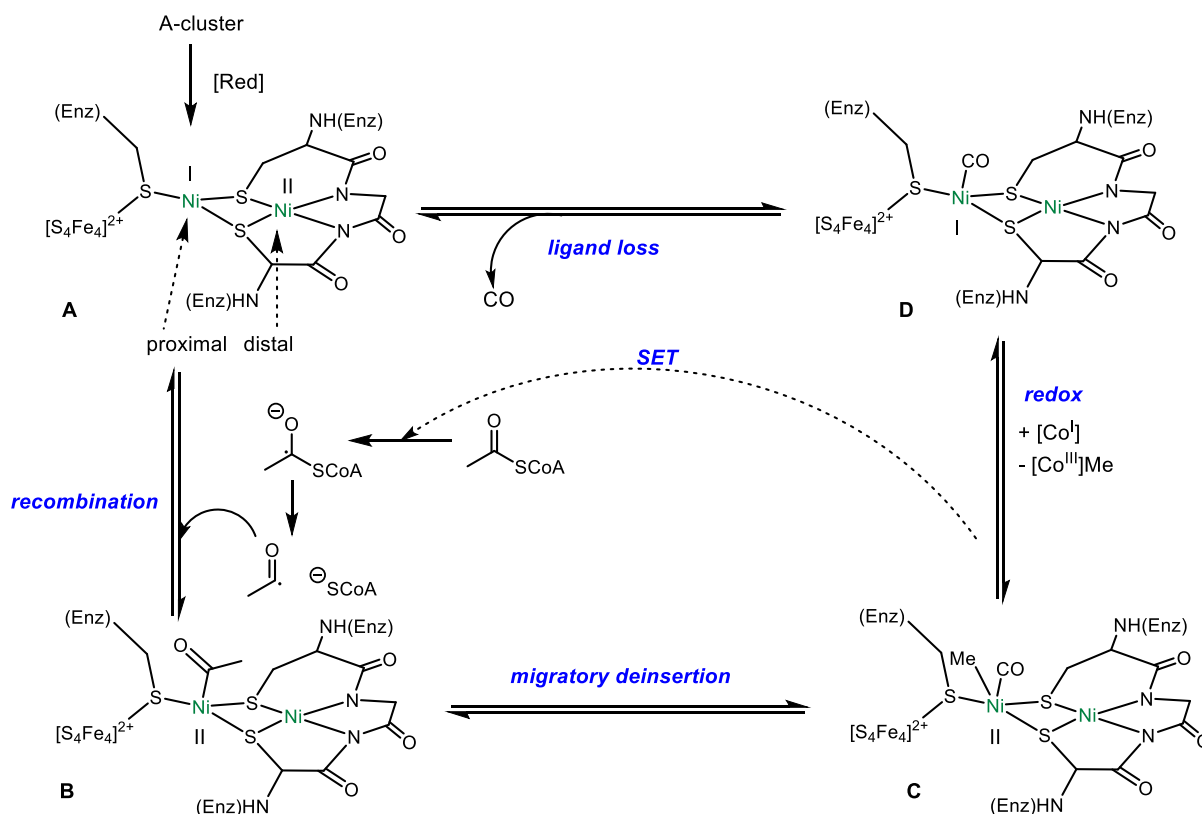
Scheme 3.2: Paramagnetic mechanism of Acetyl-CoA synthase in the unusual reversed direction utilized by methanogenic bacteria, which involves cleavage of acetyl-CoA by a Ni(I) species.

The complex enzymatic machinery capable of activation of thioesters using Ni-based organometallic chemistry is clearly an inspiration for developing Ni-based catalytic methods, which utilize thioesters in decarbonylative and CO-retentive couplings for the formation of C-C bonds. However, the synthesis of thioesters requires more energy than the synthesis of oxo-esters, and commonly active esters are employed for the synthesis of thioesters from a carboxylic acid and a thiol. Metal-catalyzed synthetic methods also offer active-ester-free routes towards thioesters, e.g. the oxidation of a thiol and an aldehyde to give a thioester and H_2,[8] or the hydrothioesterification of alkenes (Chapter 2),[9] among others.[5] Methods, which do not require covalent chemical energy for the dehydratization reaction would be highly attractive, e.g. coupling the activity of acylases with regeneratable molecular sieves to achieve thioesterification.[10]

3.1.2. Synthesis of ketones by reaction of thioesters with organometallic reagents

The reaction between selected organometallic reagents (d^1 type) and some carboxylic acid derivatives (a^1 reagents) can selectively furnish ketones (Scheme 3.3). The general text book known challenge is that the formed ketones are usually more reactive and often alcohols are formed as main products. Compounds such as Weinreb amide[11] **1** or Staab-Jost imidazolide[12] **2** are examples of amides that furnish ketones with Grignard reagents in the absence of any catalyst due to the formation of a chelate intermediate. Thioesters **3** constitute attractive alternatives to these compounds. While the

significantly more activated *S*-(2-pyridyl)thioesters, which presumably can also form a stoichiometric chelate,[13] fall partially into the area of classical a^1 reagents, other thioesters can be employed in the presence of a transition metal catalyst. In this case, two mechanistic scenarios are plausible: low-valent transition metal species undergo oxidative addition into the C-S bond (Scheme 3.3, A) or the thioester is the acceptor in a single electron transfer (SET) event (Scheme 3.3, B). It should be noted that a DFT-based computational comparison of C-S bond dissociation energies (BDE's) versus C-S bond activation energies by a Pd^0 model complex of various thioesters has shown only a weak correlation.[14] It was then proposed, at least for the more noble transition metals, that a general cross-coupling catalytic mechanism is followed. Transmetalation liberates a thiolate from the complex, which is followed by reductive elimination to regenerate the low-valent transition metal complex and release the product.

In the absence of a transition metal catalyst, only organocuprates were shown by Rosenblum to react cleanly with thioesters to give ketones,[15] presumably *via* a Cu(III) intermediate,[16] and not an addition/elimination sequence. This shows that effects other than the extent of C-M bond polarization of the organometallic coupling partner are relevant for a successful reaction of thioesters. On the other hand, it is also obvious that highly polar organometallic species (RLi, RMgX) should react with the formed ketones, which makes them disfavoured in ketone synthesis from thioesters in any case. Other effects could for example be the thiophilicity[17] of the stoichiometrically employed metal to influence the thermodynamics of the transmetalation step. Liberation of the thiolate during a reaction is the central problem when thioesters are employed as acylating agents since effective sequestration of this species must take place during the reaction to avoid a poisoning effect, a problem highly pronounced with late, thiophilic transition metals. In the following sections, selected examples on successful utilization of thioesters in ketone synthesis in metal-catalysed reactions will be discussed.

R a^1 synthon

1 R—C(O)—N(OMe)(Me)

2 R—C(O)—N(imidazole)

3 R—C(O)—SR'

R' reactivity order:
2-Pyridyl >
Aryl >
Alkyl

A *Proposed group 10 metal 2e redox catalytic cycle*

oxidative addition

reductive elimination

transmetallation

L_nM

$L_nM(RCO)(SR')$

$L_nM(RCO)(R'')$

R"M'X

(SR")M'X

R—C(O)—SR'

R—C(O)—R"

Calc. Activation free energy by Pd(PPh$_3$)$_2$ (kJ/mol)
R = Me, R' = Et: 84.5
R = Ph, R' = Et: 84.1
R = Me, R' = Ph: 67.8
R = Me, R' = pNO$_2$C$_6$H$_4$: 59.0
Ref. 13

increasing thiophilicity of M'
B Si Mg Li Zn
Cu
Ref. 16

B *Possible base metal 1e/2e redox catalytic cycle*

SET/ recombination

transmetallation

reductive elimination

L_nM-R"

$L_nM(RCO)(SR')(R'')$

$L_nM(SR')$

(SR")M'X

R"M'X

R—C(O)—SR'

R—C(O)—R"

Calc. C-S BDE (kJ/mol)
R = Me, R' = Et: 323.2
R = Ph, R' = Et: 322.2
R = Me, R' = Ph: 280.5
R = Me, R' = pNO$_2$C$_6$H$_4$: 288.3
Ref. 13

known TE C-S homolysis:
Thermal/Photochemical
Phenyl radicals (intram.)
Alkyl radicals (intram.)
Electrolysis
TE SET reduction:
SmI$_2$

Scheme 3.3: Thioesters are alternatives to classic reagents for the a^1 synthon in the synthesis of ketones. Activation with group 10 metals is proposed to follow pathway A, whereas activation with low-valent base metals could follow pathway B. BDE: Bond dissociation energy. SET: Single electron transfer. TE: Thioester.

3.1.2.1. Pd-catalyzed reactions

In 1998, Fukuyama and co-workers reported a seminal Pd-catalyzed ketone synthesis from *S*-ethyl thioesters employing primary alkyl- and aryl zinc reagents (1.5 to 3.0 equivalents) – now known as the Fukuyama coupling.[18] As expected with organozinc reagents, the functional group tolerance is excellent both in nucleophile as well as electrophile. The reaction proceeded with 5 – 10 mol% PdCl$_2$(PPh$_3$)$_2$ in THF or toluene at RT in 5 min to 3 h, giving isolated yields ranging from 50 to 99%. This reaction has been applied by Fukuyama in his synthesis of (+)-Haplophytine (Scheme 3.4).[19] The thioester group was carried through two synthetic steps unharmed, and then engaged in coupling with a functionalized alkylzinc iodide reagent to give compound **6**.
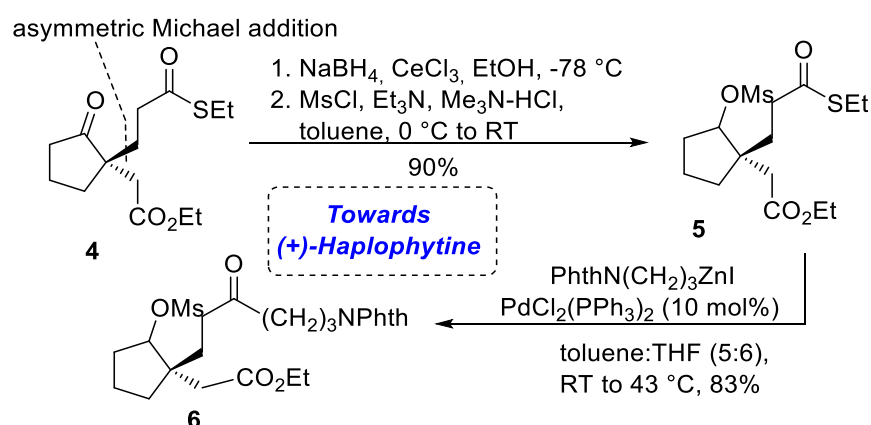
Scheme 3.4: Fukuyama's total synthesis of (+)-haplophytine employs the Fukuyama coupling reaction to give a synthetic fragment **6** in the early stages. Ms: Mesyl, PhthN: Phthalimide.

This reaction has been found in additional reports to proceed without ancillary ligand[20] or even with Pd/C,[21] from which was inferred by further experimentation that both heterogeneous and homogenous catalytic cycles are operative in the Pd/C-catalyzed Fukuyama coupling.[22] The reaction has since then been expanded to accommodate secondary organozinc coupling partners.[23] Notably, a highly stereoconvergent catalytic system, which forms tertiary stereocenters from racemic benzyl zinc reagents and thioesters **7**, has been disclosed by Maulide's group (Scheme 3.5).[24] They employed an enantiopure chiral phosphoramidite ligand (**L1**) as the stereoinducing element to affect a dynamic kinetic resolution (DKR) of the zinc reagent to give compounds of the type **8**.

Kishi pointed out that in the late stages of complex molecule synthesis, acylation chemistry should occur with optimally 1:1 stoichiometry of the coupling partners due to their high value with an additional high functional group tolerance. Thus, a one-pot Fukuyama reaction was developed by the group employing Pd$_2$dba$_3$ (5 mol%) and P(Cyclopentyl)$_3$ (10 mol%) in DMI at RT for 1 day (Scheme 3.6).[25] The aim was to extend the methodology into a macroketocyclization method in the synthesis of Eribulin. It should be noted that this reaction is not only one-pot but it also belongs to the class of cross-electrophile couplings. Presumably, the alkyl bromide is converted to the alkyl iodide in the

presence of LiI, followed by insertion of Zn dust (activated by stoichiometric triethylsilyl chloride). Either the lithium iodide or lithium bromide present could additionally facilitate zinc insertion, as this is a well-known salt effect in organozinc preparations.[26] Depending on the exact substrate class, a combination of various metal-containing additives (Co-Phthalocyanine or NbCpCl$_4$ as SET mediators, CrCl$_2$ as a deaggregating species and alkyl radical trap) in substoichiometric amounts were necessary for consistent results with the most challenging substrates. The cross-electrophile coupling of fragments **9** and **10** (Scheme 3.6) shows an impressive functional group tolerance and insensitivity to detrimental aggregate effects, which can occur when coupling fragments with large molecular weights and different solubility behaviours.
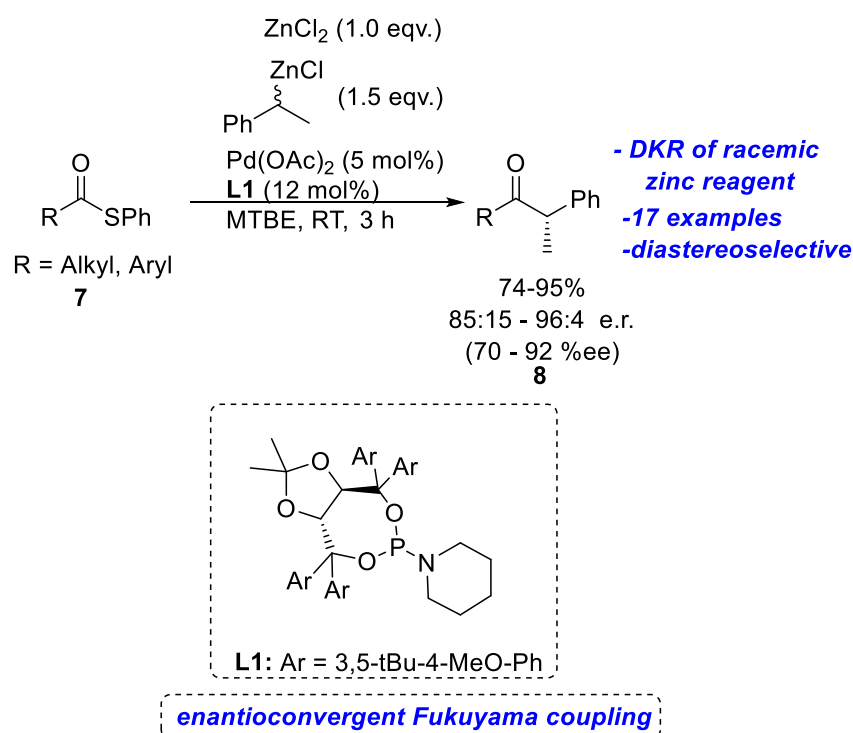
Scheme 3.5: Maulide's synthesis of tertiary stereocenters by an enantioconvergent Fukuyama reaction. MTBE: methyl-tert-butyl ether.

These studies on intermolecular reactions were followed by a synthesis of the microtubule-modulatory chemotherapeutic agent Eribulin (Halaven™, against breast cancer) featuring a macroketocyclization at a remarkably high concentration of 27 mM in DMI/THF. However, (super-)stoichiometric amounts of Pd, ligand and additives were required for attaining an acceptable yield.[27] Other catalytic (Fe, Ni) variants of this cross-electrophile coupling have been published by Kishi using S-(2-pyridyl)thioesters[28] and subsequently applied in the total synthesis to some members of the halichondrin natural product series.[28b]

Another milestone in this area is the Liebeskind-Srogl coupling, which was disclosed in 2000 (Scheme 3.7).[29] Here, aryl boronic acids were employed to render the transformation especially facile with

respect to the stoichiometric coupling partner. In this case however, Pd-S bond activation in the transmetalation (or maybe C-S activation in the oxidative addition) step must be facilitated by an additional stoichiometric Cu(I) source (**13**). The copper-bound carboxylate anion is proposed to activate the boronic acid reagent; hence the transmetalation step is thought to encompass a ternary complex. Thirteen preparative examples with diverse functional groups were shown in isolated yields up to 93% using low catalyst loading in THF at 50 °C for 18 h.
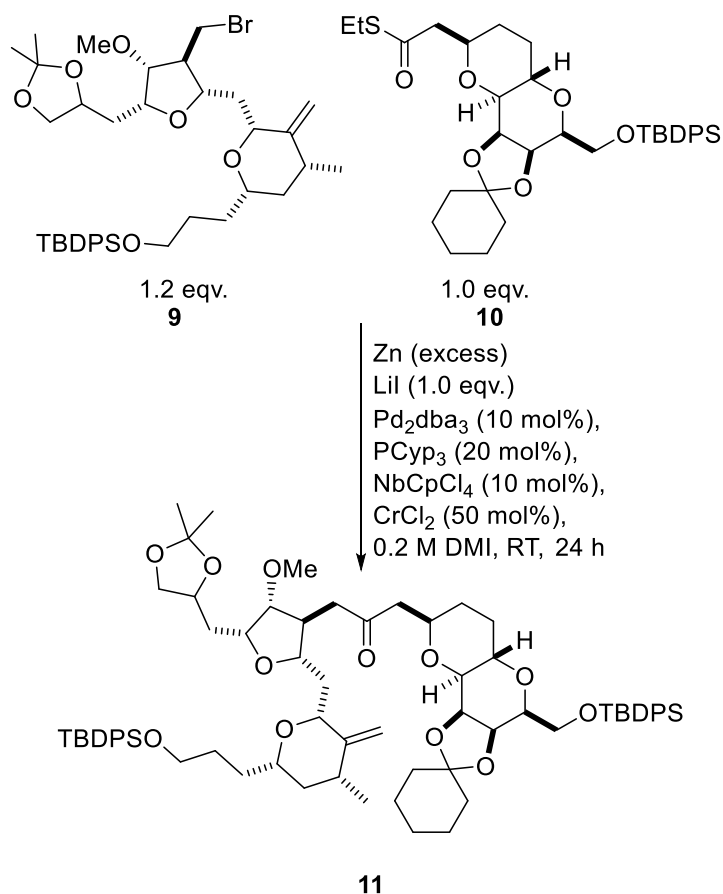
Scheme 3.6: Fukuyama-type cross-electrophile coupling of complex thioesters and alkyl bromides reported by Kishi.[61] TBDPS: Tert-butyl-diphenylsilyl, dba: dibenzylidenacetone, Cyp: cyclopentyl, Cp: cyclopentadienyl.

Since then, the scope of stoichiometric coupling partners has been extended towards 9-BBN-based alkylboronates,[30] organostannanes[31] and organoindium[32] reagents. The indium variation does not require a stoichiometric Cu(I) source, which highlights again the requirement of sufficient thiophilicity of the stoichiometric transmetalating agent. A significant advance in this area has been made by Villalobos and the original inventors of the reaction, which now allows a Cu-catalyzed (5 mol%) aerobic variation of the reaction by fine tuning the thioester moiety to an *S*-acyl thiosalicylamide.[33]   An exhaustive description of the advances and variations in this area is not the aim of this chapter; the reader is referred to a specialized review.[34]

Scheme 3.7: The Pd-catalyzed, Cu-mediated Liebeskind-Srogl coupling of arylboronic acids with thioesters. TFP: tris(2-furyl)phosphine.

Similarly non-polarized stoichiometric coupling partners are organosilanes, which were employed (1.1 to 1.2 equivalents) by Van der Eyckens and co-workers in a thioester-Hiyama coupling.[35] This method requires stoichiometric activation by fluoride (2.0 equiv.) as well as copper iodide (1.0 equiv.) in THF at 60 °C combined with Pd(PPh$_3$)$_4$ (5 mol%) to give products ranging from 79% to 98% isolated yields in 0.5–3.5 h. The other end of the polarity scale concerning the organometallic partner was covered by the same group by developing a thioester-Kumada coupling,[36] where slow addition of the Grignard solution (1.2 equivalents) by a syringe pump at room temperature was key to success combined with a catalytic system consisting of Pd(dba)$_2$ (5 mol%) and tris(2-furyl)phosphine (TFP) (10 mol%) in a THF/N-methylpyrrolidone (NMP) solvent mixture with isolated yields ranging from 23–96%.

3.1.2.1. Ni-catalyzed reactions

Seki and Shimizu were the first to report a mild Ni-catalyzed variant of the Fukuyama reaction by coupling (functionalized) aryl- and alkylzinc iodides with non-activated *S*-alkyl thioesters in 2002.[37] Interestingly, the reaction proceeds with simple Ni(acac)$_2$ (10 mol% loading) without the need for ancillary ligands. Various alkyl/alkyl, aryl/alkyl and aryl/aryl ketones were obtained using this method in yields ranging from 33% to 89%. This method was applied by the authors to obtain a late stage vinyl sulfide intermediate **16** in the synthesis of (+)-biotin by a one-pot Fukuyama coupling/condensation sequence (Scheme 3.8).

IZn(CH$_2$)$_4$CO$_2$Et (2 eqv).
Ni(acac)$_2$ (10 mol%)
DMF (50 mol%)
THF/toluene, 20 °C, 15 h;
then *p*TsOH hydrate, toluene,
20 °C, 18 h.
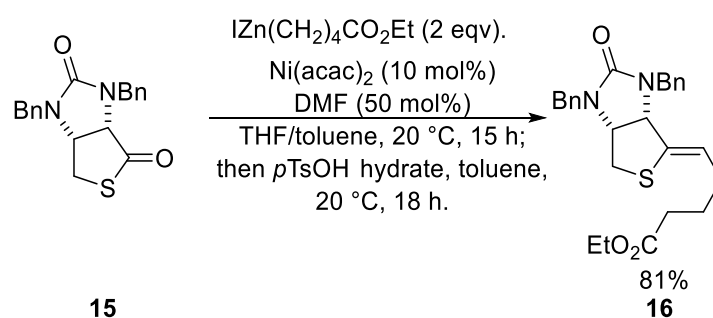
Scheme 8: Synthesis of the alkenyl sulfide intermediate 16 by a Ni-catalyzed Fukuyama coupling of thiolactone 15. acac: acetylacetonate, pTsOH: para-toluenesulfonic acid.

Zhang and Rovis reported, rather as a side note in a study on the reactivity of acyl fluorides, a Ni-catalysed variant of the Fukuyama coupling employing thioesters with diphenylzinc at room temperature with short reaction times.[38] We think the comparison in reaction times between carboxylic acid derivatives conducted by the authors is highly instructive and highlights the differences in thioester activation. The reaction times with *s*-(2-pyridyl)thioesters are significantly shorter, hinting at their different intrinsic reactivity and/or ability of the corresponding thiolates to transmetalate at a transition metal center. Key to a successful reaction was the use of the highly active bidentate *P*,*N*-ligand **L2** together with 4-fluorostyrene as a transient π-acidic ligand to facilitate reductive elimination from complex **19** (Scheme 3.9).

The first Ni-catalysed cross-electrophile coupling of a *S*-(2-pyridyl)thioester with an alkyl iodide was described by Mukaiyama *et al.*, who employed NiCl$_2$ (10 mol%) in DMF at 50 °C together with three equivalents of zinc dust to afford a dialkyl ketone in 46% yield after 5 h, whereas reactions with the corresponding carboxylates were usually higher yielding.[39] Weix and Wotal significantly improved this reaction by employing NiCl$_2$(dme)/**L3** as the catalytic system with Zn as the reductant (Scheme 3.10).[40]

Ph$_2$Zn (1.1 eqv.)
10 mol% Ni(cod)$_2$
12 mol% pyphos
20 mol% 4-F-styrene
THF, RT

17

X = SEt, 2 h, 92%
X = S(2-py), 10 min, 95%
acceleration by transient ligands

18

19
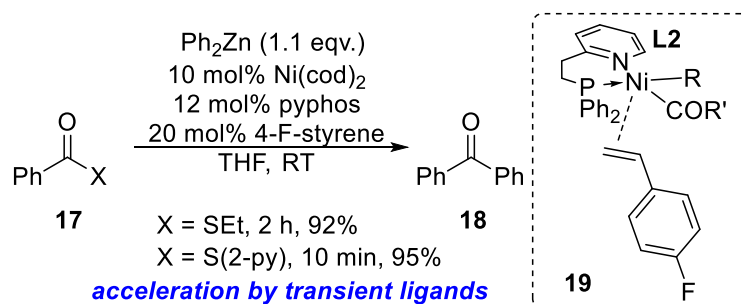
Scheme 3.9: Ni-catalysed coupling of thioesters using electron-withdrawing transient ligands. cod: 1,5-cyclooctadiene, pyphos (**L2**): 2-[2-(diphenylphosphanyl)ethyl]pyridine.

The method was applied to generate valuable polyfunctional compounds, such as "clickable" Biotin derivative **21**. In contrast to other organometallic functionalizations of Biotin, *N*-protection was not necessary, and the modest yield should be seen in relation with the reduced step count. The ketone linkage is an alternative to the usual amide bonds found in biotin derivatives, which are susceptible to hydrolysis by biotinidase. The possibility to employ downstream cross-coupling chemistry can also be introduced with no detriment as shown by the synthesis of a keto-boronate ester **23**.

20

Zn
(3 eqv.)

TIPS

5 mol% NiCl$_2$(dme)
5.5 mol% **L3**
DMAc, 0 °C or RT

22

Zn
(3 eqv.)

Bpin

L3

21
36%

TIPS
polyfunctional building blocks

23
58%
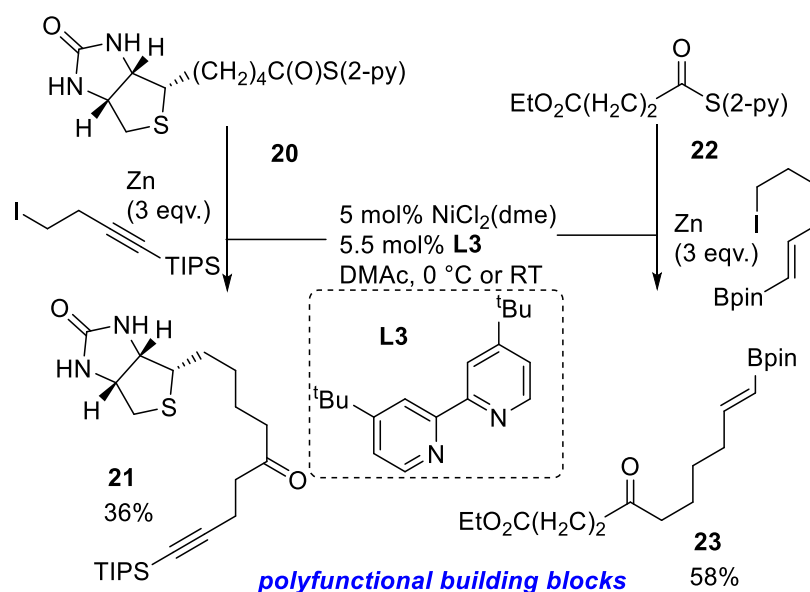
Scheme 3.10: Ni-catalysed cross-electrophile coupling for the synthesis of highly functional ketones amenable to click-chemistry (21) or cross-coupling (23). dtbpy: 4,4'-di-tert-butyl-2,2'-bipyridine, dme: 1,2-dimethoxyethane, DMAc: dimethylacetamide.

3.1.2.1. Fe-catalyzed reactions

In 1985, Marchese and co-workers presented an Fe(acac)$_3$-catalyzed (4.2 mol%) synthesis of ketones from S-phenyl thioesters by reaction with Grignard reagents (1.4 equiv.) at 0 °C in THF for 5–10 min (Scheme 3.11).[41] The obtained yields in 8 mmol scale were very good to excellent for primary, secondary and aromatic Grignard reagents, with the same variation possible in the thioester structure. Notably, the formation of a tertiary alcohol as a byproduct was not reported in this finding, meaning that the coupling reaction must be faster by several orders of magnitude. The reaction mechanism is unknown, but it stands to reason that low-valent ate species could be formed from a Grignard reagent/Fe(acac)$_3$ mixture.[42] Despite the operational advantages of this method, the use of Grignard reagents limits the functional group tolerance that has become important in the synthesis of complex structures or generally for late stage functionalization approaches.
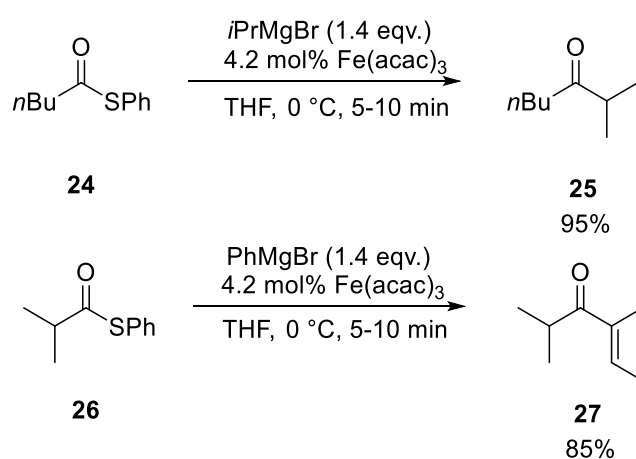
- *12 examples, 80-99% yield (GC)*
- *functional group compatability unexplored*
- *tertiary alcohol not formed!*

Scheme 3.11: Convenient iron-catalyzed coupling of S-aryl thioesters with Grignard reagents shown by Marchese et al..acac: acetylacetonate.

In addition, Oppolzer, de Brabander and co-workers could show that S-benzyl thioesters can also be applied using the same methodology (albeit with 10 mol% loading of Fe(acac)$_3$, and slightly different conditions).[43] More importantly, enantiopure thioesters with enolizable stereogenic centers (α-substituted thioesters) were converted to ketones with no erosion in enantiopurity observed. S-Benzylic thioesters were chosen as substrates due to easy access from N-acylsultam chiral auxiliaries by ate-complex mediated thiolysis. However, the use of methyl-, vinyl- and allyl magnesium halides primarily led to the corresponding tertiary alcohols. This strategy was elaborated to produce more complex building blocks, e.g. an enantiopure intermediate **29** in the synthesis of (-)-serricorole, which contained an ester as well as a silyl ether-protected alcohol (Scheme 3.12).

N-acyl sultams

BnSAlMe₃Li

BnSAlMe₃Li

28   *conservation of stereopurity*   **30**

EtMgBr (1.4 eqv.)
10 mol% Fe(acac)₃
THF, -30 °C, 1 h

EtMgBr (1.6 eqv.)
10 mol% Fe(acac)₃
THF

29
77%

31
85%
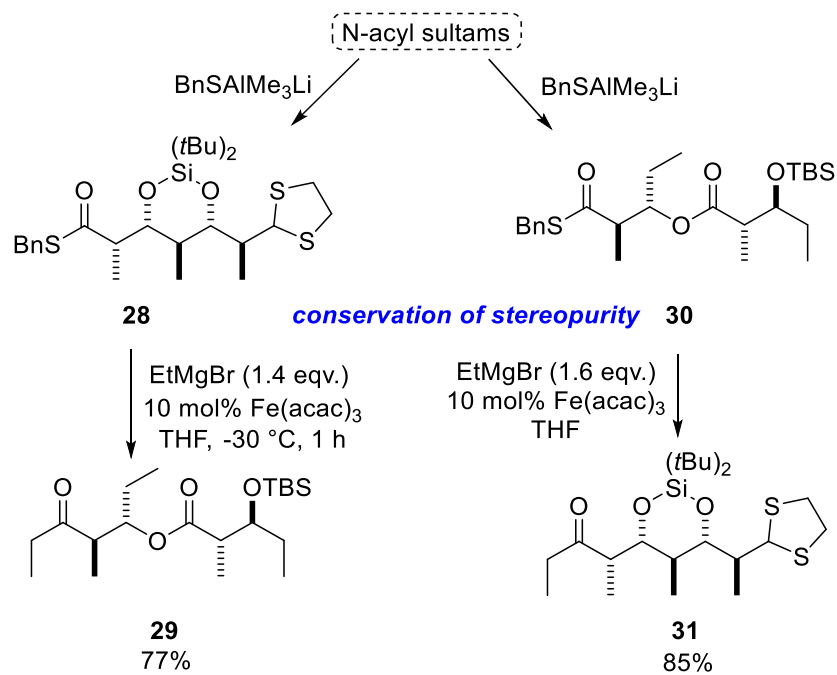
Scheme 3.12: Synthesis of functionalized, stereopure fragments **29** and **31** employing the Marchese-Fiandese cross-coupling. The thioesters were obtained by thiolytic cleavage of the amide-based chiral auxiliary.

3.1.4. Aims of this chapter

It is known that, in comparison to organolithium and organomagnesium chemistry, organozinc reagents are generally well-behaved and do not show a strong background reaction with carbonyl groups.[44] On the other hand, organozinc reagents are still more reactive than metalloid-based organometallics and transmetalate well at transition metal centers. This makes them predestined for functional-group tolerant catalysis in complex molecule synthesis. The thioester group is stable to air and normal-phase chromatography and tolerates some orthogonal chemistries.

Compared to the Pd-catalyzed Fukuyama reaction, the Ni-catalyzed Fukuyama reaction is less explored, and the mechanism is poorly understood in both cases. The major advantage is the presumed easier activation of the thioester C-S bond by low valent Ni compared to Pd complexes (see Chapter 1). This type of catalysis is inspired by the Ni-containing enzyme acetyl-CoA synthase, and in principle, decarbonylative coupling pathways should be possible as well. Knochel described a facile preparation of turbo-aryl zinc reagents (LiCl-complexed) from turbo-aryl Grignard species,[45] which is so far unexplored in the Fukuyama reaction. The combination of this salt effect with Ni-based catalysts should result in a highly active Fukuyama catalytic system for the coupling of aryl zinc halides and challenging *S*-ethyl thioesters at moderate loadings of Ni metal at room temperature, which is investigated in this chapter.

3.2 Results and discussion

3.2.1. Initial screening

The Ni-catalyzed Fukuyama reaction (FR) was investigated using hexanoic acid *S*-ethyl ester (**32**) and the LiCl-adducted phenyl zinc chloride (**33**) to give hexanophenone (**34**) under various conditions (Table 3.1).

The *S*-ethyl thioester (**32**) was chosen to ease purification. This choice deserves a short comment. A major drawback of the intermolecular Fukuyama reaction (in its original form) at the process scale is the generation of volatile, malodorous and toxic ethanethiol after acidic quenching. This means that the Fukuyama reaction will most likely stay a mainly laboratory-scale reaction unless major advances are made. In fact, the only reported process development-scale Fukuyama reaction is concerned with the activation of a thiolactone in the production of biotin.[46] The pendant thiolate re-attacks the formed ketone intermediate. Not only is this reaction relatively atom-economic but it also avoids the smell problem. Several attempts have been reported to counter above problems. Long-chain alkylthiols are known to be odourless due to their low volatility and have been employed in Fukuyama-type reactions.[47] However, chromatographic elimination of these byproducts (together with the corresponding disulfides) can be troublesome, especially with low-polarity products.[48] Thiophenols, although more activated, usually combine the most unfavourable features, namely extreme malodour coupled with relatively low volatility. Thus, *S*-ethyl thioesters were chosen in this work. These represent the most challenging coupling partners (in the context of successful activation and leaving group ability) and yet afford the most straightforward purification (rotary evaporation after acidic quench). An unexplored alternative is the use of solid-phase bound thiols.

33 was obtained by transmetalation from PhMgBr•LiCl with dry $ZnCl_2$ in THF. The aryl zinc halide was chosen over the diaryl zinc since the latter was reported to be inactive in the Pd-catalyzed Fukuyama reaction.[18, 24] While the actual composition after transmetalation is PhZnX•LiX•MgX_2 (with X = Br, Cl), the reagent will be abbreviated below as PhZnCl•LiCl. To the best of the authors knowledge, the structural details of such mixtures (containing both MgX_2 and LiX salts) have not yet been elucidated. Like other salt-adducted organozinc reagents, such mixtures will likely have ate-type character.[49] The corresponding Grignard was obtained by direct insertion of Mg turnings in the presence of LiCl, which is an established procedure from the Knochel group.[45] The presence of LiCl accelerates the direct synthesis route so that Mg insertion often occurs at lowered temperatures (as opposed to reflux conditions), which broadens the scope of compatible electrophiles in the Grignard reagent. To achieve a stoichiometric transmetalation, the resulting Grignard reagents were titrated with I_2/LiCl in THF.[50]

*Table 3.1: Optimization of the Ni-catalyzed Fukuyama reaction of phenyl zinc chloride (**33**) with thioester **32** under various conditions.*

Entry	Deviation from standard conditions	Conv. 32[a]	Yield 34[a]	Yield 35[a][b]
1	1.2 equiv. **33** instead	82%	77%	14%
2	Dropwise addn. of **33**	70%	54%	7%
3	0 °C, 2 h instead	79%	63%	10%
4	No metal, no ligand	0%	0%	0%
5	Addition of **32** to **33**	86%	70%	16%
6	5 mol% Ni(acac)$_2$ instead	95%	87%	15%
7	+5 mol% dtbbpy (**L3**)	95%	83%	19%
8	5 mol% Fe(acac)$_3$ instead	1%	1%	6%
9	10 mol% Ni-NP instead	94%	76%	12%
10	5 mol% Ni(xant)Cl$_2$ (**C1**) instead	61%	61%	11%
11	5 mol% Ni(xant)(oTol)Cl (**C2**) instead	89%	81%	9%
12	5 mol% Ni(dppf)(oTol)Cl (**C3**) instead	72	59	10
13	As 11, 1.5 h, 1.86 equiv. **33**	97	91	5

Reagents and conditions for standard run: **32** (63 mg, 333 μmol, 1equiv.), PhZnCl·LiCl (1.5 equiv.based on titre [typically 0.25 M], in THF), anhydrous NiCl$_2$ (2.2 mg, 16.6 mmol,5 mol%), dry THF (300 μL), RT, 30 min. [a] Determined by quantitative GC-FID analysis. [b] Based on $0.5*n_{PhZnCl}$. Acac:Acetylacetonate. dppf:1,1'-Diphenylphosphinoferrene. dtbbpy: 4,4'-Di-tert-butyl-2,2'-dipyridyl. NP: Nanoparticles. oTol: ortho-Tolyl, Xant:Xantphos (**L4**)

Another advantage of LiCl-adducted Grignard reagents is their increased reactivity towards electrophiles, although this behavior is not well-documented for organozinc reagents. Lewis-type activation of electrophiles and/or deaggregation of organozinc aggregates (to form ate-type species) are possible explanations for this behavior.

Interestingly, the reaction catalyzed by NiCl$_2$ (5 mol%) gave an acceptable yield of **34** at room temperature within 0.5 h reaction time. However, the discrepancy between conversion and yield was not satisfactory. During the reaction, the mixture turned deep black in color and a small exotherm was noted. After acidic quenching, organic-soluble dark precipitate was formed. Additionally, biphenyl (**35**) was detected as a byproduct. Maximally 10 mol% of biphenyl should form to reduce 5 mol% of Ni(II) precatalyst to active Ni(0) with **33**. The formation of biphenyl was initially attributed to the fast addition of **33** carried out by syringe. However, the yield was worse than when slow addition was employed (entry 2). It was concluded at this stage that a large transient excess of **33** (due to fast addition) may be beneficial to overall yield. Similarly, lower amounts of **33** did not lead to an improvement in the selectivity profile (entry 2). Kinetic control (entry 3) combined with longer reaction time also led to no improvement. The possibility of a Lewis-acid catalyzed background reaction was also ruled out (entry 5). To enforce an artificial transient excess, the electrophile **32** was added to the solution of **33**, but no improvement was found. Other Nickel salts were tested and exhibited no large difference in performance, whether in conjunction with diimine-type ligands or not (entries 6 and 7, further experiments shown in the experimental section). To test whether the coupling activity is due to residual Grignard reagent, iron catalysis was evaluated as a previously reported option.[41] Only traces of the product could be found in this case (entry 8).

From these experiments, the question was raised if a heterogeneous catalytic mode was operating or at least partially relevant for productive turnover, as is the case in the Pd-catalyzed Fukuyama reaction. The insensitivity to ligand and salt variation, the insolubility of Ni salts, as well as particle formation were interpreted as hints towards this.[51] Thus, Ni boride nanoparticles (Ni-NPs) were prepared through the reduction of NiCl$_2$ with sodium borohydride in THF under strictly inert conditions, as previously reported (and characterized).[52] The THF slurry of these nanoparticles proved to be catalytically active (entry 9), although the overall efficiency appears to be lowered (higher loading necessary). One advantage of employing NP as catalysts is their facile removal from the reaction mixture, since in this case no organic-soluble particles were noted and the NPs were simply filtered off with the aid of SiO$_2$/celite.

It was hypothesized that bidentate phosphine-ligated Ni complexes might hinder metal cluster formation and subsequently nanoparticle formation. Xantphos (**L4**) is a wide-bite angle diphosphine already known to be active in various Ni-catalyzed transformations (hydrocyanation,[53] alkyne

cyclizations[53]). The known, air-stable complex (as solid) **C1** was synthesized by reaction of $NiCl_2(H2O)_6$ with xantphos in boiling, degassed *n*-butanol. Although the activity of **C1** was disappointing (entry 10), the amount of biphenyl (**35**) was much closer to the possible theoretical amount (10 mol%). Even more promising was the excellent conversion-to-yield selectivity (1:1). The Jamison group has reported several highly active precatalysts of the type $L_2Ni(o\text{Tol})Cl$,[54] which require only a transmetalation/reductive elimination sequence to generate $L_2Ni(0)$. It was thought that rapid catalyst activation might be beneficial to overall reaction yield (as is the fast addition of **33**), and indeed the use of **C2** (synthesized from C1 by treatment with *o*TolMgCl in THF at low temperature) led to an improvement in overall yield, although the discrepancy between yield and conversion began to decrease again (entry 11). The commercially available dppf-based analogue **C3** (also a wide-bite angle ligand) showed less satisfactory catalytic performance. A slight increase in the excess of **33** and extending the reaction time led to an excellent overall yield of **34**, a smaller amount of biphenyl **35** and a small difference between yield and selectivity (entry 12).

In conclusion, the high activity of bare nickel chloride in the Fukuyama reaction is tempting but is associated with selectivity issues. Thus, to achieve acceptable levels of selectivity, activity was tamed slightly using **C2**. Although this line of optimization is uncommon in Pd-catalyzed cross-couplings (where elaborate ligand design is used to activate challenging electrophiles), it appears to be worthwhile in Ni-catalysis.[55] The successful use of both a molecular precatalyst **C2** (entry 12) and a heterogeneous (heterotopic) Ni-NP precatalyst (entry 9) is strongly similar to the Pd-catalyzed FR, where Pd/C (in various forms) was an equally effective catalyst. The only conclusion from these experiments is that the Ni-catalyzed FR may operate on both homotopic and heterotopic reaction pathways, which either intersect (termed "cocktail catalysis"[56]) or exist independently of each other. The question of open-shell reaction pathways will be addressed further below (section 3.2.4.).

3.2.2. Scope of thioesters

With optimized conditions in hand, the FR of structurally varied thioesters with aryl zinc reagents was explored (Scheme 3.13). The *S*-ethyl thioesters were prepared from the corresponding carboxylic acids by Steglich esterification, which usually proceeded well (shown in the experimental part) and allowed purification by filtration over SiO$_2$. In some cases, the *N*-acylurea byproduct had to be removed by chromatography. The synthesis of **34** was repeated on 1 g scale, giving a similar yield to the experiment evaluated with quantitative GC-FID. Various electrophilic groups are well-tolerated (**40**, **41, 46**), although the yields are moderate. This is the major advantage over Grignard-based approaches, where the synthesis of bifunctional ketones would require protecting group operations.
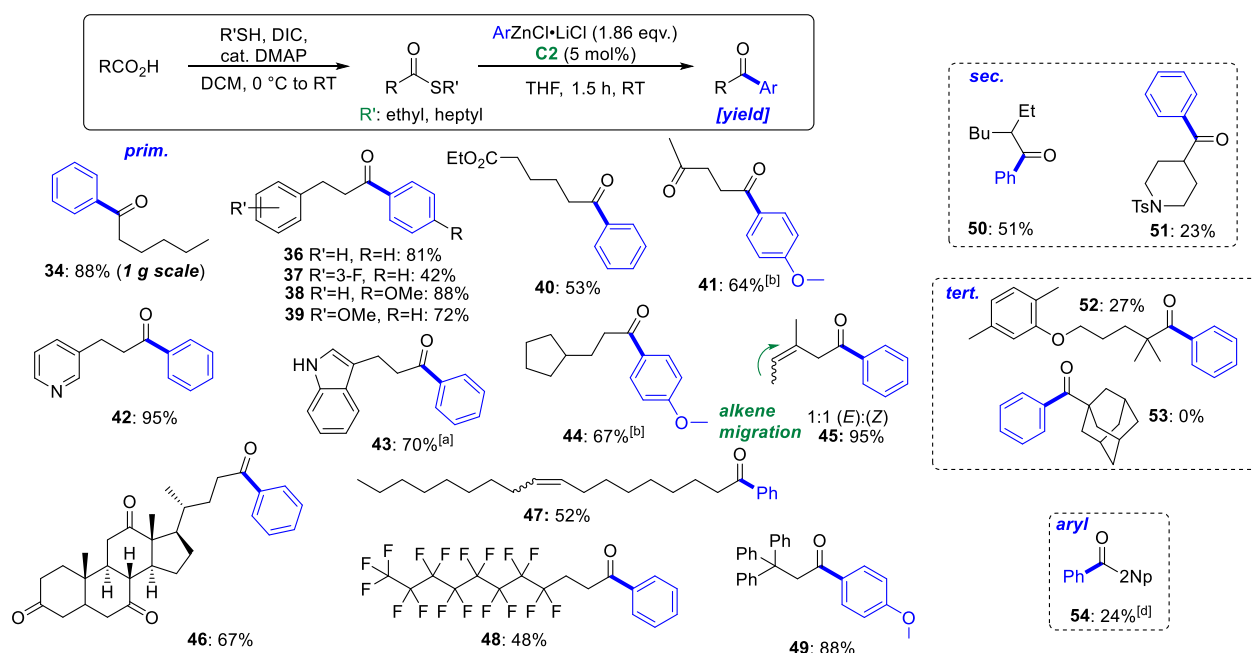
Scheme 3.13: Scope of the Ni-catalyzed Fukuyama reaction of *S*-alkyl thioesters with phenyl zinc chloride. Yields given are isolated unless stated otherwise. Reagents and conditions for standard run: Thioester (333 µmol, 1 eqv.), ArZnCl•LiCl (1.86 eqv. based on titre [typically 0.25 M], in THF), **C2** (12.7 mg, 16.6 µmol, 5 mol%), dry THF (300 µL), RT, 1.5 h. [a]: 2.86 eqv. of 4 were employed. [b]: The thioester could not be isolated in pure form. Hence, the yield given is over two steps. [c] From Knochel-type 4-Cl-C$_6$H$_4$ZnCl under standard conditions. [d] NMR yield.

Similarly, heterocycles are well-tolerated (**42** and **43**) in this reaction. Although the synthesis of **43** required a sacrificial amount of zinc reagent to deprotonate the indole ring, the yield was satisfactory. After chromatography, the product spontaneously crystallized from CDCl$_3$. Again, this result highlights the advantage of zinc reagents in conjunction with Ni catalysis since protecting group operations are limited. Since Ni catalysts are known to tightly bind to alkene groups, the effect of these groups was also tested in catalysis to give the corresponding ketones (**45** and **47**). Usually, the reaction mixture rapidly darkens upon addition of the arylzinc reagent. In the presence of alkenes, the darkening of the reaction mixture was delayed compared to the usual case. Interestingly, alkene migration to the thermodynamically favoured position was noted in product **45**, concomitant with the formation of both possible stereoisomers. A classical chain-walking mechanism with nickel hydride intermediates

appears unlikely due to the absence of obvious hydride donors. Thus, a Ni-catalyzed 1,3-*H*-shift to the thermodynamically more stable alkene is proposed which would involve nickel hydride intermediates (Scheme 3.14).
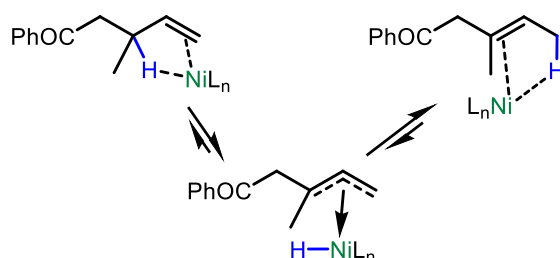
*Scheme 3.14: Explanation for the formation of product **45** by a Nickel-catalyzed 1,3-H-shift to the thermodynamically stable alkene regioisomer observed when terminal alkenes are employed as starting materials.*

Regioisomerization was not noted with product **47**, although the thermodynamic sink in this case would be the formation of a conjugated product. In this case, the first isomerization step offers no thermodynamic stabilization and makes this pathway unfavourable. Additionally, the internal alkene is more hindered towards coordination by Ni compared to the terminal alkene.

Although the yield was moderate, the successful synthesis of ketone **48** enables the use of fluorous-ponytail tagging of aryl zinc reagents as a purification strategy.[57] Sterically challenging substituents were equally tolerated with only one methylene spacer, as in compound **49**. However, more challenging acyclic secondary and tertiary thioesters gave the corresponding ketones in lower yield (**50** and **52**). When cyclic secondary and tertiary thioesters were employed, the yields were even worse, and no product **53** was observed. When a mixture of terpyridine and NiCl$_2$ was employed as the catalyst under otherwise same conditions, **51** was isolated in 87% yield and **53** in 62% yield. A strong ligand effect seems to be operative in the case of hindered thioesters.

3.2.3. Scope of aryl zinc reagents

Next, structurally varied organozinc reagents were reacted with thioester **55** (Scheme 3.15) under optimized conditions with the aim to synthesize ketones **56 – 69**. The results were compared to the yield of **50**.
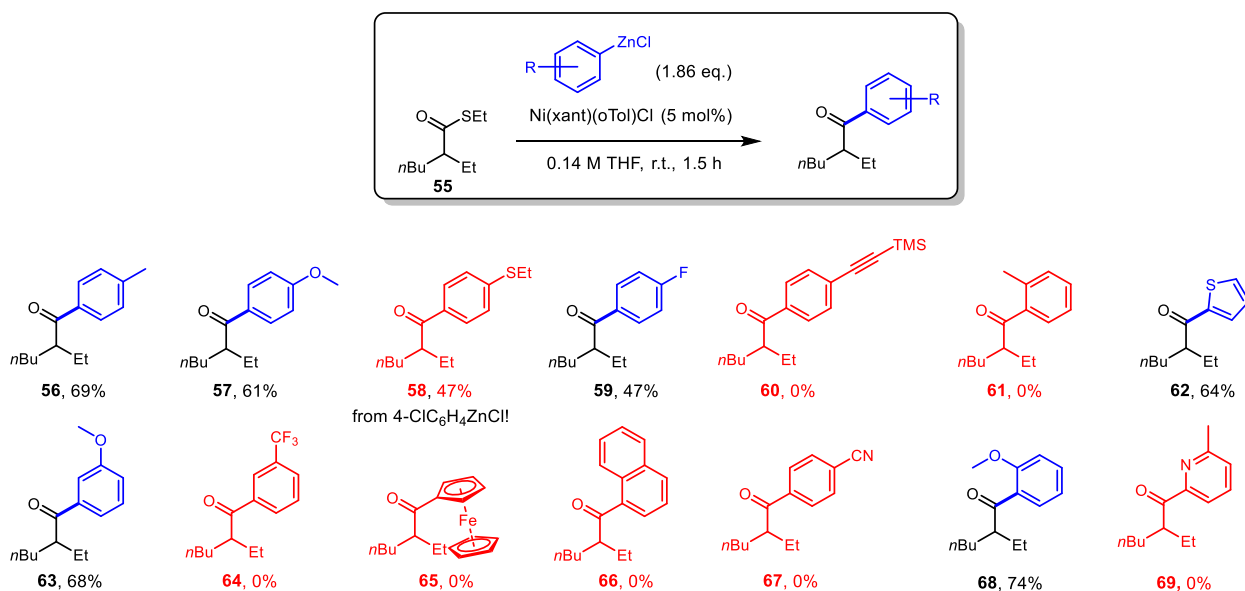
*Scheme 3.15: Scope of the Ni-catalyzed Fukuyama reaction of secondary thioester **55** with structurally varied aryl zinc halides leading to products **56 – 69**. Thioester (333 µmol, 1 eqv.), ArZnCl•LiCl (1.86 eqv. based on titre [typically 0.25 M], in THF), **C2** (12.7 mg, 16.6 µmol, 5 mol%), dry THF (300 µL), RT, 1.5 h.*

Electron-donating aryl zinc reagents generally resulted in increased yields relative to compound **50** (e.g. compounds **56**, **67**, **63**), whereas electron-poor arylzinc reagents gave usually no product (**60**, **64**, **65**, **67**). The same conclusion can be made about coordinating 2-heteroarylzinc reagents, where the electron-rich reagent leading to the product **62** was successful whereas the electron-poor reagent leading to hypothetical product **69** was not successful. The similar performance of 4-fluorophenyl zinc chloride compared to phenyl zinc chloride can be explained by looking at the Hammett σ constant of both aryl residues, which is very similar.[58] Relatively bulky arylzinc reagents were also not effective, and the desired products **61**, **65** and **66** could not be isolated. In these cases, the starting thioester **55** and the respective aromatic hydrocarbons derived from the zinc reagents were detected by GC/MS after acidic quenching.

Interestingly, a tandem Fukuyama-Migita reaction was observed when 4-chlorophenylzinc chloride was employed as the aryl zinc coupling partner. Intermediately formed EtSZnX presumably reacted with the 4-chloroarylketone to give **58**. This reaction is explored in more detail in the next chapter.

Disappointingly, alkyl-, alkenyl- and alkinylzinc reagents proved to be unreactive with **55** under standard conditions. There is generally no correlation between basicity of the carbanion to organozinc

reactivity, as there is in Grignard reagents. The reactivity order in organozinc reagents is general allyl > benzyl > aryl > alkenyl > alkyl > alkinyl.[44]

In conclusion, the combined evidence points towards the transmetalation step as overall rate-determining, since electron-poor organozinc reagents are weaker transmetalators. This result is also in line witch chemical intuition, since the high thiophilicity of Ni stabilizes an oxidative addition complex containing a Ni-bound thiolate anion, which must be displaced in an endothermic process to produce EtSZnX (X: Halide).

3.2.4. Mechanistic scenarios

While there have been proposals for a possible mechanism of the Fukuyama reaction, a complete investigation to elucidate has not been reported in the literature (Pd- or Ni-catalysis) so far. A detailed examination of the mechanism is out of the scope of this work as well. The generally postulated mechanism for both Pd- and Ni-based FR follows a classic two valence electron (2 ve) cross coupling cycle, involving oxidative addition into the thioester, transmetalation and reductive elimination.

Literature concerned with stoichiometric organometallic investigations of thioester activation however notes the occurrence of decarbonylation. Kundu reported that defined Pt-based oxidative addition complexes of thioesters underwent thermal decarbonylation (160 °C).[59] As can be expected for a 5d transition metal, thioester activation itself proceeded sluggishly (100 °C) and only with a five-fold excess of thioester. Riordan reported the decarbonylative activation of S-aryl thioesters to alkyl nickel thiolates with stoichiometric (dppe)Ni(cod) or (depe)Ni(cod) (dppe: diphenylphosphinoethane, depe: diethylphosphinoethane).[60] Acyl nickel thiolate intermediates were only detected at low temperature by ^{31}P-NMR. Various amounts of (dRpe)Ni(CO)$_2$ and (dRpe)Ni (R = p, e) were detected as side products (not explicitly quantitated in the report). Love reported decarbonylative S-ethyl and -aryl thioester activation to alkyl nickel thiolates with (dtbpe)Ni(C$_6$H$_6$).[61] The reversibility of the reaction was also shown under CO atmosphere (1 atm). Again, the corresponding dicarbonyl complex was isolated.

Based on the high stability of Nickel carbonyl complexes, it seems likely that such poisoned species are thermodynamic sinks and might offer a pathway to irreversible deactivation of FR catalysts. Secondly, no cross-coupled products derived from the corresponding alkyl nickel thiolates (from decarbonylation) were detected by GC/MS during this work, which would have implied a buildup of catalytically active (xant)Ni(CO)$_2$. Thus, this species perhaps acts as a CO-reservoir for reversible decarbonylation occurring in the Ni-catalyzed FR.

An alternative explanation for decarbonylation under reductive conditions is the existence of open-shell (radical) reaction pathways. In the beginning of this work, a C-C-coupled product **72** from a decarbonylative processes was detected by GC/MS from the reaction with **70** and PhZnCl•LiCl with various Ni(II) salts and bipyridine-type ligands (Scheme 16a). The same behavior was not observed in the same extent with **C2** as the catalyst. No decarbonylation of primary, secondary or tertiary thioesters was observed on attempted Ni-catalyzed FR with **C2** or Ni(II)/bipyridine combinations. The initial hypothesis was that this occurred due to a single electron transfer (SET) reduction of the thioester, which produces first a ketyl radical anion,[62] which then fragments to an acyl radical and a thiolate anion. This proposed key step has precedent,[62] and both redox-neutral homolytic and photochemical activation of thioesters as well as reductive electrolysis of thioesters have been

reported to yield acyl radicals as highly reactive intermediates. The rest of this mechanism would then follow closely related couplings with redox active esters,[63] with the key difference that inhibitory CO is released as opposed to relatively innocent CO_2 as in all modern redox-active ester (RAE) couplings. The difference in decarbonylative to non-decarbonylative product ratio with **C2** vs. Ni(II)/diimine systems was then explained by a difference in ligand field strength, where the strong-field phosphine ligand would make an open-shell pathway unfavourable due to a high ligand-field stabilization energy (the energetical separation of the metal HOMO and LUMO), whereas the diimine-type ligands would provide lower ligand-field stabilization energy and thus allow radical pathways.

However, a reaction with 2,2,6,6-tetramethyl-piperidine-*N*-oxide (TEMPO) as a radical trap led to a shutdown of reactivity both with **C2** and Ni diimine complexes, which was a first warning sign that there might be another aspect to the previous analysis based on ligand-field arguments. It could be argued however, that TEMPO reacts with a variety of organometallic species and thus may poison any Ni-based catalytic cycle under formally reducing conditions. For example, the reaction of Et$_2$Zn with TEMPO was reported.[64] Wolf reported the reaction of TEMPO with a Ni(I) complex.[65] In light of the oxidizing ability of electron-deficient radicals, this might not be surprising. In contrast, no decomposition of **C2** was noted in the presence of TEMPO in THF overnight (conducted in air), again underlining the high stability of this precatalyst. Since oxidation through TEMPO might effect both catalyst deactivation by quenching Ni(I, II) states or consuming the organometallic reagent, another radical trap was investigated.

It was found that the addition of ethyl acrylate to the reaction mixture leads to formation of product **74** (detected by GC/MS) both with **C2** or NiCl$_2$ (Scheme 16b). There are two possible explanations for this behavior. First, there is the possibility of a radical (paramagnetic) pathway, where the previously mentioned acyl radical undergoes addition to ethyl acrylate, producing a stabilized radical which undergoes further coupling to give **74**. The overall process would amount to a Fukuyama-Giese hybrid mechanism. The other possibility to generate this product would be the carbonickelation of ethyl acrylate, followed by further coupling to give **74** (diamagnetic mechanism). Both processes appear equally reasonable.

However, the combined evidence from both types of experiments points towards a mechanism involving acyl radicals. While the detection of ethyl-acrylate trapped product alone may not be conclusive, the observation of decarbonylation for only one type of substrate is insightful. If the decarbonylative process was due to migratory deinsertion of a acylnickel(II) species, then the decarbonylation, at least in minor amounts would have been observed for all types of structurally varied thioesters, which was not the case. This is the strongest argument against a diamagnetic pathway being operative.
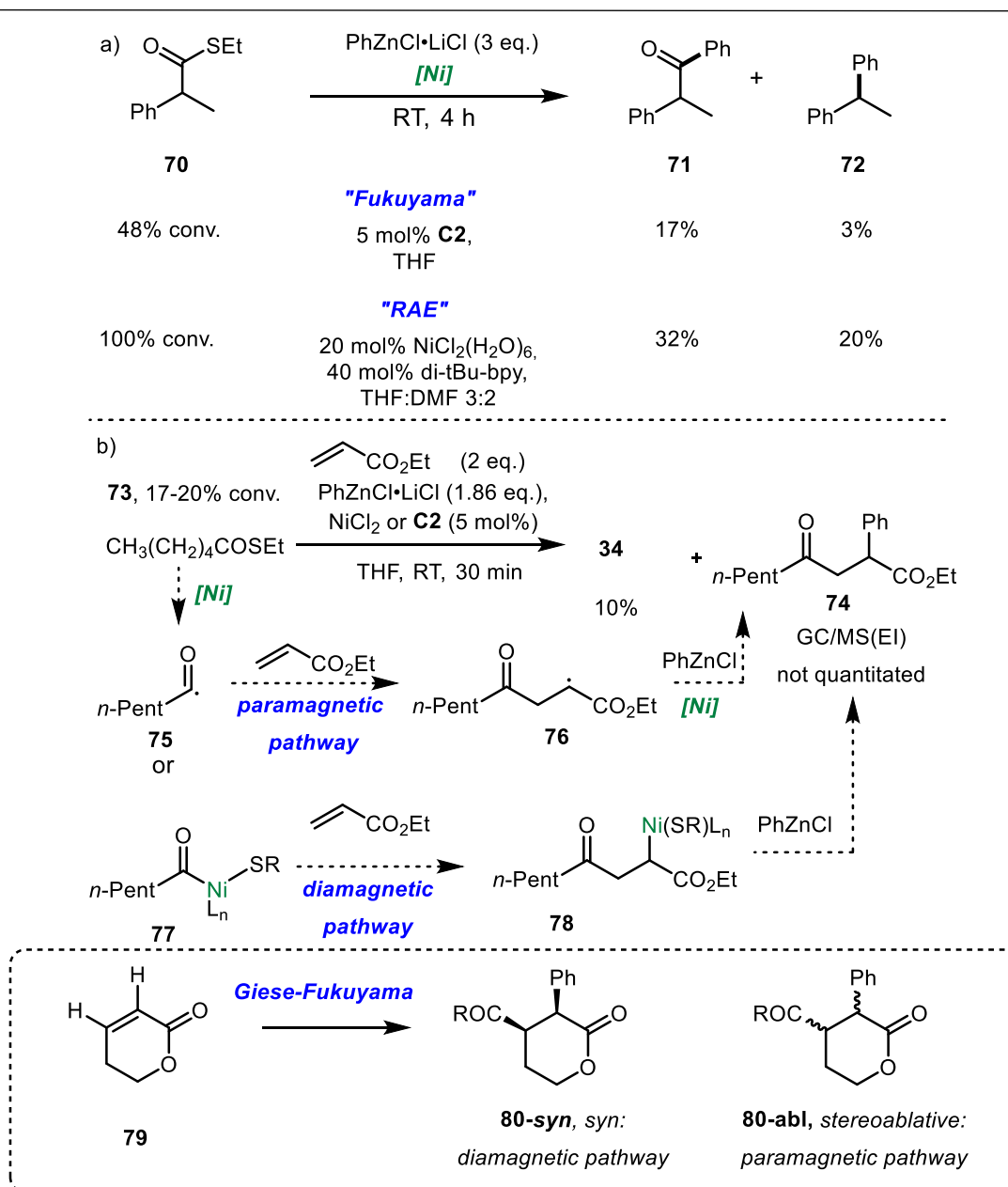
Scheme 3.16: Mechanistic investigations to discern open-shell reaction pathways (paramagnetic) from closed-shell pathways (diamagnetic).

This conclusion is supported by the rate of decarbonylation of acyl radicals. Generally, the stability of acyl radicals decreases with increasing stability of the resulting decarbonylated radical,[66] which is also connected to the reaction rate. Most of these decarbonylations are endothermic, apart from the decarbonylation of benzylic-connected acyl radicals,[67] which is not only an exothermic process but also the fastest ($k_{DCO} = 8.1 \times 10^6 - 1.5 \times 10^8\,s^{-1}$, depending on the benzylic substituents) of all acyl radical decarbonylation reactions (compared to $2.1 \times 10^2\,s^{-1}$ [primary], $1.4 \times 10^4\,s^{-1}$ [secondary] and 8.3×10^5 s^{-1} [tertiary]).[66] Dimers of the acyl radical were not detected due to the Fischer-Ingold persistent radical effect, where the Ni^I complex is the persistent radical. The generated CO gas would then be instantly trapped by the Ni complex due to high affinity of Ni to form carbonyl complexes. This in turn

poisons the catalyst. In fact, none of the Ni-catalyzed Fukuyama reactions, which feature benzylic-attached thioesters were particularly effective.

The interesting feature of a ligand framework, which supports migratory insertion, such as xantphos, is that an intermediate decarbonylated product can be "rescued" by migratory insertion of the Ni-bound CO into the Ni-C bond of the benzyl ligand. In turn, the rates of both irreversible decarbonylation and on-metal migratory (de)insertion will influence the product ratio of **71** to **72**. Where the ancillary ligand might not be as effective in promoting migratory insertion, such as for 2,2'-bipyridine or analogues, the product ratio could then be changed, leading to the observed differences in product ratio shown in Scheme 16a.
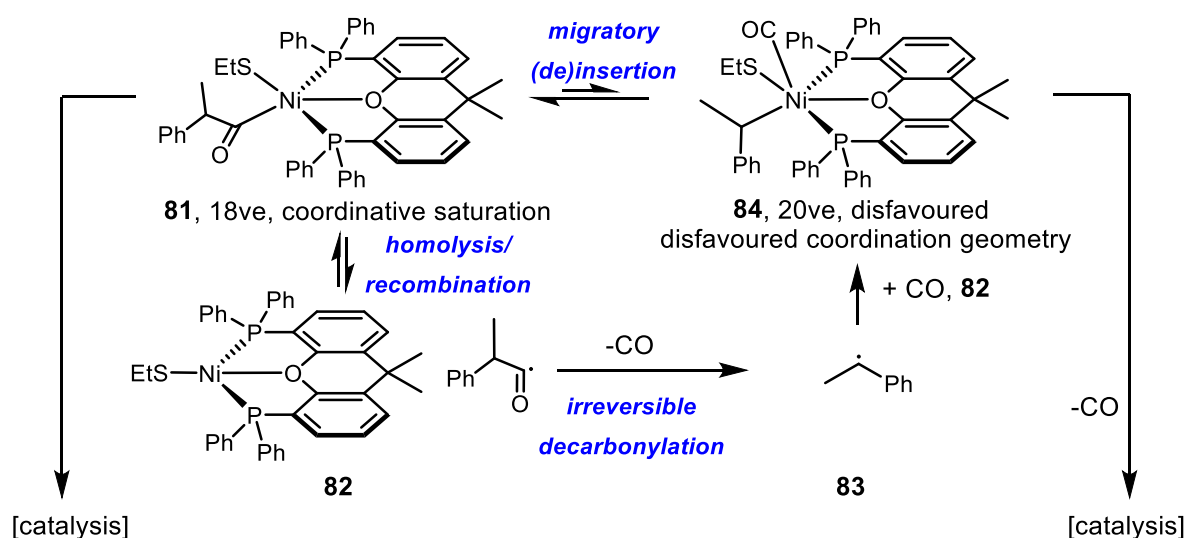
Scheme 3.17: A decarbonylated product is not direct proof of a radical pathway being operative. Ligand-dependent relative rates of migratory (de)insertion as well as the likelihood of Ni-C bond homolysis will affect the product distribution of **71** to **72**.

The last question is what redox states of Ni are involved in the Fukuyama reaction catalyzed by **C2** when a SET step is included. The most likely candidates are $Ni^{I/II/III}$ or $Ni^{0/I/II}$ cycles. A Ni^{III} intermediate, which features three possible actor X-type ligands, would also give reductive elimination products of the type ArSR. These products were not observed with **C2**. It is known that the activation pathway of **C2** by action of phenyl zinc reagents gives Ni(xant) by a transmetalation/reductive elimination sequence. Furthermore, a Ni^{I} state would readily react with an acyl radical, since it has inherent open-shell character, whereas a Ni^{II} state would require a high-spin electron configuration. In summary, the combined evidence points to a $Ni^{0/I/II}$ cycle (Scheme 3.18). At the beginning of the reaction, **C2** is activated by an aryl zinc reagent to give Ni(xant), which then promotes a SET reduction-fragmentation of the thioester to give an acyl radical and a Ni^{I} thiolate complex. This complex is short-lived since recombination with the acyl radical occurs generally before solvent cage escape and decarbonylation can take place.
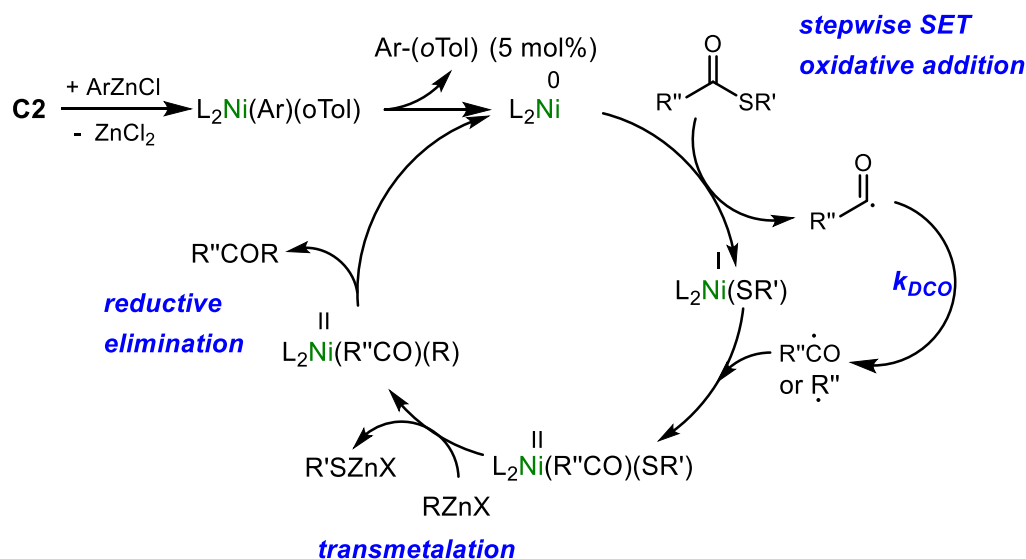
*Scheme 3.18: Proposed mechanism of the Fukuyama reaction catalyzed by **C2**. L$_2$: xantphos.*

Only in extreme cases, where the decarbonylation is thermodynamically favoured and kinetically the fastest of all possible acyl radicals, decarbonylation takes place. In this case, the formed benzyl radical then recombines with Ni^I complex as the acyl radical would and is carried through the remaining cycle in the same manner. The oxidative addition Ni^{II} complex then undergoes a transmetalation step, followed by reductive elimination to release the coupled product and regenerate the Ni^0 species. In summary, a classic cross-coupling mechanism is proposed, which however features a two-step SET oxidative addition microscopically. In Ni catalysis, such behavior is not unusual[68] and has been described early by Kochi in studies concerned with oxidative addition of Ni^0 phosphine complexes into aryl halides.[69]

To further strengthen this position, the following mechanistic experiments are proposed for follow-up work: 1. Synthesis of the oxidative addition complex (xant)Ni(SR)(COR') (**77**), from Ni(cod)$_2$, xantphos and a simple thioester. Keeping the literature in mind, this complex may not be stable and lead to decarbonylated products. However, the sensitivity of oxidative addition to radical traps could be tested in this manner (as in the work of Kochi); 2. If complex **77** is sufficiently stable, it would be interesting to see if upon exposure to ethyl acrylate, carbonickelation to **78** occurs; 3. Attempt to carry out a Giese-Fukuyama reaction on conformationally locked dihydropyrone **79** (Scheme 16, bottom box). In the case of a diamagnetic mechanism involving carbonickelation, the product **80**-*syn* would be obtained selectively; 4. Attempt to carry out a Giese-Fukuyama reaction with a tertiary thioester, where the Fukuyama reaction alone was sluggish presumably for steric reasons. By shutting down the competing pathway, more of the Giese-Fukuyama product should be obtained, since the intermediate radical formed by addition is less sterically hindered than the initial acyl radical.

3.3 Conclusion

In summary, it was shown that a Xantphos-based Jamison pre-catalyst **C2** (5 mol%) catalyzes operationally homogeneous Fukuyama reactions of LiCl-adducted aryl zinc halides with challenging *S*-ethyl thioesters at room temperature within 1.5 h. So far, the reaction conditions limit the organozinc component to aryl zinc halides (the most reactive in the organozinc series), where electron-rich, non-sterically hindered reagents perform best, as is usual for cross-coupling. However, the coupling of alkylzinc reagents with thioesters would be especially appealing in the context of natural product synthesis and is currently easily achievable with the Pd-catalyzed variant of the Fukuyama reaction. An increased molecular understanding of the differences between the Pd- and the Ni-based Fukuyama system concerning alkylzinc species is the most pressing issue of all in this area.

There is a strong dependence of the thioester structure (primary > secondary > tertiary = aryl) on the overall yield using the Jamison precatalyst, which cannot be completely explained by steric effects. As expected for organozinc reactions, the functional group tolerance is excellent, and a variety of polyfunctional ketones could be synthesized in this manner.

The first experimental proof that the Ni-catalyzed Fukuyama reaction features free acyl radical intermediates during a two-step SET-based oxidative addition of Ni(xant) into the thioester C-S bond was provided in this work. Previously, such intermediates could only be accessed by non-catalytic methods, except for one example employing photoredox catalysis. Further work should aim to strengthen this position, such as the further development of a hybrid Giese-Fukuyama reaction or the development of decarbonylative Fukuyama couplings. Furthermore, there are indications, but not proof, that the rate-determining step in the Ni-catalyzed FR could be transmetalation. Changing the stoichiometric metal or the ligand framework on Ni should give further insights in this area.

3.4. Experimental part

3.4.1. General information

All reactions with organometallic species were carried out under Ar atmosphere using dry glassware with the usual air-free techniques, unless noted otherwise. Dry THF was obtained either: by distillation of THF p.A. from purple-coloured sodium/benzophenone pots and stored over 3 Å MS (10 w/v%) in grease-free Strauß-type Schlenk flasks; use of Sigma-Aldrich anhydrous grade THF; storage of freshly distilled THF over microwave-activated 3 Å MS (20 w/v%, 3 days) in an Ar-flushed container with no large difference in performance. Chemicals were purchased from ABCR, Acros, Sigma-Aldrich, TCI or Merck. LiCl, Magnesium turnings and $NiCl_2(H_2O)_6$ (p.A. grade) were supplied by the central chemical storage, University of Tübingen. $ZnCl_2$ was supplied by either Sigma-Aldrich (anhydrous, >99.999% trace metals basis, stored in Schlenk tube) or Merck (Ph. Eur. Reagent grade) with no differences in activity; technical grade $ZnCl_2$ proved to be unsuitable for the preparation of aryl zinc halide solutions. 1,1-Diphenylethane (**72**) and 1,2-diphenylpropan-1-one (**71**) were obtained independently as calibration standards following literature procedures[S1]. Solvents for chromatography were distilled prior to use. NMR spectra were recorded using a Bruker Avance 400 ([1]H: 400 MHz, [13]C: 101 MHz), ^{13}C-NMR and ^{31}P-NMR experiments were performed in proton-decoupled mode, which is not noted explicitly. Chemical shifts are reported in parts per million relative to the residual NMR solvent signals and the *J*-coupling constants are given in Hertz with the usual designations for splitting patterns. HR-MS and LR-MS(ESI) analysis was carried out by the mass spectrometry department of the Institute of Organic Chemistry, University of Tübingen.

GC-MS was recorded on an Agilent 7820A GC system with Quadrupole MS Agilent 7820A (EI) by using dry hydrogen as carrier gas. An Agilent 190915-433UI column (30 m x 250 μm x 0.25 μm) was used. Program: Heating from 50 °C to 280 °C within 15 minutes. Constant column flow mode: 1.2 mL/min.

GC-FID (flame ionization detection) analysis was carried out on an Agilent 7820A system using dry hydrogen as carrier gas. An Agilent 19091J-431 column (30 m x 320 μm x 0.25 μm) was used. Program 50-280M12: Heating from 50 °C to 280 °C within 12 minutes. Constant column flow mode: 2.3 mL/min. In order to determine yields and conversions the internal standard method was used for quantitative GC-FID, see section 4 for determination of the respective response factors.

Column chromatography was carried out using flash-grade SiO_2 either manually or by a Puriflash system (Interchim), and TLC analysis was carried out using aluminium-backed plates coated with SiO2 60 F$_{254}$ (0.2 mm thickness) and the compounds detected under UV light (254 nm) or after staining with a $KMnO_4$, Vanilin or Anisaldehyde TLC dip solution and gentle heating.

Definition of "Gradient" used below: In separations with the Puriflash system, a gradient was developed around a suitable (target spot Rf ~ 0.3) binary eluent combination X:Y (where the latter is the strong solvent, X+Y=100) that entailed the following program – 0 to 1 CV: isocratic Y/4, 1 to 11 CV: gradient to Y*2, 11 to 12 CV isocratic Y*2. Flow rates: 23 g SiO_2 50 μm - 15 mL/min, 37 g SiO_2 50 μm – 26 mL/min.

3.4.2. General procedures

General procedure A (GP A): Steglich thioesterification[S2]

  Steglich esterifications were carried out with distilled dichloromethane under air. A RBF of suitable size with stirring bar was charged with a 0.1 - 1 M solution of the respective carboxylic acid (1.0 eqv.) in dichloromethane, followed by DMAP (5 - 10 mol%) and the thiol (1.0 – 4.0 eqv., noted in each experiment depending on the volatility of the free thiol and its disulfide and the volatility of the product). The flask was cooled to 0 °C, followed by addition of DIC (1.0 – 1.1 eqv.) by syringe. The flask was stoppered, stirred for 5 min at 0 °C, the ice bath removed and the reaction mixture allowed to warm to RT. The reaction mixture was stirred for 24 h or until completion as determined by TLC analysis. Dichloromethane was removed by careful rotary evaporation (especially important for volatile thioesters), followed by purification as detailed in individual experiments.

General procedure B (GP B): Preparation of Knochel-type aryl zinc reagents

  Following a literature procedure[S3], Mg turnings (219 mg, 9.0 mmol, 1.5 eqv.) and LiCl (318 mg, 7.5, 1.25 eqv.) were placed in a septum-capped oven-dried 25 mL Schlenk RBF with stirring bar which was flame-dried with a propane torch. After evacuating/refilling the still-warm (not hot) flask with Ar (3x repeated), the vessel contents were suspended in dry THF (3 mL), followed by addition of DIBAL-H (60 µL of a 1.0 M solution in THF, 60 µmol, 1 mol%) at RT and stirring for 5 min (gas evolution may occur). The reaction vessel was cooled to 0 °C and the corresponding aryl bromide (6.0 mmol, 1.0 eqv.) was added (if liquid – if solid, a concentrated solution of the aryl bromide in dry THF was used instead). The reaction mixture was stirred for 10 min at 0 °C, then for 1 h at RT to give Grignard reagents with 0.7 M – 1.3 M concentration as determined by titration with I_2/LiCl[50], which should be used immediately for transmetalation.

  The Knochel-Grignard reagents were transmetalated by addition to a dry THF solution of an equimolar amount of $ZnCl_2$ (prepared by charging $ZnCl_2$ into an oven-dried Schlenk RBF, flame-drying until the zinc chloride begins to melt, followed by vacuum/argon refilling cycles (3x) while the flask is still warm and dissolving the zinc chloride in the appropriate amount of dry THF by syringe addition) at RT, then stirring at the same temperature for 15 min, targeting a concentration of 0.25 M. During addition, precipitates formed in some, which redissolved when an equimolar amount of Grignard reagent was added. The reagents were in some cases titrated with the I_2/LiCl method[50] or the concentration determined by calculation of the dilution after transmetalation from the titrated concentration of the corresponding Grignard reagent.

General procedure C (GP C): Ni(xant)(oTol)Cl-catalyzed Fukuyama reaction (0.333 mmol)

A heat gun-dried 10 mL Schlenk tube with stirring bar and rubber septum under Ar was charged with **C2** (5 mol%), the thioester (1 eqv., 333 µmol) and dry THF (300 µL). The resulting orange-red solution was stirred rapidly, followed by addition of the respective Knochel-type aryl zinc halide in THF (1.86 eqv. based on the calculated titre., see **GP B**) by syringe. In most cases, a deep black color developed within seconds. The reaction mixture is stirred for 1.5 h at RT and quenched with 1 M aq. HCl (1 – 2 mL) and diluted with diethyl ether (4 mL). The phases are separated and the organic phase washed with sat. aq. NaHCO$_3$ (5 mL), then sat. brine (5 mL). The combined aq. Phases were re-extracted with diethyl ether (4 mL). The combined organic phases were dried over MgSO$_4$ and filtered to give the crude products after solvent removal by rotary evaporation. The crude products were purified by distillation or column chromatography.

General procedure C (GP D): NiCl$_2$/terpy-catalyzed Fukuyama reaction (0.333 mmol)

A heat gun-dried 10 mL Schlenk tube with stirring bar and rubber septum containing anhydrous NiCl$_2$ (2.2 mg, 16.65 µmol, 5 mol%) under Ar was charged with terpyridine (3.9 mg, 16.65 µmol, 5 mol%), thioester (1 eqv., 333 µmol) and dry THF (300 µL). The resulting suspension was stirred rapidly, followed by addition of the respective Knochel-type aryl zinc halide in THF (1.86 eqv. based on the calculated titre., see **GP B**) by syringe. In most cases, a deep black color developed within seconds. The reaction mixture is stirred for 1.5 h at RT and quenched with 1 M aq. HCl (1 – 2 mL) and diluted with diethyl ether (4 mL). The phases are separated and the organic phase washed with sat. aq. NaHCO$_3$ (5 mL), then sat. brine (5 mL). The combined aq. Phases were re-extracted with diethyl ether (4 mL). The combined organic phases were dried over MgSO$_4$ and filtered to give the crude products after solvent removal by rotary evaporation. The crude products were purified by distillation or column chromatography.

3.4.3. Experimental procedures and analytical data

3.4.3.1. Synthesis of Ni(xantphos)(oTol)Cl (**C2**)

Step 1, Ni(xant)Cl$_2$

An *n*-Butanol (25 mL) solution of NiCl$_2$ hexahydrate (p.a. grade, 798 mg, 3.36 mmol, 1 eqv.) was sparged with Argon for 15 min (step A). The resulting green solution was added to Xantphos (2.06 g, 3.36 mmol, 1 eqv.) contained in a dry, Argon-flushed three-necked RBF with stir bar and attached condenser. The reaction mixture was heated for 2 h in an oil bath (120 °C) under Ar (step B), then allowed to cool down to RT by removal from the oil bath. A purple suspension slowly formed (step C). The suspension was cooled to 0 °C for 10 min, then quickly filtered under air by vacuum over a P3 frit (step D). The product was collected and immediately placed under high vacuum vacuum to dry for 1 h, then was backfilled with Ar. The final paramagnetic product (2.14 g, 3.02 mmol, 90%) has a grey-purple appearance and was carried on to the next step without further analysis.

Step 2, Ni(xant)(*o*Tol)Cl (**C2**)

A 50 mL Schlenk RBF with a 1.5 cm long teflon stirring bar and rubber septum was flame dried with a propane torch under vacuum and then refilled with Ar (step A). While the glass was still warm, the rubber septum was removed, and Ar flow was stopped. Using a solid addition funnel, Ni(xant)Cl$_2$ (1.04 g, 1.47 mmol, 1 eqv.) was charged into the RBF (step B). The flask was refitted with the rubber septum and evacuated for 5 min, then refilled with Ar (repeated twice, step C). The purple-grey solid was suspended in dry THF (30 mL, Aldrich anhydrous), cooled to 0 °C (ice-water bath) and stirred vigorously (~1000 rpm, steps D and E). *Ortho*-Tolylmagnesium chloride (2.46 mL of a 0.6 M solution [freshly titrated] in THF, Aldrich) was added by a gas-tight Hamilton Luer-Lock syringe in a dropwise manner into the center of the vortex of the stirred suspension (step F). A colour change towards dark red occurred during addition. The mixture was stirred at 0 °C for 15 min. Under an Ar flow, the stirring bar was removed magnetically (step G). THF was removed by careful vacuum evaporation using a tepid water bath (a filter frit is recommended, step H), leaving behind an orange-red residue (step I) which was suspended in Ar-sparged (15 min) MeOH (5 mL added by syringe, HPLC grade). The suspension was agitated by sonication and swirling to remove most of the residue from the Schlenk RBF walls (step J). The suspension was cooled to 0 °C briefly, then rapidly vacuum filtered over a P3 glass frit under air, followed by washing with cold diethyl ether (dist., 2x 15 mL from a -20 °C freezer). The filter cake was dried in high vacuum to yield a fine orange-yellow powder (991 mg, 1.30 mmol, 88%) as the product (step K). We were unable to record a standard ^{13}C-NMR spectrum for this compound. ^{13}C-NMR analysis is also absent from other literature reports concerning **C2**.

m.p.: 195 °C (dec.) [Lit.: 194 – 196 °C (dec.)]

^{1}H-NMR (400 MHz, Tol-D$_8$, δ): 8.64 – 8.57 (m, 4H), 7.22 – 7.18 (m, 2H), 7.27 – 7.22 (m, 2H), 7.09 – 7.07 (m, 6H, overlaps with residual toluene signals), 6.84 – 6.75 (m, 4H), 6.65 (t, J = 7.5 Hz, 5H), 6.60 – 6.54 (m, 4H), 6.51 (d, J = 7.3 Hz, 1H), 6.31 (t, J = 6.2 Hz, 1H), 5.64 – 5.56 (m, 2H), 3.71 (s, 3H), 1.55 (s, 3H), 1.51 (s, 3H). Contains THF solvate: 3.45 (m, 4H), 1.45 (m, 4H).

^{31}P-NMR (162 MHz, Tol-D$_8$, δ): 7.42 (s, major), 2.10 (s, minor).

MS (ESI): m/z 727.1 ([M$^+$-Cl])

3.4.3.2. Screening, optimization and control experiments

Supplementary Table 1: Results from screening/optimization and control experiments obtained by quantitative GC-FID
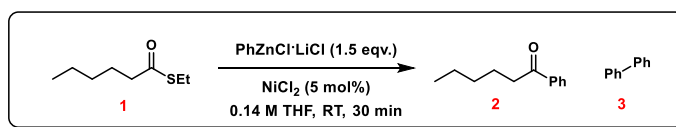
Deviation from conditions:	1 % conv.	2 % yield	3 % yield*		1 % conv.	2 % yield	3 % yield*
	97%	84%	15%	+ 5 mol% terpy	59%	56%	15%
1.2 eqv. PhZnCl LiCl	82%	77%	14%	+ 5 mol% tbubipy	95%	83%	19%
dropwise addition of PhZnCl LiCl	70%	54%	7%	+ 5 mol% meobipy	96%	74%	11%
0 °C, 2 h	79%	63%	10%	+ 5 mol% tmphen	91%	79%	14%
no metal, no ligand	0%	0%	0%	+ 5 mol% bphen, $NiCl_2$(dme) instead	89%	69%	23%
+75 mol% TEMPO	68%	1%	23%	+ 5 mol% tmphen, $NiCl_2$(dme) instead	92%	78%	20%
inverse addition	86%	70%	16%	5 mol% Ni(terpy)Cl_2 instead	51%	51%	9%
5 mol% $NiCl_2$(dme) instead	90%	60%	25%	5 mol% Ni(terpy)Cl_2 instead, 1 h	64%	60%	10%
5 mol% $NiCl_2(H_2O)_6$ instead	77%	80%	15%	5 mol% Ni(xant)(oTol)Cl instead	89%	81%	9%
10 mol% Ni nanoparticles instead	94%	76%	12%	5 mol% Ni(xant)(oTol)Cl instead, 1.86 eqv. Nu, 1.5 h	97%	91%	5%
5 mol% Ni(acac)$_2$ instead	95%	87%	15%	5 mol% Ni(xant)Cl_2 instead	61%	61%	11%
1.5 mol% $NiCl_2$	98%	85%	11%	5 mol% Ni(tbubipy)$(H_2O)_4Cl_2$ instead	88%	63%	18%
1.2 mol% $NiCl_2$, 5 min	57%	47%	12%	5 mol% Ni(dppf)(oTol)Cl instead	72%	59%	10%
5 mol% Fe(acac)$_3$ instead	1%	1%	6%	13:87 v/v toluene:THF as solvent instead	88%	82%	14%
5 mol% Ni(PPh$_3$)$_2$(oTol)Cl instead	89%	62%	25%	13:87 v/v DMAc:THF as solvent instead	53%	49%	14%
				1 mol% Ni(xant)(oTol)Cl instead	89%	24%	19%
				10 mol% Ni(xant)(oTol)Cl instead	92%	66%	57%

*based on $0.5*n_{PhZnCl}$

Screening procedure

A heat gun-dried 10 mL Schlenk tube with stirring bar and rubber septum under Ar was charged with the appropriate catalyst, the thioester **32** (1 eqv., 333 µmol) and dry THF (300 µL). The resulting solution or suspension was stirred rapidly, followed by addition of the Knochel-type phenyl zinc halide **33** in THF (the appropriate indicated equivalents based on the calculated titre., see **GP B**) by syringe. The reaction mixture was stirred for the indicated time at the indicated temperature and quenched with 1 M aq. HCl (1 – 2 mL) and diluted with diethyl ether (3 mL), followed by addition of a carefully measured amount of n-pentadecane (50 or 100 µL, dispensed by Hamilton microliter syringe) as the internal standard. An aliquot of the organic phase was filtered over a pasteur pipette plug of $MgSO_4$, basic Aluminium oxide and flash grade SiO_2 into a GC vial (ca. ¼ full) followed by addition of dist. dichloromethane into the vial. The prepared sample was analysed by quantitative GC-FID to determine yield, conversion and biphenyl byproduct.

Anhydrous $NiCl_2$

Obtained by heating green $NiCl_2(H_2O)_6$ in a Schlenk vessel under vacuum until a yellow solid was obtained. The Schlenk vessel was then refilled with Ar gas and allowed to cool to RT.

NiB nanoparticles, THF suspension

The procedure by Sato, Mashima and co-workers, who characterized the nanoparticles so obtained, was followed[52]: Sodium borohydride (1.4 mg, 38 µmol, 1.5 eqv.) and Ni(acac)$_2$ (6.4 mg, 25 µmol, 1 eqv.) were charged into a flame-dried Schlenk RBF with stirring bar under nitrogen. The solids were treated with dry THF (1.25 mL) and the reaction mixture stirred for 4 h at RT. A deep black suspension slowly formed. The nanoparticles were immediately used without further characterization as a 20 mM suspension (stirred!) in THF under nitrogen.

3.4.3.3. Detection of an acrylate-trapped acyl radical by GC/MS(EI) and NMR

The screening procedure was performed with added ethyl acrylate (2 eqv. relative to the thioester, 0.666 mmol, 71 µL added before addition of the zinc reagent) both with $NiCl_2$ and **C2**. The Fukuyama product was quantitated by our normal GC-FID method and the acrylate-trapped byproduct **33** was analyzed qualitatively by GC/MS and NMR of an enriched column chromatography fraction. The byproduct was formed in both cases, hinting at a radical pathway operative with the two Ni catalysts.
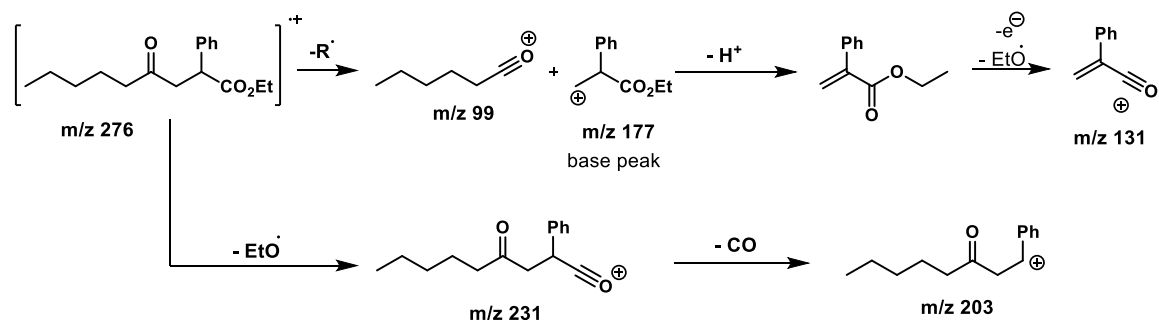
Supplementary Scheme 1: Detection of the molecular ion of the intercepted acyl radical and fragments thereof by GC/MS (EI).

3.4.3.4. Synthesis of thioesters

S-Ethyl hexanoic acid thioester (**32**)
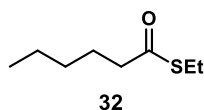
Obtained through **GP A** by employing hexanoic acid (10.75 mL, 86.1 mmol, 1 eqv.), DMAP (1.05 g, 8.6 mmol, 10 mol%), EtSH (25.5 mL, 344.4 mmol, 4 eqv.) and 5 h reaction time in DCM (87 mL). The resulting precipitate was filtered over a P3 glass frit, the filtrate was freed from solvent and excess EtSH by rotary evaporation. The crude product was purified by column chromatography on SiO_2 (PE:Et$_2$O 97.5:2.5 – 95:5 v/v), giving the product **1** as a colourless liquid (7.3 g, 45.6 mmol, 53%) with a distinct light sweet odor.

160.28 g/mol

R_f: 0.23 (PE:Et$_2$O 97.5:2.5)

m.p.: Ambient temperature.

^{1}H-NMR (400 MHz, CDCl$_3$, δ): 2.80 (q, *J* = 7.4 Hz, 2H), 2.51 – 2.41 (m, 2H), 1.67 – 1.53 (m, 2H), 1.24 (dq, *J* = 7.5, 3.4 Hz, 4H), 1.18 (t, *J* = 7.4 Hz, 3H), 0.87 – 0.76 (m, 3H).

^{13}C-NMR (101 MHz, CDCl$_3$, δ): 199.7, 44.1, 31.1, 25.4, 23.2, 22.3, 14.8, 13.9.

HR-MS (APCI): calc. for [M+H]$^+$ m/z 161.09946, found 161.09977.

S-Ethyl 2-ethylhexanoic acid thioester (**55**)

55
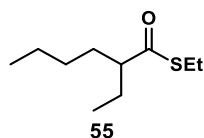
Following **GP A**, 2-ethyl hexanoic acid (1.58 mL, 10 mmol, 1 eqv.) was coupled with EtSH (721 μL, 10 mmol, 1 eqv) using DIC (1.57 mL, 10 mmol, 1 eqv.) and catalytic DMAP (61 mg, 0.5 mmol, 5 mol%) in DCM (50 mL) for 24 h to give the product as a colourless oil, having a sweet odor, (1.86 g, 9.88 mmol, 99%) after the usual workup and column chromatography on SiO_2 (PE:EA 97.5:2.5 v/v).

188.33 g/mol

R_f: 0.64 (UV, PE:Et_2O 97.5:2.5)

m.p.: Ambient temperature.

^{1}H-NMR (400 MHz, $CDCl_3$, δ): 2.80 (q, *J* = 7.4 Hz, 2H), 2.38 (tt, *J* = 8.6, 5.4 Hz, 1H), 1.67 – 1.52 (m, 2H), 1.50 – 1.32 (m, 2H), 1.29 – 1.13 (m, 7H), 0.88 – 0.76 (m, 6H).

^{13}C-NMR (101 MHz, $CDCl_3$, δ): 203.7, 56.1, 32.3, 29.4, 26.0, 23.0, 22.7, 14.9, 13.9, 11.7.

HR-MS (APCI): calc. for [M+H]$^+$ m/z 189.13076, found 189.13099.

S-Ethyl gemfibrozil thioester (**SM52**)

SM52
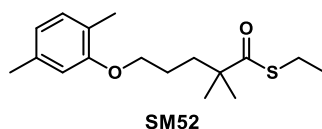
Following **GP A**, gemfibrozil (2.5 g, 10 mmol, 1 eqv.) was coupled with EtSH (721 μL, 10 mmol, 1 eqv.) using DIC (1.57 mL, 10 mmol, 1 eqv.) and catalytic DMAP (122 mg, 1 mmol, 10 mol%) in DCM (50 mL) for 24 h to give the product as a colourless oil (280 mg, 1.12 mmol, 11%) after removal of volatiles, absorbing the crude product on SiO_2 and flash chromatography on SiO_2 (gradient PE:EA 98:2 v/v).

294.45 g/mol

R_f: 0.32 (97.5:2.5 PE:EA)

m.p.: Ambient temperature.

^{1}H-NMR (400 MHz, $CDCl_3$, δ): 7.07 (d, *J* = 7.0 Hz, 1H), 6.73 (d, *J* = 7.7 Hz, 1H), 6.68 (s, 1H), 3.98 (t, *J* = 5.4 Hz, 2H), 2.93 (q, *J* = 7.4 Hz, 2H), 2.38 (s, 3H), 2.27 (s, 3H), 1.92 – 1.72 (m, 4H), 1.38 – 1.28 (m, 9H).

^{13}C-NMR (101 MHz, $CDCl_3$, δ):) 206.3, 157.0, 136.4, 130.4, 123.6, 120.8, 112.0, 67.9, 49.5, 37.6, 25.4, 24.9, 23.0, 21.5, 14.8.

HR-MS (ESI): calc. for [M+Na]$^+$ m/z 317.15457, found 317.15484

<u>*S*-Ethyl 1-adamantylcarboxylic acid thioester (**SM53**)</u>
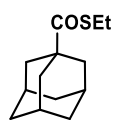
Following **GP A**, 1-Adamantylcarboxylic acid (1.8 g, 10 mmol, 1 eqv.) was coupled with EtSH (721 µL, 10 mmol, 1 eqv.) using DIC (1.57 mL, 10 mmol, 1 eqv.) and catalytic DMAP (122 mg, 1 mmol, 10 mol%) in DCM (50 mL) for 24 h to give the product as a colourless oil (1.45 g, 6.47 mmol, 65%) after removal of volatiles, followed by filtration over SiO$_2$ (PE:Et$_2$O 95:5 v/v).

224.36 g/mol

***R*$_f$**: 0.67 (PE:DCM 8:2).

m.p.: Ambient temperature.

^{1}H-NMR (400 MHz, CDCl$_3$, δ): 2.76 (q, *J* = 7.4 Hz, 2H), 2.02 – 1.92 (m, 3H), 1.89 – 1.80 (m, 6H), 1.74 – 1.59 (m, 6H), 1.16 (t, *J* = 7.4 Hz, 3H).

^{13}C-NMR (101 MHz, CDCl$_3$, δ): 206.63, 48.39, 39.27, 38.27, 36.49, 36.31, 28.21, 27.68, 22.42, 14.70.

HR-MS (ESI): calc. for [M+Na]$^+$ m/z 247.11271, found 247.11301

<u>*S*-Ethyl *N*-tosyl isonepecotic acid thioester (**SM51**)</u>
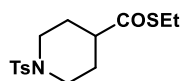
Following **GP A**, *N*-Tosyl isonepecotic acid[S4][73] (1.0 g, 3.53 mmol, 1 eqv.) was coupled with EtSH (1020 µL, 14.12 mmol, 4 eqv.) using DIC (550 µL, 3.53 mmol, 1 eqv.) and catalytic DMAP (43 mg, 353 µmol, 10 mol%) in DCM (20 mL) for 24 h to give the product as white crystals (581 mg, 1.77 mmol, 50%) after removal of volatiles, followed by flash column chromatography (SiO$_2$, gradient PE:EA 8:2 v/v).

327.46 g/mol

***R*$_f$**: 0.48 (UV, PE:EA 8:2).

m.p.: 108 °C.

^{1}H-NMR (400 MHz, CDCl$_3$, δ): 7.59 – 7.54 (m, 2H), 7.28 – 7.23 (m, 2H), 3.77 – 3.54 (m, 2H), 2.78 (q, *J* = 7.4 Hz, 2H), 2.40 – 2.26 (m, 6H), 1.93 – 1.70 (m, 4H), 1.15 (t, *J* = 7.4 Hz, 3H).

¹³C-NMR (101 MHz, CDCl₃, δ): 201.0, 143.6, 133.1, 129.7, 127.8, 49.1, 45.4, 28.0, 23.1, 21.5, 14.6.

HR-MS (ESI): calc. for [M+Na]⁺ m/z 350.08551, found 350.08542.

<u>*S*-Ethyl 3-(3-pyridyl)propionic acid thioester (**SM42**)</u>
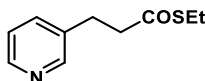
SM42

3-(3-Pyridyl)propionic acid (467 mg, 3.09 mmol) was partially dissolved in DMF (7 mL) and DCM (10 mL), followed by the addition of DMAP (37.8 mg, 310 µmol, 0.1 eqv.) and EtSH (835 µL, 11.59 mmol, 3.75 eqv.). The resulting suspension was cooled to 0 °C, to which DIC was added (484 µL, 3.09 mmol, 1.0 eqv.). The reaction mixture was stirred at 0 °C for 5 min, then 18 h at RT. The solvents were removed by rotary evaporation. The residue was adsorbed on SiO₂ (500 mg), followed by flash column chromatography (37 g SiO₂, Gradient PE:EtOAc 8:2) to furnish the product as a colourless oil (170 mg, 871 µmol, 28%) after solvent removal *in vacuo*.

195.28 mg/mmol

R_f: 0.14 (8:2 PE:EtOAc).

m.p.: Ambient temperature.

¹H-NMR (400 MHz, CDCl₃, δ): 8.58 – 8.26 (m, 2H), 7.44 (d, *J* = 7.9 Hz, 1H), 7.14 (dd, *J* = 7.8, 4.8 Hz, 1H), 2.91 (t, *J* = 7.5 Hz, 2H), 2.84 – 2.75 (m, 4H), 1.15 (t, *J* = 7.4, 3H).

¹³C-NMR (101 MHz, CDCl₃, δ): 198.1, 149.8, 147.8, 135.8, 135.5, 123.4, 44.8, 28.5, 23.4, 14.7.

HR-MS (ESI): calc. for [M+H]⁺ m/z 196.07906, found 196.07930.

<u>S-Ethyl 3-(1*H*-Indol-3-yl)-propionic acid thioester (**SM43**)</u>
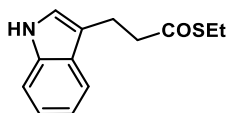
SM43

Following **GP A**, 3-(1*H*-Indol-3-yl)-propionic acid (1.89 g, 10 mmol, 1 eqv.) was coupled with EtSH (721 µL, 10 mmol, 1 eqv) using DIC (1.57 mL, 10 mmol, 1 eqv.) and catalytic DMAP (122.2 mg, 1 mmol, 10 mol%) in DCM (50 mL) for 24 h to give the product as a yellow oil (1.94 g, 8.31 mmol, 83%) after the usual workup and filtration over a pad of SiO₂ (8:2 PE:EA v/v), followed by removal of solvent by rotary evaporation. Conforms to reported analytical data.[S5]

233.33 g/mol

R$_f$: 0.44 (8:2 PE:EA).

m.p.: Ambient temperature.

^{1}H-NMR (400 MHz, CDCl$_3$, δ): 7.90 (br s, 1H), 7.51 (d, *J* = 6.7 Hz, 1H), 7.24 (d, *J* = 8.0 Hz, 1H), 7.16 – 7.02 (m, 2H), 6.88 (s, 1H), 3.05 (t, *J* = 7.8 Hz, 2H), 2.91 – 2.76 (m, 4H), 1.16 (t, *J* = 7.4 Hz, 3H).

^{13}C-NMR (101 MHz, CDCl$_3$, δ): 199.4, 136.3, 127.2, 122.1, 121.5, 119.4, 118.7, 114.6, 111.2, 44.6, 23.3, 21.3, 14.8.

GC-MS (EI): m/z 233, 143, 130.

S-Ethyl O-Ethyl adipic acid diester (**SM40**)

SM40
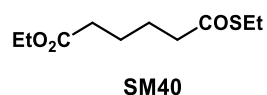
Following **GP A**, adipic acid monoethyl ester (1.74 g, 10 mmol, 1 eqv.) was coupled with EtSH (721 µL, 10 mmol, 1 eqv) using DIC (1.57 mL, 10 mmol, 1 eqv.) and catalytic DMAP (122 mg, 1 mmol, 10 mol%) in DCM (50 mL) for 24 h to give the product as a colourless oil (1.81 g, 8.86 mmol, 89%) after the removal of solvent and excess EtSH, followed by filtration over a short pad of SiO$_2$ (PE:Et$_2$O 9:1 v/v).

218.31 g/mol

R$_f$: 0.38 (85:15 PE:EA).

m.p.: Ambient temperature.

^{1}H-NMR (400 MHz, CDCl$_3$, δ) 4.06 (q, *J* = 7.1 Hz, 2H), 2.80 (q, *J* = 7.4 Hz, 2H), 2.49 (t, *J* = 7.0 Hz, 2H), 2.24 (t, *J* = 7.0 Hz, 2H), 1.69 – 1.54 (m, 4H), 1.22 – 1.13 (m, 6H).

^{13}C-NMR (101 MHz, CDCl$_3$, δ) 199.2, 173.2, 60.3, 43.6, 33.9, 25.0, 24.2, 23.2, 14.8, 14.2.

HR-MS (ESI): calc. for [M+Na]$^+$ m/z 241.08689, found 241.08713.

S-ethyl 4,4,5,5,6,6,7,7,8,8,9,9,10,10,11,11,11-heptadecafluoroundecanoic acid thioester (**SM48**)
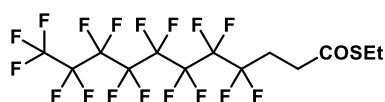
SM48

Following **GP A**, 4,4,5,5,6,6,7,7,8,8,9,9,10,10,11,11,11-heptadecafluoroundecanoic acid (984 mg, 2 mmol, 1 eqv.) was coupled with EtSH (432 µL, 6 mmol, 1 eqv) using DIC (310 mL, 2 mmol, 1 eqv.) and catalytic DMAP (12.21 mg, 0.1 mmol, 5 mol%) in DCM (10 mL) for 30 h to give the product as a crystalline solid (350 mg, 0.63 mmol, 32%) after the removal of solvent and excess EtSH, followed by column chromatography in 100% CyH.

536.25 mg/mmol

R$_f$: 0.14 (CyH)

m.p.: 36-38 ^{o}C

^{1}H-NMR (400 MHz, CDCl$_3$, δ) δ 2.97 – 2.81 (m, 4H), 2.56 – 2.41 (m, 2H), 1.26 (t, J = 7.4 Hz, 3H).

^{13}C-NMR (101 MHz, CDCl$_3$ δ$_C$) : δ 196.4, 34.5, 26.5 (t, J = 22.5 Hz), 23.5, 14.5.

^{19}F NMR (376 MHz, CDCl$_3$) δ -81.02, -114.61, -121.84, -122.07, -122.88, -123.58, -126.30.

HR-MS (ESI): calc. for [M+Na]$^+$ m/z 558.99949, found 559.00008

S-Ethyl dehydrocholic acid thioester (**SM46**)
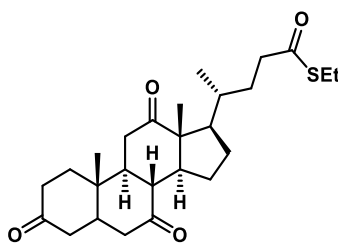
SM46

Following **GP A**, dehydrocholic acid (4.03 g, 10 mmol, 1 eqv.) was coupled with EtSH (722 µL, 10 mmol, 1 eqv.) using DIC (1.57 mL, 10 mmol, 1 eqv.) and catalytic DMAP in DCM (50 mL) for 24 h to give the product as a white solid (2.45 g, 5.49 mmol, 55%) after the removal of solvent and excess EtSH, followed by flash column chromatography (SiO$_2$, gradient 6:4 PE:EA).

446.65 g/mol

R$_f$: 0.60 (97.5:2.5 DCM:MeOH)

m.p.: 252 °C**.**

^{1}H-NMR (400 MHz, CDCl$_3$, δ): 2.90 – 2.73 (m, 5H), 2.55 (ddd, J = 14.9, 9.6, 5.2 Hz, 1H), 2.43 (ddd, J = 15.3, 9.3, 6.8 Hz, 1H), 2.32 – 1.72 (m, 14H), 1.55 (td, J = 14.2, 5.1 Hz, 1H), 1.33 (m, 4H), 1.29 – 1.21 (m, 2H), 1.18 (t, J = 7.4 Hz, 3H), 1.00 (s, 3H), 0.79 (d, J = 6.6 Hz, 3H).

^{13}C-NMR (101 MHz, CDCl$_3$, δ) δ 211.9, 209.0, 208.7, 200.0, 56.9, 51.8, 49.0, 46.9, 45.6, 45.0, 42.8, 41.3, 38.6, 36.5, 36.0, 35.4, 35.3, 31.1, 27.6, 25.1, 23.3, 21.9, 18.7, 14.8, 11.9.

HR-MS (ESI): calc. for [M+Na]$^{+}$ m/z 469.23830, found 469.23892.

<u>*S*-heptyl naphth-2-yl carboxylic acid thioester (**SM54**)</u>

SM54
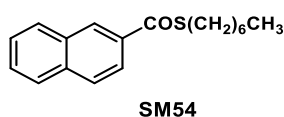
Following **GP A**, naphth-2-yl carboxylic acid (8.78 g, 51 mmol, 1 eqv.) was coupled with heptanethiol (7.99 mL, 51 mmol, 1 eqv) using DIC (7.9 mL, 51 mmol, 1 eqv.) and catalytic DMAP (624 mg, 5.1 mmol, 10 mol%) in DCM (50 mL) for 24 h to give the product as a colourless oil (10.2 g, 35.6 mmol, 70%) after the removal of solvent, followed by filtration over a short pad of SiO$_2$ (PE:EA 95:5).

286.43 g/mol

R_f: 0.47 (PE:Et$_2$O 97.5:2.5).

m.p.: Ambient temperature.

^{1}H-NMR (400 MHz, CDCl$_3$, δ): 8.54 (s, 1H), 8.00 (dd, J = 8.6, 1.8 Hz, 1H), 7.97 (d, J = 8.2 Hz, 1H), 7.93 – 7.82 (m, 2H), 7.57 (dddd, J = 17.7, 8.1, 6.8, 1.4 Hz, 1H), 3.26 – 3.03 (m, 2H), 1.80 – 1.65 (m, 2H), 1.52 – 1.40 (m, 2H), 1.39 – 1.25 (m, 7H), 0.95 – 0.81 (m, 3H).

^{13}C-NMR (101 MHz, CDCl$_3$, δ): 199.2, 173.2, 60.3, 43.6, 33.9, 25.0, 24.2, 23.2, 14.8, 14.2.

HR-MS (ESI): calc. for [M+Na]$^{+}$ m/z 309.12836, found 309.12867.

<u>*S*-ethyl 2-phenylpropionic acid thioester (**70**)</u>

70
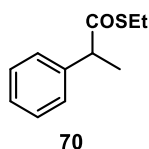
Following **GP A**, 2-phenylpropionic acid (1.37 mL, 10 mmol, 1 eqv.) was coupled with EtSH (721 µL, 10 mmol, 1 eqv) using DIC (1.57 mL, 10 mmol, 1 eqv.) and catalytic DMAP (61 mg, 500 µmol, 10 mol%) in DCM (50 mL) for 24 h to give the product as a colourless oil (1.88 g, 35.6 mmol, 97%) after the

removal of solvent and excess EtSH, followed by filtration over a short pad of SiO_2 (PE:EA 95:5). Conforms to reported analytical data.[9]

194.29 g/mol

R_f: 0.59 (PE:Et$_2$O 97.5:2.5)

m.p.: Ambient temperature.

^{1}H-NMR (400 MHz, CDCl$_3$, δ) 7.32 – 7.12 (m, 5H), 3.80 (q, *J* = 7.1 Hz, 1H), 2.83 – 2.68 (m, 2H), 1.46 (d, *J* = 7.1 Hz, 3H), 1.13 (t, *J* = 7.4 Hz, 3H).

^{13}C-NMR (101 MHz, CDCl$_3$, δ): 201.2, 140.0, 128.7, 127.9, 127.4, 54.2, 23.5, 18.4, 14.5.

GC-MS (EI): m/z 77 ($C_6H_5^+$), 105 ($C_8H_9^+$), 117 ($C_5H_9OS^+$), 165 ([M+●]-[Et●]).

<u>*S*-ethyl 3-phenylpropionic acid thioester (**SM36**)</u>
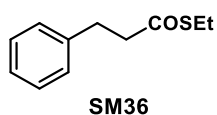
Following **GP A**, 3-phenylpropionic acid (601 mg, 4 mmol, 1 eqv.) was coupled with EtSH (865 mL, 12 mmol, 3 eqv.) using DIC (625 µL, 4 mmol, 1 eqv.) and catalytic DMAP (49 mg, 400 µmol, 1 eqv.) in DCM (20 mL) for 24 h to give the product as a colourless oil (105 mg, 540 µmol, 14%) after the removal of solvent and excess EtSH, followed by flash column chromatography (SiO$_2$, gradient 97.5:2.5 to 95:5 PE:EA). Conforms to reported analytical data.[S6][75]

194.29 g/mol

R_f: 0.54 (PE:EA 9:1).

m.p.: Ambient temperature.

^{1}H-NMR (400 MHz, CDCl$_3$, δ) 7.25 – 7.16 (m, 2H), 7.15 – 7.07 (m, 3H), 2.95 – 2.86 (m, 2H), 2.86 – 2.73 (m, 4H), 1.16 (t, *J* = 7.4 Hz, 3H).

^{13}C-NMR (101 MHz, CDCl$_3$, δ) 198.7, 140.2, 128.5, 128.3, 126.3, 45.5, 31.5, 23.3, 14.8.

GC-MS (EI): m/z 194.

<u>*S*-heptyl 3-(3-fluorophenyl)propionic acid thioester (**SM37**)</u>
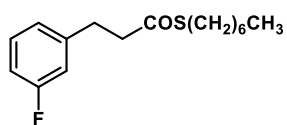
Following **GP A**, 3-(3-Fluorophenyl)propionic acid (500 mg, 2.97 mmol, 1 eqv.) was coupled with HeptSH (2.97 mmol, 1 eqv.) using DIC (3.27 mmol, 1.1 eqv.) and catalytic DMAP (32 mg, 208 µmol, 10 mol%) in DCM (10 mL) for 16 h to give the product as a colourless oil (590 mg, 2.08 mmol, 70%) after removal of volatiles, followed by filtration over SiO_2 (DCM).

282.42 g/mol

R_f: 0.73 (PE:EA 95:5).

m.p: Ambient temperature.

^{1}H-NMR (400 MHz, CDCl$_3$, δ) 7.16 (ddd, *J* = 9.0, 7.4, 5.8 Hz, 1H), 6.88 (dt, *J* = 7.8, 1.2 Hz, 1H), 6.85 − 6.76 (m, 2H), 2.94 − 2.86 (m, 2H), 2.83 − 2.72 (m, 2H), 1.63 − 1.41 (m, 2H), 1.36 − 1.10 (m, 10H), 0.84 − 0.77 (m, 3H).

^{13}C-NMR (101 MHz, CDCl$_3$, δ) 198.4, 162.9 (d, $^1J_{CF}$ = 245.7 Hz), 142.6 (d, *J* = 7.3 Hz), 129.9 (d, *J* = 8.4 Hz), 124.0 (d, *J* = 2.9 Hz), 115.3 (d, *J* = 21.1 Hz), 113.2 (d, *J* = 21.0 Hz), 45.1, 31.7, 31.1 (d, *J* = 1.8 Hz), 29.5, 29.0, 28.8 , 28.8, 22.6, 14.1.

^{19}F-NMR (376 MHz, CDCl$_3$, δ): -113.34.

HR-MS (ESI): calc. for [M+Na]$^+$ m/z 305.1346, found 305.1350.

S-ethyl 3-(4-methoxyphenyl)propionic acid thioester (**SM39**)
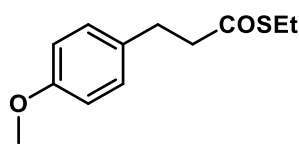
SM39

Following **GP A**, 3-(4-methoxyphenyl) propanoic acid (360.40 mg, 2 mmol, 1 eqv.) was coupled with EtSH (6 mmol, 3 eqv.) using DIC (2 mmol, 1 eqv.) and catalytic DMAP (12.21 mg, 100 μmol, 5 mol%) in DCM (10 mL) for 16 h to give the product as a colourless oil (226 mg, 1.04 mmol, 50.44%) after removal of volatiles, followed by filtration over SiO2 (gradient 97.5:2.5 to 95:5 PE : EtOAc).

MW: 224.31 g/mol

R_f: 0.84 (PE:EA 8:2)

m.p: Ambient temperature.

[1]**H-NMR** (400 MHz, CDCl$_3$, δ): δ 7.10 (d, J = 8.9 Hz, 2H), 6.83 (d, J = 8.6 Hz, 2H), 3.78 (s, 3H), 2.98 – 2.77 (m, 6H), 1.24 (t, J = 7.4 Hz, 3H)

[13]**C-NMR** (101 MHz, CDCl$_3$, δ): 198.78, 158.11, 132.19, 129.27, 113.92, 55.25, 45.83, 30.65, 23.30, 14.78

HR-MS (ESI): calc. for [M+Na]$^+$ m/z 247.07632, found 247.07663

S-heptyl 3-methylpent-4-enoic acid thioester (**SM45**)
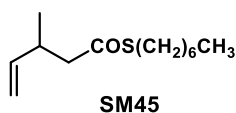
SM45

228.39 g/mol

R_f: 0.82 (PE:EA 95:5).

m.p: Ambient temperature.

[1]**H-NMR** (400 MHz, CDCl$_3$, δ): 5.68 (ddd, J = 17.2, 10.3, 6.9 Hz, 1H), 4.95 (dt, J = 17.2, 1.4 Hz, 1H), 4.89 (dt, J = 10.3, 1.3 Hz, 1H), 2.84 – 2.77 (m, 2H), 2.73 – 2.60 (m, 1H), 2.52 (dd, J = 14.5, 6.8 Hz, 1H), 2.41 (dd, J = 14.5, 7.5 Hz, 1H), 1.55 – 1.43 (m, 2H), 1.32 – 1.13 (m, 8H), 0.98 (d, J = 6.8 Hz, 3H), 0.85 – 0.76 (m, 3H).

[13]**C-NMR** (101 MHz, CDCl$_3$, δ): 198.4, 142.1, 113.5, 50.6, 35:0, 31.7, 29.6, 28.9, 28.8, 28.8, 22.6, 19.4, 14.1.

HR-MS (ESI): calc. for [M+Na]$^+$ m/z 251.14401, found 251.14441

_S_-ethyl 3,3,3-triphenylpropanoic acid thioester (**SM49**)

SM49
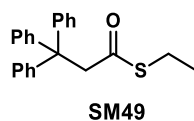
   Following GP A, 3,3,3-triphenylpropanoic acid (1.209 g, 4 mmol, 1 eqv.) was coupled with EtSH (12 mmol, 3 eqv.) using DIC (4 mmol, 1 eqv.) and catalytic DMAP (24.42 mg, 200 µmol, 5 mol%) in DCM (20 mL) for 6 h to give the product as a white solid (420 mg, 1.21 mmol, 30%) after removal of volatiles, followed by column chromatography over SiO_2 (gradient PE: EtOAc 97:3 to 92:8 v/v)

MW: 346.48 g/mol

R_f: 0.52 (PE:Et$_2$O 9:1)

m.p: 81-83 °C

^{1}H-NMR (400 MHz, CDCl$_3$, δ): 7.26 (m, 15H), 4.07 (s, 2H), 2.75 (q, J = 7.4 Hz, 2H), 1.12 (t, J = 7.4 Hz, 3H)

^{13}C-NMR (101 MHz, CDCl$_3$, δ): 196.60, 146.39, 129.26, 127.84, 126.29, 56.73, 54.90, 23.62, 14.64

HR-MS: calc. for [M+Na]$^+$ m/z 369.12836, found 369.12870

S-Ethyl octadec-9-enoic acid thioester (**SM47**)

SM47
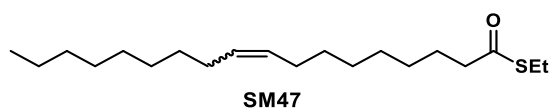
   Following **GP A**, octadec-9-enoic acid (1.47 g, 5.20 mmol, 1 eqv.) was coupled with EtSH (1.5 mL, 20.82 mmol, 4 eqv.) using DIC (890 µL, 5.72 mmol, 1.1 eqv.) and catalytic DMAP (64 mg, 520 µmol, 10 mol%) in DCM (25 mL) for 16 h to give the product as a colourless oil (1.3 g, 3.98 mmol, 77%) after removal of volatiles, followed by filtration over SiO_2 (DCM).

326.58 g/mol

R_f: 0.33 (PE:EA 97.5:2.5).

m.p.: Ambient temperature.

^{1}H-NMR (400 MHz, CDCl$_3$, δ) 5.34 − 5.25 (m, 2H), 2.80 (q, _J_ = 7.4 Hz, 2H), 2.51 − 2.41 (m, 2H), 2.03 − 1.83 (m, 4H), 1.64 − 1.47 (m, _J_ = 6.9 Hz, 2H), 1.29 − 1.14 (m, 23H), 0.87 − 0.73 (m, 3H).

13C-NMR (101 MHz, CDCl3, δ) 13C NMR (101 MHz, CDCl3) δ 199.8, 130.5, 130.2, 130.0, 129.7, 44.1, 31.9, 29.8, 29.7, 29.5, 29.3, 29.2, 29.1, 28.9, 27.2, 25.7, 23.2, 22.7, 14.8, 14.1.

HR-MS (ESI): calc. for [M+Na]+ m/z 349.25356, found 349.25376

3.4.3.5. Synthesis of ketones

1-Phenyl-hexan-1-one (**34**), 1 g scale

34
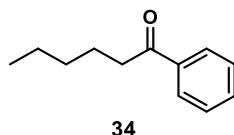
GP C was scaled to 1 g of **32** (6.24 mmol) using phenyl zinc chloride (**GP B**) as the nucleophile in glassware of appropriate size. After the usual workup, the volatiles were removed and the black residual oil purified by Kugelrohr distillation (280 °C oven temperature, 80 mbar) to give the product (964 mg, 5.47 mmol, 88%) as a colourless oil. Conforms to reported analytical data[S7][76].

176.12 g/mol

R_f: 0.5 (PE:EA 95:5)

m.p.: Ambient temperature.

1H NMR (400 MHz, CDCl3, δ) 7.96 – 7.86 (m, 2H), 7.50 – 7.44 (m, 1H), 7.41 – 7.34 (m, 2H), 2.95 – 2.83 (m, 2H), 1.75 – 1.57 (m, 2H), 1.35 – 1.21 (m, 4H), 0.90 – 0.78 (m, 3H).

13C NMR (101 MHz, CDCl3, δ) 200.6, 137.1, 132.9, 128.5, 128.1, 38.6, 31.6, 24.1, 22.6, 14.0.

GC-MS (EI)**:** m/z 176.1, 120, 105.

2-Ethyl-1-phenylhexan-1-one (**50**)
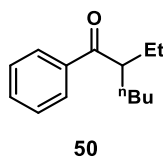
50

Following **GP C**, the thioester **SM56** (63 mg, 333 µmol, 1 eqv.) was coupled with with phenyl zinc chloride (0.25 M in THF, by **GP B**). The crude product was purified by flash column chromatography (SiO2, PE:EA gradient 98:2 v/v) to give the product as a brownish oil (35 mg, 171 µmol, 51%).

204.31 g/mol

R_f: 0.27 (PE:Et$_2$O 9:1)

m.p.: Ambient temperature.

^{1}H NMR (400 MHz, CDCl$_3$, δ) 7.89 (d, J = 7.8 Hz, 2H), 7.48 (t, J = 7.4 Hz, 1H), 7.39 (t, J = 7.6 Hz, 2H), 3.41 – 3.18 (m, 1H), 1.80 – 1.59 (m, 2H), 1.58 – 1.33 (m, 2H), 1.28 – 1.11 (m, 4H), 0.87 – 0.72 (m, 6H).

^{13}C NMR (101 MHz, CDCl$_3$, δ) 204.7, 137.8, 132.8, 128.6, 128.2, 47.6, 31.7, 29.8, 25.4, 22.9, 13.9, 11.9.

HR-MS (ESI): calc. for [M+Na]$^+$ m/z 227.14064, found 227.14099.

2-Ethyl-1-(2-methoxyphenyl)hexan-1-one (**68**)

68
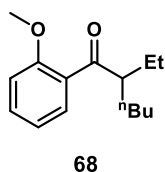
Following **GP C**, the thioester **SM56** (63 mg, 333 µmol, 1 eqv.) was coupled with with *ortho*-anisyl zinc chloride (0.25 M in THF, by **GP B**). The crude product was purified by flash column chromatography (SiO$_2$, PE:Et$_2$O gradient 95:5 v/v) to give the product as a colourless oil (40 mg, 171 µmol, 51%).

234.34 g/mol

R_f: 0.57 (PE:Et$_2$O 85:15)

m.p.: Ambient temperature.

^{1}H NMR (400 MHz, CDCl$_3$, δ) 7.43 (dd, J = 7.6, 1.8 Hz, 1H), 7.35 (ddd, J = 8.2, 7.3, 1.8 Hz, 1H), 6.92 (td, J = 7.5, 1.0 Hz, 1H), 6.87 (d, J = 8.3 Hz, 1H), 3.80 (s, 3H), 3.25 (tt, J = 7.1, 5.8 Hz, 1H), 1.76 – 1.60 (m, 2H), 1.48 – 1.29 (m, 2H), 1.26 – 1.12 (m, 4H), 0.80 (dt, J = 8.8, 7.1 Hz, 6H).

^{13}C NMR (101 MHz, CDCl$_3$, δ) 207.8, 157.8, 132.5, 130.2, 129.9, 120.7, 111.5, 55.4, 52.1, 30.8, 29.7, 24.5, 22.9, 14.0, 11.8.

HR-MS (ESI): calc. for [M+Na]$^+$ m/z 257.15120, found 257.15154.

2-Ethyl-1-(4-methylphenyl)hexan-1-one (**84**)
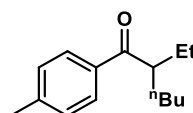
84

Following **GP C**, the thioester **SM56** (63 mg, 333 µmol, 1 eqv.) was coupled with with *para*-tolyl zinc chloride (0.25 M in THF, by **GP B**). The crude product was purified by flash column chromatography (SiO$_2$, PE:Et$_2$O gradient 98:2 v/v) to give the product as a colourless oil (50 mg, 171 µmol, 69%).

218.34 g/mol

R$_f$ 0.39 (97.5:2.5 PE:Et$_2$O).

m.p.: Ambient temperature.

^{1}H NMR (400 MHz, CDCl$_3$, δ) : 7.79 (d, *J* = 8.0 Hz, 2H), 7.18 (d, *J* = 8.0 Hz, 2H), 3.26 (tt, *J* = 7.8, 5.5 Hz, 1H), 2.33 (s, 3H), 1.80 – 1.57 (m, 1H), 1.56 – 1.33 (m, 1H), 1.27 – 1.06 (m, 2H), 0.78 (q, *J* = 7.4 Hz, 3H).

^{13}C NMR (101 MHz, CDCl$_3$, δ): 204.3, 143.5, 135.4, 129.3, 128.3, 47.5, 31.8, 29.8, 25.5, 22.9, 21.6, 14.0, 12.0.

HR-MS (ESI): m/z = calc. for [M+Na]$^+$ 241.15629, found 251.15665.

2-Ethyl-1-((4-ethylthio)phenyl)hexan-1-one (**58**)
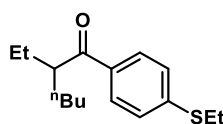
58

Following **GP C**, the thioester **SM56** (63 mg, 333 µmol, 1 eqv.) was coupled with with para-chlorophenyl zinc chloride (0.25 M in THF, by **GP B**). The crude product was purified by flash column chromatography (SiO$_2$, PE:Et$_2$O gradient 98:2 v/v) to give the product as a colourless oil (41 mg, 155 µmol, 47%).

264.43 g/mol

R$_f$ 0.25 (97.5:2.5 PE:Et$_2$O).

m.p.: Ambient temperature.

---

^{1}H NMR (400 MHz, CDCl$_3$, δ) 7.80 (d, J = 8.5 Hz, 2H), 7.24 (d, J = 8.5 Hz, 2H), 3.23 (tt, J = 7.8, 5.5 Hz, 1H), 2.95 (q, J = 7.4 Hz, 2H), 1.77 − 1.62 (m, 2H), 1.57 − 1.35 (m, 2H), 1.31 (t, J = 7.3 Hz, 2H), 1.26 − 1.08 (m, 4H), 0.83 − 0.71 (m, 7H).

^{13}C NMR (101 MHz, CDCl$_3$, δ) 203.7, 144.2, 134.4, 128.6, 126.4, 47.4, 31.8, 29.8, 26.1, 25.5, 22.9, 14.0, 13.9, 12.0.

HR-MS (ESI): m/z = calc. for [M+Na]$^+$: 287.14401, found: 287.14409.

<u>2-Ethyl-1-(4-fluorophenyl)hexan-1-one (**59**)</u>
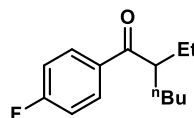
59

Following **GP C**, the thioester **SM56** (63 mg, 333 µmol, 1 eqv.) was coupled with with para-fluorophenyl zinc chloride (0.25 M in THF, by **GP B**). The crude product was purified by flash column chromatography (SiO$_2$, PE:Et$_2$O gradient 98:2 v/v) to give the product as a colourless oil (35 mg, 155 µmol, 47%).

222.30 g/mol

R$_f$ 0.42 (97.5:2.5 PE:EtOAc).

m.p.: Ambient temperature.

^{1}H NMR (400 MHz, CDCl$_3$, δ) 8.02 − 7.83 (m, 2H), 7.15 − 7.01 (m, 2H), 3.23 (tt, J = 7.7, 5.5 Hz, 1H,), 1.77 − 1.62 (m, 2H), 1.58 − 1.36 (m, 2H), 1.29 − 1.08 (m, 4H), 0.87 − 0.73 (m, 6H).

^{13}C NMR (101 MHz, CDCl$_3$, δ) 203.0, 165.6 (d, $^1J_{CF}$ = 254.2 Hz), 134.2 (d, $^4J_{CF}$ = 3.1 Hz), 130.8 (d, J_{CF} = 9.2 Hz), 115.7 (d, J_{CF} = 21.7 Hz), 47.6, 31.7, 29.8, 25.4, 22.9, 13.9, 11.9.

^{19}F NMR (376 MHz, CDCl$_3$, δ) -106.00 (m).

HR-MS (ESI): m/z = calc. for [M+Na]$^+$: 245.13121, found: 245.13155.

2-Ethyl-1-(3-methoxyphenyl)hexan-1-one (**63**)

63
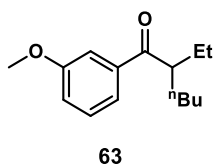
Following **GP C**, the thioester **SM56** (63 mg, 333 μmol, 1 eqv.) was coupled with with *meta*-methoxyphenyl zinc chloride (0.25 M in THF, by **GP B**). The crude product was purified by flash chromatography (SiO$_2$ 97.5:2.5 PE:EtOAc gradient) to give the product as a colourless oil (53 mg, 226 μmol, 68%).

234.34 g/mol

R$_f$ 0.42 (97.5:2.5 PE:EtOAc).

m.p.: Ambient temperature

^{1}H NMR (400 MHz, CDCl$_3$, δ) 7.46 (d, *J* = 7.8 Hz, 1H), 7.42 (dd, *J* = 2.7, 1.5 Hz, 1H), 7.30 (t, *J* = 7.9 Hz, 1H), 7.03 (ddd, *J* = 8.2, 2.7, 0.9 Hz, 1H), 3.79 (s, 3H), 3.25 (tt, *J* = 7.7, 5.5 Hz, 1H), 1.78 − 1.63 (m, 2H), 1.54 − 1.36 (m, 2H), 1.28 − 1.10 (m, 4H), 0.83 − 0.74 (m, 6H).

^{13}C NMR (101 MHz, CDCl$_3$, δ) 204.5, 159.9, 139.2, 129.5, 120.7, 119.2, 112.6, 55.4, 47.8, 31.8, 29.8, 25.5, 22.9, 13.9, 12.0.

HR-MS (ESI): m/z = calc. for [M+Na]$^+$: 257.15120, found: 257.15164.

2-Ethyl-1-(4-methoxyphenyl)hexan-1-one (**57**)

SM57
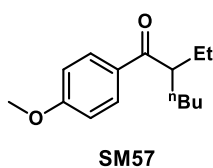
Following **GP C**, the thioester **SM56** (63 mg, 333 μmol, 1 eqv.) was coupled with with *para*-methoxyphenyl zinc chloride (0.25 M in THF, by **GP B**). The crude product was purified by flash chromatography (SiO$_2$ 95:5 PE:EtOAc gradient) to give an impure residue which was treated with dist. EtOH and filtered to remove the insoluble biaryl byproduct, giving the product as a brown oil (48 mg, 203 μmol, 61%).

234.34 g/mol

R$_f$ 0.14 (97.5:2.5 PE:EtOAc).

m.p.: Ambient temperature.

1H NMR (400 MHz, CDCl$_3$) δ 7.89 (d, J = 8.8 Hz, 2H), 6.87 (d, J = 8.8 Hz, 2H), 3.80 (s, 3H), 3.23 (tt, J = 7.8, 5.4 Hz, 1H), 1.75 – 1.63 (m, 2H), 1.58 – 1.33 (m, 2H), 1.28 – 1.06 (m, 4H), 0.78 (m, 6H).

13C NMR (101 MHz, CDCl$_3$) δ 203.2, 163.3, 130.9, 130.4, 113.7, 55.5, 47.2, 32.0, 29.8, 25.6, 22.9, 14.0, 12.0.

HR-MS (ESI): m/z = calc. for [M+Na]$^+$: 257.15120, found: 257.15150.

2-ethyl-1-(thiophen-2-yl)hexan-1-one (**62**)

62
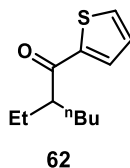
Following **GP C**, the thioester **SM56** (63 mg, 333 µmol, 1 eqv.) was coupled with with thien-2-yl zinc chloride (0.25 M in THF, by **GP B**). The crude product was purified by flash chromatography (SiO$_2$ 97.5:2.5 PE:Et2O isocratic) to give the product as a brown oil (45 mg, 213 µmol, 64%).

210.34 g/mol

R$_f$: 0.3 (97.5:2.5 PE:EtOAc).

m.p.: Ambient temperature.

1H NMR (400 MHz, CDCl$_3$, δ) 7.66 (dd, J = 3.8, 1.1 Hz, 1H), 7.56 (dd, J = 5.0, 1.1 Hz, 1H), 7.07 (dd, J = 4.9, 3.8 Hz, 1H), 3.07 (tt, J = 8.2, 5.4 Hz, 1H), 1.82 – 1.63 (m, 2H), 1.60 – 1.28 (m, 2H), 1.30 – 1.10 (m, 4H), 0.89 – 0.69 (m, 6H).

13C NMR (101 MHz, CDCl$_3$, δ) 197.5, 163.5, 145.7, 133.6, 131.6, 128.1, 50.1, 32.2, 29.9, 25.9, 22.9, 13.9, 12.1.

HR-MS (ESI): calc. for [M+Na]$^+$ m/z 233.09706, found 255.09742.

5-(2,5-dimethylphenoxy)-2,2-dimethyl-1-phenylpentan-1-one (**52**)
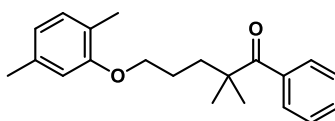
52

Following **GP C**, the thioester **SM52** (98 mg, 333 µmol, 1 eqv.) was coupled with with phenyl zinc chloride (0.25 M in THF, by **GP B**). The crude product was purified by flash chromatography (SiO$_2$ 95:5 PE:Et$_2$O gradient) to give the product as a colourless oil (28 mg, 90 µmol, 27%).

310.44 g/mol

R$_f$: 0.15 (97.5:2.5 PE:EA)

m.p.: Ambient temperature.

^{1}H-NMR (400 MHz, CDCl$_3$, δ): 7.67 − 7.56 (m, 2H), 7.42 − 7.35 (m, 1H), 7.35 − 7.28 (m, 2H), 6.92 (dd, J = 7.5, 1.0 Hz, 1H), 6.63 − 6.54 (m, 1H), 6.53 − 6.45 (m, 1H), 3.82 (t, J = 6.1 Hz, 2H), 2.22 (s, 3H), 2.06 (s, 3H), 1.96 − 1.80 (m, 2H), 1.74 − 1.59 (m, 2H), 1.29 (s, 6H).

^{13}C-NMR (101 MHz, CDCl$_3$, δ): 208.9, 156.9, 139.0, 136.5, 130.9, 130.3, 128.2, 127.6, 123.5, 120.7, 111.8, 67.8, 47.6, 37.5, 26.2, 25.1, 21.4, 15.8.

HR-MS (ESI): calc. for [M+Na]$^+$ m/z 333.18250, found 333.18250.

Phenyl(1-tosylpiperidin-4-yl)methanone (**51**)
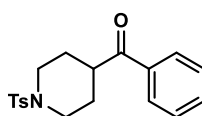
51

Following **GP C**, the thioester **SM51** (109 mg, 333 µmol, 1 eqv.) was coupled with with phenyl zinc chloride (0.25 M in THF, by **GP B**). The crude product was purified by flash chromatography (SiO$_2$ 8:2 PE:Et$_2$O gradient) to give the product as a white solid (26 mg, 76 µmol, 23%). Conforms to reported analytical data[S8].

343.44 g/mol

R$_f$: 0.17 (8:2 PE:Et$_2$O)

m.p.: 130 °C (Lit. [S8]: 90 − 91 °C)

^{1}H-NMR (400 MHz, CDCl$_3$, δ): 7.87 − 7.82 (m, 2H), 7.66 (d, J = 8.2 Hz, 2H), 7.57 − 7.52 (m, 1H), 7.43 (dd, J = 8.3, 7.0 Hz, 2H), 7.34 (d, J = 8.1 Hz, 2H), 3.85 − 3.70 (m, 2H), 3.19 (tt, J = 10.2, 4.3 Hz, 1H), 2.59 − 2.48 (m, 2H), 2.45 (s, 3H), 1.98 − 1.80 (m, 4H).

13C-NMR (101 MHz, CDCl$_3$, δ): 201.4, 143.6, 135.6, 133.3, 133.1, 129.7, 128.8, 128.2, 127.7, 45.6, 42.3, 27.9, 21.6.

LR-MS (ESI): (m/z) 382.0 ([M+K]$^+$), 366.0 ([M+Na]$^+$), 344.1 ([M+H]$^+$)

1-Phenyl-3-(pyridin-3-yl)propan-1-one (**42**)
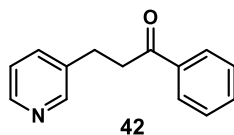
Following **GP C**, the thioester **SM42** (65.1 mg, 333 μmol, 1 eqv.) was coupled with with phenyl zinc chloride (0.25 M in THF, by **GP B**). The crude product was purified by flash column chromatography (SiO$_2$, DCM:MeOH gradient 95:5 v/v) to give the product as a white solid (67 mg, 317 μmol, 95%). Conforms to reported analytical data[S9].

211.26 g/mol

R$_f$: 0.1 (7:3 PE:EtOAc)

m.p.: 86 °C (Lit.[S9]: 84 – 86 °C).

1H-NMR (400 MHz, CDCl$_3$, δ): 8.43 (d, J = 33.8 Hz, 2H), 7.90 – 7.84 (m, 2H), 7.57 – 7.50 (m, 1H), 7.49 – 7.45 (m, 1H), 7.45 – 7.35 (m, 2H), 7.15 (s, 1H), 3.24 (t, J = 7.4 Hz, 2H), 3.01 (t, J = 7.4 Hz, 2H).

13C-NMR (101 MHz, CDCl$_3$, δ): 198.4, 149.8, 147.5, 136.6, 136.3, 133.3, 128.7, 128.0, 123.5, 39.7, 27.1.

GC-MS: (m/z) 211.1, 207, 105, 91.

4,4,5,5,6,6,7,7,8,8,9,9,10,10,11,11,11-heptadecafluoro-1-phenylundecan-1-one (**48**)
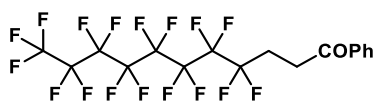
Following **GP C**, the thioester **SM48** (179 mg, 333 μmol, 1 eqv.) was coupled with with phenyl zinc chloride (0.25 M in THF, by **GP B**). The crude product was purified by flash chromatography (SiO$_2$ 97.5:2.5 PE:Et$_2$O gradient) to give the product as a white solid (74 mg, 160 μmol, 48%).

The ^{13}C-resonances of quarternary fluorocarbons were not detected by our standard ^{13}C-NMR method. This is in accordance with standard ^{13}C-NMR analysis of the parent acid and a reported decarboxylated-alkylated derivative. Two factors play a role in giving particularly weak signals: ^{19}F induced signal splitting and long relaxation times typical for quarternary fluorocarbon signals.

462.63 g/mol

R$_f$: 0.40 (97.5:2.5 PE:Et$_2$O)

m.p.: 55 °C.

^{1}H-NMR (400 MHz, CDCl$_3$, δ): 7.99 – 7.84 (m, 2H), 7.60 – 7.48 (m, 1H), 7.42 (dd, J = 8.4, 7.1 Hz, 2H), 3.31 – 3.16 (m, 2H), 2.54 (tt, J = 19.1, 7.8 Hz, 2H).

^{13}C-NMR (101 MHz, CDCl$_3$, δ): 196.4, 136.1, 133.6, 128.8, 128.0, 29.5, 25.6 (t, J = 21.9 Hz).

^{19}F-NMR (376 MHz, CDCl$_3$, δ): -80.82, -114.13, -114.84, -121.68, -121.92, -122.73, -123.42, -126.14.

HR-MS (ESI): calc. for [M+Na]$^+$ m/z 575.02742, found 575.02750.

[(8R,9S,10S,13R,14S,17R)-10,13-Dimethyl-17-((R)-5-oxo-5-phenylpentan-2-yl)dodecahydro-3H-cyclopenta[a]phenanthrene-3,7,12(2H,4H)-trione (**46**)]{.underline}

46
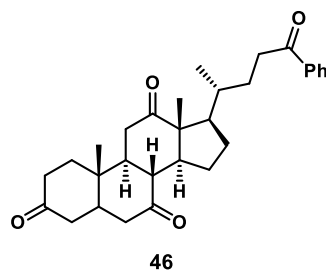
Following **GP C**, the thioester **SM46** (149 mg, 333 μmol, 1 eqv.) was coupled with with phenyl zinc chloride (0.25 M in THF, by **GP B**). The crude product was purified by flash column chromatography (SiO$_2$, PE:EtOAc gradient 6:4 v/v) to give the product as a white solid (103 mg, 223 μmol, 67%). Conforms to reported analytical data[S10].

462.63 g/mol

R$_f$: 0.46 (97.5:2.5 DCM:MeOH)

m.p.: 229 °C (dec.)

^{1}H-NMR (400 MHz, CDCl$_3$, δ): 7.92 – 7.86 (m, 2H), 7.52 – 7.45 (m, 1H), 7.39 (t, J = 7.6 Hz, 2H), 3.03 – 2.93 (m, 1H), 2.92 – 2.74 (m, 4H), 2.34 – 1.86 (m, 12H), 1.80 (td, J = 11.5, 7.1 Hz, 1H), 1.55 (td, J = 14.2, 5.1 Hz, 1H), 1.49 – 1.38 (m, 1H), 1.33 (s, 3H), 1.27 – 1.16 (m, 2H), 1.02 (s, 3H), 0.85 (d, J = 6.6 Hz, 3H).

^{13}C-NMR (101 MHz, CDCl$_3$, δ): 212.0, 209.0, 208.7, 200.7, 137.1, 132.9, 128.6, 128.0, 56.9, 51.8, 49.0, 46.9, 45.7, 45.6, 45.0, 42.8, 38.7, 36.5, 36.0, 35.5, 35.3, 29.8, 27.6, 25.2, 21.9, 18.9, 11.9.

HR-MS (ESI): calc. for [M+Na]$^+$ m/z 485.26623, found 485.26645.

3-methyl-1-phenylpent-3-en-1-one (**45**)
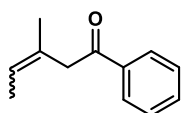
45

Following **GP C**, the thioester **SM45** (58 mg, 333 µmol, 1 eqv.) was coupled with with phenyl zinc chloride (0.25 M in THF, by **GP B**). The crude product was purified by filtration over a pad of SiO_2 (95:5 PE:Et2O) to give the product **17** as a colourless oil (55 mg, 316 µmol, 95%). Conforms to reported analytical data[S11].

174.23 g/mol

R$_f$: 0.41 (95:5 PE:Et$_2$O)

m.p.: Ambient temperature.

^{1}H-NMR (400 MHz, CDCl$_3$, δ): 7.92 – 7.87 (m, 2H), 7.51 – 7.44 (m, 1H), 7.42 – 7.34 (m, 2H), 5.43 (dddt, J = 8.1, 6.8, 5.5, 1.3 Hz, 1H, Diastereomer 1), 5.31 (dddq, J = 8.0, 6.7, 5.3, 1.3 Hz, 1H, Diastereomer 2), 3.64 (s, 2H, Diastereomer 1), 3.59 – 3.55 (m, 2H, Diastereomer 2), 1.66 (t, J = 1.5 Hz, 3H, Diastereomer 1), 1.62 – 1.60 (m, 3H, Diastereomer 2), 1.58 – 1.57 (m, 3H, Diastereomer 1), 1.56 – 1.55 (m, 1H, Diastereomer 2).

^{13}C-NMR (101 MHz, CDCl$_3$, δ): 198.8, 198.2, 137.1, 133.0, 130.1, 129.7, 128.5, 128.2, 123.7, 122.8, 49.3, 41.8, 24.1, 16.3, 13.8, 13.7.

GC-MS: (m/z) 174.1, 160.1, 143.1, 131.1, 105, 91.1, 77.1 (the isomers were separated on the GC column and gave identical fragmentation patterns).

3-(3-fluorophenyl)-1-phenylpropan-1-one (**37**)
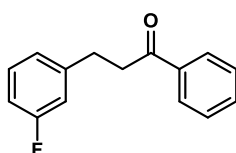
37

Following **GP C**, thioester **SM37** (71 mg, 0.333 mmol, 1 eqv.) was coupled with phenyl zinc chloride (0.25 M in THF, by **GP B**). The crude product was purified by column chromatography (SiO_2, PE:EtOAc 97.5:2.5 v/v) to give the product as a colorless oil (32 mg, 140 µmol, 42%). Conforms to reported analytical data[S12].

228.27 g/mol

R$_f$: 0.24 (97.5:2.5 PE:EA)

m.p.: Ambient temperature.

^{1}H-NMR (400 MHz, CDCl$_3$, δ): 7.92 – 7.84 (m, 2H), 7.53 – 7.44 (m, 1H), 7.43 – 7.33 (m, 2H), 7.23 – 7.13 (m, 1H), 6.96 (dd, J = 7.7, 0.8 Hz, 1H), 6.92 – 6.87 (m, 1H), 6.82 (tdd, J = 8.6, 2.7, 1.0 Hz, 1H), 3.23 (t, J = 7.7 Hz, 2H), 3.00 (t, J = 7.6 Hz, 2H).

^{13}C-NMR (101 MHz, CDCl$_3$, δ): 198.8, 162.9 (d, J = 245.5 Hz), 143.8 (d, J = 7.3 Hz), 136.8 , 133.2, 129.9 (d, J = 8.3 Hz), 124.1 (d, J = 2.9 Hz), 115.3 (d, J = 21.0 Hz), 113.0 (d, J = 21.0 Hz), 40.0, 29.8.

^{19}F-NMR (376 MHz, CDCl$_3$, δ): -113.5.

GC-MS: (m/z) 228.1, 212.1, 197.1, 109.1, 105.1, 77.1.

1-(4-methoxyphenyl)pentane-1,4-dione (**41**)

41
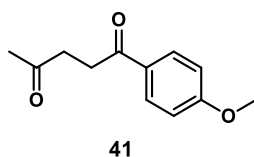
Following **GP A**, 4-Oxopentanoic acid (1.0 g, 881 µL, 8.61 mmol, 1 eqv.) was coupled with EtSH (2.49 mL, 34.45 mmol, 4 eqv.) using DIC (1.35 mL, 8.61 mmol, 1 eqv.) and catalytic DMAP (105 mg, 861 µmol, 10 mol%) in DCM (20 mL) for 24 h. After the usual workup, the crude material was passed over a pad of SiO$_2$ (95:5 CyH:EtOAc) to give a crude material (825 mg, 5.25 mmol, 61%) which could not be purified further and was thus directly used in the next step assuming full purity.

Following **GP C**, crude **SM41** (53 mg, 0.333 mmol, 1 eqv.) was coupled with 4-methoxyphenyl zinc chloride (0.25 M in THF, by **GP B**). The crude product was purified by column chromatography (SiO$_2$, PE:EtOAc gradient 95:5 v/v) to give the productas a paste (44 mg, 213 µmol, 64% over two steps). Conforms to reported analytical data[S13] with the exception that the product did not solidify in our hands.

206.24 g/mol

R$_f$: (9:1 PE:EA)

^{1}H-NMR (400 MHz, CDCl$_3$, δ): δ 7.89 (d, J = 8.9 Hz, 2H), 6.86 (d, J = 8.9 Hz, 2H), 3.80 (s, 3H), 3.17 (t, J = 6.4 Hz, 2H), 2.80 (t, J = 6.3 Hz, 2H), 2.19 (s, 3H).

^{13}C-NMR (101 MHz, CDCl$_3$, δ): 207.5, 197.0, 163.5, 130.3, 129.8, 113.7, 55.5, 37.2, 32.1, 30.2.

GC-MS: (m/z) 206.1, 188.1, 173.1, 135.1, 77.1.

1-(4-methoxyphenyl)-3,3,3-triphenylpropan-1-one (**49**)

49
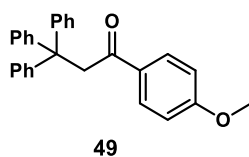
Following **GP C**, the thioester **SM49** (115 mg, 333 µmol, 1 eqv.) was coupled with with phenyl zinc chloride (0.25 M in THF, by **GP B**). The crude product was purified by flash chromatography (SiO$_2$ 9:1 PE:EA gradient) to give the product as an amorphous white paste (113 mg, 287 µmol, 87%).

392.50 g/mol

R$_f$: 0.42 (9:1 PE:EA)

^{1}H-NMR (400 MHz, CDCl$_3$, δ): 7.73 (d, J = 8.9 Hz, 2H), 7.23 – 7.01 (m, 15H), 6.75 (d, J = 8.9 Hz, 2H), 4.31 (s, 2H), 3.73 (s, 3H).

^{13}C-NMR (101 MHz, CDCl$_3$, δ): 195.6, 163.2, 147.1, 131.2, 130.2, 129.3, 127.8, 126.0, 113.5, 56.0, 55.5, 48.9.

HR-MS: calc. for [M+Na]$^+$ m/z 415.16685, found 415.16695.

1-phenyloctadec-9-en-1-one (**47**)

47
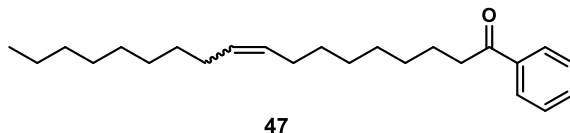
Following **GP C**, thioester **SM47**(109 mg, 0.333 mmol, 1 eqv.) was coupled with phenyl zinc chloride (0.25 M in THF, by **GP B**). The crude product was purified by column chromatography (SiO$_2$, PE:EtOAc 97.5:2.5 v/v) to give the product as a colorless oil (59 mg, 172 µmol, 52%). Conforms to reported analytical data[S14].

342.57 g/mol

R$_f$: 0.22 (97.5:2.5 PE:EA)

m.p.: Ambient temperature.

^{1}H-NMR (400 MHz, CDCl$_3$, δ): 7.88 (d, J = 7.2 Hz, 2H), 7.51 – 7.44 (m, 1H), 7.38 (t, J = 7.6 Hz, 2H), 5.38 – 5.21 (m, 2H), 2.88 (t, J = 7.4 Hz, 2H), 2.05 – 1.80 (m, 4H), 1.70 – 1.58 (m, 2H), 1.62 – 1.50 (m, J = 7.1 Hz, 1H), 1.36 – 1.14 (m, 19H), 0.80 (td, J = 6.9, 1.7 Hz, 3H).

^{13}**C-NMR** (101 MHz, CDCl$_3$, δ): 200.5, 137.1, 132.8, 130.5, 123.0, 128.5, 128.1, 60.1, 38.6, 34.4, 32.6, 31.9, 29.8, 29.7, 29.7, 29.7, 29.6, 29.6, 29.5, 29.5, 29.4, 29.4, 29.3, 29.2, 29.2, 29.1, 29.0, 27.2, 24.99, 24.4, 22.7, 14.7, 14.1.

GC-MS: (m/z) 342.2.

Ethyl 6-oxo-6-phenylhexanoate **(40)**

40
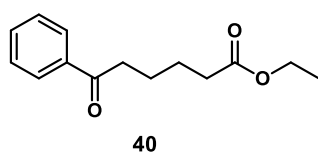
Following **GP C**, thioester **SM40** (72 mg, 0.333 mmol, 1 eqv.) was coupled with phenyl zinc chloride (0.25 M in THF, by **GP B**). The crude product was purified by column chromatography (SiO$_2$, PE:EtOAc 9.5:0.5 v/v) to give the product as a colorless oil (41 mg, 175 μmol, 52%). Conforms to reported analytical data.[S15]

234.30 g/mol

R$_f$: 0.22 (9:1 PE:EA)

m.p.: Ambient temperature.

^{1}**H-NMR** (400 MHz, CDCl$_3$, δ): 7.97 – 7.93 (m, 2H), 7.58 – 7.53 (m, 1H), 7.48 – 7.43 (m, 2H), 4.12 (q, J = 7.1 Hz, 2H), 2.99 (t, J = 7.0 Hz, 2H), 2.36 (t, J = 7.1 Hz, 2H), 1.84 – 1.66 (m, 4H), 1.25 (t, J = 7.1 Hz, 3H)

^{13}**C-NMR** (101 MHz, CDCl$_3$, δ): 199.8, 173.5, 136.9, 133.0, 128.6, 128.0, 60.3, 38.2, 34.2, 24.6, 23.7, 14.3

GC-MS: (m/z) 233.1

3-(1H-indol-3-yl)-1-phenylpropan-1-one (**43**)

43
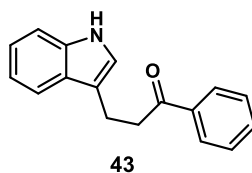
Following **GP C**, thioester **SM43** (77 mg, 0.333 mmol, 1 eqv.) was coupled with phenyl zinc chloride (2.86 eqv. instead, 0.25 M in THF, by **GP B**). The crude product was purified by column chromatography (SiO$_2$, PE:EtOAc 95:5 v/v) to give the product as a maroon colored solid (58 mg, 233 μmol, 70%). Conforms to reported analytical data[S16] with the exception that a white solid was expected.

249.31 g/mol

R_f: 0.43 (PE:EA 85:15)

mp: 128-130 °C (Lit.[S16]: 124 – 126 °C).

¹H NMR (400 MHz, CDCl₃, δ) 8.02 – 7.90 (m, 3H), 7.64 (d, J = 7.8 Hz, 1H), 7.55 (t, J = 7.4 Hz, 1H), 7.45 (t, J = 7.7 Hz, 2H), 7.37 (d, J = 8.3 Hz, 1H), 7.21 (ddd, J = 8.2, 7.0, 1.3 Hz, 1H), 7.14 (ddd, J = 8.0, 6.9, 1.1 Hz, 1H), 7.06 (t, J = 1.4 Hz, 1H), 3.43 – 3.36 (dd, 2H), 3.23 (dd, J = 8.2, 6.8 Hz, 2H).

¹³C NMR (101 MHz, CDCl₃, δ) δ 199.9, 137.0, 136.3, 133.3, 133.0, 128.6, 128.1, 127.3, 122.1, 121.6, 119.4, 118.7, 115.5, 111.2, 39.4, 19.7.

GC-MS (EI)**:** (m/z) 249.1.

3-(4-methoxyphenyl)-1-phenylpropan-1-one (**39**)
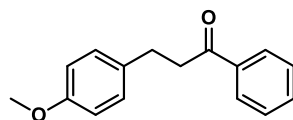
39

Following **GP C**, thioester **SM39** (74 mg, 0.333 mmol, 1 eqv.) was coupled with phenyl zinc chloride (0.25 M in THF, by **GP B**). The crude product was purified by column chromatography (SiO₂, PE: EtOAc 97 : 3 to 90 : 10 v/v) to give the product as a light yellow solid (58 mg, 241 µmol, 73.23 %). Conforms to reported analytical data[S17] with the exception that a colourless solid was expected.

240.302 g/mol

R_f: 0.24 (PE:EA 9:1)

mp: 63-65 °C. (Lit.[S17]: 66 °C).

¹H NMR (400 MHz, CDCl₃, δ) 8.02 – 7.92 (m, 2H), 7.59 – 7.51 (m, 1H), 7.46 (ddt, J = 8.2, 6.7, 1.1 Hz, 2H), 7.23 – 7.13 (m, 2H), 6.85 (d, J = 8.6 Hz, 2H), 3.79 (s, 3H), 3.33 – 3.22 (t, 2H), 3.02 (t, J = 8.3, 7.0 Hz, 2H).

¹³C NMR (101 MHz, CDCl₃, δ) δ 199.4, 158.0, 136.9, 133.3, 133.0, 129.4, 128.6, 128.1, 114.0, 55.3, 40.7, 29.3.

GC-MS (EI): m/z 240.1

3-cyclopentyl-1-phenylpropan-1-one (**44**)

44
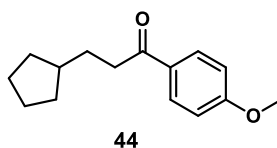
Following **GP A**, 3-cyclopentylpropanoic acid (0.568 g, 4 mmol, 1 eqv.) was coupled with EtSH (0.86 mL, 12 mmol, 3 eqv.) using DIC (618 µL, 4 mmol, 1 eqv.) and catalytic DMAP (24.42 mg, µmol, 5 mol%) in DCM (20 mL) for 24 h. All attempts towards purification of crude *S*-ethyl 3-cyclopentylpropanethioate failed. The result was isolation of (246 mg, 1.32 mmol, 33%) crude *S*-ethyl 3-cyclopentylpropanethioate. Hence, the crude thioester was used for the next step.

Assuming complete purity, following **GP C**, *S*-ethyl 3-cyclopentylpropanethioate (61 mg, 0.333 mmol, 1 eqv.) was coupled with 4-methoxy phenyl zinc chloride (0.25 M in THF, by **GP B**). The crude product was purified by column chromatography (SiO$_2$, PE:EtOAc 98:2 to 95:5 v/v) to give the product as a light yellow solid (34.8 mg, 149 µmol, 67%) over two steps. Conforms to reported analytical data[S18]

232.32 g/mol

R_f: 0.45 (CyH: EA 9:1)

m.p.: Ambient temperature.

¹H NMR (400 MHz, CDCl$_3$, δ) 7.94 (d, J = 8.8 Hz, 2H), 6.92 (d, J = 8.8 Hz, 2H), 3.86 (s, 3H), 2.96 – 2.87 (m, 2H), 2.16 (s, 1H), 1.84 – 1.70 (m, 5H), 1.61 (dt, J = 7.2, 2.7 Hz, 1H), 1.55 – 1.45 (m, 2H), 1.18 – 1.10 (m, 2H).

¹³C NMR (101 MHz, CDCl$_3$, δ) 199.4, 163.3, 130.3, 130.2, 113.7, 55.4, 39.9, 37.6, 32.6, 30.9, 25.2.

GC-MS (EI)**:** m/z 232.1

HRMS (ESI): calc. for [M+Na]$^+$ m/z 255.13555, found 255.13588.

1-(4-methoxyphenyl)-3-phenylpropan-1-one (**38**)

38
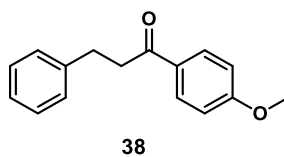
Following **GP C**, thioester **SM36** (64 mg, 0.333 mmol, 1 eqv.) was coupled with 4-methoxyphenyl zinc chloride (0.25 M in THF, by **GP B**). The crude product was purified by column chromatography (SiO$_2$, PE:EtOAc 97:3 to 85:15 v/v) to give the product as a colourless oil (70 mg, 266 μmol, 88%). Conforms to reported analytical data[S19] but the product did not solidify in our hands.

240.30 g/mol

R$_f$: 0.17 (PE: EA 9:1)

m.p.: Ambient temperature.

^{1}H NMR (400 MHz, CDCl$_3$, δ) 7.96 (d, J = 8.9 Hz, 2H), 7.26 (m, 5H), 6.94 (d, J = 8.9 Hz, 2H), 3.88 (s, 3H), 3.27 (t, J = 7.9 Hz, 2H), 3.12 – 3.01 (t, 2H).

^{13}C NMR (101 MHz, CDCl$_3$, δ) 197.8, 163.5, 141.5, 130.3, 130.0, 128.5, 128.4, 126.1, 113.7, 55.5, 40.1, 30.4.

GC-MS (EI)**:** (m/z) 240.1.

1,3-Diphenylpropan-1-one (**36**)

36
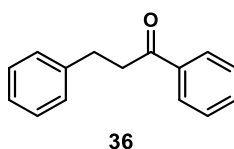
Following **GP C**, thioester **SM36** (78 mg, 0.333 mmol, 1 eqv.) was coupled with phenyl zinc chloride (0.25 M in THF, by **GP B**). The crude product was purified by column chromatography (SiO$_2$, PE:EtOAc 97.5:2.55 v/v) to give the product as a colourless solid (56 mg, 266 μmol, 80%). Conforms to reported analytical data[S20].

210.28 g/mol

R$_f$: 0.48 (PE: EA 9:1)

m.p.: 73-75 °C

---

¹H NMR (400 MHz, Chloroform-d): δ 7.97 (dd, J = 8.4, 1.4 Hz, 2H), 7.61 – 7.52 (m, 1H), 7.50 – 7.43 (m, 2H), 7.26 (m, 5H), 3.31 (d, J = 1.7 Hz, 2H), 3.09 (d, J = 8.0 Hz, 2H).

¹³C NMR (101 MHz, CDCl₃): δ 199.2, 141.3, 136.9, 133.1, 128.6, 128.5, 128.4, 128.1, 126.1, 40.5, 30.2.

GC-MS (EI)**:** m/z 210.2

3.4.3.6 Tolerance of steric hindrance by catalysts other than Ni(xant)(oTol)Cl

To prove that that other catalysts do not show the preference for primary thioesters as **C2** does, we selected a model catalyst consisting of NiCl₂ and terpy (as outlined in **GP D**) and conducted some comparative experiments (same timescale, starting material scale and catalyst loading) with one secondary and one tertiary thioester.

Phenyl(1-tosylpiperidin-4-yl)methanone (**51**) by **GP D**

GP D was followed using thioester **SM51**. Isolation was carried out as detailed in section 3.5 for compound **51**. The product was isolated in 87% yield with the same analytical data as above, compared to a yield of 23% when **C2** was used as catalyst.

(Adamantan-1-yl)(phenyl)methanone (**53**) by **GP D**

53
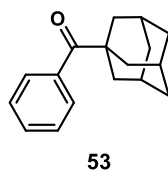
Following **GP D**, the thioester **SM53** (98 mg, 333 μmol, 1 eqv.) was coupled with with phenyl zinc chloride (0.25 M in THF, by **GP B**). The crude product was purified by flash chromatography (SiO₂ 97.5:2.5 PE:Et₂O isocratic) to give the product as a white solid (50 mg, 206 μmol, 62%). Conforms to reported analytical data[S21]. No product is obtained when **C2** was used as catalyst (**GP C**).

240.34 g/mol

R_f: 0.23 (9:1 PE:DCM)

m.p.: 51 °C (Lit.[S22]: 50-52 °C)

¹H-NMR (400 MHz, CDCl₃, δ): 7.50 – 7.43 (m, 2H), 7.39 – 7.24 (m, 3H), 1.99 (s, 3H), 1.93 (s, 6H), 1.67 (s, 6H).

¹³C-NMR (101 MHz, CDCl₃, δ): 210.1, 139.6, 130.1, 127.9, 127.1, 46.9, 39.1, 36.6, 28.2.

GC-MS: (m/z) 240.2, 224, 135.1.

3.5. References

[1]   M. C. Kohler, J. M. Yost, M. R. Garnsey, D. M. Coltart, *Organic Letters* **2010**, *12*, 3376-3379.

[2]   C. D. Duve, in *The Molecular Origins of Life: Assembling Pieces of the Puzzle* (Ed.: A. Brack), Cambridge University Press, Cambridge, **1998**, pp. 219-236.

[3]   G. Wächtershäuser, *Progress in Biophysics and Molecular Biology* **1992**, *58*, 85-201.

[4]   H. S. Bernhardt, *Biology Direct* **2012**, *7*, 23.

[5]   V. Hirschbeck, P. H. Gehrtz, I. Fleischer, *Chemistry – A European Journal* **2017**, *24*, 7092-7107.

[6]   M. C. Weiss, F. L. Sousa, N. Mrnjavac, S. Neukirchen, M. Roettger, S. Nelson-Sathi, W. F. Martin, *Nature Microbiology* **2016**, *1*, 16116.

[7]   M. Can, F. A. Armstrong, S. W. Ragsdale, *Chemical Reviews* **2014**, *114*, 4149-4174.

[8]   Y.-T. Huang, S.-Y. Lu, C.-L. Yi, C.-F. Lee, *The Journal of Organic Chemistry* **2014**, *79*, 4561-4568.

[9]   V. Hirschbeck, P. H. Gehrtz, I. Fleischer, *Journal of the American Chemical Society* **2016**, *138*, 16794-16799.

[10]   N. Weber, E. Klein, K. Vosmann, K. D. Mukherjee, *Biotechnology Letters* **1998**, *20*, 687-691.

[11]   S. Nahm, S. M. Weinreb, *Tetrahedron Letters* **1981**, *22*, 3815-3818.

[12]   H. A. Staab, E. Jost, *Justus Liebigs Annalen der Chemie* **1962**, *655*, 90-94.

[13]   M. Araki, S. Sakata, H. Takei, T. Mukaiyama, *Bulletin of the Chemical Society of Japan* **1974**, *47*, 1777-1780.

[14]   Y. Tian, L. Wang, H.-Z. Yu, *RSC Advances* **2016**, *6*, 61996-62004.

[15]   R. J. Anderson, C. A. Henrick, L. D. Rosenblum, *Journal of the American Chemical Society* **1974**, *96*, 3654-3655.

[16]   N. Yoshikai, R. Iida, E. Nakamura, *Advanced Synthesis & Catalysis* **2008**, *350*, 1063-1072.

[17]   K. P. Kepp, *Inorganic Chemistry* **2016**, *55*, 9461-9470.

[18]   H. Tokuyama, S. Yokoshima, T. Yamashita, T. Fukuyama, *Tetrahedron Letters* **1998**, *39*, 3189-3192.

[19]   H. Ueda, H. Satoh, K. Matsumoto, K. Sugimoto, T. Fukuyama, H. Tokuyama, *Angewandte Chemie International Edition* **2009**, *48*, 7600-7603.

[20]   K. Kunchithapatham, C. C. Eichman, J. P. Stambuli, *Chemical Communications* **2011**, *47*, 12679-12681.

[21]   T. Shimizu, M. Seki, *Tetrahedron Letters* **2001**, *42*, 429-432.

[22]   Y. Mori, M. Seki, *Advanced Synthesis & Catalysis* **2007**, *349*, 2027-2038.

[23]   A. H. Cherney, S. E. Reisman, *Tetrahedron* **2014**, *70*, 3259-3265.

[24]   R. Oost, A. Misale, N. Maulide, *Angewandte Chemie International Edition* **2016**, *55*, 4587-4590.

[25]   J. H. Lee, Y. Kishi, *Journal of the American Chemical Society* **2016**, *138*, 7178-7186.

[26]   A. Krasovskiy, V. Malakhov, A. Gavryushin, P. Knochel, *Angewandte Chemie* **2006**, *118*, 6186-6190.

[27]   J. H. Lee, Z. Li, A. Osawa, Y. Kishi, *Journal of the American Chemical Society* **2016**, *138*, 16248-16251.

[28]   a) V. P. Kumar, V. S. Babu, K. Yahata, Y. Kishi, *Organic Letters* **2017**, *19*, 2766-2769; b) K. Yahata, N. Ye, Y. Ai, K. Iso, Y. Kishi, *Angewandte Chemie International Edition* **2017**, *56*, 10796-10800; c) Y. Ai, N. Ye, Q. Wang, K. Yahata, Y. Kishi, *Angewandte Chemie International Edition* **2017**, *56*, 10791-10795.

[29]   L. S. Liebeskind, J. Srogl, *Journal of the American Chemical Society* **2000**, *122*, 11260-11261.

[30]   Y. Yu, L. S. Liebeskind, *The Journal of Organic Chemistry* **2004**, *69*, 3554-3557.

[31]   R. Wittenberg, J. Srogl, M. Egi, L. S. Liebeskind, *Organic Letters* **2003**, *5*, 3033-3035.

[32]   B. W. Fausett, L. S. Liebeskind, *The Journal of Organic Chemistry* **2005**, *70*, 4851-4853.

[33]   J. M. Villalobos, J. Srogl, L. S. Liebeskind, *Journal of the American Chemical Society* **2007**, *129*, 15734-15735.

[34]   H. Prokopcová, C. O. Kappe, *Angewandte Chemie International Edition* **2009**, *48*, 2276-2286.

[35]   V. P. Mehta, A. Sharma, E. Van der Eycken, *Advanced Synthesis & Catalysis* **2008**, *350*, 2174-2178.

[36]   V. P. Mehta, S. G. Modha, E. Van der Eycken, *The Journal of Organic Chemistry* **2009**, *74*, 6870-6873.

[37]   T. Shimizu, M. Seki, *Tetrahedron Letters* **2002**, *43*, 1039-1042.

[38]   Y. Zhang, T. Rovis, *Journal of the American Chemical Society* **2004**, *126*, 15964-15965.

[39]   O. Makoto, M. Yoshio, M. Teruaki, *Chemistry Letters* **1981**, *10*, 531-534.

[40]   A. C. Wotal, D. J. Weix, *Organic Letters* **2012**, *14*, 1476-1479.

[41]   C. Cardellicchio, V. Fiandanese, G. Marchese, L. Ronzini, *Tetrahedron Letters* **1985**, *26*, 3595-3598.

[42]   T. Parchomyk, K. Koszinowski, *Chemistry – A European Journal* **2016**, *22*, 15609-15613.

[43]   W. Oppolzer, C. Darcel, P. Rochet, S. Rosset, J. De Brabander, *Helvetica Chimica Acta* **1997**, *80*, 1319-1337.

[44]   H. L. Paul Knochel, Liu-Zhu Gong, Sylvie Perrone, Florian F. Kneisel, in *The Chemistry of Organozinc Compounds* (Ed.: I. M. Zvi Rappoport), John Wiley & Sons, Ltd, **2007**, pp. 287-393.

[45]   F. M. Piller, P. Appukkuttan, A. Gavryushin, M. Helm, P. Knochel, *Angewandte Chemie International Edition* **2008**, *47*, 6802-6806.

[46]   T. Shimizu, M. Seki, *Tetrahedron Letters* **2000**, *41*, 5099-5101.

[47]   T. Miyazaki, Y. Han-ya, H. Tokuyama, T. Fukuyama, *Synlett* **2004**, *2004*, 477-480.

[48]   M. Asadi, S. Bonke, A. Polyzos, D. W. Lupton, *ACS Catalysis* **2014**, *4*, 2070-2074.

[49]   a) K. Koszinowski, P. Böhrer, *Organometallics* **2009**, *28*, 771-779; b) E. Hevia, J. Z. Chua, P. García-Álvarez, A. R. Kennedy, M. D. McCall, *Proceedings of the National Academy of Sciences* **2010**, *107*, 5294-5299; c) J. E. Fleckenstein, K. Koszinowski, *Organometallics* **2011**, *30*, 5018-5026.

[50]   A. Krasovskiy, P. Knochel, *Synthesis* **2006**, *2006*, 0890-0891.

[51]   R. H. Crabtree, *Chemical Reviews* **2012**, *112*, 1536-1554.

[52]   T. Yurino, Y. Ueda, Y. Shimizu, S. Tanaka, H. Nishiyama, H. Tsurugi, K. Sato, K. Mashima, *Angewandte Chemie International Edition* **2015**, *54*, 14437-14441.

[53]   L. Bini, C. Müller, D. Vogt, *Chemical Communications* **2010**, *46*, 8325-8334.

[54]   E. A. Standley, S. J. Smith, P. Müller, T. F. Jamison, *Organometallics* **2014**, *33*, 2012-2018.

[55]   V. P. Ananikov, *ACS Catalysis* **2015**, *5*, 1964-1971.

[56]   V. P. Ananikov, I. P. Beletskaya, *Organometallics* **2012**, *31*, 1595-1604.

[57]   W. H. Pearson, D. A. Berry, P. Stoy, K.-Y. Jung, A. D. Sercel, *The Journal of Organic Chemistry* **2005**, *70*, 7114-7122.

[58]   C. Hansch, A. Leo, R. W. Taft, *Chemical Reviews* **1991**, *91*, 165-195.

[59]   S. Kundu, W. W. Brennessel, W. D. Jones, *Organometallics* **2011**, *30*, 5147-5154.

[60]   P. W. G. Ariyananda, M. T. Kieber-Emmons, G. P. A. Yap, C. G. Riordan, *Dalton Transactions* **2009**, 4359-4369.

[61]   A. N. Desnoyer, F. W. Friese, W. Chiu, M. W. Drover, B. O. Patrick, J. A. Love, *Chemistry – A European Journal* **2016**, *22*, 4070-4077.

[62]   P. Blakskjær, B. Høj, D. Riber, T. Skrydstrup, *Journal of the American Chemical Society* **2003**, *125*, 4030-4031.

[63]   J. Cornella, J. T. Edwards, T. Qin, S. Kawamura, J. Wang, C.-M. Pan, R. Gianatassio, M. Schmidt, M. D. Eastgate, P. S. Baran, *Journal of the American Chemical Society* **2016**, *138*, 2174-2177.

[64]   K. Budny-Godlewski, D. Kubicki, I. Justyniak, J. Lewiński, *Organometallics* **2014**, *33*, 5093-5096.

[65]   U. Chakraborty, F. Urban, B. Mühldorf, C. Rebreyend, B. de Bruin, N. van Velzen, S. Harder, R. Wolf, *Organometallics* **2016**, *35*, 1624-1631.

[66]   C. Chatgilialoglu, D. Crich, M. Komatsu, I. Ryu, *Chemical Reviews* **1999**, *99*, 1991-2070.

[67]   L. Lunazzi, K. U. Ingold, J. C. Scaiano, *The Journal of Physical Chemistry* **1983**, *87*, 529-530.

[68]   J. A. Labinger, *Organometallics* **2015**, *34*, 4784-4795.

[69]   T. T. Tsou, J. K. Kochi, *Journal of the American Chemical Society* **1979**, *101*, 6319-6332.

[S1]   a) S. Sawadjoon, A. Lundstedt and J. S. M. Samec, *ACS Catalysis* **2013**, 3, 635-642; b) L. De Luca, G. Giacomelli and M. Taddei, *The Journal of Organic Chemistry*, **2001**, 66, 2534-2537.

[S2]   B. Neises and W. Steglich, *Angewandte Chemie International Edition in English* **1978**, 17, 522-524.

[S3]   F. Sandfort, M. J. O'Neill, J. Cornella, L. Wimmer and P. S. Baran, *Angewandte Chemie International Edition* **2017**, 56, 3319-3323.

[S4]   E. Nyfeler and P. Renaud, *Organic Letters* **2008**, 10, 985-988.

[S5]   G. Hobley, J. C. McKelvie, J. E. Harmer, J. Howe, P. C. F. Oyston and P. L. Roach, *Bioorganic & Medicinal Chemistry Letters* **2012**, 22, 3079-3082.

[S6]   N. Li, J. Ou, M. Miesch and P. Chiu, *Organic & Biomolecular Chemistry* **2011**, 9, 6143-6147.

[S7]   J. Ruan, O. Saidi, J. A. Iggo and J. Xiao, *Journal of the American Chemical Society* **2008**, 130, 10510-10511.

[S8]   F. Wu, W. Lu, Q. Qian, Q. Ren and H. Gong, *Organic Letters* **2012**, 14, 3044-3047.

[S9]   T. Kuwahara, T. Fukuyama and I. Ryu, *Organic Letters* **2012**, 14, 4703-4705.

[S10]   Lukas J. Gooßen and K. Ghosh*, European Journal of Organic Chemistry*, **2002**, 3254-3267.

[S11]   Q.-A. Chen, D. K. Kim and V. M. Dong, *Journal of the American Chemical Society* **2014**, 136, 3772-3775.

[S12]   J. Yang, Y. W. Seto and N. Yoshikai, *ACS Catalysis* **2015**, 5, 3054-3057.

[S13]   A. P. Kozikowski and A. Ames, *Tetrahedron* **1985**, 41, 4821-4834.

[S14]   D. L. Boger, H. Sato, A. E. Lerner, M. P. Hedrick, R. A. Fecik, H. Miyauchi, G. D. Wilkie, B. J. Austin, M. P. Patricelli and B. F. Cravatt, *Proceedings of the National Academy of Sciences* **2000**, 97, 5044-5049.

[S15]   Y. Mori and M. Seki, *The Journal of Organic Chemistry* **2003**, 68, 1571-1574.

[S16]   F. Portela-Cubillo, B. A. Surgenor, R. A. Aitken and J. C. Walton, *The Journal of Organic Chemistry* **2008**, 73, 8124-8127.

[S17]   M. Hofmann, N. Hampel, T. Kanzian and H. Mayr, *Angewandte Chemie International Edition* **2004**, 43, 5402-5405.

[S18]   H. Stephan, G. Geipel, G. Bernhard, P. Comba, G. Rajaraman, U. Hahn and F. Vögtle, *European Journal of Inorganic Chemistry* **2005**, 4501-4508.

[S19]   S. A. Babu, M. Yasuda and A. Baba, *Organic Letters* **2007**, 9, 405-408.

[S20]   D. J. Fox, D. S. Pedersen and S. Warren, *Organic & Biomolecular Chemistry 2006*, 4, 3102-3107.

[S21]   S. Roslin and L. R. Odell, *Chemical Communications* **2017**, 53, 6895-6898.

[S22]   M. J. Lo Fiego, M. T. Lockhart and A. B. Chopa, *Journal of Organometallic Chemistry* **2009**, 694, 3674-3678.

Peer-reviewed work has been used to assemble sections of this chapter.

Sections 4.2., 4.3., 4.4. without the computational analysis:

Author	Author position	Scientific ideas %	Data generation %	Analysis & Interpretation %	Paper writing %
P.H. Gehrtz	First	87.5%	87.5%	87.5%	100%
V. Geiger	Second	5%	5%	5%	0%
T. Schmidt	Second	5%	5%	5%	0%
L. Srsan	Third	2.5%	2.5%	2.5%	0%
I. Fleischer	Supervisor				
Title of paper:		Cross-coupling of chloro(hetero)arenes with thiolates employing a well-defined Ni catalyst, *Org. Lett.* **2019**, *21*, 50-55			
Status in publication process:		Published			

4. Nickel-catalyzed coupling of zinc thiolates with chloroarenes

4.1. Introduction

4.1.1. Aryl thioethers in pharmaceuticals, agrochemicals and materials

Aryl thioethers - meaning either diaryl thioethers or aryl alkyl thioethers - are a common structural motif in functional, non-natural organic compounds with applications in pharmaceutical chemistry, agrochemistry and material design (Figure 4.1). For example, aryl alkyl thioethers as well as diaryl thioethers are found in pharmaceuticals across several medical indications (**1**, axitinib: anti-tumoral; **2**, 2C-T-7: psychotomimetic; **3**, vortioexetin: anti-depressant; **4**, cangrelor: thrombocyte aggregation inhibitor) with diverse biomacromolecular targets. A 2014 analysis has shown that of the Top 200 US drugs by prescription or retail sales, 25% and 23% respectively of these sets contain a sulfur heteroatom.[1] Of all sulfur-containing FDA-approved drugs, the thioether functional group is the third most prevalent (8.8% of the total share) after sulfonamides (29%) and β-lactams (10.5%).[1]

To understand the unique structural properties conferred by introduction of the aryl thioether motif, a comparison to the oxygen analogues is warranted in the context of medicinal chemistry. As an example, albendazole (**9**, a microtubule-modifying antihelminthic) was chosen (Scheme 4.1).[2] The hypothetic oxygen analogue **10** is less lipophilic (as seen by the decreased logD value) than **9**. This has important effects on membrane permeability, absorption and metabolism of the compound in humans.

Furthermore, the oxygen atom has a stronger *H*-bonding acceptor ability than the sulfur atom and thus may engage in completely different intermolecular interactions, which can have important effects in target selectivity. However, anti-bonding σ* C-S orbitals have been postulated as stereoelectronic design elements for medicinal chemistry as well.[3] While having a similar mesomeric effect, the oxygen atom possesses a more distinct negative inductive effect, which can impact the pK_a or pK_{aH} of neighbouring functional groups (e.g. making the second-most acidic proton slightly less acidic by oxygen-to-sulfur switch). Compared to the oxoethers, thioethers have a reduced C-S-C bond angle, approaching a right angle. Finally, the incorporation of sulfur atoms allows fine-tuning of metabolism, including shortening of blood plasma half-life ($t_{1/2}$) and reducing bioavailability (%*F*) through oxidation to the sulfoxide and sulfone. In conclusion, a seemingly innocent structural change can influence pharmacodynamics and pharmacokinetic parameters of a drug in a drastic manner.

Drugs
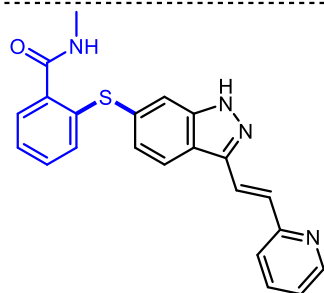
Axitinib (1)
Tyr kinase inhibitor
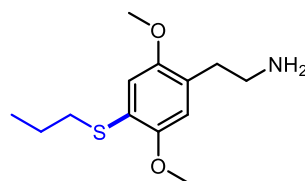
2C-T-7 (2)
5HT$_{2A}$R agonist
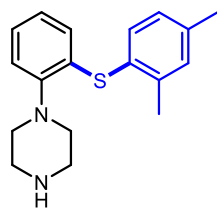
Vortioxetin (3)
5HTR modulator
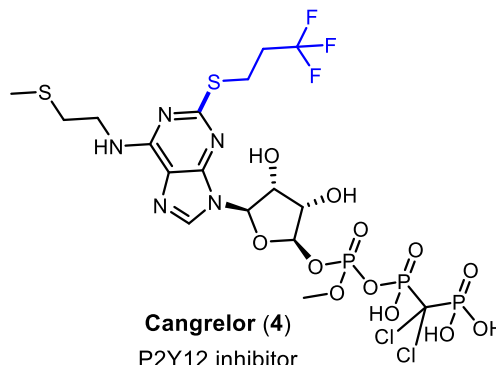
Cangrelor (4)
P2Y12 inhibitor

Materials
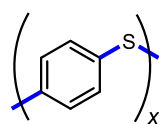
PPS (5)
high-performance structural polymer
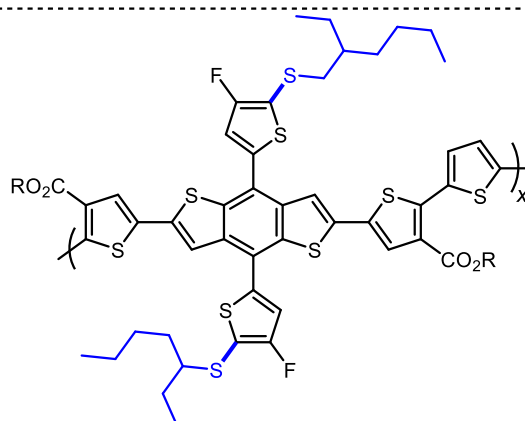
PDTB-EF-T (6)
organic solar cell donor-type polymer

Agrochemicals
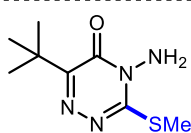
Metribuzin (7)
photosynthesis inhibitor herbicide
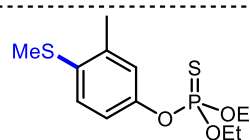
Fenthion (8)
AChE inhibitor insecticide

Figure 4.1: Diaryl sulfides and aryl alkyl sulfides as common motifs in non-natural functional molecules.
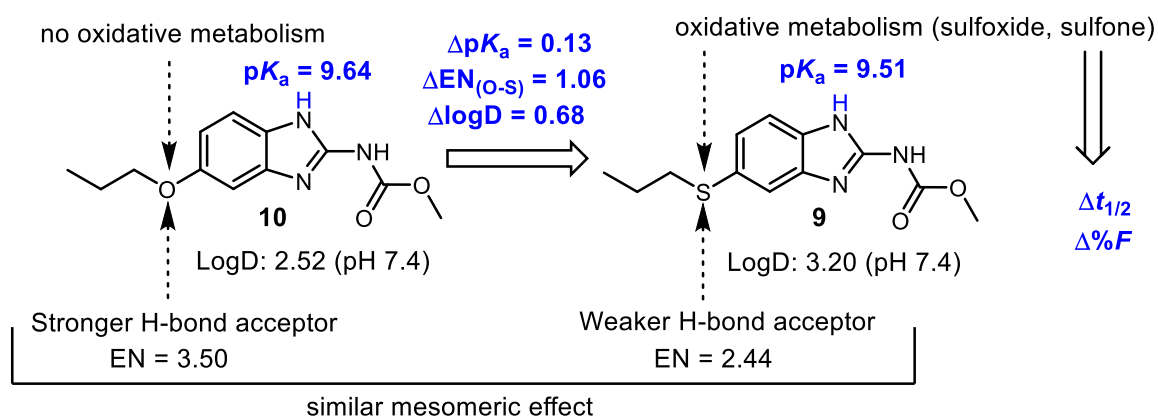
Scheme 4.1: Physicochemical differences imparted by oxygen-to-sulfur exchange and possible effects in metabolic profiles using albendazole (**9**) as an exemplary bioactive compound.

The possibility of isosteric replacement is formalized in the classic divalent series -CH$_2$-, -O-, -S-, -NH-.[4] Thioethers can also be found in various materials (Figure 4.1, compounds **5 – 6**) and agrochemicals (Figure 4.1, compounds **7 – 8**). A famous example is poly-phenylsulfide (PPS, **5**), a high-performance polymer. Selectivity for soft Mercury ions in metal-organic-frameworks has been achieved by incorporating aryl thioether structural motifs.[5] Recently, efficient polymeric organic solar cell components have been developed, which contain aryl alkyl thioether motifs in the monomer unit, such as in **6**.[6]
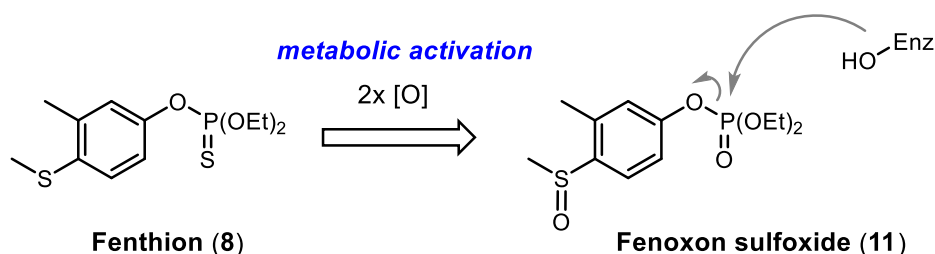
Scheme 4.2: Metabolic activation of the insecticide Fenthion (**8**) by oxidation to a highly active electrophile **11** for inhibition of insect acetylcholine esterase (denoted as Enz-OH).

In the insecticidal agrochemical Fenthion (**8**, Bayer AG), oxidative metabolism of the thioether (transport form) to the sulfoxide generates the active toxic substance by increasing the leaving group ability of the phenolate (Scheme 4.2). Disappointingly, both forms of Fenthion still display high toxicity towards other organisms; it is currently not approved for use.

Aryl thioethers appear to be less common in natural products, but are not completely absent (Figure 4.2, compounds **12** to **14**). Lissoclibadin 5 (**12**) belongs to a series of sulfur-rich dopamine-derived alkaloid natural products,[7] some of which have displayed anti-tumoral properties in cell culture experiments.[8] Chuangxinmycin (**13**) is an microbially produced antibiotic compound, derived from tryptophan.[9] In this case, it is known that the final C$_{aryl}$-S bond formation is carried out by a Cytochrome P$_{450}$ enzyme catalyzed oxidation and that the sulfur originates from cystein. A total

synthesis has been achieved by Greco and Kozikowski in 1980.[10] Nasturlexin B (**14**) is biosynthetically derived from tyrosine.[11] Compound **14** belongs to the class of phytoalexins, showing antimicrobial activity, which are produced by certain plants in response to (a)biotic stressors. Thus, the biosynthetic genes for phytoalexins have attracted interest as potential resistance traits transferable to agriculturally relevant plants by breed crossing.[12]

Lissoclibadin 5 (**12**)   **Chuangxinmycin** (**13**)   **Nasturlexin B** (**14**)
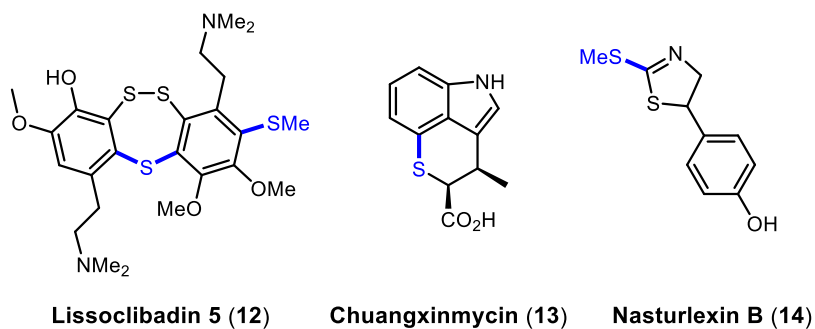
Figure 4.2: Exemplary natural products containing diaryl sulfides or alkyl aryl sulfides.

4.1.2. Synthetic methods to access aryl thioethers

In the following section, common methods for the construction of aryl thioethers (diaryl sulfides and aryl alkyl sulfides of the type **15**) will be critically discussed, meaning that their practicality will be assessed together with their mechanistic uniqueness, while a focus on transition-metal catalyzed methods will be laid. Mechanistically similar variants of parent reactions will not be discussed.

The most obvious disconnection of an aryl alkyl sulfide functionality is to cut retrosynthetically at the C_{sp3}-S bond, but a discussion of available synthetic methods for this disconnection is outside of the scope of this introduction. However, a range of classic organic reactions (S_N2, Michael addition, etc.) is applicable in this case. This is also relevant for the disconnection of dialkyl sulfides. Depending on the synthetic strategy, or the structural features of the reactant, this disconnection may not be available.
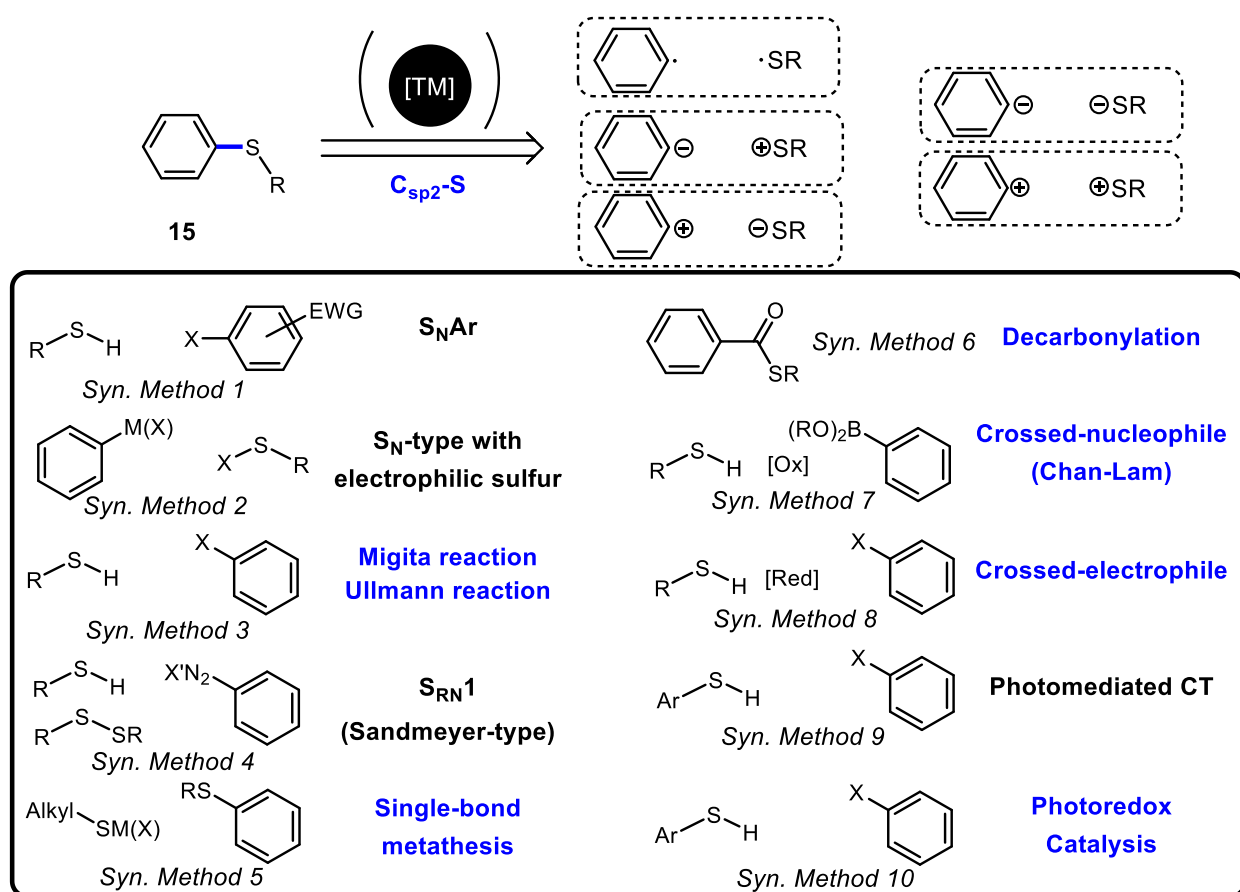
Scheme 4.3: Synthesis of alkyl aryl sulfides or diaryl sulfides: an overview of C_{sp2}-S disconnections leading to five unique synthon combinations, which are discussed below. [TM]: Transition metal; [Ox]: Oxidant; [Red]: Reductant.

The alternative disconnection (C_{sp2}-S) then might become attractive (Scheme 4.3). In general, for all hypothetic synthons (ionic-polar and radical) and their shown combinations, a real forward transformation exists (synthetic methods 1 – 10). For aryl halides, the S_NAr pathway is only efficient in the presence of electron-withdrawing groups on the arene, and still may require forcing conditions even with reactive, nucleophilic thiolates (Synthetic method 1). Polarity reversal of inherently

nucleophilic thiols has been achieved with oxidizing agents (synthetic method 2). *N*-Chlorosuccinimide was used by Lee and co-workers to give sulfenyl chlorides, which showed excellent reactivity with aryl Grignard reagents to give aryl alkyl sulfides.[13]

The Migita and Ullmann reactions are C-S cross-coupling reactions, which in a broad sense follow the general mechanistic steps of late-transition metal-catalyzed cross-couplings with 2 valence-electron redox cycles (synthetic method 3). The Migita reaction is closely related mechanistically to the Buchwald-Hartwig amination and etherification and will be discussed in more detail later (sections 4.1.2.1.-4.1.2.3.). It is known to be catalyzed by several different transition metals whereas the Ullmann reaction refers specifically to catalysis by copper species. Various Ullmann C-heteroatom cross-couplings have been comprehensively reviewed.[14] An interesting example was presented by Snieckus demonstrating high tolerance of the Ullman method towards protic functionality (Scheme 4.4).[15]
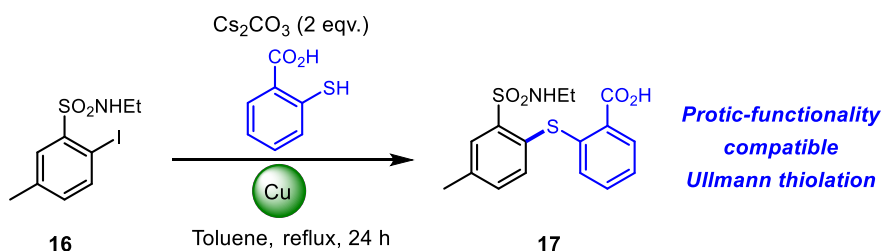
Scheme 4.4: Functional-group tolerant Ullman thiolation reported by Snieckus.

Arenediazonium salts can be conveniently exploited as facile sources of aryl radicals by single electron transfer (SET) reductants, such as excited state organic photocatalysts or simply by thermo- or photoinitiation - the thermodynamic driving force being the formation of nitrogen. This reaction type shares mechanistic similarities with the Sandmeyer-reaction (synthetic method 4). The aryl radicals combine with thiyl radicals (recombination) or disulfides (recombination and chain elongation by production of another thiyl radical) to give the desired aryl sulfide products. Jacobi von Wangelin and co-workers have shown a broad scope of these dark and photocatalyzed reactions in a series of articles,[16] including an interesting trifluoromethylthiolation reaction of relevance in an agrochemical and pharmaceutical context.

Morandi recently reported a Pd-catalyzed (0.4 – 0.8 mol%) single bond metathesis approach to alkyl aryl sulfides from other alkyl aryl sulfides or thiophenols by applying an excess of lithium thiolate (2.6 to 3.9 eqv.) and allowing thermal equilibration (synthetic method 5).[17] The key to designing successful single-bond metathesis catalysts for C-S bond formation is complete reversibility of the elementary organometallic steps. So far, relatively harsh thermal conditions (100 °C for thioethers, 160 °C for thiophenols) were required to access the target structures. The most impressive feature of this

reaction is however the demonstrated success in depolymerizing polyphenyl sulfide **5** to a single non-polymeric dithioether.

Sanford has reported the redox neutral, thermal (130 – 150 °C) Pd- and Ni-catalyzed (10 mol%) decarbonylation of *S*-aryl thioesters to yield diaryl sulfides after 20 h reaction time (synthetic method 6).[18] Szostak and Liu have reported a similar Ni-catalyzed reaction.[19] The reaction is mechanistically intriguing since the final thermodynamic fate of the catalysts appear to be the corresponding metal carbonyls, which seems to be countered by the high temperature to enable thermolysis of the Metal-CO bond. *S*-alkyl thioesters proved to be unreactive under the conditions reported by Sanford. Although the reaction is redox neutral, the preparation of thioesters as starting materials is necessary. This can be an advantage considering the wide availability of benzoic acid derivatives.

The Copper-catalyzed Chan-Lam reaction (synthetic method 7) is a cross-nucleophile coupling between an organoboronic acid (**18**) or ester (**19**) and a heteroatom nucleophile (amine or thiol such as **20**) requiring an oxidant (Scheme 4.5).
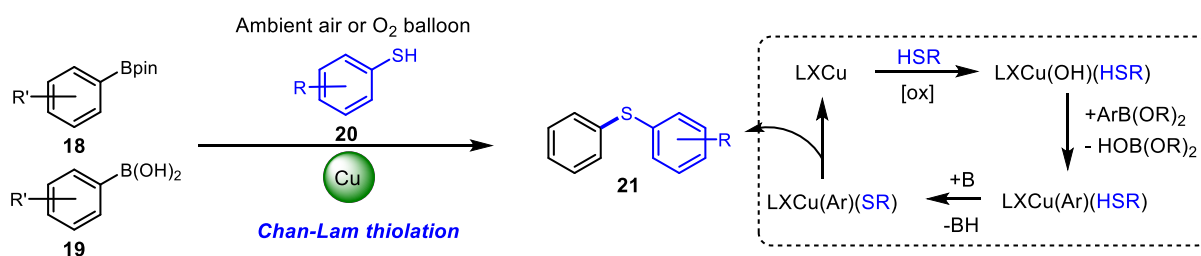
Scheme 4.5: Generalized scheme for the reported crossed-nucleophile Chan-Lam Cu-catalyzed reaction of aryl boronic acid(s) (esters) with thiophenols. A simplified mechanism is shown on the right.

From a handling perspective, it is an attractive alternative since it can be conducted in aerobic conditions (or in an atmosphere of pure oxygen). It has therefore gained attention from the pharmaceutical industry. Significant advances have been made in the Chan-Lam coupling of thiophenols with arylboronic acids. Fang, Xu and co-workers reported a $CuSO_4$/Phenanthroline catalyzed system (5 mol%) each to give a large set of diaryl sulfides (48 examples, 40 – 85% yield) at RT under an oxygen atmosphere in EtOH solvent within 8 h.[20] Watson and co-workers at GlaxoSmithKline reported in a mainly mechanistic study the Chan-Lam coupling of aryl boronic pinacol esters with thiophenols (2 examples) using $Cu(OAc)_2$ (20 mol%) under an oxygen atmosphere at 80 °C in acetonitrile solvent in the presence of powdered molecular sieves and boric acid for 24 h.[21] The Chan-Lam coupling of aliphatic thiols with aryl boronic acids is currently only possible by employing stoichiometric copper, which is an unsolved severe limitation of this otherwise attractive synthetic method.

Cross-electrophile thiolations (synthetic method 8) combine disulfides and aryl halides in the presence of a metallic reducing agent. Only aryl iodides have been shown to be competent coupling partners under Ni catalysis (with various ligand frameworks) and elemental Zn as the reductant.[22] It has been shown for related cross-electrophile couplings that the mechanism may diverge from simple metalation of the stronger electrophile, followed by a classical cross-coupling mechanism. Indeed, all the above cited studies propose various mechanisms that diverge completely from the typical cross-coupling mechanism by accounting for single electron transfer reductions. For example, Nevado has shown an organic reductant to be highly active in a Ni-catalyzed cross-electrophile coupling.[23]

A mechanistically interesting example was presented by Miyake and co-workers for the synthesis of diaryl sulfides under visible light irradiation from electronically differentiated coupling partners **22** and **23** in basic conditions at RT (Scheme 4.6).[24]
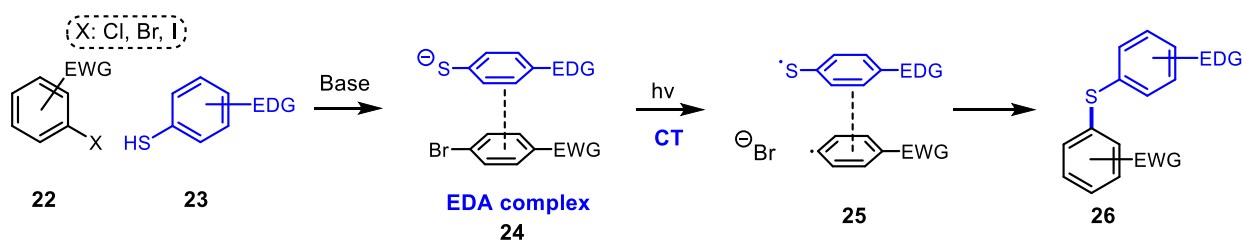
Scheme 4.6: Mechanistic proposal of a transition-metal-free, light-mediated charge transfer from an electron donor-acceptor-complex (EDA complex) to give aryl-thiyl radical coupling products as reported by Miyake.

An electron-donor-acceptor (EDA) complex **24** was proposed, which after charge-transfer would give two radical species (complex **25**), which would recombine to give the desired product **26** (synthetic method 9). The proposed mechanism was supported by UV/Vis experiments and the fact that alkanethiols were incompetent nucleophiles. The possibility of "hidden" transition-metal catalysis was ruled out using high purity cesium carbonate as base. While the reaction represents an interesting alternative to thermal S_NAr reactions, it is still limited by the necessary electronic differentiation of the substrates into electron-rich nucleophile (**23**) combined with electron-poor electrophile (**22**).

Before the report of Miyake, approaches utilizing photoredox catalysis (synthetic method 10) to produce aryl sulfides have been published. Fu and co-workers reported an effective combination of the photoredox catalyst [*fac*-Ir(ppy)$_3$] and Cs_2CO_3 to generate thiyl radicals from the excited state photocatalyst and cesium thiolate.[25] The reduced photocatalyst then reduces the aryl halide (X= I, Br, Cl) to an aryl halide radical anion, which couples with the thiyl radical to give a thioether radical, which undergoes oxidation to generate the diaryl thioether product and another thiolate equivalent (Scheme 4.7).
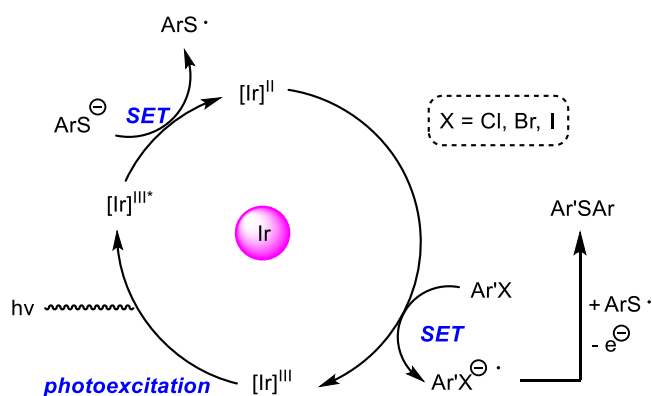
Scheme 4.7: General mechanistic proposal for the Ir-photoredox catalyzed thiolation of aryl halides as reported by Fu and co-workers. SET: single electron transfer.

However, there are similarities between Fu's and Miyake's work. Interestingly, control experiments in Fu's work without added photocatalyst did not give appreciable yields of aryl sulfide. Additionally, aliphatic thiols were rather incompetent coupling partners, giving only 52% isolated yield with less challenging aryl iodide partners.

In a related approach reported by Johannes, dual photoredox-nickel catalysis was employed (Scheme 4.8).[26] Again, a photoexcited Ir catalyst was used as an oxidant to generate a thiyl radical which oxidizes a Ni(I) species to give a Ni(II) complex carrying the thiolate. Reduction of the Ni species by the reduced photocatalyst gives a Ni(I) thiolate which undergoes a typical cross-coupling sequence leading to the desired thioether product and a Ni(I) halide ready to reenter the catalytic cycle by combination/SET with a thiyl radical. While aliphatic thiols were well-tolerated, the electrophile scope was limited to aryl iodides. While photo-mediated or photo-catalytic synthetic methods have their unique advantages, technical issues can arise upon scale-up by action of the Lambert-Beer law.
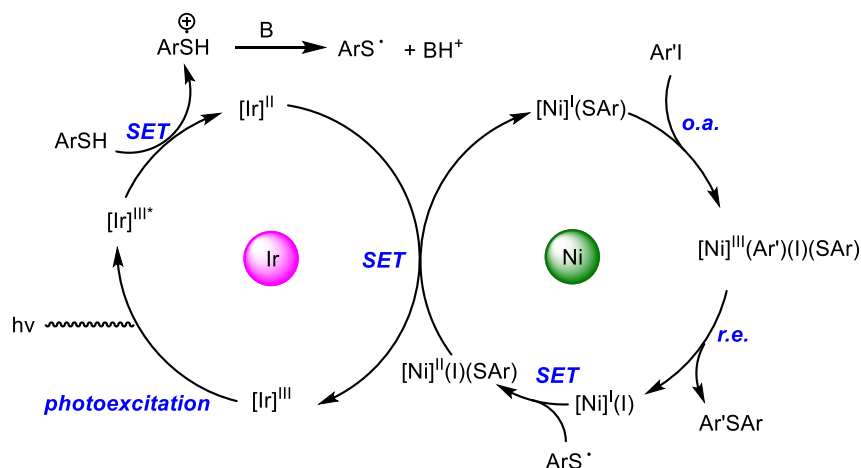
Scheme 4.8: General mechanistic proposal for the dual Ir-photoredox/Ni-catalyzed thiolation of aryl iodides as reported by Johannes and co-workers. SET: single electron transfer; o.a.: oxidative addition; r.e: reductive elimination.

Molander used a base-free approach by combining dual photoredox-nickel catalysis with *H*-atom transfer reagents. A hypervalent alkylsilicate reagent **27** is reduced by a photoexcited Ruthenium catalyst, to give an alkyl radical which rapidly generates a thiyl radical by *H*-atom abstraction (Scheme 4.9).[27] These thiyl radicals then enter a Ni-catalyzed cross-coupling cycle similar as to the one reported by Johannes and co-workers.
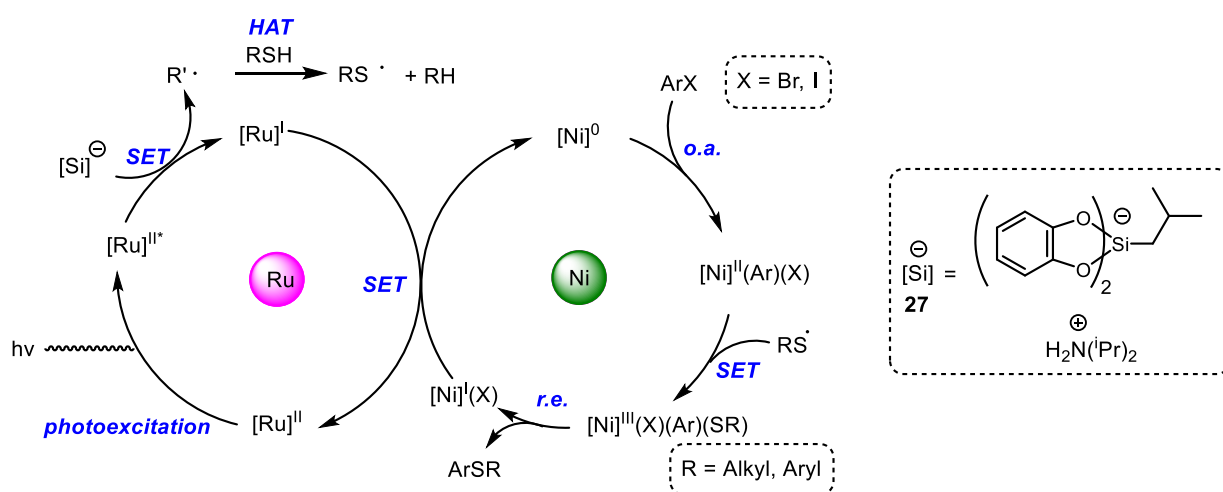
Scheme 4.9: General mechanistic proposal for the dual Ir-photoredox/Ni-catalyzed thiolation of aryl iodides as reported by Molander and co-workers. SET: single electron transfer; o.a.: oxidative addition; r.e: reductive elimination; HAT: H-atom transfer.

Thiophenols were unreactive coupling partners, and the aryl halide scope is currently limited to aryl bromides and iodides. Since the reaction is occurring base-free, interesting applications in bioorganic chemistry are opened up and have been reported subsequently by Molander.[28] A highlight in the follow-up publication is the selective arylation of a cysteine residue in a highly functionalized, unprotected linear octapeptide within 1.5 h at RT in DMF.

4.1.2.1. Pd-catalyzed Migita reactions

In 1978, Toshihiko Migita and co-workers from Gunma University in Japan reported the $Pd(PPh_3)_4$-catalyzed (4 mol%) reaction of aryl iodides and bromides with sodium alkyl- and arylthiolates in DMSO for 18 h at 100 °C.[29] Aryl chlorides were reported to be unreactive under these conditions. The chemical literature in some cases does not acknowledge this historic development, and the Migita reaction is in some cases confusingly referenced as the Buchwald-Hartwig(-Migita) thiolation.[30] Interestingly, Migita also contributed heavily to the development of the Pd-catalyzed Buchwald-Hartwig amination of aryl halides through discovery of the Pd-catalyzed reaction of tin amides with aryl halides.[31] It was found by the same group that alcoholic solvents exhibit an overall better performance than DMSO.[32] In the following years, the reaction scope was extended towards other metal thiolates, as well as alkenyl and alkynyl bromides and iodides by various groups. Progress in this area has been reviewed up to 2011.[33] A generally accepted mechanism for Pd(0/II) systems is presented below (Scheme 4.10) and is basically equivalent to the Buchwald-Hartwig amination. It consists of oxidative addition to an C_{sp2}-X electrophile, transmetalation of a metal thiolate and reductive elimination to release the product and regenerate the Pd^0 species.
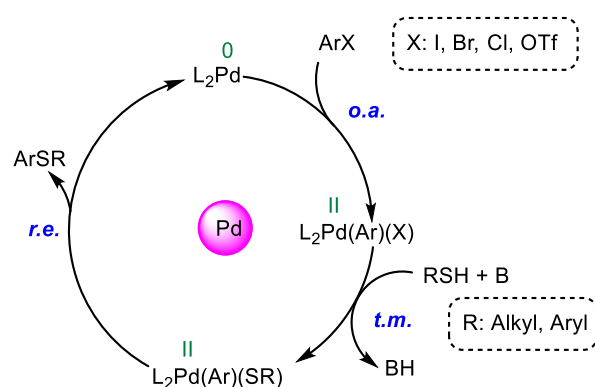
Scheme 4.10: General mechanism of the Pd-catalyzed Migita reaction with a 2-valence electron redox cycle. In some cases, an adduct of the thiol with the oxidative addition complex was detected.

The first reports of successful aryl chloride activation in the Pd-catalyzed Migita reaction appeared from 2000 onwards. In 2001, Li and co-workers at DuPont Company reported air-stable dimeric Pd^{II} complexes from secondary phosphine oxides, which were active in the Migita reaction of some aryl chlorides.[34] Electron rich aryl chlorides showed less satisfactory performance.[35]

In 2004, Buchwald disclosed a $Pd(OAc)_2$/dippf-catalyzed Migita reaction (dippf: 1,1'-bis(diisopropylphosphino)ferrocene) for the transformation of various aryl chlorides at 100 °C for 18 h.[36] Hartwig reported on a Pd-catalyzed Migita reaction of aryl chlorides with Pd loadings as low as 0.01 mol% (usually 0.5 − 2 mol%) in various solvents at 110 °C for 2 − 24 h.[37] In this case, a Josiphos-type chiral ligand showed superior performance to other bidentate phosphines, however the chiral information was obviously not necessary *per se*. The last two systems are generally the strongest

performers in the area of Pd-catalysis. A minor drawback is the requirement for air-sensitive and costly designer phosphine ligands.

In 2018, the Schönebeck group reported a Migita reaction of aryl bromides and iodides selectively over aryl triflates (e.g. DPEphos/Pd mixtures were reported to selectively activate aryl triflates over bromides) with pre-formed sodium thiolates by using air- and moisture-stable [(μ-Br)Pd(P^{t}Bu$_3$)]$_2$ (5 mol%) at 40 - 60 °C in toluene for 3 – 12 hours.[38] A major advantage of the method appears to be the tolerance of the reaction towards reactants with protic functionality. The proposed catalytic cycle differs from the standard cross-coupling cycle; transmetalation is followed by oxidative addition to give a dinuclear Pd(II) complex which undergoes reductive elimination.
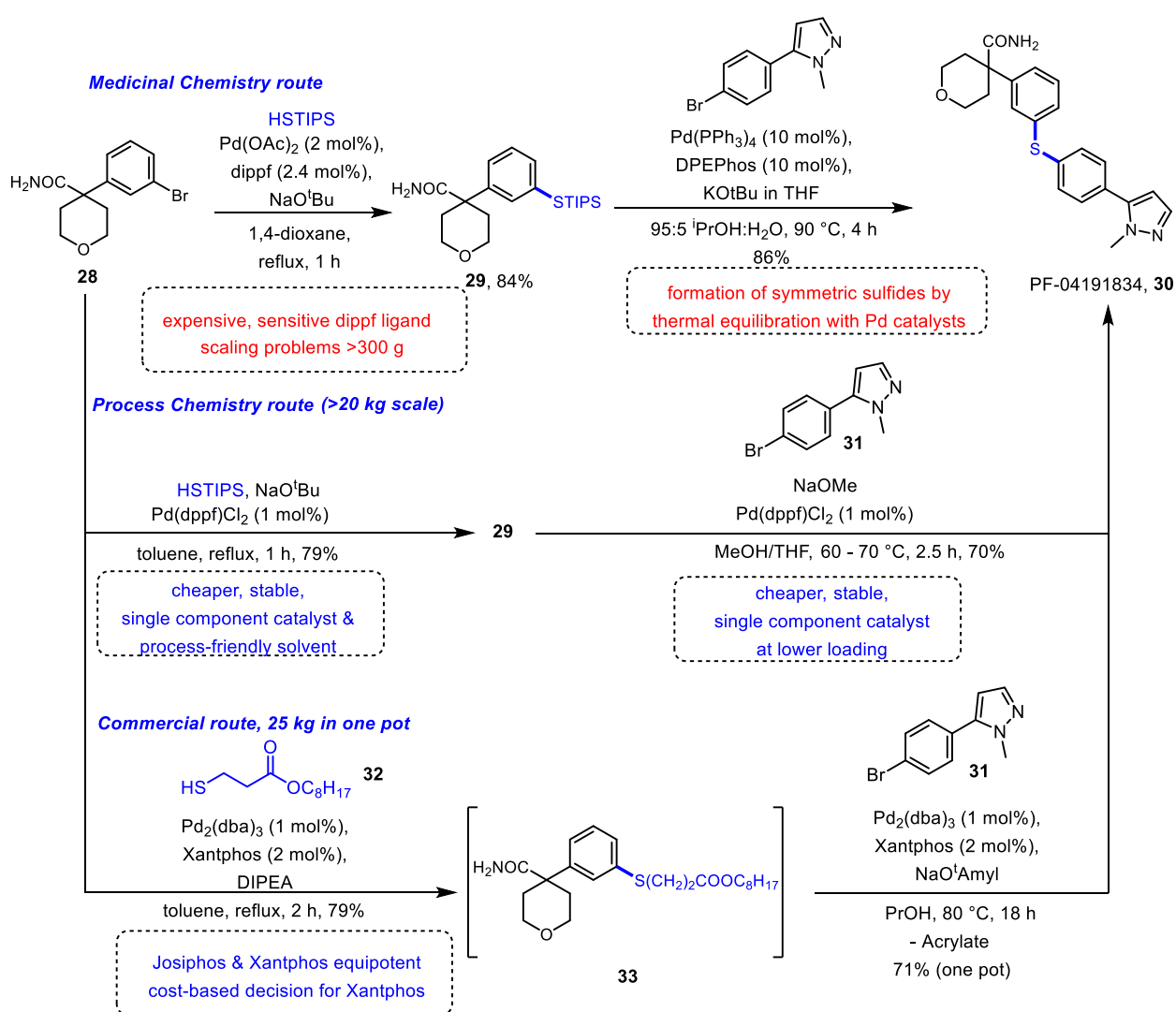
Scheme 4.11: Uses of the Pd-catalyzed Migita reaction in the process development and commercial manufacture of a lipoxygenase inhibitor **30** from Pfizer.

It is interesting to note that the Pd-catalyzed Migita reaction has found its way into pharmaceutical process chemistry.[39] Pfizer developed the Lipoxygenase inhibitor PF-04191834 (**30**) containing a central diaryl sulfide motif, which required changes to the discovered medicinal chemistry synthetic

route to facilitate multi-kg production for clinical trials. The chemical evolution of the route into commercial production has been documented by two published reports. Initially, the medicinal chemistry route used (^{i}Pr)$_3$SiSH (TIPS-SH) as a sulfide surrogate to construct the central C-S bonds in two subsequent Migita reactions. While the overall strategy was kept in the subsequent process development, the Buchwald catalytic system (Pd(OAc)$_2$/dippf) was exchanged due to scale-up and cost problems towards a more robust dppf-based precatalyst operating at lower loadings (from **28** to **29**).[40] A similar tactic was executed for the second step (from **29** to **30**).

Finally, in the commercial route, 3-mercaptopropionate (**32**) was chosen as a sulfide surrogate instead and a one-pot process was developed with an excellent overall yield.[41] The propionate moiety is eliminated as an acrylate under the basic conditions of the second step (from **33** to **30**). Again, this was achieved by a re-evaluation of catalytic systems for the Migita reaction. A Xantphos-based system was found to be equally potent to the Hartwig system (Josiphos-based), and thus the former was selected based on estimated operating costs. The conclusion from this case study is that in process chemistry robustness and cost are key issues in transition metal catalysis, leading to the preference towards non-designer ligands, low metal loadings, short reaction times and process-friendly solvents over highly performant catalytic systems.

4.1.2.2. Ni-catalyzed Migita reactions

Cristau reported the first Ni-catalyzed Migita reaction of aryl bromides using 0.3 mol% of Ni(dppBz)Br$_2$ (dppBz: 1,2-bis(diphenylphosphino)benzene) at 200 °C in glycol for 24 h.[42] Following this seminal report, Ni-catalyzed Migita couplings generally remained limited to aryl bromides, iodides and mesylates as the electrophilic coupling partner; the progress up to 2011 has been reviewed.[33] While a 2 valence-electron redox cycle similar to the Pd-catalyzed Migita reaction appears likely, other mechanistic scenarios (such as the involvement of Ni(I) species) should not be ruled out.

In 2015, the Schönebeck group discovered a Ni-catalyzed trifluoromethylthiolation of aryl chlorides at 45 °C in toluene for 24 h using Ni(cod)$_2$/dppf (10 mol% each) to form the active catalyst *in situ*.[43] The resulting aryl trifluoromethyl sulfides are high-value structures in medicinal chemistry. Some key discoveries were made: 1. The addition of nitrile additives lowers the energetic span of the catalytic cycle by destabilizing the zerovalent Ni complex relative to the cod-ligated analogue, thus leading to a lower barrier for oxidative addition, which was rationalized by DFT calculations; 2. Ni(dppf)Cl was formed from the oxidative addition of Ni(dppf)(cod) into chlorobenzene 3. Ni(dppf)Cl was catalytically inactive, which supports a Ni(0/II) redox cycle analogous to the Pd-catalyzed process.

In 2017, the Stewart group and co-workers at Bayer reported the Ni-catalyzed Migita coupling of arylthiols with chloroarenes using Ni[P(O*p*Tol)$_3$]$_4$ (5 − 10 mol%) and Xantphos (5 − 10 mol%) in toluene at 110 °C for 16 h.[44] Alkylthiols were unsuitable coupling partners. Interestingly, the Xantphos ligand

was found the most effective by simple empirical screening of 28 bidentate commercially available phosphine ligands using a GC/MS-based assay. Stoichiometric zinc was necessary as an additive to suppress the formation of aryl disulfides.

Table 4.1 reviews all reported Ni-catalyzed Migita reactions of aryl halides (and some alkenyl halides) with thiols or thiolates by comparing all important reaction parameters. To allow for a fair comparison, an idealized turnover frequency (TOF) was calculated from the turnover number (TON) assuming complete catalyst selectivity and no deactivation over the course of the reaction over time t. This TOF value should not be confused with a rate based TOF, which changes over the course of a reaction. It should be noted that no normalization of temperature was carried out.

$$\text{TOF (h}^{-1}) = \text{TON}/t = (100\%/[\text{Ni loading}])/t \qquad \text{(Equation 1)}$$

There are two overall themes: Most reactions are performed in polar aprotic solvents (e.g DMF) and secondly most reactions target aryl iodides and bromides. The average (considering all electrophiles) Ni-catalyzed Migita reaction is performed at around 90 °C, for 13 hours with a Ni loading of approximately 7 mol% and a TOF of 18 h^{-1}. These benchmark values allow for method comparison and highlight the underdeveloped status of Migita reactions targeting aryl chlorides and operating under milder conditions, most desirably at room temperature. For an exemplary comparison, Hartwigs Pd/Josiphos-catalyzed Migita reaction of chloroarenes typically operates at 0.1 mol% metal loading, going to completion within 4 h (at 110 °C), giving an idealized TOF of 250 h^{-1}.[37b]

Table 4.1: Comparison of literature-known Ni-catalyzed Migita reactions of aryl halides with thiols or thiolates in various reaction parameters.

	ArX [a]	RSH	Base	Reductant	Catalyst	Ni loading (mol%)[b]	Ligand	Ligand loading (mol%)	Solvent	T (°C) [b]	t (h)[b]	TOF (h^{-1})[c]
1[44]	Cl	Ar	KOtBu	Zn (100 mol%)	Ni[P(OpTol)$_3$]$_4$	10	Xantphos	20	Toluene	110	16.0	0.6
2[45]	I	Ar, Alkyl	Pyridine	Zn (200 mol%)	[Ni•Py•2EC]	30		90	MeOH	25	5.0	0.7
3[42]	Br	Ar	NaSR		Ni(dppBz)Br$_2$	0.3			Glycol	200	24.0	13.9
4[46]	OMs	Ar	NaSR	Zn	Ni(dppf)Cl$_2$	10	dppf	20	DMF	80	21.5	0.5
5[43]	Cl	CF$_3$	Me$_4$NSCF$_3$		Ni(cod)$_2$	10	dppf	10	Toluene/MeCN	45	15.0	0.7
6[47]	Br*	Ar, Alkyl	KO^{t}Bu		Ni(OAc)$_2$	10	IPr	5	DMF	70	2.0	5.0
7[48]	Br**	Ar	K$_2$CO$_3$	Zn (20 mol%)	NiBr$_2$	4	dppf	8	NMP	60	10.0	2.5
9[49]	Br	Ar, Alkyl	NaH or Et$_3$N or PhNEt$_2$		Ni[P(OEt)$_3$]$_4$	5			DMF/(THF)	120	24.0	0.8
10[50]	I	Ar, Alkyl	KOH		NiCl$_2$(H$_2$O)$_6$	5			TBAB molten salt	110	10.0	2.0
11[51]	Br	Ar, Alkyl	KO^{t}Bu		(34)$_2$Ni	4			DMF	110	16.0	1.6
12[52]	Cl	Ar	KOH		(35)$_2$Ni	5			DMF	70	2.0	10.0
13[53]	Br**	Ar	NaO^{t}Bu		(36)Ni(allyl)Cl	1			DMF	100	24.0	4.2
14[54]	I	Ar	KOH		NiCl$_2$/Ni(cod)$_2$	1	Ph$_2$P(O)H	10	DMF	80	2.0	50.0
15[55]	I***	Ar	KOH		Ni(cod)$_2$	0.5	37	0.5	DMF	80	1.0	200.0
16[56]	Br	Ar, Alkyl	NaOH	Zn (15 mol%)	NiBr$_2$	10			PEG400	120	12.0	0.8
17[57]	Br	Ar	NaO^{t}Bu		(IPr)Ni(allyl)Cl	5			DMF	100	24.0	0.8
Average						6.9				92.5	13.0	18.4

[a]: Only the aryl halide with the strongest C-X bond is mentioned. [b]: Highest value during substrate screening. [c]: Assuming complete conversion after the reaction and complete product selectivity per mol% of catalyst during all stages of the reaction. *: ArCl examples are reported only with strongly electron-withdrawing nitro groups. **: ArCl examples below 15% yield. ***: One example with ArBr. cod: 1,8-cyclooctadiene; dppBz: 1,2-bis(diphenylphosphino)benzene; dppf: 1,1'-diphenylphosphinoferrocene; IPr: 1,3-Bis(2,6-diisopropylphenyl)imidazolylidene; TBAB: tetrabutyl ammonium bromide; pTol: para-tolyl; PEG400: polyethylene glycol of average molecular weight 400; NMP: N-Methylpyrrolidine; DMF: N,N-Dimethylformamide; EC: Ethylcrotonate; Py: Pyridine; 34: 1,3-Bis[benzyl]imidazolylidene 35: 2-(((2-(benzylthio)phenyl)imino)methyl)phenolate 36: 1,3-Bis[2,6-bis(diphenylmethyl)-4-methoxy-phenyl]imidazolylidene; 37: 1,1'-Bis(phenylphosphineoxide)diphenylether.

4.1.2.3. Migita reactions catalyzed by other (transition) metals

The iron-catalyzed Migita reaction is a highly attractive method. The high earth-crust abundance of this metal coupled with its low toxicity makes it attractive for pharmaceutical process chemistry. In 2009, Bolm reported the Fe-catalyzed (10 mol%) Migita coupling of aryl iodides with various (hetero)arenethiols at 135 °C for 24 h in toluene employing a diamine ligand.[58] Lee extended the scope to alkylthiols with a similar system using Xantphos as a ligand.[59] It was however conclusively shown copper contamination present in non-high-purity commercial batches of iron precursor salts is causing the cross-coupling activity.[60] The copper-catalyzed Migita reaction is synonymous to the Ullmann thiolation and was briefly discussed above. It is currently unclear if an iron-catalyzed Migita reaction is feasible at all, and significant experimental work will have to be dedicated to exclude catalysis by transition metal contaminants.

In 2008, Rao and co-workers presented an Indium-catalyzed Migita reaction of aryl iodides with thiophenols and alkanethiols in DMSO at 135 °C for 24 h.[61] The necessity of an amine ligand and the fact that Indium is a simple Lewis acid unable to undergo typical transition metal redox cycles make the mechanism of this reaction intriguing and calls for investigation of "hidden" metal catalysis in this case. Rao has since then shown that indium oxide nanoparticles alone are able to catalyze similar Migita reactions.[62]

In 2006, Cheng and co-workers reported an attractive Cobalt-catalyzed (1-2 mol%) Migita reaction operant on aryl iodides and bromides in acetonitrile at 80 °C.[63] Various alkanethiols and thiophenols were efficiently coupled using simple pyridine as the stoichiometric base. However, a stoichiometric reductant (Zn) was required. The authors postulated a $Co^{I/III}$ 2-valence electron redox cycle where the reductant performs an initial reduction of a Co^{II} precursor salt.

4.1.3. Aims of the chapter

As can be seen from the preceding sections, the Migita reaction can be a valuable tool in the synthesis of non-natural aryl thioether compounds, up to process chemistry scale. A rather large set of methods is available, which utilize Pd or Ni catalysts to activate aryl bromides or iodides, whereas the activation of chloroarenes is relatively underdeveloped.

The typically observed activity row ArI > ArBr = ArOTf > ArCl (which corresponds to the reported bond dissociation energy trend)[64] in Pd-catalyzed cross-coupling (there are exceptions to the presented order) is appealing to the synthetic chemist, allowing in principle programmable, sequential functionalizations of polyhalogenated arenes,[38] especially in the context of increasing automatization of cross-coupling

sequences.[65] However, cross-coupling systems for functionalizing stable chloroarenes remain rare and may require designer phosphine ligands (e.g. Josiphos)[37b] or air-sensitive ligands (e.g. dippf)[36] in the realm of Pd catalysis. Ni catalysis offers the opportunity to activate challenging electrophiles with ease (see chapter 1), but severe limitations exist which may hinder method uptake by the wider synthetic community, including: 1. limited functional group and heterocycle tolerance, 2. high Nickel loadings, 3. harsh thermal conditions and prolonged reaction times.

Thus, in this chapter, an exceptionally mild Migita reaction of zinc thiolates with chloroarenes was discovered as a side-reaction of the Ni-catalyzed Fukuyama reaction (Chapter 3). A similar observation has been made by Stambuli during investigation of the Pd-catalyzed Fukuyama reaction, where aryl bromides were activated. Thus, a robust Ni-catalyzed Migita reaction of challenging chloroarenes with *in situ* generated zinc alkyl- and arylthiolates will be presented in the following sections, which compares favorably in various metrics to established Pd and Ni-based systems.

4.2. Results and discussion

4.2.1. Initial optimization

Based on the initial observation of the Migita coupling in the context of the Fukuyama coupling using **C1**, a set of screening reactions between chlorobenzene (**38**) and heptane-1-thiol (HeptSH, **39**) was conducted in THF at RT using 0.5 mol% **C1** loading. The results were analyzed by quantitative GC-FID (Table 4.2).

Table 4.2: Initial optimization of the Migita coupling of chlorobenzene with heptane-1-thiol.
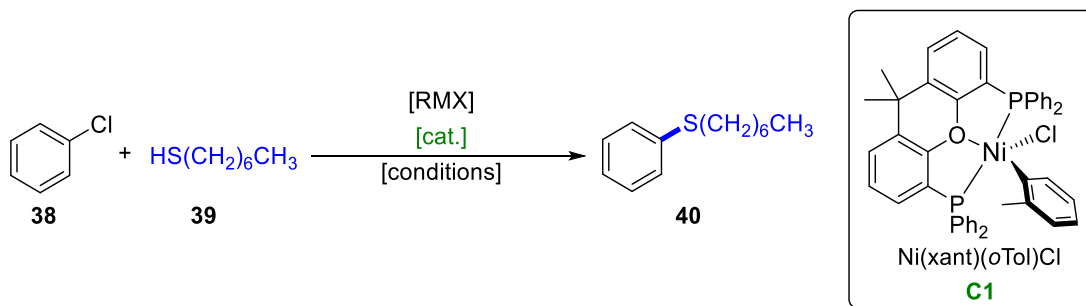
Entry	RMX	Cat.	Conditions	Conv.^{a}	Yield^a
1	PhMgBr•LiCl (1.1 eqv)	**C1** (0.5 mol%)	15 min, 0°C to RT	100%	93%
2	PhMgBr•LiCl (1.1 eqv)	**C1** (0.5 mol%)	5 min, 0 °C to RT	36%	33%
3	PhMgBr•LiCl (1.1 eqv)	**C1** (0.5 mol%)	15 min, 0 °C to RT, in air	13%	13%
4	PhMgBr•LiCl (1.1 eqv)	NiCl$_2$ (0.5 mol%)	15 min, 0 °C to RT	35%	0%
5	PhMgBr•LiCl (1.5 eqv)	None	15 min, 0 °C to RT	6%	1%
6	PhMgBr•LiCl (1.1 eqv)	Ni-NP (0.5 mol%)^b	30 min, 0 °C to RT	31%	0%
7	PhMgBr•LiCl (1.1 eqv)	**C1** (0.5 mol%)	30 min, 0°C to RT, dark	100%	65%

PhCl (50 μL, 500 μmol), heptane-1-thiol (80 μL, 500 μmol) PhMCl·LiCl (1.2 mmol based on titre [typically 0.5 M], in THF), **C1** (2.0 mg, 2.5 μmol, 0.5 mol%), dry THF (500 μL), 0 °C to RT, 15 or 30 min. ^{a}Determined by quant. GC-FID analysis. ^{b}Prepared as a THF slurry by a literature procedure (SI).

PhMgBr•LiCl (**41**) was chosen as a readily accessible organometallic base, which was added with ice-water bath cooling to avoid undesired Kumada-coupled side products. Pleasingly, full conversion of **38** and an excellent yield of the aryl sulfide **40** was observed after 15 min reaction time with only 0.5 mol% catalyst loading (entry 1). Shorter reaction times proved detrimental (entry 2), perhaps since the reaction required warming to RT to achieve full catalytic efficiency. To rule out a mechanism involving oxidation of the thiolate to deliver a potent disulfide electrophile which would be attacked by the Grignard reagent to give the desired product **40**, the reaction was conducted in air, which gave the expected negative result (entry 3). The use of ligand-free anhydrous $NiCl_2$ as a substitute for **C1** resulted in a negative result as well, pointing towards a strong ligand effect (entry 4). Similarly, the use of preformed NiB nanoparticles or metal-free conditions did not lead to any significant product formation (entries 5 and 6). Curiously, under dark (laboratory lights turned off & reaction vessel shielded by a cardboard box) conditions, a lowered yield was observed (entry 7). However, removal of the ice bath under dark conditions proved to be difficult and this result may be accounted by a simple experimental error. However, re-evaluation of this result might represent a future direction of mechanistic research. The photocatalyst-free acceleration of the organozinc-mediated reduction of Ni^{II} salts to Ni^0 catalysts in flow-reactor Negishi Ni-catalyzed reactions has been conclusively proven by NMR experiments.[66] MacMillan and co-workers have proposed photoexcited states driving thermodynamically unfavoured C-O reductive elimination from Ni^{II} alkoxide complexes.[67]

Next, ligand effects were investigated (Table 4.3). The selection encompassed the small bite angle ligand dppe, monodentate PPh_3 and the wide bite angle ligand dppf. To allow for a fair comparison, the corresponding $L_2Ni(oTol)Cl$ complexes were synthesized (**C2** – **C3**) by the Jamison route[68] or acquired (**C4**). It was found that only the Xantphos-ligated precatalyst **C1** gave the desired product in the required timeframe. Use of the dppf-ligated prectalyst **C4** furnished little product, whereas the dppe- and PPh_3-ligated complexes **C2** and **C3** were inactive. The conclusion from these experiments is that a wide bite angle bidentate phosphine seems to be a prerequisite for high activity in the Migita reaction. However, further requirements seem to be either the rigidity afforded by the Xantphos backbone (compared to dppf, which has Fe-Cp rotatable axes) or the possibility of a hemilabile κ^3-P,O,P coordination mode.[69]

Table 4.3: Screening of $L_2Ni(oTol)Cl$-based complexes with different phosphane ligands in the Migita reaction.
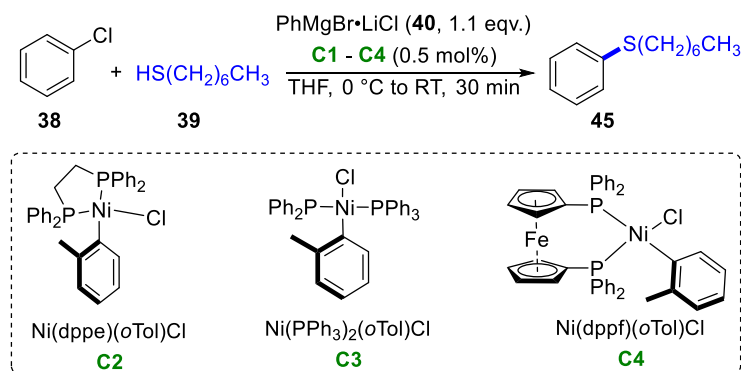
Entry	Cat.	Conv.[a]	Yield[a]
1	**C1** (0.5 mol%)	100%	93%
2	**C2** (0.5 mol%)	2%	0%
3	**C3** (0.5 mol%)	10%	0%
4	**C4** (0.5 mol%)	8%	7%

PhCl (50 µL, 500 µmol), heptane-1-thiol (80 µL, 500 µmol) PhMgBr·LiCl (1.2 mmol based on titre [typically 1.3 M], in THF), **C1** – C4 (2.5 µmol, 0.5 mol%), dry THF (500 µL), 0 °C to RT, 30 min. [a]Determined by quant. GC-FID analysis.

To avoid a competing Kumada coupling occurring with Grignard bases, aryl zinc halides were chosen as substitutes. In this case, the reaction could be carried out at room temperature without a competing Negishi reaction taking place (Table 4.4, entry 1). Despite repeated attempts, reactions with preformed thiolates or substitution of the reductant with a simpler inorganic base led to inferior results (entry 2). Furthermore, arylzinc bases seem to be optimal, and use of highly reactive turbo-Grignard base did not lead to product formation (entry 3). It was concluded that the organometallic base fulfills a dual role of pre-catalyst reductant and stoichiometric base.

Table 4.4: Screening of different bases in the Ni-catalyzed Migita reaction.
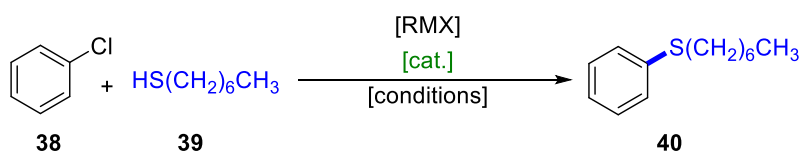
Entry	RMX	Cat.	Conditions	Conv.[a]	Yield[a]
1	PhZnCl•LiCl (2.0 eqv.)	**C1** (0.5 mol%)	15 min, RT	96%	96%
2	HeptSZnCl•LiCl (1.28 eqv.)[b]	**C1** (0.5 mol%)	10 min, RT	18%	18%
3	iPrMgCl•LiCl (1.1 eqv.)	**C1** (0.5 mol%)	60 min, 0 °C to RT	3%	2%

PhCl (50 µL, 500 µmol), heptane-1-thiol (80 µL, 500 µmol), base/reductant, **C1** (2.0 mg, 2.5 µmol, 0.5 mol%), dry THF (500 µL), 0 °C to RT or RT, 10, 15 or 30 min. [a]Determined by quant. GC-FID analysis [b]HeptSZnCl·LiCl was generated from thiol and PhZnCl·LiCl, which was prepared from PhMgBr·LiCl.

4.2.2. Scope of chloro(hetero)arenes

Next, the scope of electrophilic reaction partners was studied (Scheme 4.12). Electron-poor and electron-rich chloroarenes are equally well-tolerated. Various monosubstituted chloroarenes reacted with heptanethiol using either organozinc or organomagnesium bases. Protic functionality was not tolerated.
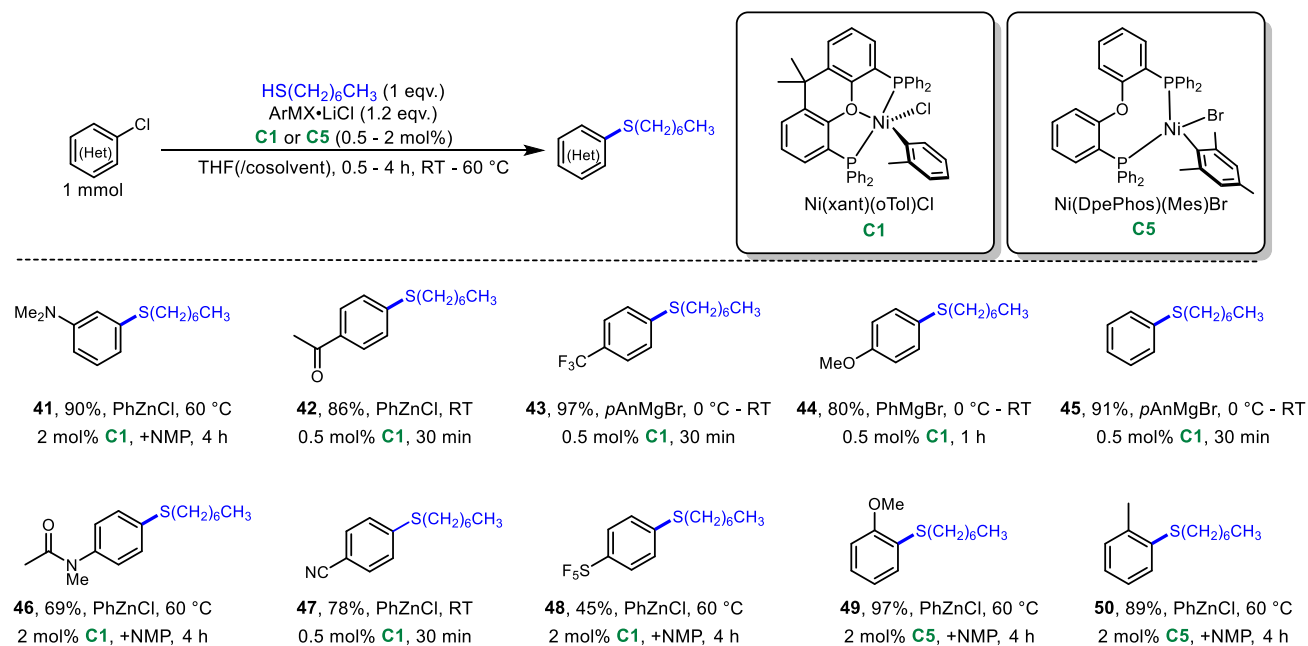
Scheme 4.12: The Ni-catalyzed Migita reaction of various monosubstituted chloroarenes with heptane-1-thiol. Conditions: Chloroarene (1.0 mmol), thiol (1.0 mmol), PhZnCl·LiCl or PhMgBr·LiCl (1.2 mmol of a titrated solution in THF), dry NMP or THF (400 µL), C1 or C5 (0.5–2.0 mol%), 0.5 to 4.0 h, RT–60 °C (for RZnX) or 0 °C–RT (for RMgX, removal of ice-water bath after Grignard addition).

Pleasingly, electrophilic (e.g. in compounds **42** and **47**) as well as Lewis-basic functionality (e.g. in compound **46** or **41**) was generally tolerated. The presence of Michael acceptors as in 4-trimethylsilyl-ethynyl-chlorobenzene led to product mixtures as determined by qualitative GC/MS analysis, which did not enable isolation. Some Lewis-basic functionalized chloroarenes (e.g. 3-chloropyridine, *N*-acetyl-*N*-methyl-4-chloroaniline) did not show any reactivity in pure THF. Catalyst poisoning by coordination of Lewis-basic (or π-basic) functionalities to low-valent Ni^0 complexes was considered a possibility. Schönebeck employed nitrile additives to displace inhibitory cod ligand (originating from the use of $Ni(cod)_2$ as a precatalyst), which lowered the overall energetic span of oxidative addition (determined computationally).[43] Applying this strategy in the present work did not lead to an improved outcome. Either, inhibitory Lewis-basic substituents were not easily replaced by nitrile functionality, or

the origin of inhibition was to be found elsewhere. The second option could be deleterious coordination of Lewis-basic groups to the zinc thiolate, which could inhibit its reactivity by aggregation in solution. Indeed, by addition of a polar-aprotic additive (*N*-methylpyrrolidinone) the reactivity of Lewis-basic chloroarenes in the Migita reaction could be restored. It was found during the scope evaluation that organozinc bases generally possess higher functional group tolerance, as magnesium thiolates were found to cause transesterification of carboxylic acid derivatives.

Ortho-substituted chloroarenes proved to be highly problematic substrates. Using catalyst **C1**, no reactivity of these substrates even under forcing conditions was found. Sawatzky and Stradiotto reported the use of **C5** in cross-coupling chemistry. Interestingly, the tolyl-based analogue of **C5** was not stable upon isolation, which required the use of mesityl-substitution. It was speculated that the decreased stability of *ortho*-substituted oxidative addition complexes with the DPEPhos framework would lead to a catalytic activity of *ortho*-substituted chloroarenes. Indeed, this tactic proved to be valuable in converting two ortho-substituted chloroarenes to the corresponding heptyl aryl sulfides **49** and **50** in excellent yields. However, there might be alternative explanations for the increased performance of the complex **C5** rather than the simple stability arguments presented here.

The reactivity of heterocyclic chloroarenes was evaluated as well (Scheme 4.13). Such motifs are widely found in pharmaceutical chemistry and often cause problematic behavior in cross-coupling chemistry. Pleasingly, the found system was quite robust to various heterocyclic electron-rich and electron-poor systems under the previously established more robust conditions (2 mol% Ni, 60 °C, THF/NMP, 4 h). The presence of Michael acceptor systems was not tolerated well due to competing 1,4-addition of the thiolate under the reaction conditions. However, this may be dependent on the exact electronic and steric requirements of the electrophilic conjugate position. For example, compound **59** still gave acceptable yields of the cross-coupled product, whereas compound **58** was isolated in poor yield. Finally, potentially bioactive compounds were also converted in moderate to good yield, such as 8-chlorocaffeine (to thioether **B1**) or indomethacin ethyl ester (to thioether **B2**).

51, 81%, PhZnCl, 60 °C
2 mol% **C1**, +NMP, 4 h

52, 87%, PhZnCl, 60 °C,
0.5 mol% **C1**, +NMP, 4 h

53, 96%, PhZnCl, 60 °C
2 mol% **C1**, +NMP, 4 h

54, 95%, PhZnCl, 60 °C
2 mol% **C1**, +NMP, 4 h

55, 41%, PhZnCl, RT
0.5 mol% **C1**, 30 min

56, 79%, PhZnCl, 60 °C
0.5 mol% **C1**, +ACN, 4 h

57, 61%, PhZnCl, 60 °C,
2 mol% **C1**, +NMP, 4 h

58, 23%, PhZnCl, 60 °C
0.5 mol% **C1**, +NMP, 4 h

59, 67%, PhZnCl, 60 °C
0.5 mol% **C1**, +NMP, 4 h

60, 82%, PhZnCl, 60 °C
2 mol% **C1**, +NMP, 4 h

B1, 54%, PhMgBr, 0 °C to RT,
0.5 mol% **C1**, 1 h

B2, 86%, PhZnCl, 60 °C,
2 mol% **C1**, + NMP, 4 h
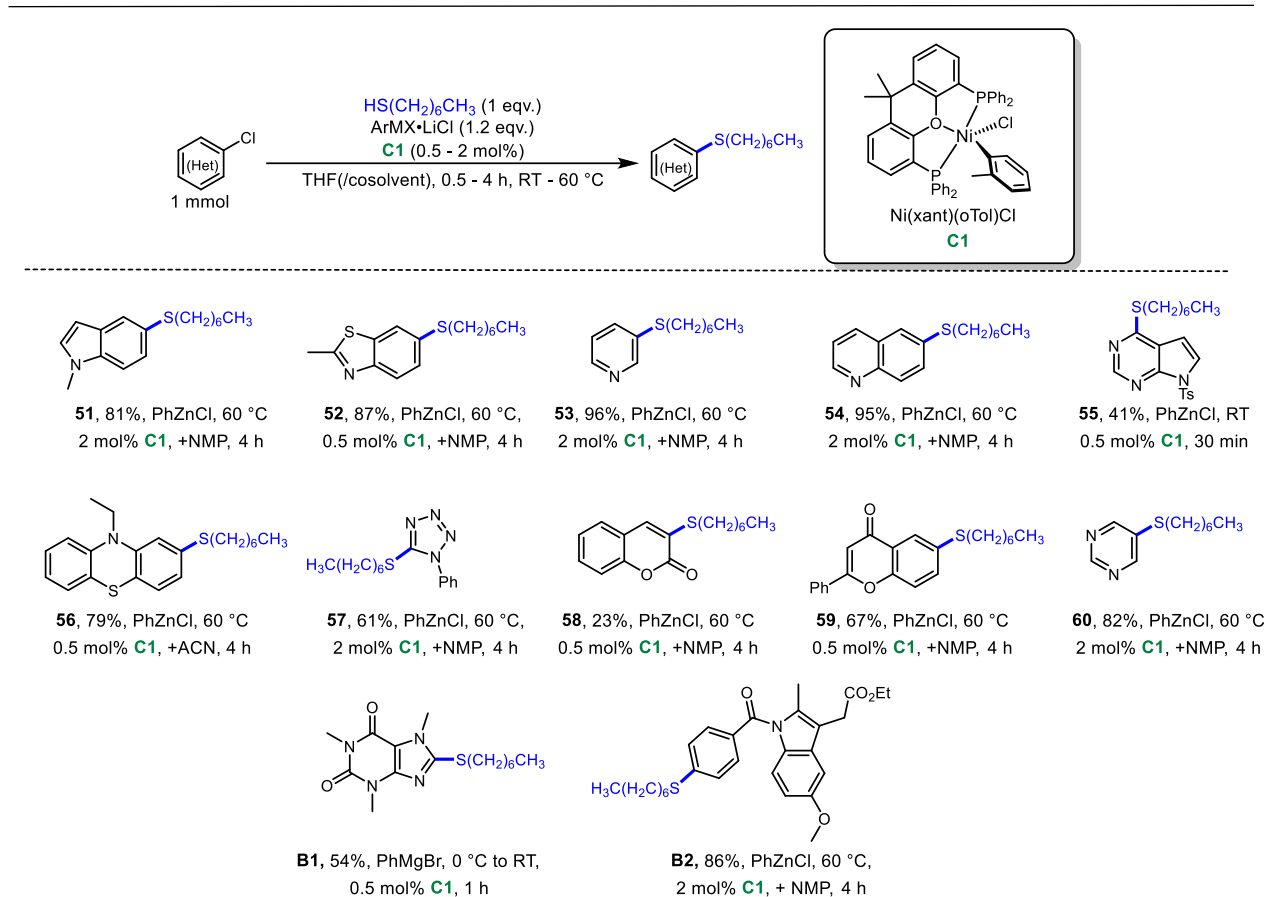
Scheme 4.13: The Ni-catalyzed Migita reaction of various heterocyclic chloroarenes with heptane-1-thiol. Conditions: Chloroarene (1.0 mmol), thiol (1.0 mmol), PhZnCl·LiCl or PhMgBr·LiCl (1.2 mmol of a titrated solution in THF), dry NMP or THF (400 µL), C1 or C5 (0.5–2.0 mol%), 0.5 to 4.0 h, RT–60 °C (for RZnX) or 0 °C–RT (for RMgX, removal of ice-water bath after Grignard addition).
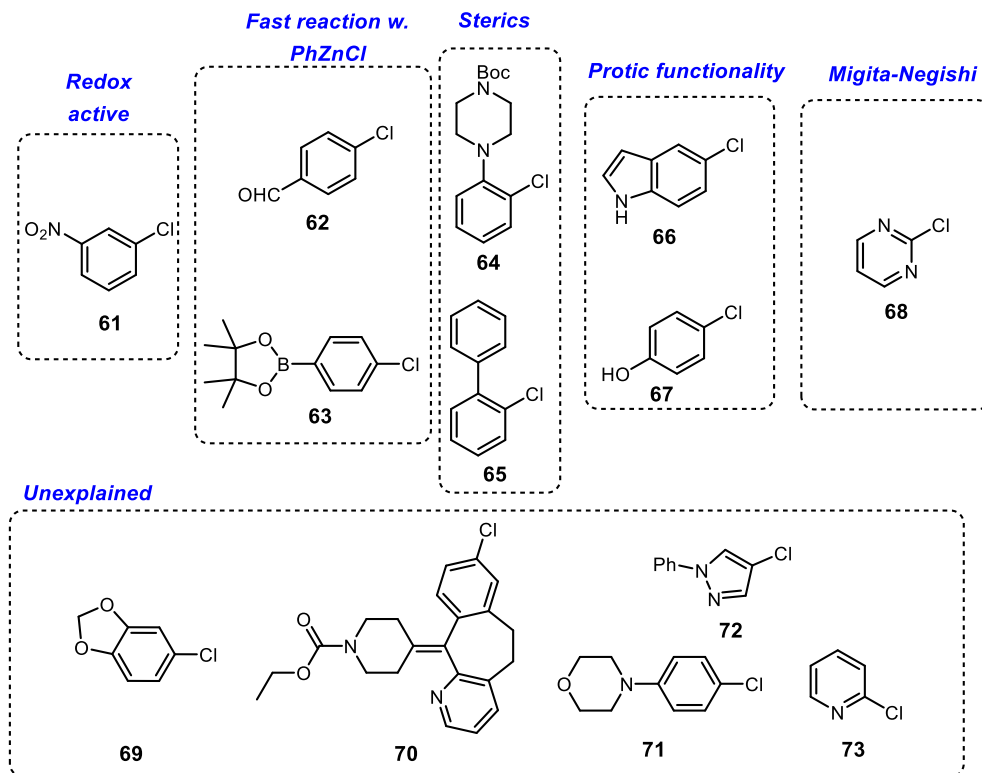
Figure 4.3: Chloro(hetero)arenes which showed no reactivity or deleterious side reactions upon attempted reaction with HeptSH under various conditions and catalysts. The molecules are grouped based on their presumed mode of failure. One group of molecules with an unexplained failure mode remained.

Analysis of the aryl chlorides (**61 – 73**) that showed no reactivity with HeptSH led to the identification of several problematic properties (Figure 4.3): 1. Redox active substituents (e.g. **61**), 2. Substituents which compete with HeptSH for reaction with PhZnCl due to their high electrophilicity (e.g. **62** - **63**), 3. Sterically demanding systems (**65**) – although coordinative effects in this case can be not ruled out (e.g. **64**), 4. Protic functionality – the activity of chloroarenes with such functionality can be observed after addition of more base. However, the approximate conversion by GC/MS remains at an unsatisfactory 50% in the same timeframe (tested by GC/MS for compound **66**). The reaction of 2-chloropyrimidine (**68**) under robust conditions led to the formation of the Negishi product mixed with the desired aryl sulfide as determined by GC/MS analysis. Knochel reported the Negishi-type reaction of 2-heteroaryl alkyl thioethers with organozinc reagents, which would explain this peculiar behavior.[70] Five unreactive chloroarenes remain, which elude this simple analysis (compounds **69 – 73**). The common denominator in this series is the presence of heterocycles having free electrons available for metal coordination. Only in the case of 2-chloropyridine (**73**) is the reactive site only one bond away from a Lewis-basic heteroatom. However, a range of other chloroheteroarenes posed no problem in the Ni-catalyzed MR.

To aid an understanding of the relationship between aryl chloride structure and observed yield in the catalytic reactions, several descriptive values were generated from the set of 20 successfully converted chloroarenes with the help of an online tool.[1] The observed yield of a given substrate was plotted against the value of the descriptor in question. Then, a simple linear regression model was constructed for every descriptor generated (see Figures 4.5 – 4.8 for models with explanatory power). Division of the data into training and evaluation sets was not carried out. The fraction of sp³-hybridized atoms (F_{sp3}), computed lipophilicity (cLogP), atom count polarizability and molecular weight as descriptors possess little to no explanatory power. A measure of π-bond distalness (for an explanation, see Figure 4.4) to the reactive center (ArC-Cl) was introduced as a descriptor (Figure 4.7), which however showed only a weak correlation, similarly to the negative correlation of the observed yield with increasing computed ¹³C-NMR shift at the ArC-Cl position (Figure 4.8). This descriptor is supbar since it is strongly related to the number of Lewis-basic sites in a molecule as well. A stronger negative correlation was found with the number of hydrogen bond acceptors present in the chloroarene (Figure 4.9). This correlation perhaps has the causal background that Lewis basic sites non-productively compete for binding sites on the active Ni center.
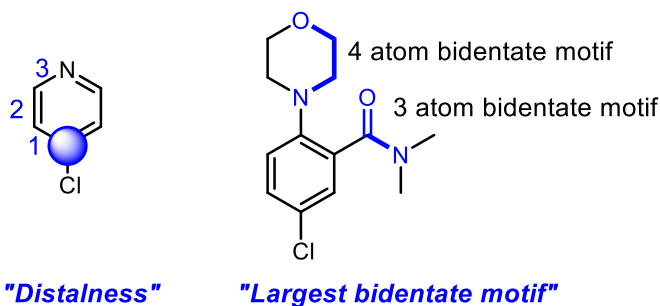
Figure 4.4: Visual explanation of new molecular descriptors for data analysis.

This led to the manual introduction of a descriptor that counts the number of atoms connecting two Lewis basic sites and selects the largest count number below 7, which showed an even stronger negative correlation to the observed yield (Figure 4.10). The reasoning behind this descriptor was to account for the formation of inhibitory metallacycles, which however are less common for metallacycle sizes of 9 and larger (see Figure 4.6).

---

[1] The tool used was ChemAxon. The outliers were removed since competing mechanisms (non-chemoselective oxidative addition in **48** and Michael addition in **58**) were suspected.
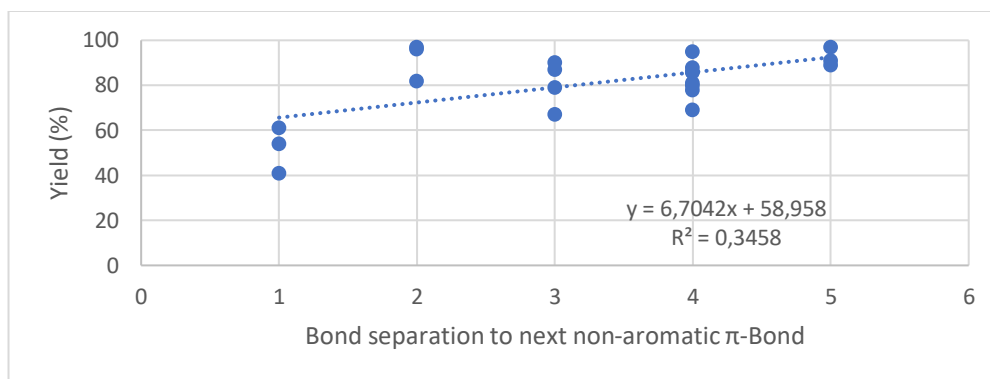
Figure 4.5: Plot of π-Bond distalness of the aryl chloride set against isolated yield and results of a linear regression.
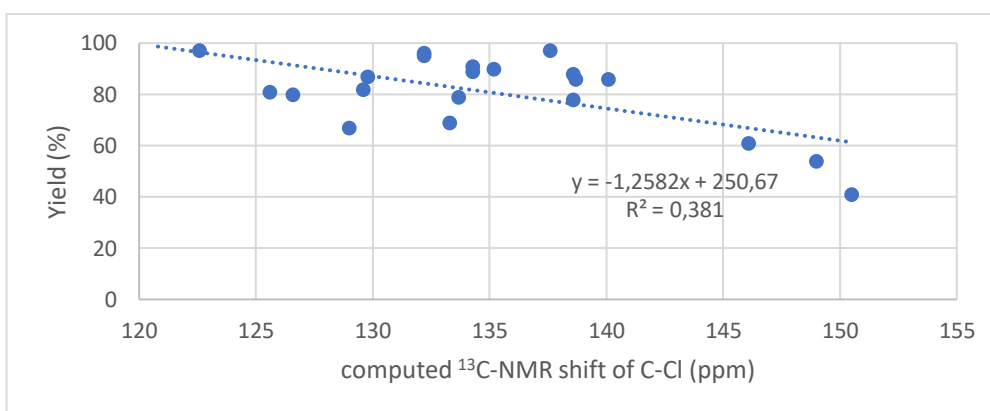
Figure 4.6: Plot of the computed ^{13}C-NMR shift of the aryl chloride set against isolated yield and results of a linear regression.
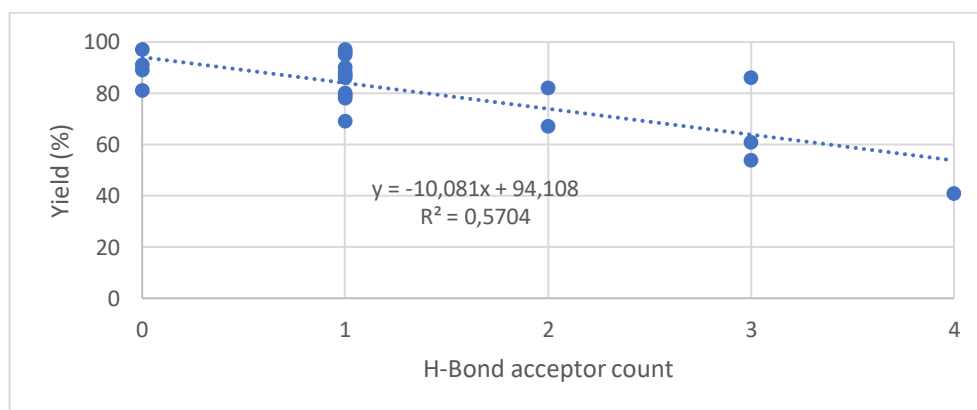
Figure 4.7: Plot of the H-bond acceptor count of the aryl chloride set against isolated yield and results of a linear regression.

The plot shows Yield (%) on the y-axis (ranging from 20 to 100) versus Size of largest bidentate Lewis-basic motif on the x-axis (ranging from 0 to 6). The linear regression equation is:

$$y = -7{,}1522x + 90{,}884$$
$$R^2 = 0{,}6884$$
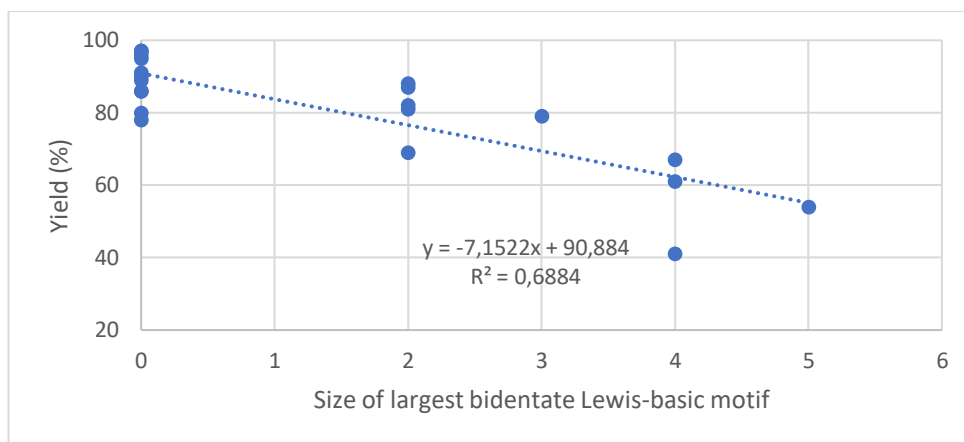
Figure 4.8: Plot of the size of the largest bidentate Lewis basic motif of the aryl chloride set against isolated yield and results of a linear regression.

While these models lack predictive power to account for the failure of several heterocyclic chloroarenes in the Migita reaction (so-called activity cliffs), a clear negative influence of Lewis basic atoms on the overall yield can be seen. The situation seems to be aggravated in the presence of bidentate motifs of an appropriate size. The formation of transient off-cycle species may lead to various irreversible deactivation pathways, which may cause no conversion of the observed extreme examples. One possibility to rationally overcome this problem by catalyst design is to speed up productive reactions and thereby to distribute the total catalyst amount mainly on-cycle. Another possibility would be to employ appropriate solvent mixtures which lead to deaggregation (solvation). It is reasonable to assume that polar co-solvents not only deaggregate zinc thiolate species, but also change the interaction energies between bidentate motifs and the Ni active center. Another approach would be to establish an H-bonding network between the Lewis-basic H-bond acceptors and an H-bond donor cosolvent. In turn, the H-bonding network would have to reorganize before any interaction with the Ni center could take place, which may come with a thermodynamic penalty. This idea is not new and has been brought forward in the context of Pd-catalyzed cross coupling in a review by Fleckenstein and Plenio.[71] Solvents with heteroatom-bound protons (e.g. water, ethanol) are ruled out since they interfere with the catalytic process. A relatively straightforward measure of the ability of a solvent to act as an H-bond donor is the Kamlet-Taft α parameter.[72] Using the preceding criterion, suitable cosolvents for establishing an H-bond network could be chloroform (α = 0.44), methylene chloride (α = 0.30), nitromethane (α = 0.22), acetonitrile (α = 0.19) and acetone (α = 0.08).

4.2.4. Scope of alkylthiols

The scope of alkylthiols was evaluated next. The yields of the reaction of ethyl 4-chlorobenzoate with thiols follow the trend secondary > primary >> tertiary thiol (Scheme 4.14). The reaction of primary and secondary thiols is preparatively useful, whereas the tertiary thiols would require longer reaction times.
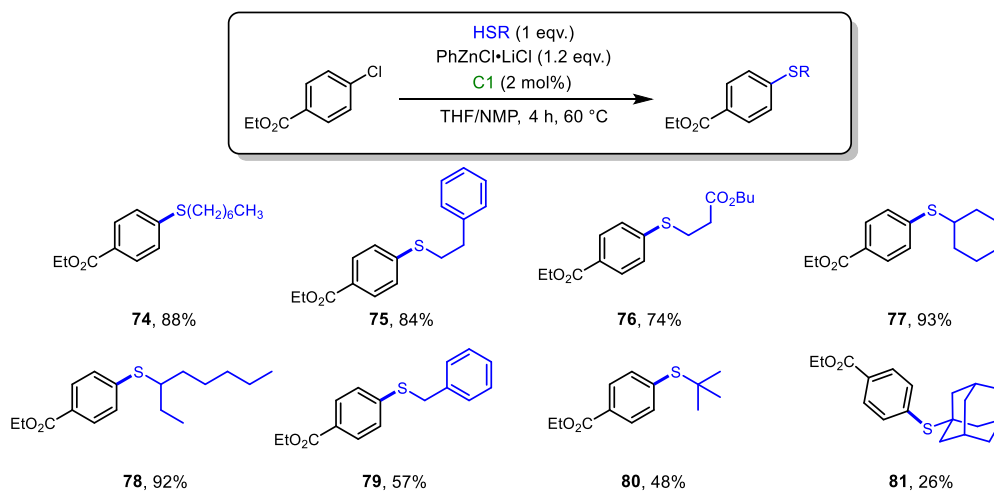
Scheme 4.14: The Ni-catalyzed Migita reaction of ethyl 4-chlorobenzoate with structurally varied alkylthiols. Conditions: Chloroarene (1.0 mmol), thiol (1.0 mmol), PhZnCl·LiCl (1.2 mmol of a titrated solution in THF), dry NMP or THF (400 µL), C1 or C5 (0.5–2.0 mol%), 0.5 to 4.0 h, RT–60 °C.

The reaction of the electronically less activated benzylthiol with ethyl 4-chlorobenzoate provided the product **79** in only moderate yield. It appears that the high nucleophilicity and moderate steric bulk of secondary thiols allow for optimal yields (aryl sulfides **77** and **78**), whereas sterically demanding tertiary thiols give decreased yields of the corresponding products (compounds **80** and **81**). While there is no difference between the performance of acyclic and cyclic secondary thiols (compare yield of **77** to **78**), the performance of cyclic tertiary thiols is significantly worse than that of the acyclic ones (compare yield of **80** to **81**). Mechanistically, structural variation of the thiolate will impact the rates of transmetalation and reductive elimination at the Ni center.

4.2.5. Scope of arylthiols

In line with the observation of diminished yields with electronically deactivated thiols, thiophenols gave no conversion with ethyl 4-chlorobenzoate under robust conditions (2 mol% Ni, NMP cosolvent, 60 °C, 4 h). Since thiophenols have a similar steric profile compared to secondary alkylthiols, this should be an exclusively electronic effect. It was suspected that the problem simply resided in slow transmetalation. As such, magnesium thiolates were evaluated as alternatives. The addition of Grignard reagents as bases however gave complex product mixtures containing symmetric and asymmetric sulfides and biaryls. The situation did not improve when highly hindered aryl Grignard reagents were employed as bases (e.g. MesMgBr). One of the side reactions led to asymmetric biaryls (a desulfenylative Kumada cross-coupling) and was explored seperately (see section 4.2.6.). During screening of Grignard bases, it was found by chance that toluene had a positive influence on the product distribution – more of the targeted asymmetric sulfide was produced with commercial aryl Grignards supplied in toluene independent of the Grignard structure.
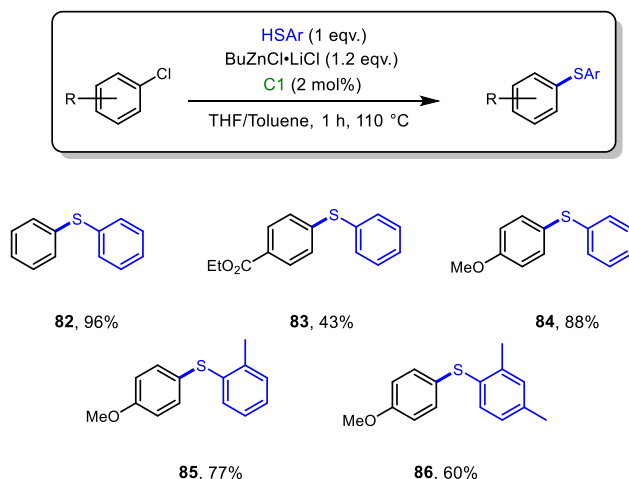
Scheme 4.15: *The Ni-catalyzed Migita reaction of various chloroarenes with structurally varied thiophenols. Conditions: Chloroarene (1.0 mmol), arenethiol (1.0 mmol), BuZnCl·LiCl (1.2 mmol of a THF solution [typically 0.5 M]), **C1** (2 mol%), toluene (usually 2.4 mL, equal to THF volume), 1 h, 110 °C.*

The use of PhZnCl•LiCl (prepared in THF) at 110 °C in toluene for 1 h led to the formation of the desired non-symmetric sulfide, together with formation of the non-symmetric biaryl. The transition-metal free desulfenylative coupling of Knochel-type aryl zinc reagents with thiophenols has been recently described.[73] In this study was observed that no coupling occurred with alkyl zinc bases. Thus, BuZnCl•LiCl (conveniently prepared from ^{n}BuLi and $ZnCl_2$ in THF) was used as a base at 110 °C for 1 h. To our delight, it led to the formation of the desired disulfides (**82 – 86**) with no Negishi-type alkyl-aryl-coupled byproduct (Scheme 4.15).

However, depending on the electronic structure of the coupling partners, symmetric sulfides are still produced, especially with electron-poor coupling partners (e.g. leading to product **83**). Two independent literature reports arrived at the same explanation for this phenomenon.[48]

It is argued that product activation by oxidative addition of intermediate L_nNi^0 occurs in the initially formed non-symmetric diaryl sulfide compounds at both possible sites (Scheme 4.16). Transmetalation of the oxidative addition complex **87a** by transient (e.g. in the beginning stages of the reaction, where a large amount of thiolate is available) excess zinc benzenethiolate (**89**) leads to complex **88a** that will generate the first symmetric sulfide (Ph$_2$S, **82**) upon reductive elimination. At the same time, another thiolate **90** is formed which is then transferable to the other possible oxidative addition complex (**87b**) of the initial product **83**, to give the intermediate **88b**, which after reductive elimination will give the other possible symmetric disulfide **91**, under the presumption that all these processes are in equilibrium.
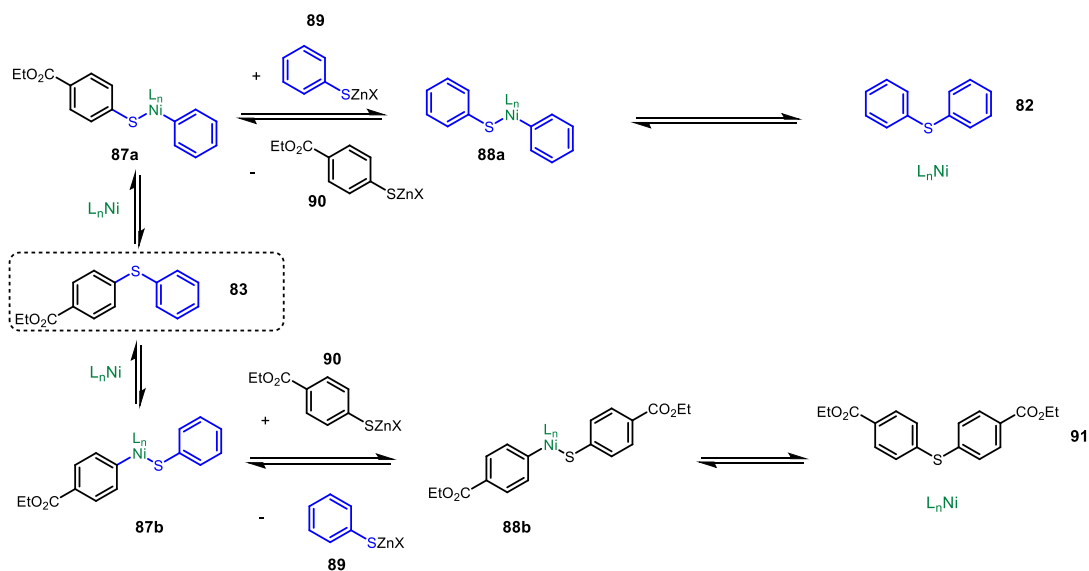
*Scheme 4.16: Mechanistic explanation of thiolate scrambling using the observed behaviour of compound **82** as an example.*

The interplay between relative C-S bond strengths at the different possible insertion sites in **83** in combination with the relative nucleophilicities of the intermediate thiolates **89, 90** and the kinetic effects will determine the final relative composition of all possible products. In the example case presented here, the low nucleophilicity (and relatively better leaving group ability of thiolate **90**) leads to the situation that formation of symmetric Ph$_2$S is favoured over formation of the symmetric sulfide **91**. The relatively bad leaving group ability of of 4-methoxy-thiophenolate coupled with the disfavoured insertion into the electron-rich C-S bond explains the predominant formation of the desired non-symmetric coupling product **84** over the possible symmetric sulfides.

This deleterious behavior was reported in the case for Ni-based catalysts. Interestingly, symmetrical sulfide byproducts were not noted by Stewart and co-workers at Bayer concerning the Migita reaction of chloroarenes with thiophenols.[44, 46] A dedicated study in comparing reaction parameters could reveal additives used in the work by Stewart which inhibit thiolate scrambling. Thiolate scrambling can be driven in one predominant direction by applying Le Chateliers principle. This has been employed by Morandi to effect single bond metathesis to give Migita-type products via Pd-catalyzed reversible arylation.[17] For the aforementioned reasons, this only works selectively when alkanethiols are employed as coupling partners. Symmetrical disulfide formation has also been reported in the Pd/Josiphos-catalyzed Migita reaction by Hartwig.[37b]

4.2.6. Desulfenylative Kumada-type reaction
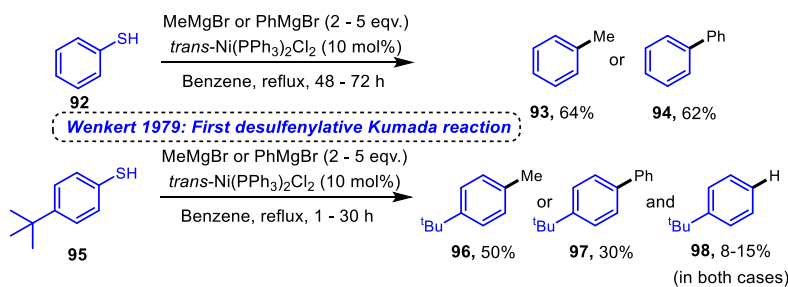
Scheme 4.17: Wenkert performed the first desulfenylative Ni-catalyzed Kumada reaction in 1979.

In 1979, Wenkert described the Ni-catalyzed desulfenylative Kumada coupling (Scheme 4.17) of benzenethiol (**92**) and 4-*tert*-butylbenzenethiol (**95**) with MeMgBr and PhMgBr in refluxing benzene requiring in some cases prolonged reaction times (1 – 72 h, unspecified for the examples shown) to give C-C coupled products (**93**, **94**, **96** and **97**).[74] During the reaction, the generated sulfide anion is stabilized by magnesium (to give MgS), which upon acidic workup releases H$_2$S.
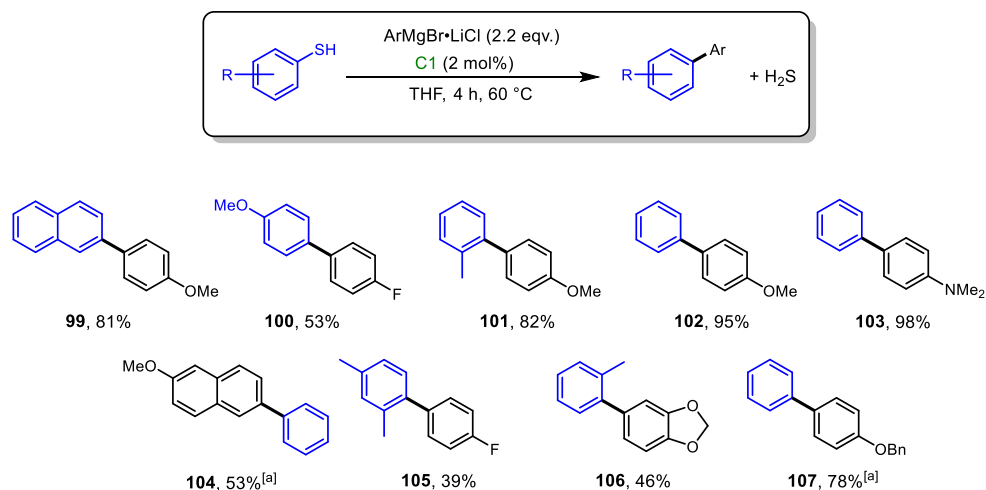
Scheme 4.18: The Ni-catalyzed desulfenylative Kumada reaction of thiophenols with Knochel-type Grignard reagents.^{a}Conditions: Arenethiol (1.0 mmol), ArMgBr·LiCl (2.2 mmol of a THF solution [typically 1 M]), **C1** (2 mol%), THF (0.5–1.0 mL), 4.0 h, 60 °C. ^{a}The product could not be completely purified. In these cases, yields were determined by quantitative NMR methods.

Two equivalents of the Grignard are necessary for an effective conversion based on the kinetically fast deprotonation of the thiophenol component with organometallic bases. During this work, Wenkert's

desulfenylative Kumada reaction catalyzed by **C1** was observed even in the presence of competing chloroarene electrophiles.

In frame of a master thesis, Valentin Geiger confirmed the presence of hydrogen sulfide after acidic workup by precipitation of lead sulfide (by passing the reaction headspace gas over lead acetate). The reaction scope was studied in more depth, which furnished several biaryls (**99** − **107**) after isolation in poor to good yield (Scheme 4.18). The reaction generally works excellent with electron-rich Grignard reagents and electron-poor thiophenols and *vice versa*, which is a common observation in cross-coupling method development.

While the present work using catalytic **C1** displays better parameters (Ni loading, reaction times) than the original report, the question of synthetic utility of this method remains. Thiophenols are non-natural air-sensitive compounds. Compared to air-stable aryl halides, easily prepared by S_EAr methods, benzenethiols seem to be inferior cross-coupling partners.

4.2.7. Tandem Fukuyama-Migita reaction

Based on the best performing substrates for the Fukuyama reaction (primary thioesters) and the Migita reaction (primary thiols) an intramolecular tandem Fukuyama-Migita reaction was investigated using the thioester **108** and a zinc reagent **109** containing the required chloride functionality. The reaction was performed under conditions optimized for the Fukuyama coupling. The overall yield of the thioketone **110** (62%) is moderate.
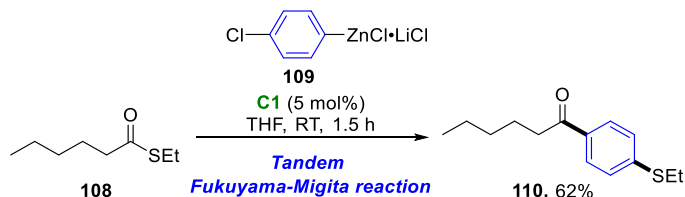
Scheme 4.19: Intramolecular tandem Fukuyama-Migita reaction of thioester **107** with a chloro-functionalized aryl zinc reagent **108** to give the thioketone **109**. Conditions: **107** (0.5 mmol), 4-Cl-C$_6$H$_4$ZnCl·LiCl (3.6 mL of a 0.25 M THF solution), **C1** (2 mol%), THF (0.5 mL), 1.5 h, RT.

Considering the isolated yields of the single reactions, the expected yield should be at least 75%. The possible explanation arises from closer look at possible catalytic species. Ni^I intermediates were postulated for the Ni-catalyzed Fukuyama reaction (Chapter 3). However, Ni^I precatalysts have shown an inhibitory effect in Ni-catalyzed Suzuki-Miyaura couplings[75] or Buchwald-Hartwig aminations[76] involving Ni$^{0/II}$ redox cycles. The same situation could apply to the present system. In conclusion, a deeper mechanistic understanding may be required to achieve an efficient tandem process.

However, the potential rewards are opportunities in biological and medicinal chemistry as well as the streamlining of synthetic sequences. This will be briefly elaborated below.

Linker chemistry in biological chemistry heavily relies on the ease and modularity of amide bond formation *via* the assistance of active ester methods. While the amide bond is usually regarded as relatively inert to chemical cleavage by laboratory methods, the half-life of these molecules in biological systems can be reduced by action of amidases. This behavior can be a problem in bioconjugate chemistry and the design of biologically active chimeric molecules for targeted protein degradation. One well-known example is the action of biotinidase upon amide-bond connected conjugates of biotin. Strategies to combat this have usually employed introduction of steric bulk around the amide bond, e.g. by amide bond formation with valine derivatives or other bulky amino acids.[77] Since the intramolecular F-MR reaction results in the formal insertion of a phenylene spacer into the C-S bond of the thioester, the resulting keto-thioethers should exhibit improved metabolic stability compared to the starting material. Therefore,

a reaction sequence to design metabolically stable linkers ready for further reaction is presented using biotin as an example (Scheme 4.20, top). A similar idea has been executed by Weix,[78] however in their case, the thiolate moiety was not incorporated into the final product (a TIPS-alkyne-terminated keto-biotin).
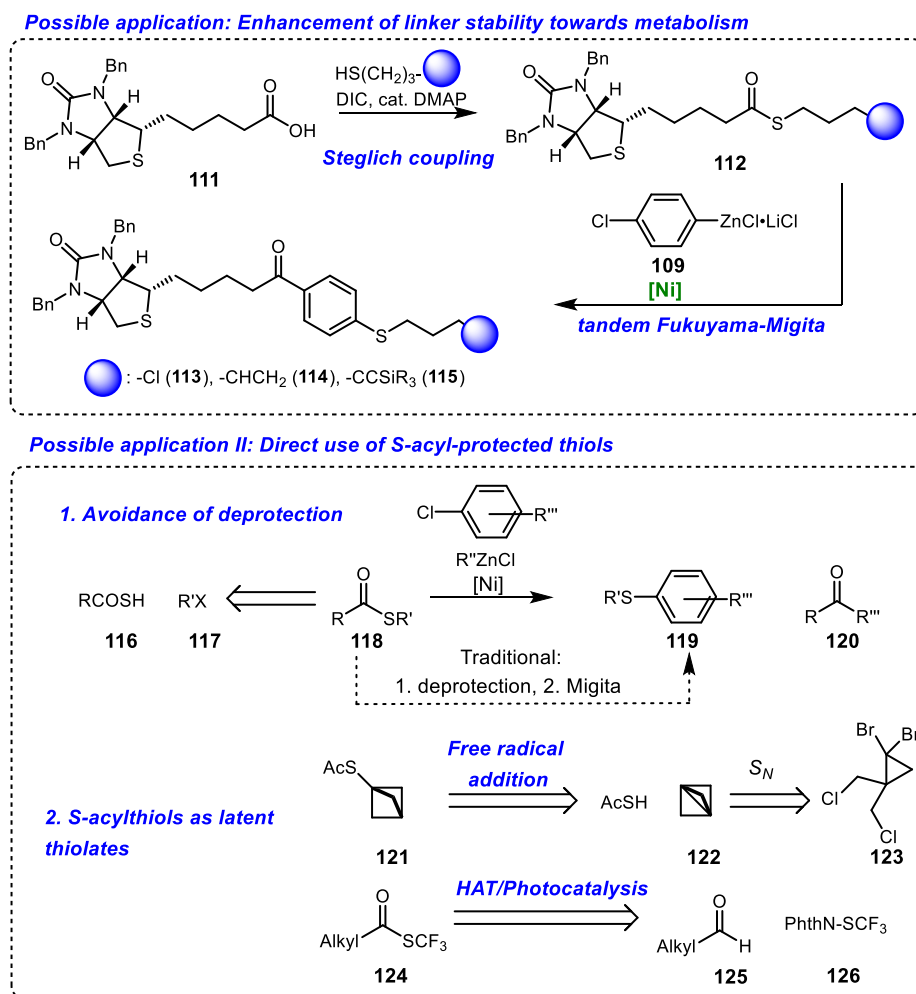
Scheme 4.20: Possible applications of the tandem Fukuyama-Migita reaction (F-MR). Top: The intramolecular F-MR results in the insertion of a phenyl spacer into a thioester C-S bond. The resulting keto-thioethers could be a replacement for metabolically labile amide bonds in bioconjugation chemistry. Bottom: The intermolecular F-MR would allow direct use of S-acyl thiols as air-stable thiol surrogates. Secondly, it would enable the facile transfer of unstable or high-value thiolates for medicinal chemistry programs.

Since the F-MR reaction conditions will not be tolerant towards protic functionality, the biotin recognition element needs to be protected as the N,N-dibenzylated version (111). For the same reasons, the other coupling partner of the linker element needs to be attached after the F-MR, which requires the introduction of a further aprotic functional group (either chloro-substituted, or a terminal alkene/alkyne)

at the thiol. Then, the thioester of the type **112** would be formed by a reliable Steglich coupling reaction, followed by phenylene insertion by the F-MR to give **113 - 115**. *N*-Deprotection, followed by a Finkelstein reaction of **113** using NaI in acetone would give a highly reactive electrophile for bioconjugation. Similarly, the alkene **114** could be used in cross-metathesis, although applications of this reaction in aqueous systems remain rare.[79] Most importantly, desilylation and *N*-debenzylation of **115** would give a building block ready for click chemistry which is known to be generally compatible in biological, aqueous systems. The longest sequence possible consists of five synthetic steps until the ready-to-use biotin derivative would be available. Synthesis of such building blocks furthermore allow for further functionalization at the keto group (e.g. hydrazone formation) or at the sulfur atom (oxidation).

Secondly, the F-MR would allow a step count reduction if thiols were to be synthesized via their S-acyl protected form (Scheme 4.20, bottom). This approach is commonplace for the preparation of functional thiols from the corresponding functional alkyl halides. In this case, reaction of a thioacyl acid **116** with the appropriate functional electrophile **117** yields *S*-acylthiols **118**, which require separate deprotection before they can be employed in a Migita reaction. The F-MR would make this deprotection step unnecessary. However, a ketone **120** is produced as stoichiometric waste. Thus, any development in this area should aim at the production of volatile waste to aid purification of the Migita product. The optimal waste product would therefore be acetone, which would require however the development of an efficient Ni-catalyzed Fukuyama reaction with alkylzinc reagents. Such a reaction is currently not possible with the Ni-catalyzed approach.

In other circumstances, the usage of S-acyl protected thiols for the Migita reaction could circumvent tedious technical or synthetic issues. For example, trifluoromethanethiol is a toxic, unstable gas. Due to its unique high lipophilicity coupled with a strong electron-withdrawing ability, it is a sought-after motif in pharmaceutical and agrochemical research.[80] While various electrophilic and nucleophilic SCF$_3$ transfer reagents exist, these differ in stability and synthetic tractability. The Glorius group has reported the photocatalytic synthesis of air- and chromatography-stable *S*-trifluoromethanethioesters (**124**),[81] which could be used as SCF$_3$ transfer reagents in the F-MR.

Another example would be the use of bicyclo[1.1.1]pentane-1-thiol (BCP-1-thiol) in Migita reactions. Based on recent successes in medicinal chemistry with bioisosteric switches using strained bicycloalkyls,[82] BCP-1-thiol would represent a new bioisostere of thiophenol with similar steric, but not electronic properties. Besides various changes in physicochemical properties, the main difference would be the removal of π-interactions with other compounds while keeping the spatial properties of

thiophenol. Undoubtedly, such bioisosteres are useful tools for drug discovery. The phenyl-to-BCP switch has been reported by various medicinal chemistry research groups, including teams from the pharmaceutical industry.[83] However, the synthesis of such exotic and strained compounds is often tedious. For example, the phenyl-to-cubane bioisosteric switch is even better in the sense that the steric properties of phenyl ring are more closely replicated,[84] but the synthesis of such building blocks is cumbersome, which is reflected in the pricing of functionalized cubanes. Fortunately, the BCP motif is readily available from [1.1.1]propellane (**122**) by various reactions with the main thermodynamic driving force being the alleviation of ring strain. Bräse and co-workers investigated the known, but not thoroughly investigated reaction of [1.1.1]propellane with various thiols.[85] The group was able to confirm the previously suspected free-radical addition mechanism by labeling experiments. A fast click-type reaction (Et$_2$O as solvent, 15 min, RT) was found with generally good yields for various thiols. Although attempted, BCP-1-thiol could not be easily accessed from **122** by reaction with hydrogen sulfide (a symmetric BCP-sulfide was formed) or benzylthiol (the deprotection led to decomposition). Based on S-H bond dissociation energy considerations,[86] the reaction of **122** with thioacetic acid should be feasible. The produced building block **121** could then be utilized in a F-MR sequence to produce aryl BCP sulfides, an unexplored substance class.
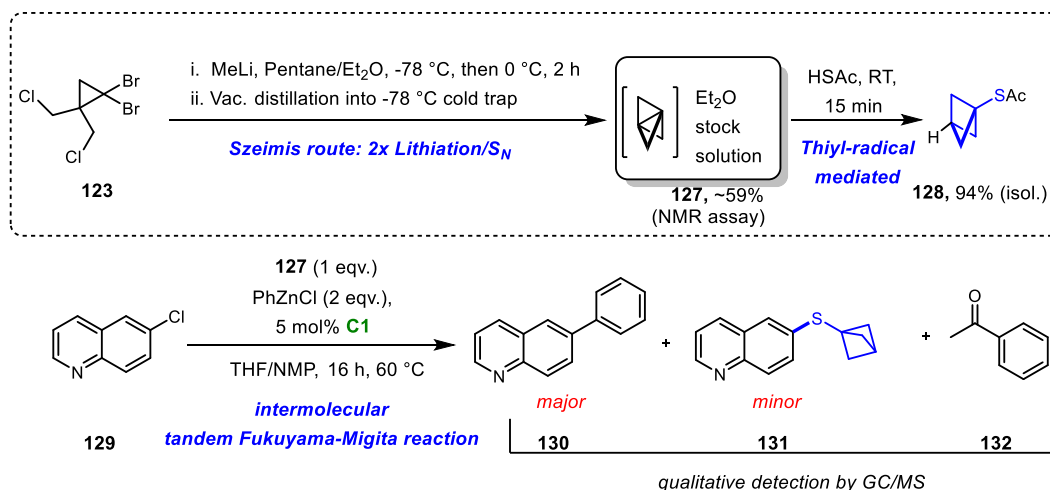
Scheme 4.21: Synthesis of S-acetyl-BCP-1-thiol () from a commercially available precursor in two steps and subsequent use in an intermolecular tandem Fukuyama-Migita reaction.

In a brief investigation, it was found that the formation of *S*-acetyl-BCP-1-thiol (**128**) indeed succeeded in two steps from the commercially available building block **123** *via* the propellane intermediate.[87] The reactivity of **128** was then tested in the F-MR reaction of chloroquinoline **129**. The expected m/z pattern of **131** was confirmed by qualitative GC/MS analysis. This minor peak in the chromatogram was however

accompanied by the major peak corresponding to the Negishi product **130**. The sluggish reactivity of tertiary thiols in the found MR explains why leftover PhZnCl (the excess found to be necessary to give efficient Fukuyama couplings, see Chapter 3) preferably reacted with **129**.

While this is a promising result, the F-MR clearly deserves further attention to achieve selectivities that would warrant isolation of the aryl sulfide products. Based on the premise that the Negishi reaction of alkylzincs would be disfavoured over the coupling with arylzincs (as seen in section 4.2.6.), further improvements will most likely hinge again on the development of an efficient Ni-catalyzed Fukuyama reaction with alkylzinc reagents.

4.2.8. Mechanistic scenarios

The obtained results suggest that a classical group 10 metal cross-coupling mechanism consisting of oxidative addition, transmetalation and reductive elimination is operative (Scheme 4.22, right-hand cycle). Additional details on the various elementary steps are provided below.
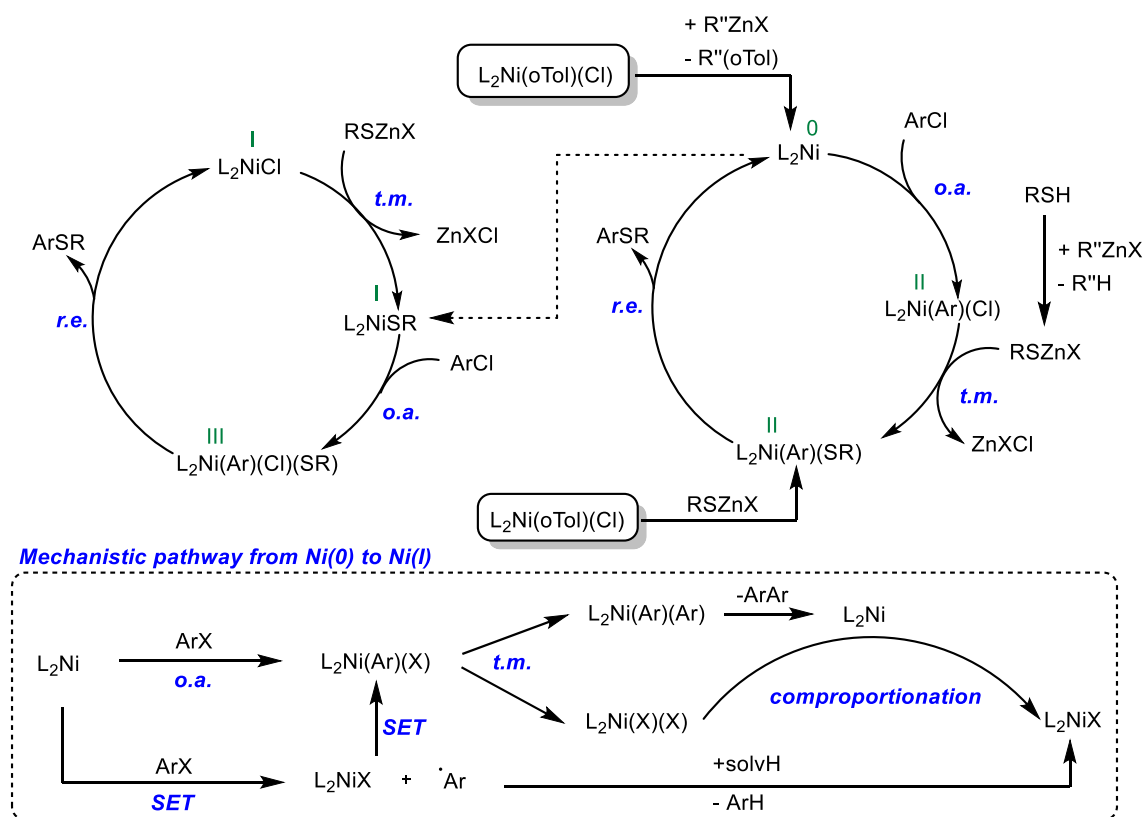
Scheme 4.22: Proposed possible mechanisms of the Ni-catalyzed Migita reaction involving 2 valence electron redox cycles. Ni(I) species can be obtained from Ni(0) by comproportionation or solvent-interrupted stepwise oxidative addition. O.a.: Oxidative addition; r.e.: reductive elimination; SET: single electron transfer; t.m.: transmetalation.

Oxidative addition of Ni(0) into aryl halides can occur via three distinct mechanisms: 1. Concerted three-centre-, 2. Stepwise S_NAr-type-, 3. Stepwise double SET-oxidative addition (Kochi-type). For the reaction of Ni(cod)(dppf) with ArBr, the first possibility was found to be the most likely from kinetic studies by Nelson and Sproules.[88] The exact mechanism may however be strongly ligand-dependent and is unknown for the present system.

The zinc thiolate is generated by organometallic deprotonation. In contrast to other heteroatom cross-coupling reactions, this is not an equilibrium reaction, which results in a high concentration of the reactive zinc thiolate and an alkane or arene as the organic byproduct. In other heteroatom cross-couplings using

equilibrium bases, such as in the Pd-catalyzed Buchwald-Hartwig amination, a pre-equilibrium step is invoked consisting of a coordination of the nucleophile to the Pd center before deprotonation takes place, which then leads to transmetalation.[89] In other cases, bases were postulated to coordinate to the active site first, which then deprotonates the nucleophile. For group 10 metals, such a mechanism would require a third vacant coordination site, which can be easily achieved for sterically bulky monodentate phosphines in Pd catalysis. In Ni-catalysis using bidentate ligands, this behavior however would imply ligand hemilability to provide a vacant coordination site.

To answer the question whether Ni(xant)(oTol)Cl requires base for transmetalation, a toluene-d_8 solution of the complex in air was treated with an excess of base-free HeptSH, followed by the acquisition of ^{31}P-NMR spectra. The mixture darkened over the course of several hours, while the ^{31}P-NMR signals characteristic of **C1** disappeared and the signals corresponding to free xantphos enhanced. The organic phase contained HeptS(oTol) as the major organic product (besides excess HeptSH). This proves that **C1** is a competent intermediate for transmetalation with alkanethiols even under aerobic, neutral conditions in a relatively non-polar solvent, with subsequent fast reductive elimination (the combined process was finished within a few hours) at room temperature. This reaction provided the cross-coupled aryl sulfide and a Ni(0) species, which rapidly decomposed in air to give unidentified Ni products and free xantphos (**C1** does not decompose in a THF solution under air overnight, nor in the presence of TEMPO as a single-electron oxidant). This implies that transmetalation of simple alkanethiolates should be even faster due to the increased nucleophilicity of the anionic form. Secondly, it shows that the precatalyst should not be stirred too long in the presence of thiols before the start of the reaction. Notably, this opens up opportunities in stoichiometric Ni-mediated bioconjugation chemistry of Cysteine residues in peptides or proteins, similar to the system reported by Buchwald.[90]

The organozinc reactant can activate the precatalyst by a transmetalation/reductive elimination sequence to give Ph(oTol) and a zerovalent Ni species. Alternatively, the zinc thiolate may transmetalate at the precatalyst species to generate RS(oTol) and the same Ni species. Both activation byproducts were detected qualitatively by a GC/MS assay of a standard reaction with PhCl, HeptSH as the nucleophile and PhZnCl•LiCl as the base.

It remains puzzling why preformed zinc thiolates perform significantly worse in catalysis compared to their *in situ* formation by an excess of reductant (20 mol%). A variety of Ni-catalyzed Migita reactions operate in the presence of added reductant. An exciting, if less likely, possibility would be catalysis by anionic nickelate complexes (giving a redox cycle involving 0/II oxidation states at formally anionic Ni).

Anionic transition states have been invoked in Pd-catalyzed cross coupling reactions.[91] The existence of nickelates is implied from computational studies by Wang and Uchiyama in the Kumada reaction of aryl methyl ethers.[92] Oxidative addition would give a Ni(II) biaryl complex, which would require transmetalation by the zinc thiolate to explain aryl sulfide formation. However, this mechanism would lead to scrambled aryl sulfide products if the transmetalation is not controlled adequately by electronic factors. Since such scrambled products were not observed, an anionic mechanism is currently ruled out. Finally, the possibility of Ni(I) species as active catalysts should be considered (Scheme 4.22, left-hand cycle), where the order of elementary steps is shuffled. Ni(I) species can be generated from Ni(II) oxidative addition complexes by ligand scrambling/comproportionation[93] or from Ni(0) species by solvent-interrupted stepwise oxidative addition as suggested by Kochi (Scheme 4.22., bottom).[94] The composition ratio of organic byproducts (ArH or ArAr) may be a hint towards which mechanism is operative. Hydrodehalogenated compounds or symmetric biaryls resulting from aryl chlorides were not isolated during the scope evaluation. The catalytic competency of Ni(I) species could be evaluated in the future by testing Ni(xantphos)(Cl) or Ni(dpephos)(Cl) as precatalysts, which however would require the synthesis of these previously unreported, air-sensitive compounds. Stolley has accessed Ni(xantphos)Br from comproportionation of Ni(xantphos)Br$_2$ with Ni(cod)$_2$ in THF.[95]

The question of homo- vs. heterotopicity of the catalytic system was also briefly investigated. No visible bulk particles or metal mirror were formed during the reaction or after aqueous workup. A strong ligand effect was observed, with many other phosphine-based precatalysts being completely inactive. Preformed NiB nanoparticles were also catalytically incompetent. A lag phase during time-point kinetic measurements, which is typical for heterogeneous catalysis, was not observed. Furthermore, time-point kinetic studies with added DCT (result: inhibition) or Hg (result: no inhibition) gave clear-cut results. With the possible interpretative pitfalls of these latter experiments in mind, the combined evidence strongly points towards an exclusively molecular mechanism of catalysis. These results however do not rule out the existence of catalytically inactive Ni thiolate clusters, nanoparticles or sparsely visible bulk particles.

Thiols are often implicated as poisons for transition metals. Therefore, a short discussion of possible off-cycle species is necessary (Scheme 4.23). Alvaro and Hartwig conducted a detailed mechanistic study concerning off-cycle species in the Pd-catalyzed Migita reaction.[96] The team identified Pd dithiolates and hydrido palladium thiolates as key off-cycle species. Whether the same situation exists for the present catalytic system is unknown so far. The existence of hydrido nickel thiolates is a possibility. However, two extremes of coordination are possible, and in the case of a side-on sigma complex formation, the Ni center

simply acts as an acidifying agent to ease deprotonation of the thiol. Since deprotonation by the organometallic base is a non-equilibrium reaction, the existence of these hydrido Nickel thiolate off-cycle species is less of a concern.

The existence of $L_2Ni(SR)_2$ complexes could, upon ligand loss lead to the formation of soluble Nickel thiolate clusters up to the formation of insoluble polymeric forms. This presents a problem since these complexes can be remarkably stable and may be a thermodynamic sink, which slowly, but irreversibly reduces the concentration of on-cycle catalyst. Highly lipophilic impurities were noted during chromatography (no retention on normal-phase SiO_2 upon elution with hexane) of Migita reactions with primary and secondary alkanethiols. The discoloration was not observed with tertiary alkanethiols or thiophenols. It is likely that cyclic hexameric clusters of the type $Ni_6(SR)_{12}$ or higher order versions of these form as deactivation products. For example, cyclic $Ni_6(SEt)_{12}$ is described as an air-stable black diamagnetic compound which is soluble (wine-red solution) in aromatic solvents, dichloromethane but not in acetone, MeCN, DMSO and water.[97] Cyclic $Ni_6(SCH_2CH_2Ph)_{12}$ exhibits similar properties.[98] Nickel thiolate clusters containing secondary and tertiary thiolates have also been isolated, but their degree of air-sensitivity was not reported.[99] The similarities to the observed impurities in chromatography are striking and deserve further study. The first experiment in this direction could be to test if a defined, hexameric Ni cluster is able to catalyze the Migita reaction in the presence of xantphos, i.e. if cluster formation is reversible under catalytically relevant conditions.

Such clusters are simply prepared from alcoholic solutions of $NiCl_2$ in air by reaction with metal thiolates, although the formation of pure $Ni_6(SEt)_{12}$ without the excessive formation of insoluble polymers required reaction with $(EtS)_2SnMe_2$.[100] Considering this, it becomes clear why $L_2Ni(oTol)(Cl)$ precatalysts may be superior to L_2NiCl_2 precatalysts in the presence of metal thiolates. Secondly, the requirement for purified thiols is explained.

The reinsertion of L_2Ni^0 into the C_{sp2}-S bond of sulfide products was proven by the observation of thiolate scrambling when thiophenols underwent Migita coupling (see Section 4.2.5.). The scrambling did not occur when alkanethiols underwent coupling which proves that C_{sp3}-S bonds of sulfide products are not activated. The inhibition by Lewis basic sites most likely affects the zerovalent state of Ni. The transient off-cycle complexes may be involved in irreversible deactivation pathways (e.g. ligand exchange or cyclometalation). A countering strategy by establishing an H-bonding network was discussed in section 4.2.2.
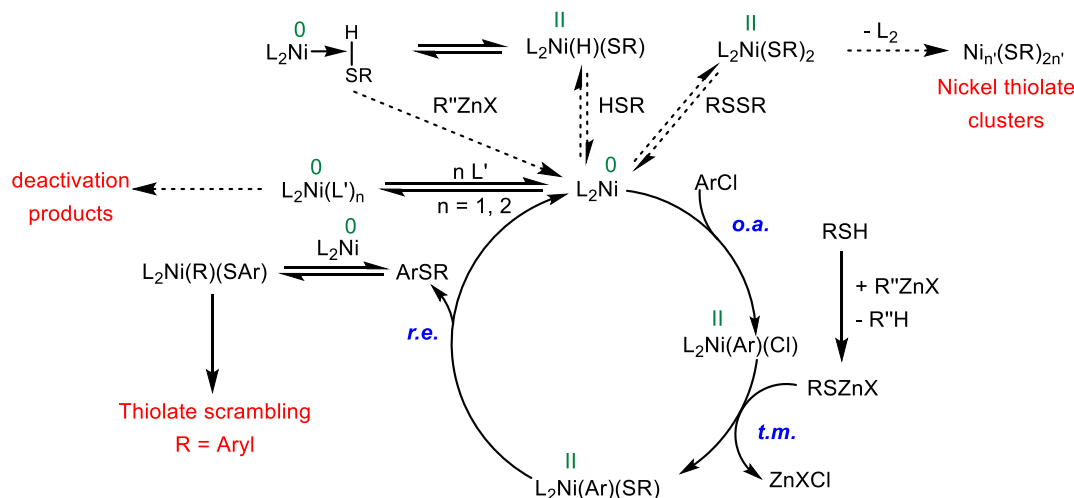
Scheme 4.23: Possible off-cycle species and deactivation modes for the Ni-catalyzed Migita reaction. Dashed lines represent non-proven, but likely reactions. o.a.: oxidative addition; t.m.: transmetalation; r.e.: reductive elimination. L_2: Xantphos or DPEPhos.

In conclusion, two plausible off-cycle species were identified that could lead to irreversible catalyst deactivation. While non-productive coordination may be inhibited by solvent choice and Ni dithiolate formation by controlling reagent purity, the most likely successful strategy will be to make the productive cycle faster by ligand design. This requires identification of the rate-determining (r.d.) step. Compared to catalysis by Pd, oxidative addition is favoured with Ni complexes. The rate of transmetalation in Pd^{II} complexes follows the trend Cl > Br > I for the leaving group, indicating that polarization of the metal centre is a major determinant for successful transmetalation.[93] Thus, the first two steps should be favoured in the present system, but it is not known whether reductive elimination is rate-determining. However, the exceptional activity of wide-bite angle ligands in the discovered system hints at reductive elimination as the r.d.-step. Wide-bite angle ligands enhance reductive elimination by a stereoelectronic (as can be seen from a qualitative Walsh diagram[101]) as well as a steric effect (relief of intra- or interligand steric strain by reducing the coordination number).[102]

One strategy, which has been elegantly shown to work for Ni-catalyzed Buchwald-Hartwig-aminations[103] and -etherifications[104] by the group of Stradiotto, is to reduce electron density on the ligand phosphorus atoms, which would speed up transmetalation (to compensate a negative partial charge at Nickel in the transition state), as well as reductive elimination (to compensate for the extra electron pair after reduction of Nickel). Stradiotto introduced further steric bulk by ligand design to favour reductive elimination (low coordination reduces steric strain). At the same time, steric bulk disfavours

transmetalation (increase of steric strain in the transition state). The combination of a relatively bulky, electron-poor organophosphine was found in the 1,3,5,7-tetramethyl-2,4,8-trioxa-6-phosphaadamantane fragment (CgP). The Stradiotto group then designed bidentate ligands containing the CgP fragment in combination with a "normal" phosphine arm to not overload on steric bulk. To transfer this concept to the xantphos-type ligands, synthetic tractability needs to be evaluated as well (Scheme 4.24). Thus, first one electron-rich and one electron-poor symmetric xantphos-type ligand should be evaluated, possibly the Furyl-Xantphos (**135**) as well as the *para*-Anisyl-Xantphos (**136**)[105] by the double Directed-o*rtho*-metalation (DoM) route typical for the synthesis of Xantphos ligands.
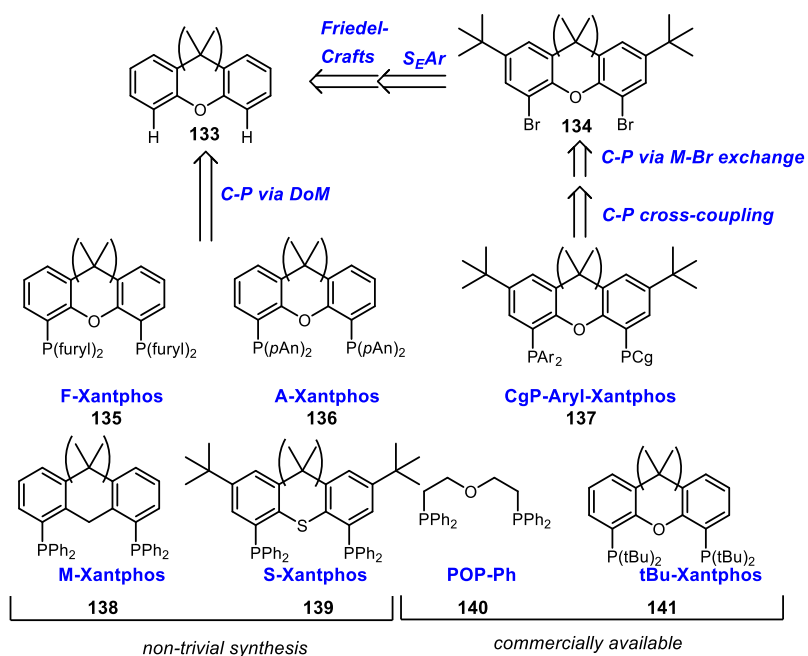
Scheme 4.24: Proposed ligand structures to be synthesized to facilitate mechanistic understanding of the Migita reaction. The construction of non-symmetric Xantphos-type ligands will require considerable synthetic effort, as shown by a simple retrosynthetic analysis (top). Other ligands are commercially available or require high synthetic effort.

Both chlorodiorganophosphines should be readily available from reaction of the corresponding Grignards with PCl$_3$. The synthesis of electronically and sterically differentiated Xantphos-type ligands appears more complicated (**137**). The double DoM route should be replaced by sequential metal-halogen exchange. To avoid double DoM to introduce the necessary halogens, a S$_E$Ar reaction is required, which however requires the blockage of the activated *para*-oxy position. After bromination (**134**), and the first metal halogen exchange followed by chlorophosphine quench, the CgP fragment could be introduced by cross-coupling. Another question that could be answered by ligand synthesis is the importance of flexibility and alternative coordination modes. Thus the synthesis or acquisition of M-Xantphos (**138**)[106],

S-Xantphos (**139**)[107], POP-Ph (**140**, commercially available) and tBu-Xantphos (**141**, commercially available) as well as the DPEPhos-type analogues, is proposed. To reduce the workload for screening the corresponding $L_2Ni(oTol)(Cl)$ complexes, *in situ* ligand exchange of *trans*-$(Ph_3P)_2Ni(oTol)(Cl)$ or $(tmeda)Ni(oTol)(Cl)$[108] is proposed instead of the dedicated synthesis of the corresponding complexes *via* the Jamison route.[68] While $Ni(cod)_2$ is the most obvious pre-catalyst for screening in a glovebox, the presence of cod could inhibit catalysis.

To gain further mechanistic insight, a series of DFT calculations were carried out, assuming a $Ni^{0/II}$ redox cycle with concerted oxidative addition and reductive elimination steps. The calculation was carried out at the B3LYP/6-31G* level of theory since it is common in the literature, offers a good mixture of speed and accuracy and allows modeling of first row transition metals. It is acknowledged at this point that more accurate methods exist, but the application and comparison of such methods is outside the scope of this experimentally focused work.

A thermodynamic cycle was established by modeling PhCl, PhSMe, $ZnCl_2$ and MeSZnCl and calculating the respective thermodynamic energies (after vibrational analysis). The presented results hold true to a reaction in the gas phase, and dispersion interactions are not accounted for (for further details, see the experimental part). The overall free Gibbs energy under standard conditions for the reaction of chlorobenzene with zinc chloride methanethiolate amounts to ΔG^0_{total} = -47.90 kJ mol^{-1}, meaning the reaction should occur spontaneously at room temperature, which is in line with the experimental result in liquid phase.

Next, the above cycle was broken down by adding intermediates corresponding to the oxidative addition complex, the transmetalated complex and finally, the zerovalent complex Ni(xant). In the same manner, the overall energies were calculated using the previous results. Oxidative addition was calculated to be exergonic (ΔG^0_{OA} = -192.89 kJ mol^{-1}), whereas transmetalation (ΔG^0_{TM} = +51.82 kJ mol^{-1}) and reductive elimination (ΔG^0_{RE}= +93.16 kJ mol^{-1}) were calculated to be endergonic. Consequently, the oxidative addition complex **143** should be the resting state of the catalytic cycle (the catalytic intermediate with the highest concentration during the reaction), which should be verified experimentally. One problem with this type of energy calculation, while thermodynamically correct, is that it may not reproduce the actual intermediates crossed by the reaction on the potential energy surface. In the gas phase, chlorobenzene and phenyl methyl sulfide may coordinate to the zerovalent Ni(xant) (14 ve) and exert a stabilizing effect to give a post- and pre-reaction complex (post- and pre-RC, **145** and **142** both 16 ve) lower in energy. Therefore, the geometries and energies of the post- and pre-RC were calculated by the same method. The

overall results are presented below (Figure 4.9.). They are similar to the calculation, which excluded pre- and post-reaction complexes. The transition state for transmetalation could not be located readily and appears to be rarely modeled in the literature.
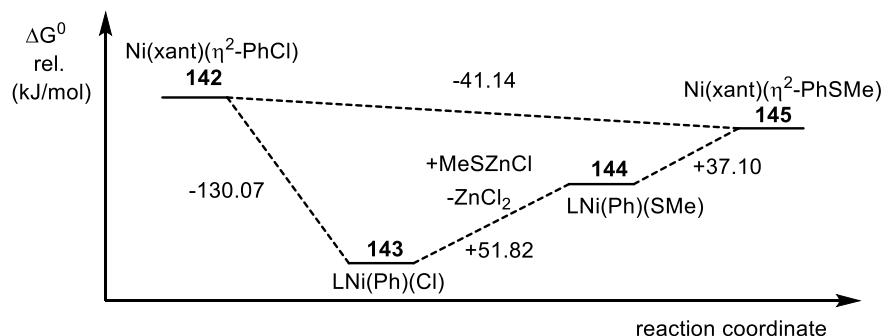

Figure 4.9: Energy profile (qualitative, axes not to scale) of the Migita reaction of chlorobenzene with zinc methylthiolate catalyzed by Ni(xant) in the gas phase at the B3LYP/6-31G* level of theory.

While the overall reaction thermochemistry is favorable, there are low-energy intermediates, which means that the following reactions are endergonic. Addition of an excess amount of thiolate may be helpful to shift the equilibrium of the reaction from **143** to **144**. While this is intuitively clear for the Ni-arylthiolate **144** (due to the strong thiophilic interaction), the low energy of the oxidative addition complex **143** is surprising, but perhaps reflects the instability of Ni(0) complexes in general. However, these results are in line with calculations of Shaik who modeled the Pd-catalyzed reaction of chlorobenzene with HS$^-$ at the same level of theory, also in the gas phase, which gave the same overall qualitative result.[109] The Schönebeck group arrived at a slightly endergonic thermochemistry result of the oxidative addition of Ni(dppf) into chlorobenzene, however their model accounted for solvation and dispersion effects.[43] The Stradiotto group also calculated the oxidative addition of a bidentate phosphine (or dppf) Ni(0) complex into PhCl, and arrived at the result that oxidative addition is exergonic (-109.20 kJ/mol for the former and -88.33 kJ/mol for the latter) in the gas phase with corrections for dispersion interactions.[76] The results presented here are interesting starting points for further calculations which include such important effects.

4.3. Conclusion

In conclusion, a general Ni-catalyzed Migita reaction of chloro(hetero)arenes with *in situ* formed zinc or magnesium thiolates by employing organometallic bases was developed. Unfunctionalized reaction partners show high turnover frequencies with alkylthiols (15 min reaction time, TOF_{max} = 800 h^{-1}) even at low catalyst loading (0.5 mol%) at room temperature in THF. Functionalized electrophilic and Lewis basic coupling partners as well as heterocycles relevant to pharmaceutical chemistry were reacted with alkylthiols to the aryl sulfides under slightly more demanding, but still moderate conditions (2 mol% catalyst, 60 °C, 4 h, THF/NMP solvent mixture).

Arylthiols reacted sluggishly and required harsh thermal conditions (2 mol% catalyst, 110 °C, 1 h, THF/Toluene solvent mixture) for turnover. Even in the presence of chloroarenes, thiophenols undergo a desulfenylative Kumada coupling when a Grignard reagent was chosen as the basic component. A small scope evaluation was carried out for the first time, and the typical electronic trends influencing cross-coupling were found to be operative. The developed system (2 mol% catalyst, 4 h, 60 °C, THF) is generally superior to the singular example reported earlier.[74] Although unsolved problems remain, the tandem Fukuyama-Migita reaction offers a promising route to access either the keto-thioether substance class in an atom-economic fashion or make use of air-stable *S*-acylthiols as latent thiolates for the transfer of high-value building blocks.

A possible mechanism was presented together with preliminary mechanistic investigations (catalyst topicity and precatalyst activation). The available evidence points towards a classical C-heteroatom group 10 metal cross-coupling cycle being active with a clear molecular mode of catalysis. Possible deactivation pathways were discussed. Based on the hypothesis that reductive elimination is the rate-determining step, several close analogues to xantphos were suggested for synthesis and screening in the Ni-catalyzed Migita reaction to interrogate the mechanism and generate more robust catalysts.

The use of stoichiometric organometallic bases to effect cross-coupling presents a cost disadvantage on scale. The use of substoichiometric reducing agents in the presence of stoichiometric inorganic bases is certainly another avenue for future investigations. On the other hand, the reaction takes place in a single phase (as opposed to cross-couplings with insoluble inorganic bases), which positions this system as inherently suitable for scale-down (i.e. high-throughput experimentation) or for liquid-liquid flow reactor setups.

4.4. Experimental part

4.4.1. General information

All reactions with organometallic species and catalytic Ni were carried out under Ar or N_2 atmosphere using dry glassware with the usual air-free techniques, unless noted otherwise. Dry THF was obtained either: by use of Sigma-Aldrich or Acros anhydrous grade THF in septum capped-bottles; storage of freshly distilled THF over microwave-activated 3 Å MS (20 w/v%, 3 days) in an Ar-flushed container with no large difference in performance. PhMgBr solution in THF, iPrMgCl•LiCl solution in THF and N-Methylpyrrolidone (SureSeal) and **C4** were obtained from Sigma-Aldrich. **C1**, **C2**, **C3** and **C5** were prepared according to published procedures[S1] (additionally, a visual guide on the preparation of **C1** is available from our group[S2] and the procedure can be carried out analogously for the preparation other precatalysts). 8-Chlorocaffeine was prepared from 8-chlorotheophylline by a literature procedure.[S3] 6-chloro-9-tosyl-9H-purine was prepared from 6-chloro-9H-purine by a literature procedure.[S4] LiCl, Magnesium turnings and $NiCl_2(H_2O)_6$ (p.A. grade) were supplied by the central chemical storage, University of Tübingen. $ZnCl_2$ was supplied by either Sigma-Aldrich (anhydrous, >99.999% trace metals basis, stored in Schlenk tube or reagent grade, stored in a screw-capped plastic bottle), TCI or Merck (Ph. Eur. Reagent grade) with no differences in activity; technical grade $ZnCl_2$ proved to be unsuitable for the preparation of aryl zinc halide solutions. Other chemicals were purchased from ABCR, Acros, Sigma-Aldrich, TCI, ChemPUR or Merck. Thiols were either distilled under inert atmosphere/vacuum and stored at -10 °C in Schlenk vessels or transferred to an Ar-filled Glovebox for handling and storage. Aryl chlorides were handled in air and stored at the supplier-recommended temperature in screw-capped bottles.

Solvents for chromatography were distilled prior to use. NMR spectra were recorded using a Bruker Avance 400 (^{1}H: 400 MHz, ^{13}C: 101 MHz), ^{13}C-NMR and ^{31}P-NMR experiments were performed in proton-decoupled mode, which is not noted explicitly. Chemical shifts are reported in parts per million relative to the residual NMR solvent signals and the J-coupling constants are given in Hertz with the usual designations for splitting patterns. HR-MS(ESI, APCI, EI) and LR-MS(ESI, APCI) analysis was carried out by the mass spectrometry department of the Institute of Organic Chemistry, University of Tübingen. LR-MS(EI) analysis was carried out by our standard GC/MS method (see below).

Melting point determination was carried out using a MPM HV 3 machine with automated or visual detection (heating rate 1 °C/min). FT-IR spectra were recorded using a Cary 630 FTIR by applying the sample neat on a diamond ATR sampler.

GC-MS was recorded on an Agilent 7820A GC system with Quadrupole MS Agilent 7820A (EI) by using dry hydrogen as carrier gas. An Agilent 190915-433UI column (30 m x 250 μm x 0.25 μm) was used. Program: Heating from 50 °C to 280 °C within 15 minutes. GC-FID (flame ionization detection) analysis was carried out on an Agilent 7820A system using dry hydrogen as carrier gas. An Agilent 19091J-431 column (30 m x 320 μm x 0.25 μm) was used. Program 50-280M12: Heating from 50 °C to 280 °C within 12 minutes.

Preparative TLC was carried out on 20 x 20 cm glass plates with a 1 mm layer of SiO_2 containing fluorescence indicator (F_{254}) by applying a concentrated DCM solution of the crude product as a thin band, development in the appropriate solvent system in a large TLC tank, scraping off the appropriate band, extracting the product with MeOH (HPLC grade) and filtering off SiO_2, followed by solvent removal. Column chromatography was carried out using flash-grade SiO_2 either manually or by a Puriflash system (Interchim), and TLC analysis was carried out using aluminium-backed plates coated with SiO_2 60 F_{254} (0.2 mm thickness) and the compounds detected under UV light (254 nm) or after staining with a $KMnO_4$, Vanilin or Anisaldehyde TLC dip solution and gentle heating.

Definition of "Gradient" used below: In separations with the Puriflash system, a gradient was developed around a suitable (target spot Rf ~ 0.3) binary eluent combination X:Y (where the latter is the strong solvent, X+Y=100) that entailed the following program – 0 to 1 CV: isocratic Y/4, 1 to 11 CV: gradient to Y*2, 11 to 12 CV isocratic Y*2. Flow rates: 23 g SiO_2 50 μm - 15 mL/min, 37 g SiO_2 50 μm – 26 mL/min.

4.4.2. General procedures

General procedure A (GP A): Preparation of PhZnCl•LiCl from PhMgBr•LiCl or PhMgBr

Following a literature procedure[S5], Mg turnings (219 mg, 9.0 mmol, 1.5 eqv.) and LiCl (318 mg, 7.5, 1.25 eqv.) were placed in a septum-capped oven-dried 25 mL Schlenk RBF with stirring bar, which was flame-dried with a propane torch. After evacuating/refilling the still-warm (not hot) flask with Ar (3× repeated), the vessel contents were suspended in dry THF (3 mL), followed by addition of DIBAL-H (60 µL of a 1.0 M solution in THF, 60 µmol, 1 mol%) at RT and stirring for 5 min (gas evolution may occur). The reaction vessel was cooled to 0 °C and bromobenzene (6.0 mmol, 1.0 eqv.) was added. The reaction mixture was stirred for 10 min at 0 °C (or until the major exotherm subsided), then for 1 h at RT to give a solution of PhMgBr•LiCl in THF, typically in a concentration of 1.3 M as determined by titration with I_2/LiCl[S6], which should be used immediately for reaction or transmetalation.[2]

The Grignard reagents were transmetalated by addition to a dry THF solution of $ZnCl_2$ (1.1 eqv. relative to the amount of Grignard to be transmetalated; prepared by charging $ZnCl_2$ into an oven-dried Schlenk RBF with stir bar, flame-drying until the zinc chloride began to melt, followed by vacuum/argon refilling cycles (3×) while the flask is still warm and dissolving the zinc chloride in the appropriate amount of dry THF by syringe addition) at RT, then stirring at the same temperature for 15 min, targeting a concentration of 0.5 M in THF. During the early stages of Grignard addition, a precipitate formed, which redissolved in the later stages of addition. The obtained reagent in THF (clear brown-metallic solution) was usually not again titrated, but should be used immediately for best results. *para*-anisylmagnesium bromide lithium chloride adduct and its corresponding zinc reagent were prepared analogously using the procedure outlined above.

General procedure B (GP B): Ni-catalyzed Migita reaction with alkylthiols (1 mmol scale)

A 10 to 20 mL Schlenk tube with stir bar was dried under vacuum using a heat gun and then refilled with Ar. The cooled vessel was charged with the appropriate catalyst **C1** or **C5** (0.5 – 2.0 mol% relative to the aryl chloride), followed by the aryl chloride (1.0 mmol, 1.0 eqv., if solid) and thiol (1.0 mmol, 1.0 eqv., if solid). The vessel was then evacuated and backfilled with Ar (2× repeated), followed the addition of aryl chloride (1.0 mmol, 1.0 eqv., if liquid) and thiol (1.0 mmol, 1.0 eqv., if liquid). The contents were then dissolved or suspended under stirring by addition of either dry THF or NMP (400 µL). Grignard reagents

---

[2] In our hands, scaling up this reaction tenfold did not lead to major problems besides a more defined exotherm and slightly lower final Grignard concentrations. At large scale, it became important to dry the inorganic salts thoroughly.

(2.4 mL of a 0.5 M THF solution, 1.2 mmol, 1.2 eqv.) were added dropwise under rapid stirring and ice-water bath cooling, followed by removal of the ice bath and stirring for 15 min to 1 h at room temperature. Organozinc reagents (2.4 mL of a 0.5 M THF solution, 1.2 mmol, 1.2 eqv.) were added dropwise under rapid stirring at room temperature, followed by stirring at the same temperature for 15 min to 4 h or heating to 60 °C using an oil bath or aluminum heating block. After the appropriate reaction time, any heating source was removed and the reaction solution allowed to cool to RT. The Mg thiolates were quenched with sat. aq. NH_4Cl solution (2 mL, dropwise), the Zn thiolates with brine (2 mL) under rapid stirring. The reaction mixture was diluted with EtOAc (5 mL). After phase separation, the aqueous phase was removed and the organic phase washed with brine (5 mL). If required, the combined aqueous phases can be re-extracted with EtOAc. The (combined) organic phase(s) were dried over $MgSO_4$ or Na_2SO_4, followed by solvent removal using a rotary evaporator or directly adsorbed on SiO_2. The products were isolated by chromatography.

General procedure C (GP C): Ni-catalyzed Migita reaction with arylthiols (1 mmol scale)

Couplings were carried out analogously to **GP B**, with the following differences: The reaction was carried out at 110 °C for 1 h using catalyst **C1** (2 mol% relative to the aryl chloride) in a 20 mL Schlenk-type pressure vessel using BuZnCl•LiCl as the base (1.2 eqv. of a THF solution, usually 0.5 M) with toluene as the cosolvent (equal to the THF volume). BuZnCl•LiCl was prepared as a 0.5 M THF solution from the reaction of commercially available, freshly titrated ^{n}BuLi with a dry THF solution of $ZnCl_2$.

Caution: Butane formation occurs! Do not carry out the thiol deprotonation in a closed vessel! On larger scale, BuLi should be replaced with HexLi.

General procedure D (GP D): Ni-catalyzed desulfenylative Kumada reaction (1 mmol scale)

Under nitrogen atmosphere, **C1** (2 mol% relative to thiol), thiol (1.00 mmol, 1 equiv.) and dry and degassed THF (0.5 mL) are placed in a heat gun dried 10 mL Schlenk tube with stir bar and sealed with a rubber septum. While stirring, a freshly titrated solution of Knochel-type Grignard reagent (2.20 mmol, 2.2 equiv.) is added *via* a syringe at room temperature. The reaction mixture is placed in an oil bath and stirred for 4 h at 60 °C. Then, the reaction is quenched by addition of saturated NH_4Cl solution (3 mL). Diethyl ether (3 mL) is added and the organic layer is separated from the aqueous layer. The aqueous phase is extracted with diethyl ether (3×5 mL). The collected organic phases are dried over anhydrous $MgSO_4$, filtered and purified by chromatography.

General procedure E (GP E): Ni-catalyzed Migita reaction with alkylthiols (screening/controls)

Couplings were carried out analogously to **GP B**, with the following differences: The reaction was carried out at 0.5 mmol scale with the appropriate catalyst (or no catalyst) and reaction condition/temperature/time. After the reaction, an accurately measured volume of *n*-pentadecane was added *via* a microliter syringe to the reaction mixture, followed by quenching and dilution with EtOAc or Et$_2$O as in **GP B**. A sample (approximately 1 mL) of the organic phase was dried over MgSO$_4$, filtered over a Pasteur pipette plug of MgSO$_4$ and SiO$_2$ into a 2 mL GC vial, which was filled to about 1/4 of its height. The filtrate was diluted with methylene chloride until the vial was full and analysed by GC-FID. In order to determine yields and conversions, the internal standard method was used for quantitative analysis, see section 5 for determination of the respective response factors. See section 1 for GC-FID parameters.

4.4.3. Experimental procedures and analytical data

4.4.3.1. Synthesis of thioethers

Heptyl(phenyl)sulfane (**45**)

45
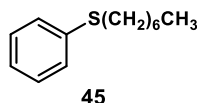
The product (190 mg, 911 µmol, 91%) was obtained as a colourless oil by **GP B** from chlorobenzene (100 µL, 1 mmol) and dist. HeptSH (160 µL, 1 mmol, 1 eqv.), with 4-methoxyphenyl-MgBr•LiCl as the base, THF (400 µL) as solvent at RT for 0.5 h catalyzed by **C1** (0.5 mol%), followed by flash column chromatography (37 g SiO$_2$, gradient to 95:5 PE:EA over 10 CV). Conforms to reported analytical data.[S7]

208.36 g/mol

R$_f$: 0.47 (Cyclohexane)

m.p.: Ambient temperature.

^{1}H-NMR (400 MHz, CDCl$_3$, δ): 7.27 – 7.16 (m, 4H), 7.11 – 7.06 (m, 1H), 2.87 – 2.81 (t, J = 7.2 Hz, 2H), 1.58 (m, 2H), 1.41 – 1.29 (m, 2H), 1.28 – 1.09 (m, 6H), 0.86 – 0.76 (m, 3H).

^{13}C-NMR (101 MHz, CDCl$_3$, δ): 137.1, 128.8, 128.8, 125.6, 33.6, 31.7, 29.2, 28.9, 28.8, 22.6, 14.1.

GC-MS (EI): m/z 208.1, 123.0, 110.1.

N,*N*-Dimethyl-3-(heptylthio)aniline (**41**)

41
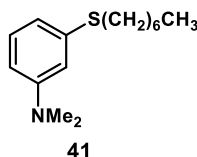
The product (227 mg, 904 µmol, 90%) was obtained as a black oil by applying **GP B** using *N*,*N*-Dimethyl-3-chloroaniline (140 µL, 1 mmol, 1 eqv.) and dist. HeptSH (160 µL, 1 mmol, 1 eqv.), with PhZnCl•LiCl as the base, NMP (400 µL) as co-solvent at 60 °C for 4 h catalyzed by **C1** (2 mol%), followed by flash column chromatography (24 g SiO$_2$, gradient to 9:1 Hexane:EtOAc over 10 CV).

251.43 g/mol

R~f~: 0.59 (PE:EtOAc 9:1)

m.p.: Ambient temperature.

1H-NMR (400 MHz, CDCl$_3$, δ): 7.13 – 7.01 (m, 1H), 6.62 (m, 2H), 6.47 (d, *J* = 2.6 Hz, 1H), 2.87 (s, 6H), 1.67 – 1.50 (m, 2H), 1.41 – 1.29 (m, 2H), 1.26 – 1.14 (m, 6H), 0.91 – 0.69 (m, 3H).

13C-NMR (101 MHz, CDCl$_3$, δ): 137.6, 129.3, 117.0, 113.1, 110.4, 40.6, 33.7, 31.7, 29.3, 28.9, 22.6, 14.1.

HR-MS (EI): m/z calc. for [M]$^{+\bullet}$ 251.170221, found 251.17135.

IR (ATR, $\tilde{v}$ [cm^{-1}]): 1587, 1490, 1438, 1345, 1230, 1177, 1103, 1062, 987, 957, 827, 760, 685.

4'-(Heptylthio)acetophenone (**42**)
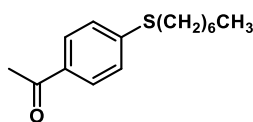
42

  The product (216 mg, 863 µmol, 86%) was obtained as a colourless crystalline solid by **GP A** from 4'-chloroacetophenone (210 µL, 1 mmol, 1 eqv.) and dist. HeptSH (160 µL, 1 mmol, 1 eqv.), with PhZnCl•LiCl as the base, THF (400 µL) as solvent at RT for 0.5 h catalyzed by **C1** (0.5 mol%),   followed by flash column chromatography (24 g SiO$_2$, gradient to 85:15 Hexane:Et$_2$O over 15 CV). Conforms to reported analytical data.[S8]

250.40 g/mol

R~f~: 0.20 (PE:Et$_2$O 95:5)

m.p.: 58 °C (Lit.[S8]: 60 – 61 °C).

1H-NMR (400 MHz, CDCl$_3$, δ): 7.75 (d, *J* = 8.5 Hz, 2H), 7.19 (d, *J* = 8.5 Hz, 2H), 2.89 (t, *J* = 7.5 Hz, 2H), 2.47 (s, 3H), 1.61 (p, *J* = 7.3 Hz, 2H), 1.42 – 1.31 (m, 2H), 1.28 – 1.14 (m, 6H), 0.83 – 0.74 (m, 3H).

13C-NMR (101 MHz, CDCl$_3$, δ): 197.0, 145.0, 133.7, 128.7, 126.2, 31.9, 31.7, 28.9, 28.8, 28.7, 26.4, 22.6, 14.1.

GC-MS (EI): m/z 250.2, 235.2, 152.1, 137.1.

Heptyl-(4-trifluoromethyl)phenylsulfane (**43**)

43
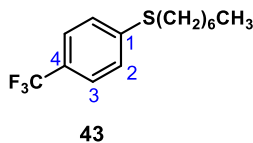
The product (267 mg, 966 µmol, 97%) was obtained as a black oil by applying **GP B** using 4-chlorobenzotrifluoride (135 µL, 1 mmol, 1 eqv.) and dist. HeptSH (160 µL, 1 mmol, 1 eqv.), with 4-methoxyphenyl-MgBr•LiCl as the base, THF (400 µL) as solvent at RT for 0.5 h catalyzed by **C1** (0.5 mol%), followed by standard workup and removal of volatiles. The crude mixture was partially dissolved in cyclohexane, followed by vacuum filtration over a pad of SiO_2 (1. 50 mL CyH; 2. CyH:Et_2O 95:5 v/v until the first brown brown band elutes).

276.36 g/mol

R_f: 0.39 (Cyclohexane)

m.p.: Ambient temperature.

¹H-NMR (400 MHz, $CDCl_3$, δ): 7.50 (d, J = 8.2 Hz, 2H), 7.34 (d, J = 8.1 Hz, 2H), 2.97 (t, J = 7.4 Hz, 2H), 1.69 (p, J = 7.4 Hz, 2H), 1.50 – 1.39 (m, 2H), 1.36 – 1.11 (m, 6H), 0.89 (t, J = 6.7 Hz, 3H).

¹³C-NMR (101 MHz, $CDCl_3$, δ): 142.8 (d, J = 1.7 Hz, C^1), 127.1 (s, C^2), 127.1 (q, $^2J_{CF}$ = 32.6 Hz, C^4) 125.6 (q, $^3J_{CF}$ = 3.8 Hz, C^3), 124.3 (q, $^1J_{CF}$ = 271.6 Hz, CF_3)[3 & S9], 32.4, 31.7, 28.8, 28.8, 28.6, 22.6, 14.0.

¹⁹F-NMR (377 MHz, $CDCl_3$, δ): –62.4.

HR-MS (EI): m/z calc. for [M][•+] 276.115407, found 276.11584.

IR (ATR, $\tilde{v}$ [cm⁻¹]): 2926, 2855, 1606, 1323, 1162, 1121, 1095, 1062, 1013, 820.

---

[3] Not all peaks of the quartet could be detected. The visible upfield shifted signal next to the visible peak at 122.9 ppm is separated by 271.6 Hz, which is the coupling constant observed for the quartet CF_3-signal in 4-trifluoromethyl-thioanisole. The downfield shifted signal (separation by 271.6 Hz) to the visible peak at 122.9 ppm should have the same intensity (1:3:3:1 intensity pattern), but is not observed since it overlaps with the signal of C^3. Based on these observations, the quartet should be centered at 124.2 ppm, which is agreement with the above mentioned compound (centered at 124.4 ppm). See the supporting information of reference 9 for more details.

Heptyl(4-methoxyphenyl)sulfane (**44**)

44
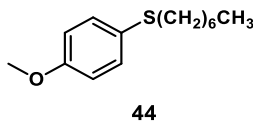
    The product (191 mg, 801 µmol, 80%) was obtained as a colourless oil by applying **GP B** using 4-chloroanisole (125 µL, 1 mmol, 1 eqv.) and dist. HeptSH (160 µL, 1 mmol, 1 eqv.), with PhMgBr•LiCl as the base, THF (400 µL) solvent at RT for 1 h catalyzed by **C1** (0.5 mol%), followed by flash column chromatography (37 g SiO_2, gradient to 9:1 CyH:EtOAc over 10 CV).

238.39 g/mol

R_f: 0.67 (PE:EA 9:1)

m.p.: Ambient temperature.

^{1}H-NMR (400 MHz, $CDCl_3$, δ): 7.30–7.35 (d, J = 8.7 Hz, 2H), 6.80–6.86 (d, J = 8.7 Hz, 2H), 3.78 (s, 3H), 2.80 (t, J = 7.4 Hz, 2H), 1.53–1.61 (m, 2H), 1.18–1.43 (m, 8H), 0.83–0.90 (m, 3H).

^{13}C-NMR (101 MHz, $CDCl_3$, δ): 158.7, 132.9, 127.0, 114.5, 55.3, 35.8, 31.7, 29.3, 28.8, 28.6, 22.6, 14.0.

HR-MS (APCI): m/z calc. for $[M+H]^+$ 239.14641, found 239.14676.

IR (ATR, $\tilde{v}$ [cm^{-1}]): 2922, 2855, 1591, 1490, 1461, 1282, 1241, 1174, 1032, 823.

N-(4-(heptylthio)phenyl)-*N*-methylacetamide (**46**)

46
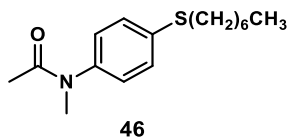
    The product (193 mg, 691 µmol, 69%) was obtained as a colourless oil by applying **GP C** using **SM10** (184 mg, 1 mmol, 1 eqv.) and dist. HeptSH (160 µL, 1 mmol, 1 eqv.), with PhZnCl•LiCl as the base, NMP (400 µL) as cosolvent at 60 °C for 4 h catalyzed by **C1** (2 mol%), followed by flash column chromatography (24 g SiO_2, 75:25 Hexane:EtOAc to 50:50 Hexane:EtOAc over 15 CV).

279.44 g/mol

R_f: 0.39 (PE:EA 1:1)

R_f: 0.39 (PE:EA 1:1)

m.p.: Ambient temperature.

^{1}H-NMR (400 MHz, CDCl$_3$, δ): 7.25 (d, J = 8.4 Hz, 2H), 7.02 (d, J = 8.4 Hz, 2H), 3.17 (s, 3H), 2.87 (t, J = 7.4 Hz, 2H), 1.80 (s, 3H), 1.60 (p, J = 7.3 Hz, 2H), 1.42 – 1.31 (m, 2H), 1.29 – 1.15 (m, 6H), 0.87 – 0.75 (m, 3H).

^{13}C-NMR (101 MHz, CDCl$_3$, δ): 170.6, 142.0, 137.2, 129.3, 127.4, 37.1, 33.4, 31.7, 29.0, 28.8, 22.6, 14.1.

HR-MS (ESI): m/z calc. for [M+Na]$^+$ 302.15491, found 302.15513.

IR (ATR, $\tilde{v}$ [cm^{-1}]): 2922, 2855, 1654, 1490, 1371, 1345, 1293, 1140, 1095, 1013, 972, 827, 745.

4-(Heptylthio)benzonitrile (**47**)

47
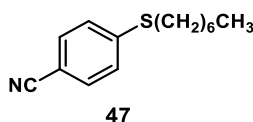
The product (181 mg, 776 µmol, 78%) was obtained as a colourless oil by **GP B** from 4-chlorobenzonitrile (137.57 mg, 1 mmol, 1 eqv.) and dist. HeptSH (160 µL, 1 mmol, 1 eqv.), with PhZnCl•LiCl as the base, THF (400 µL) as solvent at RT for 0.5 h catalyzed by **C1** (2 mol%), followed by flash column chromatography (24 g SiO$_2$, 5 CV 100% Hexane, over 10 CV to 80:20 Hexane:Et$_2$O).

233.37 g/mol

R_f: 0.36 (PE:EtOAc 95:5)

m.p.: Ambient temperature.

^{1}H-NMR (400 MHz, CDCl$_3$, δ): 7.41 (d, J = 8.5 Hz, 2H), 7.19 (d, J = 8.5 Hz, 2H), 2.87 (t, J = 7.4 Hz, 2H), 1.60 (p, J = 7.2 Hz, 2H), 1.41 – 1.30 (m, 2H), 1.28 – 1.06 (m, 6H), 0.86 – 0.71 (m, 3H).

^{13}C-NMR (101 MHz, CDCl$_3$, δ): 145.4, 132.1, 126.6, 118.9, 107.8, 31.9, 31.7, 28.8, 28.8, 28.6, 22.6, 14.1.

HR-MS (EI): m/z calc. for [M]$^{•+}$ 233.123271, found 233.12413.

IR (ATR, $\tilde{v}$ [cm^{-1}]): 2926, 2855, 2225, 1725, 1591, 1483, 1088, 820.

4-(Heptylthio)pentafluorosulfanylbenzene (**48**)
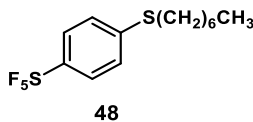
The product (150 mg, 448 μmol, 45%) was obtained as a colourless oil by **GP B** from 4-chloropentafluorosulfanylbenzene (239 mg, 1 mmol, 1 eqv.) and dist. HeptSH (160 μL, 1 mmol, 1 eqv.), with PhZnCl•LiCl as the base, NMP (400 μL) as cosolvent at 60 °C for 4 h catalyzed by **C1** (2 mol%), followed by preparative TLC (Hexane).

334.41 g/mol

R_f: 0.6 (Hexane)

m.p.: Ambient temperature.

^{1}H-NMR (400 MHz, CDCl$_3$, δ): 7.55 (d, J = 8.8 Hz, 2H), 7.21 (d, J = 8.8 Hz, 2H), 2.89 (t, J = 7.4 Hz, 2H), 1.62 (p, J = 7.4 Hz, 2H), 1.45 – 1.32 (m, 2H), 1.29 – 1.17 (m, 6H), 0.81 (t, J = 6.7 Hz, 3H).

^{13}C-NMR (101 MHz, CDCl$_3$, δ): 143.1, 128.0 (d, J = 159.4 Hz), 126.5, 126.2 (t, J = 4.7 Hz), 32.3, 31.7, 28.8, 28.8, 28.7, 22.6, 14.1.

^{19}F-NMR (659 MHz, CDCl$_3$, δ): 85.07 (p, J = 150.6 Hz), 63.33 (d, J = 150.7 Hz).[4]

HR-MS (EI): m/z calc. for [M]$^{•+}$ 334.084284, found 334.08090.

IR (ATR, $\tilde{v}$ [cm^{-1}]): 2926, 2855, 1580, 1487, 1397, 1080, 823, 723, 663.

---

[4] We were unable to record a standard ^{19}F-NMR spectrum for this compound. This spectrum was acquired by Priska Kolb from the NMR department, Central Chemical Institute, University of Tübingen on a 700 MHz NMR spectrometer. The observed signals and splitting patterns are typical for Aryl-SF$_5$ compounds.

2-(Heptylthio)anisole (**49**)
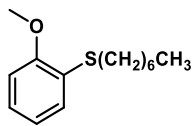
49

The product (231 mg, 969 µmol, 97%) was obtained as a black oil by **GP B** from 2-chloroanisole (130 µL, 1 mmol, 1 eqv.) and dist. HeptSH (160 µL, 1 mmol, 1 eqv.), with PhZnCl•LiCl as the base, NMP (400 µL) as cosolvent at 60 °C for 4 h catalyzed by **C1** (2 mol%), followed by flash column chromatography (24 g SiO$_2$, 5 CV hexane, then gradient to 8:2 Hexane:Et$_2$O over 10 CV).

238.39 g/mol

R_f: 0.58 (95:5 Hexane:Et$_2$O)

m.p.: Ambient temperature.

^{1}H-NMR (400 MHz, CDCl$_3$, δ): 7.18 (d, J = 8.5 Hz, 1H), 7.09 (t, J = 7.8 Hz, 1H), 6.85 (t, J = 7.5 Hz, 1H), 6.77 (d, J = 8.2 Hz, 1H), 3.82 (s, 3H), 2.81 (t, J = 7.4 Hz, 2H), 1.59 (p, J = 7.5 Hz, 2H), 1.42 − 1.31 (m, 2H), 1.22 (m, 6H), 0.80 (t, J = 6.6 Hz, 3H).

^{13}C-NMR (101 MHz, CDCl$_3$, δ): 157.1, 128.7, 126.6, 125.3, 121.0, 110.3, 55.8, 31.9, 31.7, 28.9, 28.9, 22.6, 14.1.

HR-MS (EI): m/z calc. for [M]$^{•+}$ 238.138587, found 238.14131.

IR (ATR, $\tilde{v}$ [cm^{-1}]): 2922, 2851, 1576, 1461, 1271, 1237, 1073, 1025, 741, 685.

2-(Heptylthio)toluene (**50**)
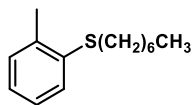
50

The product (198 mg, 890 µmol, 89%) was obtained as a red-black oil by **GP B** from 2-chlorotoluene (115 µL, 1 mmol, 1 eqv.) and dist. HeptSH (160 µL, 1 mmol, 1 eqv.), with PhZnCl•LiCl as the base, NMP (400 µL) as cosolvent at 60 °C for 4 h catalyzed by **C5** (2 mol%), followed by flash column chromatography (wet load, 24 g SiO$_2$, 10 CV 100% Hexane).

222.39 g/mol

R_f: 0.48 (Hexane)

m.p.: Ambient temperature.

¹H-NMR (400 MHz, CDCl₃, δ): 7.20 – 7.15 (m, 1H), 7.08 (m, 2H), 7.00 (m, 1H), 2.80 (t, *J* = 7.4 Hz, 2H), 2.29 (s, 3H), 1.59 (p, *J* = 7.2 Hz, 2H), 1.41 – 1.32 (m, 2H), 1.29 – 1.15 (m, 6H), 0.81 (t, *J* = 6.8 Hz, 3H).

¹³C-NMR (101 MHz, CDCl₃, δ): 137.2, 136.4, 123.0, 127.3, 126.3, 125.2, 32.8, 31.7, 29.0, 29.0, 28.9, 22.6, 20.3, 14.1.

HR-MS (EI): m/z calc. for [M]•⁺ 222.143672, found 222.14529.

IR (ATR, $\tilde{v}$ [cm⁻¹]): 2922, 2855, 1587, 1464, 1379, 1274, 1066, 738.

5-(Heptylthio)-1-methyl-1*H*-indole (**51**)

51
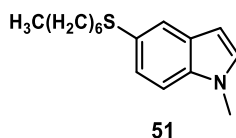
The product (211 mg, 807 µmol, 81%) was obtained as a black oil by applying **GP B** using 5-chloro-1-methylindole (166 mg, 1 mmol, 1 eqv.) and dist. HeptSH (160 µL, 1 mmol, 1 eqv.), with PhZnCl•LiCl as the base, NMP (400 µL) as cosolvent at 60 °C for 4 h catalyzed by **C1** (2 mol%), followed by flash column chromatography (24 g SiO₂, from 100% hexane to 90:10 hexane:EtOAc over 10 CV).

261.43 g/mol

R_f: 0.64 (PE:Et₂O 95:5)

m.p.: Ambient temperature.

¹H-NMR (400 MHz, CDCl₃, δ): 7.64 (dd, *J* = 1.7, 0.7 Hz, 1H), 7.23 (dd, *J* = 8.5, 1.7 Hz, 1H), 7.19 – 7.15 (m, 1H), 6.96 (d, *J* = 3.0 Hz, 1H), 6.36 (dd, *J* = 3.2, 0.8 Hz, 1H), 3.70 (s, 3H), 2.79 (t, *J* = 7.4 Hz, 2H), 1.57 – 1.47 (m, 2H), 1.32 (m, 2H), 1.25 – 1.12 (m, 6H), 0.79 (t, *J* = 6.8 Hz, 3H).

¹³C-NMR (101 MHz, CDCl₃, δ): 135.9, 129.5, 129.1, 126.0, 125.4, 124.7, 109.6, 100.7, 36.6, 32.9, 31.8, 29.5, 28.9, 28.8, 22.6, 14.1.

HR-MS (ESI): m/z calc. for [M+Na]⁺ 284.14434, found 284.14448.

IR (ATR, $\tilde{v}$ [cm⁻¹]): 2922, 2851, 1509, 1472, 1375, 1274, 1241, 1080, 879, 793, 752, 715.

5-(heptylthio)-2-methylbenzo[*d*]thiazole (**52**)
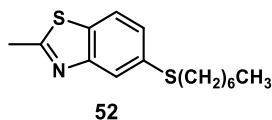
The product (243 mg, 871 µmol, 87%) was obtained as a colourless crystalline solid by applying **GP B** using 5-Chloro-2-methylbenzothiazole (184 mg, 1 mmol, 1 eqv.) and dist. HeptSH (160 µL, 1 mmol, 1 eqv.), with PhZnCl•LiCl as the base, NMP (400 µL) as cosolvent at 60 °C for 4 h catalyzed by **C1** (2 mol%), followed by flash column chromatography (24 g SiO_2, 100% Hexane to 85:15 Hexane:EtOAc over 20 CV).

279.44 g/mol

R_f: 0.8 (PE:Et_2O 8:2)

m.p.: 43 °C.

^{1}H-NMR (400 MHz, $CDCl_3$, δ): 7.90 (d, *J* = 1.8 Hz, 1H), 7.69 (d, *J* = 8.4 Hz, 1H), 7.31 (dd, *J* = 8.3, 1.8 Hz, 1H), 2.95 (t, *J* = 7.5 Hz, 2H), 2.82 (s, 3H), 1.66 (p, *J* = 7.3 Hz, 2H), 1.41 (m, 2H), 1.27 (m, 6H), 0.89 – 0.82 (m, 3H).

^{13}C-NMR (101 MHz, $CDCl_3$, δ): 167.8, 154.0, 135.1, 133.1, 126.3, 122.3, 121.4, 34.2, 31.7, 29.1, 28.8, 28.8, 22.6, 20.2, 14.1.

HR-MS (ESI): m/z calc. for [M+Na]$^+$ 280.11882, found 280.11904.

IR (ATR, $\tilde{v}$ [cm^{-1}]): 1587, 1520, 1438, 1300, 1170, 1084, 995, 913, 846, 808, 723.

3-(Heptylthio)pyridine (**53**)
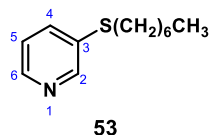
The product (202 mg, 965 µmol, 97%) was obtained as a colourless oil by applying **GP B** using 3-chloropyridine (94 µL, 1 mmol, 1 eqv.) and dist. HeptSH (160 µL, 1 mmol, 1 eqv.), with PhZnCl•LiCl as the base, NMP (400 µL) as cosolvent at 60 °C for 4 h catalyzed by **C1** (2 mol%), followed by flash column chromatography (24 g SiO_2, 5 CV 100% Hexane, over 5 CV to 75:25 Hexane:EtOAc, hold 1 CV, over 1 CV to 68:32 Hexane:EtOAc, hold 4 CV).

209.12 g/mol

R_f: 0.25 (PE:Et$_2$O 8:2)

m.p.: Ambient temperature.

^{1}H-NMR (400 MHz, CDCl$_3$, δ): 8.46 (s, 1H, H^2), 8.30 (d, J = 3.6 Hz, 1H, H^6), 7.53 (dd, $^3J_{H4-H5}$ = 8.1, $^4J_{H4-H2}$ = 1.8 Hz, 1H, H^4), 7.09 (dd, J = 8.1, 4.4 Hz, 1H, H^5), 2.82 (t, J = 7.4 Hz, 2H), 1.54 (p, J = 7.3 Hz, 2H), 1.38 – 1.27 (m, 6H), 1.26 – 1.10 (m, 6H), 0.81 – 0.76 (m, 3H).

^{13}C-NMR (101 MHz, CDCl$_3$, δ): 149.9, 146.7, 136.5, 134.1, 123.4, 33.6, 31.6, 29.1, 28.7, 28.6, 22.5, 14.0.

HR-MS (EI): m/z calc. for [M]$^{•+}$ 209.123271, found 209.12144.

IR (ATR, $\tilde{v}$ [cm^{-1}]): 2952, 2922, 2855, 1558, 1464, 1401, 1107, 1017, 790, 704.

6-(heptylthio)quinoline (**54**)

54
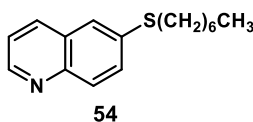
The product (245 mg, 944 µmol, 94%) was obtained as a turbid oil by applying **GP B** using 6-chloroquinoline (164 mg, 1 mmol, 1 eqv.) and dist. HeptSH (160 µL, 1 mmol, 1 eqv.), with PhZnCl•LiCl as the base, NMP (400 µL) as cosolvent at 60 °C for 4 h catalyzed by **C1** (2 mol%), followed by flash column chromatography (14 g SiO$_2$, gradient to 6:4 Hexane:Et$_2$O over 10 CV). The compound solidifies to a white paste after brief storage at -10 °C.

259.41 g/mol

R_f: 0.26 (PE:Et$_2$O 8:2)

m.p.: Ambient temperature.

^{1}H-NMR (400 MHz, CDCl$_3$, δ): 8.97 – 8.60 (m, 1H), 7.95 – 7.85 (m, 2H), 7.57 – 7.49 (m, 2H), 7.26 (dd, J = 8.3, 4.2 Hz, 1H), 2.93 (t, J = 7.4 Hz, 2H), 1.67 – 1.56 (p, J = 7.2 Hz, 2H), 1.41 – 1.31 (m, 2H), 1.19 (m, 6H), 0.82 – 0.73 (m, 3H).

^{13}C-NMR (101 MHz, CDCl$_3$, δ): 149.6, 146.6, 136.3, 134.9, 130.3, 129.7, 128.7, 125.0, 121.6, 33.2, 31.7, 28.9, 28.8, 28.8, 22.6, 14.1.

HR-MS (ESI): m/z calc. for [M+H]$^+$ 260.14675, found 260.14716.

IR (ATR, $\tilde{v}$ [cm^{-1}]): 2922, 2851, 1610, 1584, 1487, 1367, 1304, 1236, 1185, 1121, 1069, 1032, 943, 864, 827, 790, 764, 723.

9-Tosyl-6-heptylthio-9*H*-purine (**55**)

51
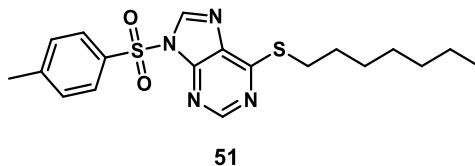
The product (165 mg, 407 μmol, max. 41%, containing an unknown impurity) was obtained as an off-white solid by **GP B** from 9-Tosyl-6-chloro-9*H*-purine (309 mg, 1 mmol, 1 eqv.) and dist. HeptSH (160 μL, 1 mmol, 1 eqv.), with PhZnCl•LiCl as the base, THF as solvent at 60 °C for 0.5 h catalyzed by **C1** (0.5 mol%), after washing the crude solid obtained after workup, drying and solvent removal with dist. *n*-Hexane (4 x 5 mL).

404.55 g/mol

R$_f$: 0.44 (DCM:MeOH 9:1)

m.p.: 115 °C (dec.)

^{1}H-NMR (400 MHz, CDCl$_3$, δ): 8.78 (s, 1H), 8.51 (s, 1H), 8.10 (d, *J* = 8.4 Hz, 2H), 7.38 – 7.27 (m, 2H), 2.49 – 2.41 (m, 2H), 2.37 (s, 3H), 1.54 (p, *J* = 7.2 Hz, 2H), 1.24 – 1.17 (m, 6H), 0.84 – 0.78 (m, 5H).

^{13}C-NMR (101 MHz, CDCl$_3$, δ): 153.6, 152.3, 150.2, 147.6, 142.5, 133.2, 131.5, 130.4, 128.8, 34.1, 31.7, 28.7, 28.4, 24.7, 22.6, 21.9, 14.1.

HR-MS (ESI): m/z calc. for [M+Na]$^+$ 427.12329, found 427.12389.

IR (ATR, $\tilde{v}$ [cm^{-1}]): 2995, 2922, 2851, 1558, 1438, 1334, 1162, 1069, 1013, 972, 928, 812, 704, 667.

10-ethyl-2-(heptylthio)-10*H*-phenothiazine (**56**)

56
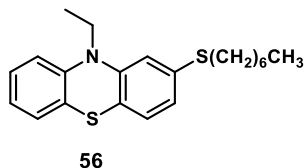
The product (284 mg, 794 μmol, 79%) was obtained as a colourless oil by applying **GP B** using 2-Chloro-10-ethyl-10*H*-phenothiazine (262 mg, 1 mmol, 1 eqv.) and dist. HeptSH (160 μL, 1 mmol, 1 eqv.), with PhZnCl•LiCl as the base, NMP (400 μL) as cosolvent at 60 °C for 4 h catalyzed by **C1** (2 mol%), followed by flash column chromatography (23 g SiO$_2$, Hexane).

357.57 g/mol

R_f: 0.13 (Hexane)

m.p.: Ambient temperature.

^{1}H-NMR (400 MHz, CDCl$_3$, δ): 7.08 – 6.71 (m br, 7H), 2.80 (s br, 2H), 1.55 (p, *J* = 7.2 Hz, 2H), 1.39 – 1.28 (m, 6H), 1.27 – 1.12 (m, 7H), 0.84 – 0.73 (m, 3H).[5]

^{13}C-NMR (101 MHz, CDCl$_3$, δ): 145.4, 144.7, 135.9, 127.4, 127.3, 124.4, 123.3, 122.5, 116.6, 115.3, 41.9, 34.3, 31.7, 29.7, 28.8, 28.8, 22.6, 14.1, 13.1.

HR-MS (ESI): m/z calc. for [M+Na]$^+$ 357.15794, found 357.15796.

IR (ATR, $\tilde{v}$ [cm^{-1}]): 2922, 2851, 1565, 1449, 1401, 1315, 1278, 1230, 1133, 1039, 924, 801, 745.

---

[5] We observed line broadening in both ^{1}H- and ^{13}C-NMR spectra. Due to this, some ^{13}C signals could not be detected.

5-(Heptylthio)-1-phenyl-1H-tetrazole (**57**)
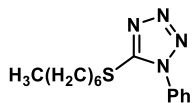
57

The product (169 mg, 611 µmol, 61%) was obtained as a colourless oil by applying **GP B** using (181 mg, 1 mmol, 1 eqv.) and dist. HeptSH (160 µL, 1 mmol, 1 eqv.), with PhZnCl•LiCl as the base, NMP (400 µL) as cosolvent at 60 °C for 4 h catalyzed by **C1** (2 mol%), followed by flash column chromatography (24 g SiO$_2$, from 100% hexane to 70:30 hexane:Et$_2$O over 10 CV). The analytical data conforms to the reported literature.[S10]

276.40 g/mol

R$_f$: 0.17 (PE:Et$_2$O 9:1)

m.p.: Ambient temperature.

^{1}H-NMR (400 MHz, CDCl$_3$, δ): 7.56 – 7.42 (m, 5H), 3.32 (t, J = 7.4 Hz, 2H), 1.75 (p, J = 7.4 Hz, 2H), 1.42 – 1.32 (m, 2H), 1.30 – 1.14 (m, 6H), 0.81 (t, J = 6.7 Hz, 3H).

^{13}C-NMR (101 MHz, CDCl$_3$, δ): 154.5, 133.8, 130.1, 129.8, 123.9, 33.4, 31.6, 29.1, 28.7, 28.6, 22.6, 14.0.

LR-MS (ESI): 277.1 (MH$^+$)

3-(Heptylthio)-coumarin (**58**)
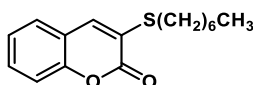
58

The product (63 mg, 227 µmol, 23%) was obtained as an off-white solid by applying **GP C** using 3-Chloro-coumarin (181 mg, 1 mmol, 1 eqv.) and dist. HeptSH (160 µL, 1 mmol, 1 eqv.), with PhZnCl•LiCl as the base, NMP (400 µL) as cosolvent at 60 °C for 4 h catalyzed by **C1** (2 mol%), followed by flash column chromatography (24 g SiO$_2$, 100% Hexane to 70:30 Hexane:EtOAc over 20 CV).

276.39 g/mol

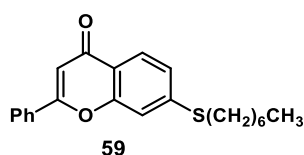**R$_f$**: 0.12 (9:1 Hexane:EtOAc)

m.p.: 97 °C.

¹H-NMR (400 MHz, CDCl₃, δ): 7.41 – 7.17 (m, 5H), 2.86 (t, *J* = 7.3 Hz, 2H), 1.67 (p, *J* = 8.8, 2H), 1.46 – 1.35 (m, 2H), 1.33 – 1.13 (m, 6H), 0.82 (t, *J* = 6.7 Hz, 3H).

¹³C-NMR (101 MHz, CDCl₃, δ): 159.3, 151.7, 134.0, 130.1, 128.4, 126.3, 124.6, 119.6, 116.5, 31.7, 31.3, 28.9, 28.8, 28.0, 22.6, 14.1.

HR-MS (ESI): m/z calc. for [M+Na]⁺ 299.10762, found 299.10796.

IR (ATR, $\tilde{v}$ [cm⁻¹]): 2955, 2918, 2851, 1763, 1662, 1595, 1550, 1360, 1278, 1028, 984, 939, 905, 834, 749.

6-(Heptylthio)-flavone (**59**)

59

The product (279 mg, 673 μmol, 67%) was obtained as an off-white solid by applying **GP B** using 6-Chloro-flavone (256 mg, 1 mmol, 1 eqv.) and dist. HeptSH (160 μL, 1 mmol, 1 eqv.), with PhZnCl•LiCl as the base, NMP (400 μL) as cosolvent at 60 °C for 4 h catalyzed by **C1** (2 mol%), followed by flash column chromatography (24 g SiO₂, 100% Hexane to 70:30 Hexane:EtOAc over 20 CV).

279.44 g/mol

*R*f: 0.11 (PE:EtOAc 9:1)

m.p.: 83 °C.

¹H-NMR (400 MHz, CDCl₃, δ): 8.02 (d, *J* = 2.4 Hz, 1H), 7.88 – 7.80 (m, 2H), 7.54 (dd, *J* = 8.7, 2.4 Hz, 1H), 7.49 – 7.38 (m, 4H), 6.77 (s, 1H), 2.94 (t, *J* = 7.4 Hz, 2H), 1.61 (tt, *J* = 7.5, 6.1 Hz, 2H), 1.43 – 1.31 (m, 2H), 1.28 – 1.09 (m, 6H), 0.87 – 0.73 (m, 3H).

¹³C-NMR (101 MHz, CDCl₃, δ): 177.7, 163.4, 154.5, 135.2, 134.4, 131.7, 131.7, 129.1, 126.3, 124.3, 123.9, 118.6, 107.6, 33.7, 31.7, 28.8, 28.8, 22.6, 14.1.

HR-MS (ESI): m/z calc. for [M+Na]⁺ 375.13892 found 375.13871.

IR (ATR, $\tilde{v}$ [cm⁻¹]): 1625, 1561, 1498, 1449, 1356, 1289, 1248, 1140, 1025, 909, 823, 767, 685.

5-(Heptylthio)pyrimidine (**60**)

60
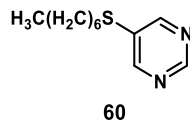
The product (173 mg, 822 µmol, 82%) was obtained as a colourless oil by applying **GP B** using (115 mg, 1 mmol, 1 eqv.) and dist. HeptSH (160 µL, 1 mmol, 1 eqv.), with PhZnCl•LiCl as the base, NMP (400 µL) as cosolvent at 60 °C for 4 h catalyzed by **C1** (2 mol%), followed by flash column chromatography (24 g SiO$_2$, from 100% hexane to 90:10 hexane:EtOAc over 10 CV).
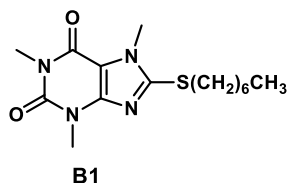
210.34 g/mol

R$_f$: 0.55 (PE:EtOAc 8:2)

m.p.: Ambient temperature.

^{1}H-NMR (400 MHz, CDCl$_3$, δ): 8.95 (s, 1H), 8.60 (s, 2H), 2.88 (t, *J* = 7.4 Hz, 2H), 1.59 (p, *J* = 7.3 Hz, 2H), 1.43 – 1.29 (m, 2H), 1.30 – 1.18 (m, 6H), 0.89 – 0.74 (m, 3H).

^{13}C-NMR (101 MHz, CDCl$_3$, δ): 156.6, 155.6, 33.5, 31.6, 29.1, 28.7, 28.6, 22.6, 14.0.

HR-MS (ESI): m/z calc. for [M+Na]$^+$ 211.12635 found 211.12640.

IR (ATR, $\tilde{v}$ [cm^{-1}]): 2922, 2855, 1539, 1461, 1401, 1155, 1073, 1028, 887, 719.

8-(Heptylthio)caffeine (**B1**)

B1

The product (175 mg, 539 µmol, 54%) was obtained as a white solid by **GP B** from 8-chlorocaffeine (229 mg, 1 mmol, 1 eqv.) and heptanethiol (160 µL, 1 mmol, 1 eqv.) with PhMgBr•LiCl as the base, THF (400 µL) as solvent at RT for 1 h catalyzed by **C1** (0.5 mol%), followed by flash column

chromatography (37 g SiO_2, gradient to 8:2 PE:EA over 10 CV). The obtained spectroscopic data is in accordance with the literature.[S11]

324.44 g/mol

R_f: 0.65 (1:1 PE:EA)

m.p.: 60 °C.

¹H-NMR (400 MHz, CDCl₃, δ): 3.77 (s, 3H), 3.49 (s, 3H), 3.32 (s, 3H), 3.19 (t, J = 7.3 Hz, 2H), 1.68 (p, J = 7.4 Hz, 2H), 1.45 – 1.30 (m, 2H), 1.32 – 1.14 (m, 6H), 0.82 (t, J = 6.7 Hz, 3H).

¹³C-NMR (101 MHz, CDCl₃, δ): 154.6, 151.6, 151.4, 148.5, 108.5, 32.8, 32.2, 31.6, 29.7, 29.6, 28.7, 28.6, 27.8, 22.6, 14.1.

HR-MS (ESI): m/z calc. for [M+Na]⁺ 347.15122, found 347.15164.

IR (ATR, $\tilde{v}$ [cm⁻¹]): 2955, 2914, 2851, 1695, 1662, 1453, 1401, 1364, 1285, 1218, 1032, 972, 745.

Ethyl 2-(1-(4-(heptylthio)benzoyl)-5-methoxy-2-methyl-1H-indol-3-yl)acetate (**B2**)

B2
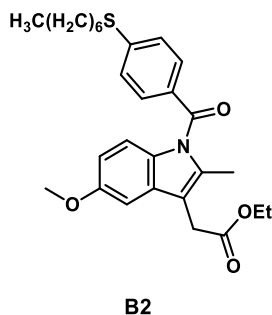
The product (206 mg, 855 µmol, 86%) was obtained as a yellow oil by **GP B** from Indometacin ethyl ester (**SM26**, 193 mg, 0.5 mmol, 1 eqv.) and dist. heptanethiol (80 µL, 0.5 mmol, 1 eqv.) with PhZnCl•LiCl as the base, NMP (400 µL) as cosolvent at 60 °C for 4 h catalyzed by **C1** (2 mol%), followed by flash column chromatography (23 g SiO_2, 4 CV Hexane, gradient to 75:25 Hexane:EtOAc over 6 CV, 1 CV hold, gradient to 65:35 Hexane:EtOAc over 4 CV, 2 CV hold). The product solidified at -10 °C.

481.65 g/mol

R_f: 0.23 (8:2 PE:Et₂O)

m.p.: 67 °C.

¹H-NMR (400 MHz, CDCl₃, δ): 7.62 (d, *J* = 8.4 Hz, 2H), 7.31 (d, *J* = 8.4 Hz, 2H), 6.97 (d, *J* = 2.5 Hz, 1H), 6.92 (d, *J* = 9.0 Hz, 1H), 6.66 (dd, *J* = 9.0, 2.6 Hz, 1H), 4.16 (q, *J* = 7.1 Hz, 2H), 3.84 (s, 2H), 3.00 (t, *J* = 7.4 Hz, 2H), 2.39 (s, 3H), 1.72 (p, *J* = 7.3 Hz, 2H), 1.52 – 1.40 (m, 2H), 1.37 – 1.21 (m, 9H), 0.94 – 0.84 (m, 3H).

¹³C-NMR (101 MHz, CDCl₃, δ): 171.0, 168.9, 155.8, 145.1, 136.0, 131.5, 131.0, 130.5, 130.4, 126.3, 114.9, 112.1, 111.5, 101.1, 61.0, 55.7, 32.0, 31.7, 30.5, 28.9, 28.8, 28.7, 22.6, 14.3, 14.1, 13.3.

HR-MS (ESI): m/z calc. for [M+Na]⁺ 504.21790 found 504.21807.

IR (ATR, $\tilde{v}$ [cm⁻¹]): 2926, 2855, 1733, 1677, 1587, 1476, 1397, 1353, 1308, 1259, 1222, 1140, 1088, 1032, 924, 827, 801, 752, 693.

Ethyl 4-(heptylthio)benzoate (**74**)

74
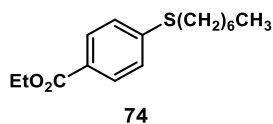
The product (246 mg, 877 µmol, 88%) was obtained as a colourless oil by applying **GP B** using ethyl 4-chlorobenzoate (155 µL, 1 mmol, 1 eqv.) and heptanethiol (160 µL, 1 mmol, 1 eqv.) with PhZnCl•LiCl as the base, with NMP (400 µL) as cosolvent at 60 °C for 4 h catalyzed by **C1** (2 mol%), followed by flash chromatography (14 g SiO₂, 5 CV Hexane, gradient to 8:2 Hexane:EtOAc over 20 CV, hold 5 CV).

280.43 g/mol

***R*ₓ**: 0.13 (95:5 PE:Et₂O)

m.p.: Ambient temperature.

¹H-NMR (400 MHz, CDCl₃, δ): 7.82 (d, *J* = 8.5 Hz, 2H), 7.17 (d, *J* = 8.5 Hz, 2H), 4.25 (q, *J* = 7.1 Hz, 2H), 2.85 (t, *J* = 7.4 Hz, 2H), 1.58 (p, *J* = 7.2 Hz, 2H), 1.39 – 1.11 (m, 11H), 0.83 – 0.74 (m, 3H).

¹³C-NMR (101 MHz, CDCl₃, δ): 166.2, 144.4, 129.8, 126.9, 126.2, 60.8, 32.1, 31.7, 28.9, 28.8, 28.8, 22.6, 14.3, 14.0.

HR-MS (EI): m/z calc. for [M]⁺• 280.149152, found 280.14748.

IR (ATR, $\tilde{v}$ [cm⁻¹]): 2926, 2855, 1714, 1591, 1461, 1397, 1364, 1267, 1103, 1017, 842, 760.

Ethyl 4-(phenethylthio)benzoate (**75**)

75
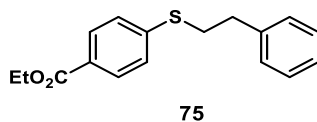
   The product (228 mg, 797 μmol, 80%) was obtained as a red-black oil by applying **GP B** using ethyl 4-chlorobenzoate (155 μL, 1 mmol, 1 eqv.) and butyl 3-mercaptopropionate (160 μL, 1 mmol, 1 eqv.) with PhZnCl•LiCl as the base, with NMP (400 μL) as cosolvent at 60 °C for 4 h catalyzed by **C1** (2 mol%), followed by flash chromatography (14 g SiO$_2$, Hexane).

286.39 g/mol

R_f: 0.27 (95:5 PE:Et$_2$O)

m.p.: Ambient temperature.

^{1}H-NMR (400 MHz, CDCl$_3$, δ): 7.87 (d, J = 8.5 Hz, 2H), 7.27 − 7.21 (m, 4H), 7.19 − 7.12 (m, 3H), 4.29 (q, J = 7.1 Hz, 2H), 3.21 − 3.12 (t, J = 7.8 Hz, 2H), 2.96 − 2.84 (t, J = 7.8 Hz, 2H), 1.31 (t, J = 7.1 Hz, 3H).

^{13}C-NMR (101 MHz, CDCl$_3$, δ): 166.3, 143.5, 139.8, 130.0, 128.6, 128.5, 127.3, 126.7, 126.6, 60.9, 35.2, 33.7, 14.4.

HR-MS (ESI): m/z calc. for [M+Na]$^+$ 309.09197, found 309.09220.

IR (ATR, $\tilde{v}$ [cm^{-1}]): 3060, 3026, 2978, 2929, 1707, 1591, 1490, 1453, 1397, 1364, 1267, 1177, 1103, 1013, 842, 756, 693.

Ethyl 4-((3-butoxy-3-oxopropyl)thio)benzoate (**76**)

76
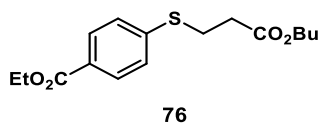
   The product (229 mg, 737 μmol, 74%) was obtained as a red-black oil by applying **GP B** using ethyl 4-chlorobenzoate (155 μL, 1 mmol, 1 eqv.) and butyl 3-mercaptopropionate (160 μL, 1 mmol, 1 eqv.) with PhZnCl•LiCl as the base, with NMP (400 μL) as cosolvent at 60 °C for 4 h catalyzed by **C1** (2 mol%), followed by flash chromatography (23 g SiO$_2$, 5 CV Hexane, gradient to 87:13 Hexane:EtOAc over 4 CV, hold 1 CV, gradient to 8:2 Hexane:EtOAc over 2 CV, hold 2 CV, gradient to 7:3 Hexane over 4 CV, hold 1 CV).

310.41 g/mol

R_f: 0.39 (9:1 Hexane:EtOAc)

m.p.: Ambient temperature.

^{1}H-NMR (400 MHz, CDCl$_3$, δ): 7.88 (d, J = 8.4 Hz, 2H), 7.25 (d, J = 8.4 Hz, 2H), 4.29 (q, J = 7.1 Hz, 2H), 4.03 (t, J = 6.7 Hz, 2H), 3.18 (t, J = 7.4 Hz, 2H), 2.60 (t, J = 7.4 Hz, 2H), 1.60 – 1.50 (m, 2H), 1.32 (t, J = 7.1 Hz, 3H), 0.86 (t, J = 7.4 Hz, 3H).

^{13}C-NMR (101 MHz, CDCl$_3$, δ): 171.53, 166.21, 142.45, 130.03, 127.71, 127.16, 64.82, 60.96, 34.01, 30.59, 27.46, 19.11, 14.34, 13.69.

HR-MS (ESI): m/z calc. for [M+Na]$^+$ 333.11310, found 333.11365.

IR (ATR, $\tilde{v}$ [cm^{-1}]): 2959, 2870, 1710, 1595, 1461, 1397, 1364, 1267, 1177, 1105, 1013, 842, 760.

Ethyl 4-(cyclohexylthio)benzoate (**77**)
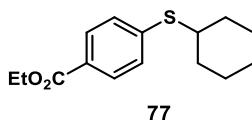
The product (232 mg, 878 µmol, 88%) was obtained as a red-black oil by applying **GP B** using ethyl 4-chlorobenzoate (155 µL, 1 mmol, 1 eqv.) and cyclohexanethiol (120 µL, 1 mmol, 1 eqv.) with PhZnCl•LiCl as the base, with NMP (400 µL) as cosolvent at 60 °C for 4 h catalyzed by **C1** (2 mol%), followed by flash chromatography (23 g SiO$_2$, 5 CV Hexane, gradient to 87:13 Hexane:EtOAc over 8 CV, hold 2 CV, gradient to 8:2 Hexane:EtOAc over 1 CV, hold 2 CV). The analytical data conforms to the reported literature.[S12]

264.38 g/mol

R_f: 0.62 (9:1 Hexane:EtOAc)

m.p.: Ambient temperature.

^{1}H-NMR (400 MHz, CDCl$_3$, δ): 7.93 (d, J = 8.5 Hz, 2H), 7.34 (d, J = 8.5 Hz, 2H), 4.36 (q, J = 7.1 Hz, 2H), 3.35 – 3.22 (m, 1H), 2.09 – 1.98 (m, 2H), 1.85 – 1.74 (m, 2H), 1.67 – 1.58 (m, 1H), 1.50 – 1.11 (m, 8H).

^{13}C-NMR (101 MHz, CDCl$_3$, δ): 166.3, 142.8, 129.8, 128.6, 127.5, 60.9, 45.2, 33.1, 26.0, 25.7, 14.4.

LR-MS (EI): m/z 264, 219, 182, 154, 137, 122, 105, 83.

IR (ATR, $\tilde{v}$ [cm^{-1}]): 2978, 2929, 2851, 1710, 1591, 1446, 1364, 1267, 1174, 1103, 1017, 842, 760, 693.

Ethyl 4-(octan-3-ylthio)benzoate (**78**)

78
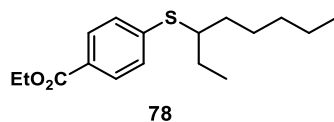
The product (272 mg, 924 µmol, 92%) was obtained as a red-black oil by applying **GP B** using ethyl 4-chlorobenzoate (155 µL, 1 mmol, 1 eqv.) and octane-3-thiol (145 µL, 1 mmol, 1 eqv.) with PhZnCl•LiCl as the base, with NMP (400 µL) as cosolvent at 60 °C for 4 h catalyzed by **C1** (2 mol%), followed by flash chromatography (23 g SiO$_2$, Hexane).

294.45 g/mol

R_f: 0.60 (9:1 Hexane:Et$_2$O)

m.p.: Ambient temperature.

^{1}H-NMR (400 MHz, CDCl$_3$, δ): 7.85 (d, J = 8.5 Hz, 2H), 7.22 (d, J = 8.5 Hz, 2H), 4.28 (q, J = 7.1 Hz, 2H), 2.88 (d, J = 6.3 Hz, 2H), 1.55 (p, J = 6.2 Hz, 1H), 1.46 – 1.33 (m, 3H), 1.31 (t, J = 7.1 Hz, 4H), 1.27 – 1.16 (m, 4H), 0.88 – 0.78 (m, 6H).

^{13}C-NMR (101 MHz, CDCl$_3$, δ): 166.4, 144.8, 129.8, 126.8, 126.4, 60.8, 38.7, 36.5, 32.5, 28.8, 25.7, 22.9, 14.4, 14.1, 10.8.

HR-MS (ESI): m/z calc. for [M+Na]$^+$ 317.15457, found 317.15485.

IR (ATR, $\tilde{v}$ [cm^{-1}]): 2959, 2926, 2858, 1714, 1591, 1461, 1397, 1364, 1267, 1177, 1103, 1017, 842, 760.

Ethyl 4-(benzylthio)benzoate (**79**)

79
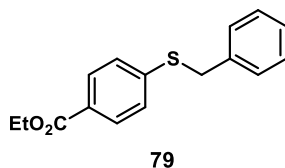
   The product (156 mg, 573 µmol, 57%) was obtained as a brownish solid by applying **GP B** using ethyl 4-chlorobenzoate (155 µL, 1 mmol, 1 eqv.) and benzylthiol (120 µL, 1 mmol, 1 eqv.) with PhZnCl•LiCl as the base, with NMP (400 µL) as cosolvent at 60 °C for 4 h catalyzed by **C1** (2 mol%), followed by flash chromatography (23 g SiO₂, 5CV Hexane, gradient to 9:1 Hexane:EtOAc over 10 CV, hold for 5 CV). The analytical data conforms to the reported literature.[S13]

272.36 g/mol
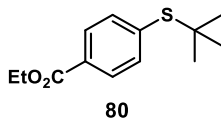
R_f: 0.53 (9:1 Hexane:EtOAc)

m.p.: 65 °C.

¹H-NMR (400 MHz, CDCl₃, δ): 7.84 (d, *J* = 8.5 Hz, 2H), 7.34 – 7.12 (m, 7H), 4.28 (q, *J* = 7.1 Hz, 2H), 4.13 (s, 2H), 1.30 (t, *J* = 7.1 Hz, 3H).

¹³C-NMR (101 MHz, CDCl₃, δ): 166.3, 143.5, 136.4, 129.9, 128.8, 128.7, 127.5, 127.5, 127.1, 60.9, 37.4, 14.3.

LR-MS (EI): m/z 272, 227, 182, 165, 150, 137, 122, 105, 91.

IR (ATR, $\tilde{v}$ [cm⁻¹]): 3026, 2981, 2933, 1699, 1587, 1442, 1397, 1364, 1271, 1185, 1110, 1025, 842, 756, 715, 689.

Ethyl 4-(*tert*-butylthio)benzoate (**80**)

80

   The product (115 mg, 483 µmol, 26%) was obtained as a colourless liquid by applying **GP B** using ethyl 4-chlorobenzoate (155 µL, 1 mmol, 1 eqv.) and tert-butanethiol (110 µL, 1 mmol, 1 eqv.) with PhZnCl•LiCl

as the base, with NMP (400 µL) as cosolvent at 60 °C for 4 h catalyzed by **C1** (2 mol%), followed by preparative TLC (9:1 Hexane:EtOAc).

238.35 g/mol

R_f: 0.69 (Hexane:EtOAc 9:1)
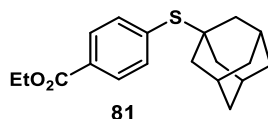
m.p.: Ambient temperature.

1H-NMR (400 MHz, CDCl$_3$, δ): 7.98 (d, J = 8.3 Hz, 2H), 7.59 (d, J = 8.3 Hz, 2H), 4.38 (q, J = 7.1 Hz, 2H), 1.39 (t, J = 7.1 Hz, 3H), 1.31 (s, 9H).

13C-NMR (101 MHz, CDCl$_3$, δ): 166.3, 138.8, 136.8, 130.5, 129.4, 61.1, 46.7, 31.1, 14.3.

HR-MS (ESI): m/z calc. for [M+Na]$^+$ 261.09197, found 261.09196.

IR (ATR, $\tilde{v}$ [cm^{-1}]): 2963, 1714, 1595, 1457, 1394, 1364, 1267, 1107, 1017, 853, 764, 697.

Ethyl 4-(adamant-1-ylthio)benzoate (**81**)

The product (82 mg, 259 µmol, 26%) was obtained as a white solid by applying **GP B** using ethyl 4-chlorobenzoate (155 µL, 1 mmol, 1 eqv.) and adamantane-1-thiol (168 mg, 1 mmol, 1 eqv.) with PhZnCl•LiCl as the base, with NMP (400 µL) as cosolvent at 60 °C for 4 h catalyzed by **C1** (2 mol%), followed by flash chromatography (23 g SiO$_2$, 5 CV Hexane, gradient to 9:1 Hexane:Et$_2$O over 18 CV).

316.46 g/mol

R_f: 0.54 (Hexane:Et$_2$O 9:1)

m.p.: 70 °C.

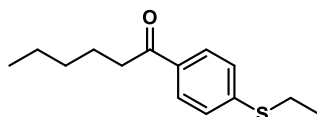**1H-NMR** (400 MHz, CDCl$_3$, δ): 7.97 (d, J = 8.3 Hz, 2H), 7.56 (d, J = 8.3 Hz, 2H), 4.38 (q, J = 7.1 Hz, 2H), 2.04 – 1.97 (m, 3H), 1.82 (d, J = 3.0 Hz, 6H), 1.69 – 1.50 (m, 6H), 1.39 (t, J = 7.1 Hz, 3H).

13C-NMR (101 MHz, CDCl$_3$, δ): 166.3, 137.2, 136.7, 130.4, 129.2, 61.1, 48.9, 43.7, 36.1, 30.0, 14.3.

HR-MS (ESI): m/z calc. for [M+Na]$^+$ 339.13892, found 339.13932.

IR (ATR, $\tilde{v}$ [cm^{-1}]): 2899, 2851, 1714, 1595, 1453, 1394, 1267, 1103, 1017, 853, 760, 697.

4'-(Ethylthio)hexanophenone (**110**)

110

Hexanoic acid *S*-ethyl thioester (**108**)[2] (73 mg, 0.5 mmol, 1.0 eqv.) and **C1** (19 mg, 5 mol%) were dissolved in dry THF (500 µL) in a Schlenk vessel with stirring bar and rubber septum. 4-Chlorophenyl-ZnCl•LiCl (3.6 mL of a 0.25 M solution in THF, 0.9 mmol, 1.8 eqv.) was added via syringe and the resulting reaction mixture stirred for 1.5 h at RT. The mixture was quenched with sat. aq. NH4Cl solution, extracted three times with EtOAc (5 mL each) and dried over MgSO$_4$. The solvent was evaporated under reduced pressure. The crude product was purified by column chromatography (Hexane/Et$_2$O 97.5:2.5) delivered the product as a crystalline solid (74 mg, 312 µmol, 62%).

***R*$_f$**: 0.17 (Hexane/Et$_2$O 97.5:2.5)

m.p.: 51 °C.

^{1}H-NMR (400 MHz, CDCl$_3$, δ): 7.86 (dd, *J* = 8.60, 4.84 Hz, 2 H, Ar-*H*), 7.29 (dd, *J* = 8.60, 4.84 Hz, 2 H, Ar-*H*), 3.02 (q, *J* = 7.38 Hz, 2 H, C*H*$_2$SAr), 2.91 (t, *J* = 7.44 Hz, 2 H, C*H*$_2$COAr), 1.76–1.69 (m, 2 H, C*H*$_2$CH$_2$COAr), 1.39–1.33 (m, 7 H), 0.90 (t, *J* = 7.06 Hz, 3 H).

^{13}C-NMR (101 MHz, CDCl$_3$, δ): 199.8, 144.3, 133.9, 128.7, 126.5, 38.5, 31.7, 26.2, 24.3, 22.7, 14.1 (2 C).

LR-MS (EI): m/z 236, 220, 193, 180, 165, 151, 137, 120, 105, 91, 77.

IR (ATR, $\tilde{v}$ [cm^{-1}]): 3079, 2952, 2866, 1674, 1588, 1465, 1398, 1320, 1256, 1185, 1088, 1055, 1006, 977, 813, 760, 731.

(4-Methoxyphenyl)(phenyl)sulfane (**84**)
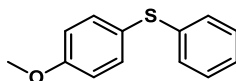
84

Following **GP C**, thiophenol (100 µL, 1.0 mmol, 1.0 eqv.) was coupled with 4-chloroanisole (100 µL, 1.0 mmol, 1.0 eqv.). Isolation by flash chromatography (23 g SiO$_2$, Hexane) delivered the product (191 mg, 883 µmol, 88%) as a colourless oil. The analytical data conforms to the reported literature.[S14]

216.30 g/mol

*R*f: 0.62 (9:1 Hexane:EtOAc)

m.p.: Ambient temperature.

1H-NMR (400 MHz, CDCl$_3$, δ): 7.32 (d, *J* = 8.8 Hz, 2H), 7.19 – 6.94 (m, 5H), 6.80 (d, *J* = 8.8 Hz, 2H), 3.72 (s, 3H).

13C-NMR (101 MHz, CDCl$_3$, δ): 159.9, 138.6, 135.4, 129.0, 128.3, 125.8, 124.4, 115.0, 55.4.

LR-MS (EI): m/z 216, 201, 184, 169, 141, 129, 115, 108, 78.

Diphenylsulfane (**82**)
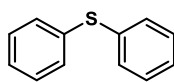
82

Following **GP C**, thiophenol (100 µL, 1.0 mmol, 1.0 eqv.) was coupled with chlorobenzene (100 µL, 1.0 mmol, 1.0 eqv.). Isolation by flash chromatography (23 g SiO$_2$, Hexane) delivered the product (179 mg, 961 µmol, 96%) as a colourless oil. The analytical data conforms to the reported literature.[S14]

186.27 g/mol

*R*f: 0.78 (9:1 Hexane:EtOAc)

m.p.: Ambient temperature.

1H-NMR (400 MHz, CDCl$_3$, δ): 7.51 – 7.46 (m, 4H), 7.44 – 7.38 (m, 4H), 7.38 – 7.32 (m, 2H).

13C-NMR (101 MHz, CDCl$_3$, δ): 135.9, 131.1, 129.3, 127.1.

LR-MS (EI): m/z 186, 171, 154, 78.

Ethyl 4-(phenylthio)benzoate (**83**)

83
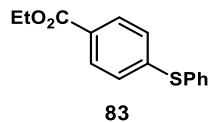
Following **GP C**, thiophenol (100 µL, 1.0 mmol, 1.0 eqv.) was coupled with ethyl 4-chlorobenzoate (155 µL, 1.0 mmol, 1.0 eqv.). Isolation by flash chromatography (23 g SiO2, 3 CV Hexane, then gradient to 9:1 Hexane:EtOAc over 11 CV) delivered the product (113 mg, 437 µmol, 44%) as a colourless oil. The analytical data conforms to the reported literature.[S15]

258.34 g/mol

R_f: 0.56 (9:1 Hexane:EtOAc)

m.p.: Ambient temperature.

1H-NMR (400 MHz, CDCl$_3$, δ): 7.81 (d, J = 8.5 Hz, 2H), 7.41 – 7.34 (m, 2H), 7.31 – 7.25 (m, 3H), 7.12 (d, J = 8.5 Hz, 2H), 4.26 (q, J = 7.1 Hz, 2H), 1.27 (t, J = 7.1 Hz, 3H).

13C-NMR (101 MHz, CDCl$_3$, δ): 166.2, 144.1, 133.6, 132.6, 130.1, 129.6, 128.6, 127.9, 60.9, 14.4.

LR-MS (EI): m/z 258, 243, 230, 213, 198, 184, 152, 122, 105, 91, 78.

(2,4-dimethylphenyl)(4-methoxyphenyl)sulfane (**86**)

86
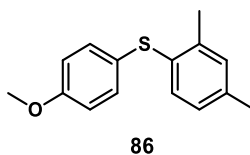
Following **GP C**, 2,4-dimethylthiophenol (135 µL, 1.0 mmol, 1.0 eqv.) was coupled with 4-chloroanisole (155 µL, 1.0 mmol, 1.0 eqv.). Isolation by flash chromatography (23 g SiO2, 18 CV Hexane) delivered the product (162 mg, 663 µmol, 66%) as a colourless oil. The analytical data conforms to the reported literature.[S16]

244.35 g/mol

R_f: 0.26 (Hexane)

m.p.: Ambient temperature.

^{1}H-NMR (400 MHz, CDCl$_3$, δ): 7.23– 7.20 (m, 2H), 7.00 – 6.99 (m, 2H), 6.88 – 6.85 (m, 1H), 6.82 – 6.79 (m, 2H), 3.73 (s, 3H), 2.32 (s, 3H), 2.25 (s, 3H).

^{13}C-NMR (101 MHz, CDCl$_3$, δ): 159.1, 138.2, 136.8, 133.2, 132.6, 131.3, 131.0, 127.4, 126.0, 114.9, 55.4, 21.0, 20.4.

LR-MS (EI): m/z 244, 229, 212, 197, 179, 171, 165, 136, 108, 91, 77.

<u>(2-methylphenyl)(4-methoxyphenyl)sulfane (**85**)</u>

85

Following **GP C**, 2 -methylthiophenol (118 µL, 1.0 mmol, 1.0 eqv.) was coupled with 4-chloroanisole (155 µL, 1.0 mmol, 1.0 eqv.). Isolation by flash chromatography (23 g SiO2, 18 CV Hexane, then gradient to 1:1 Hexane:EtOAc over 7 CV) delivered the product (162 mg, 703 µmol, 70%) as a colorless oil. The analytical data conforms to the reported literature.[S17]

230.33 g/mol

R$_f$: 0.28 (Hexane)

m.p.: Ambient temperature.

^{1}H-NMR (400 MHz, CDCl$_3$, δ): 7.29-7.25 (m, 2H), 7.12 – 7.10 (m, 1H), 7.05 – 6.97 (m, 2H), 6.94 – 6.92 (m, 1H), 6.84 – 6.80 (m, 2H), 3.74 (s, 3H), 2.42 (s, 3H), 2.37 (s, 3H).

^{13}C-NMR (101 MHz, CDCl$_3$, δ): 159.6, 137.2, 137.1, 134.7, 130.3, 129.2, 126.6, 126.2, 124.5, 115.1, 55.4, 20.4.

LR-MS (EI): m/z 230, 215, 198, 183, 171, 165, 153, 139, 122, 108, 91, 78.

4.4.3.2. Synthesis of biaryls

4-Fluoro-4'-methoxy-1,1'-biphenyl (**100**)

100
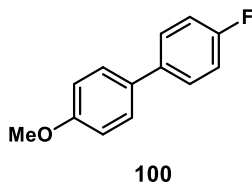
Using 4-methoxybenzenethiol (125 μL, 1.00 mmol, 1 equiv.) and 4-fluorophenylmagnesium bromide lithium chloride complex (1.23 M in THF; 1.79 mL, 2.20 mmol, 2.2 equiv.), **GP D** was followed. Purification by flash column chromatography (hexane to hexane:ethyl acetate 99:1 to 9:1) yielded the product (107 mg, 529 μmol, 53 %) as a white solid. The analytical data conforms to the reported literature.[S18]

202.23 g/mol

R_f: 0.59 (9:1 PE:EtOAc)

m.p.: 89 °C (Lit.: 87-89 °C[18])

1H-NMR (400 MHz, CDCl₃, δ): 7.52 − 7.43 (m, 4H), 7.10 (t, J = 8.7 Hz, 2H), 6.97 (d, J = 8.8 Hz, 2H), 3.85 (s, 3H).

13C-NMR (101 MHz, CDCl₃, δ): 162.1 (d, J = 245.4 Hz), 159.1, 137.0 (d, J = 3.1 Hz), 132.8, 128.2 (d, J = 8.0 Hz), 128.0, 115.5 (d, J = 21.3 Hz), 114.3, 55.4.

19F-NMR (376 MHz, CDCl₃, δ): -116.84 (m).

LR-MS (EI): m/z 202, 187, 170, 159, 133, 101.

2-Methyl-4'-methoxy-1,1'-biphenyl (**101**)
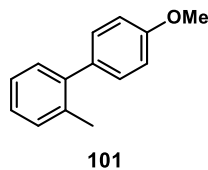
101

Using 2-methylbenzenethiol (118 μL, 1.00 mmol, 1 equiv.) and 4-methoxyphenylmagnesium bromide lithium chloride complex (0.867 M in THF; 2.54 mL, 2.20 mmol, 2.2 equiv.), **GP D** was followed. Purification

by flash-column chromatography (hexane to hexane:ethyl acetate 9:1) yielded the product (163 mg, 822 µmol, 82 %) as a colorless oil. The analytical data conforms to the reported literature.[S 18]
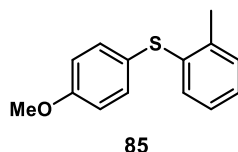
198.27 g/mol

R_f: 0.27 (Hexane)

m.p.: Ambient temperature.

¹H-NMR (400 MHz, CDCl$_3$, δ): 7.24 – 7.07 (m, 6H), 6.92 – 6.80 (m, 2H), 3.75 (s, 3H), 2.25 – 2.10 (m, 3H).

¹³C-NMR (101 MHz, CDCl$_3$, δ): 158.5, 141.6, 135.5, 134.4, 130.3, 129.9, 129.5, 127.0, 125.8, 113.9, 113.5, 55.3, 20.6.

LR-MS (EI): m/z 198, 183, 167, 155, 139, 128, 115.

4-methoxy-1,1'-biphenyl (**102**)
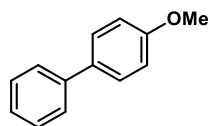
102

Using thiophenol (102 µL, 1.00 mmol, 1 equiv.) and 4-methoxyphenylmagnesium bromide lithium chloride complex (0.867 M in THF; 2.54 mL, 2.20 mmol, 2.2 equiv.), **GP D** was followed. Purification by preparative TLC (hexane) yielded the product (176 mg, 953 µmol, 95 %) as a white solid. The analytical data conforms to the reported literature.[S19]

184.24 g/mol

R_f: 0.69 (Hexane:EtOAc 9:1)

m.p.: 84 °C (Lit.[19]: 87-88 °C)

¹H-NMR (400 MHz, CDCl$_3$, δ): 7.61 – 7.52 (m, 4H), 7.46 – 7.39 (m, 2H), 7.34 – 7.29 (m, 1H), 6.99 (d, J = 8.8 Hz, 2H), 3.86 (s, 3H).

¹³C-NMR (101 MHz, CDCl$_3$, δ): 159.2, 140.8, 133.8, 128.7, 128.2, 126.8, 126.7, 114.2, 55.4.

LR-MS (EI): m/z 184, 169, 152, 141, 126, 115.

2-methoxy-6-phenylnaphthalene (**104**)
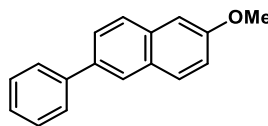
104

Using thiophenol (100 µL, 1 mmol, 1 equiv.) and 6-Methoxynaphth-2-ylmagnesium bromide lithium chloride complex (1.0 M in THF; 2.2 mL, 2.2 mmol, 2.2 equiv.), **GP D** was followed. Purification by flash chromatography (23 g SiO$_2$, 6 CV hexane, gradient to 95:5 hexane:EtOAc over 3 CV, hold 8 CV, gradient to 9:1 hexane:EtOAc over 4 CV, hold 2 CV) yielded a mixture (141 mg) containing the product and 2-methoxynaphthalene (identified by GC/MS). The mixture was placed in high vacuum at 40 °C overnight to remove the majority of the contaminant. DCE (30 µL, 37.5 mg, 379 µmol) was added to the impure compound as an internal standard, and the mixture dissolved in 1400 µL CDCl$_3$.

The sample concentration was determined by the formula:

$$c_P = I_P/I_S * N_S/N_P * c_S$$

$$= 3/2.84 * 4/3 * (379\ \mu mol/1400\ \mu L) = 0.378\ M$$

$$n_P = 529\ \mu mol = 0.378\ M * 1400\ \mu L$$

giving a NMR yield of 53%.

N: Nuclei count

I: NMR integral

P: Product

S: Standard

234.30 g/mol

R_f: 0.59 (9:1 Hexane:EtOAc)

LR-MS (ESI): m/z 234, 219, 204, 191, 176, 165, 152, 139, 128, 117, 110.

4'-Methoxy-2,4-dimethyl-1,1'-biphenyl (**105**)

105
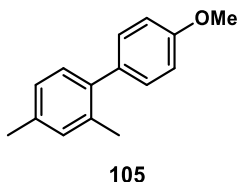
Using 2,4-dimethylbenzenethiol (135 μL, 1.00 mmol, 1 equiv.) and *para*-anisylmagnesium bromide lithium chloride complex (0.867 M in THF; 2.54 mL, 2.20 mmol, 2.2 equiv.), **GP D** was followed. Purification by flash chromatography (23 g SiO_2, gradient from Hexane to 95:5 Hexane:EtOAc over 18 CV) yielded the product (83 mg, 389 μmol, 39%) as a colourless oil. The analytical data conforms to the reported literature.[S20]

212.29 g/mol

R_f: 0.28 (Hexane)

m.p.: 52 °C.

1H-NMR (400 MHz, CDCl$_3$, δ): 7.19 – 7.13 (m, 2H), 7.06 – 6.99 (m, 2H), 6.98 – 6.93 (m, 1H), 6.89 – 6.83 (m, 2H), 3.76 (s, 3H), 2.27 (s, 3H), 2.17 (s, 3H).

13C-NMR (101 MHz, CDCl$_3$, δ): 158.4, 138.7, 136.6, 135.3, 134.4, 131.1, 130.3, 129.9, 126.5, 113.5, 55.3, 21.2, 20.5.

LR-MS (EI): m/z 212, 197, 181, 165, 154, 171, 128, 115, 105.

5-(*o*-tolyl)benzo[*d*][1,3]dioxole (**106**)
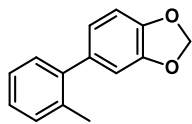
106

Using 2-methylbenzenethiol (118 µL, 1.00 mmol, 1 equiv.) and 3,4-(methylenedioxy)-magnesium bromide lithium chloride complex (1.50 M in THF; 1.47 mL, 2.20 mmol, 2.2 equiv.), **GP D** was followed. Purification by flash chromatography (23 g SiO$_2$, 1 CV Hexane, gradient from Hexane to 90:10 Hexane:EtOAc over 3 CV, hold for 6 CV) yielded the product (97 mg, 461 µmol, 46%) as a colourless oil. The analytical data conforms to the reported literature.[S21]

212.25 g/mol

R$_f$: 0.48 (30:1 Hexane:EtOAc)

m.p.: Ambient temperature.

^{1}H-NMR (400 MHz, CDCl$_3$, δ): 7.42–7.37 (m, 4H), 7.04–6.92 (m, 3H), 6.16 (s, 2H), 2.45 (s, 3H).

^{13}C-NMR (101 MHz, CDCl$_3$, δ): 147.4, 146.5, 141.7, 136.0, 135.6, 130.4, 129.9,127.3, 125.9, 122.6, 109.9, 108.1, 101.1, 20.6.

LR-MS (EI): 212, 181, 165, 153, 141, 139, 128, 115, 105, 91, 76.

2-(4-methoxyphenyl)naphthalene (**99**)
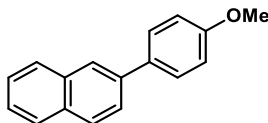
99

Using 2-naphtylthiol (160.3 mg, 1.00 mmol, 1 equiv.) and 4-methoxymagnesium bromide lithium chloride complex (0.867 M in THF; 2.54 mL, 2.20 mmol, 2.2 equiv.), **GP D** was followed. Purification by flash chromatography (23 g SiO$_2$, 15 CV Hexane, gradient from Hexane to 70:30 Hexane:EtOAc over 10 CV) and additional recrystallization in pure Hexane yielded the product (190 mg, 810 µmol, 81%) as a crystalline solid. The analytical data conforms to the reported literature.[S22]

234.30 g/mol

R_f: 0.37 (30:1 Hexane:EtOAc)

m.p.: 136 °C (Lit.[S22]: 130-132 °C)

1H-NMR (400 MHz, CDCl3, δ): 7.99 (s, 1H), 7.90–7.84 (m, 3H), 7.72 (dd, J = 8.6, 1.8 Hz, 1H), 7.66 (m, 2H), 7.52–7.43 (m, 2H), 7.03 (m, 2H), 3.88 (s, 3H).

13C-NMR (101 MHz, CDCl3, δ): 159.3, 138.2, 133.8, 133.7, 132.3, 128.4, 128.3, 128.1, 127.6 126.2, 125.7, 125.4, 125.0, 114.3, 55.4,

LR-MS (EI): 234, 219, 202, 191,189, 165, 117, 101, 95, 88, 82.

4-(benzyloxy)-1,1'-biphenyl (**107**)

44
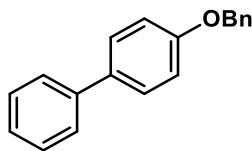
  Using thiophenol (50 µL, 0.50 mmol, 1 equiv.) and 4-benzyloxyphenylmagnesium bromide lithium chloride complex (1.0 M in THF; 1.1 mL, 1.1 mmol, 2.2 equiv.), **GP D** was followed. Purification by flash chromatography yielded a mixture of the product contaminated with benzyl phenyl ether (identified by GC/MS) as a yellowish solid (m_{total} = 161 mg). The mixture was analyzed by 1H-NMR to determine the relative composition R using the benzylic/methylene proton signal sets from both compounds.

$$R = n_P/n_C = (I_P/N_P)/(I_C/N_C)= 2.00 / 1.57 = 1.27$$

$$m_{total} = m_p + m_c$$

  from which follows:

$$m_{total} = M_p*n_p + M_c*(n_p/R)$$

rearrangement gives:

$$n_P = m_{total}/((M_c/R)+M_p) = 161 \text{ mg}/((184.24 \text{ mg mmol}^{-1} / 1.27) + 260.34 \text{ mg mmol}^{-1}) = 397 \text{ μmol}$$

giving a NMR yield of 79%.

N: Nuclei count

I: NMR integral

P: Product

C: Contaminant

260.34 g/mol

R_f: 0.62 (9:1 Hexane:EtOAc)

LR-MS (EI): m/z 260, 244, 207, 182, 170, 165, 154, 141, 121, 115, 91.

_N_,_N_-dimethyl-[1,1'-biphenyl]-4-amine (**103**)
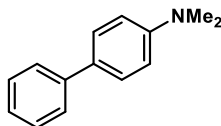
103

Using thiophenol (100 μL, 1.00 mmol, 1 equiv.) and _N_,_N_-dimethyl-4-aminophenylmagnesium bromide lithium chloride complex (1.0 M in THF; 2.2 mL, 2.20 mmol, 2.2 equiv.), **GP D** was followed. Purification by flash chromatography (23 g SiO_2, 2 CV hexane, gradient to 1:1 hexane:EtOAc over 13 CV, hold 2 CV) yielded the product (193 mg, 978 μmol, 98%) as a white solid. The analytical data conforms to the reported literature.[S23]

197.28 g/mol

R_f: 0.56 (9:1 Hexane:EtOAc)

**m.p.**: 120 °C (Lit.[S24]: 121 – 122 °C)

¹H-NMR (300 MHz, CDCl₃, δ): 7.81 – 7.67 (m, 4H), 7.65 – 7.53 (m, 2H), 7.51 – 7.38 (m, 1H), 6.97 (dd, *J* = 8.9, 2.0 Hz, 2H), 3.13 (s, 6H).

¹³C-NMR (75 MHz, CDCl₃, δ): 150.2, 141.4, 129.4, 128.9, 127.9, 126.5, 126.2, 113.0, 40.7.

LR-MS (EI): m/z 197, 181, 167, 152, 139, 127, 115, 98, 90.

4.4.3.3. Synthesis of starting materials and calibration standards

Heptyl(phenyl)sulfane (**40**) (independent synthesis)

40
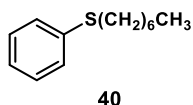
A 50 mL RBF with stirring bar under air was charged with thiophenol (513 µL, 5 mmol, 1 eqv.), heptyl bromide (785 µL, 5 mmol, 1 eqv.) and K₂CO₃ (1.04 g, 7.5 mmol, 1.5 eqv), followed by addition of dist. acetone (20 mL). The reaction vessel was fitted with a glass stopper and stirred for 18 h at RT. K₂CO₃ was removed by vacuum filtration over a glass frit and acetone was removed by rotary evaporation to give the product as a colourless oil.

Analytical data as above.

Indometacin *O*-Ethyl ester (**SM-B2**)
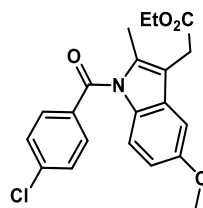
SM-B2

In a 25 mL RBF with stirring bar, Indometacin (647 mg, 1.81 mmol, 1 eqv.) and *N,N*-Dimethyl-4-aminopyridine (22 mg, 181 µmol, 10 mol%) were dissolved in DCM (9 mL) and EtOH (400 µL) followed by the addition of *N,N'*-Diisopropylcarbodiimide (280 µL, 1.81 mmol, 1 eqv.). The resulting mixture was stirred for 16 h at room temperature. The precipitate was removed by filtration and the yellow filtrate freed from solvent and then filtered over SiO₂ using DCM as the eluent. The solvent was removed to give the ethyl ester product as a light yellow solid (679 mg, 1.76 mmol, 97%). The analytical data conforms to the reported literature.[S25]

385.84 g/mol

R$_f$: 0.39 (8:2 hexane:Et$_2$O)

m.p.: 97 °C.

^{1}H-NMR (400 MHz, CDCl$_3$, δ): 7.66 (m, 2H), 7.47 (m, 2H), 6.97 (d, J = 2.5 Hz, 1H), 6.88 (d, J = 9.0 Hz, 1H), 6.67 (dd, J = 9.0 Hz, 2.5 Hz, 1H), 4.16 (q, J = 7.1 Hz, 2H), 3.84 (s, 3H), 3.65 (s, 2H), 2.38 (s, 3H), 1.26 (t, J = 7.1 Hz, 3H).

^{13}C-NMR (101 MHz, CDCl$_3$, δ): 135.3, 130.2, 129.6, 125.2, 121.9, 120.3, 110.3, 100.7, 33.1.

LR-MS (EI): 385, 371, 351, 337, 321, 299, 278, 264, 247, 234, 218, 207, 174, 139, 130, 11, 105, 91, 77.

10-Ethyl-2-chlorophenothiazine (**SM56**)

SM56

2-Chlorophenothiazine (2.38 g, 10.18 mmol) was dissolved in 30 mL DMF with stirring under air, followed by the addition of NaOH pellets (1.22 g, 30.55 mmol, 3 eqv.). The resulting reaction mixture was stirred for 1 h at RT, followed by the addition of EtI (1.22 mL, 15.28 mmol, 1.5 eqv.). A slight exotherm reaction resulted and the mixture was stirred for 18 h at RT. The reaction mixture was quenched with brine (50 mL) and extracted with diethyl ether (2 x 50 mL). The aqueous phase appears bluish and the organic phase deep dark red, which can be hard to distinguish. The combined organic phases were dried over MgSO$_4$ and adsorbed on SiO$_2$ (6 g), followed by vacuum filtration over SiO$_2$ (80 g) with hexane (500 mL) and hexane/diethyl ether 95:5 (250 mL). All the collected filtrate was freed from solvent to give a white solid (1.2 g, 4.58 mmol, 45%).

261.77 g/mol

R$_f$: 0.34 (hexane)

m.p.: 121 °C (Lit[S26]: 120 °C).

---

¹H-NMR (400 MHz, CDCl₃, δ): 7.12 – 7.03 (m, 1H), 7.03 (dd, *J* = 7.7, 1.5 Hz, 1H), 6.93 (d, *J* = 8.1 Hz, 1H), 6.89 – 6.76 (m, 3H), 6.74 (d, *J* = 2.0 Hz, 1H), 3.81 (s br, 2H), 1.34 (t, *J* = 7.0 Hz, 3H).

¹³C-NMR (101 MHz, CDCl₃, δ): 146.2, 144.3, 133.2, 127.8, 127.4, 124.2, 122.9, 122.8, 122.1, 115.4, 41.9, 12.9.

HR-MS (ESI): m/z calc. for [M]⁺ 261.03735, found 261.03758.

IR (ATR, $\tilde{v}$ [cm⁻¹]): 2974, 2862, 1561, 1442, 1401, 1319, 1282, 1248, 1125, 1095, 1036, 950, 916, 861, 812, 752, 678.

4-Chloro-*N*-methylacetanilide (**SM46**)

SM46
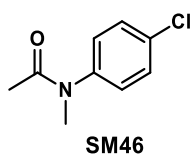
According to a known procedure[27], 4-Chloroacetanilide (5.00 g, 29.48 mmol) was dissolved in freshly distilled THF (50 mL) under stirring in an Ar-purged reaction vessel. The THF solution was sparged with Ar for 15 min, followed by the careful portionwise addition of NaH (1.49 g of a 57% w/w oil dispersion, 35.38 mmol, 1.2 eqv.) with ice-bath cooling (Caution: gas evolution). After complete addition, methyl iodide (2.20 mL, 35.38 mmol, 1.2 eqv.) was added dropwise with ice-bath cooling and stirred after complete addition for a further 30 min at the same temperature. The ice-bath was removed and the reaction stirred for 1 d at RT. The reaction mixture was diluted with EtOAc (20 mL) washed with sat. aq. NH₄Cl (2 x 25 mL), the organic phase dried over MgSO₄ and the solvent removed to give a crude yellow oil, which solidified at -20 °C within a few hours. The still-cold solid was washed with cold water (20 mL) over a fritted funnel and then thouroughly dried to yield a yellowish solid (3.84 g, m.p. 85 °C) which was recrystallized from boiling hexane (20 mL, the hot clear hexane solution is decanted off from a yellow oil into a hot beaker) to give the product as colourless plates (2.53 g, 13.77 mmol, 47%) after cooling to RT. The analytical data conforms to the reported literature.

183.64 g/mol

*R*f: 0.27 (PE:EtOAc 1:1)

---

m.p.: 92 °C (Lit.[S28]: 91 °C).

^{1}H-NMR (400 MHz, CDCl$_3$, δ): 7.31 (d, J = 8.5 Hz, 2H), 7.08 (d, J = 8.6 Hz, 2H), 3.16 (s, 3H), 1.79 (s, 3H).

^{13}C-NMR (101 MHz, CDCl$_3$, δ): 170.2, 143.1, 133.4, 129.9, 128.4, 37.1, 22.3.

GC-MS (EI): m/z 183.1, 168, 149, 141, 111.

5-Chloro-1-methylindole (**SM51**)

SM51

Sodium hydride (300 mg of 60% w/w mineral oil suspension, 7.5 mmol, 1.5 eqv.) was added in portions to a stirred solution of 5-chloroindole (755 mg, 5.0 mmol, 1 eqv.) in dry THF (17 mL) in a 50 mL Schlenk flask at 0 °C. After complete addition, the reaction mixture is stirred for 10 min at the same temperature. Methyl iodide (405 µL, 6.5 mmol, 1.3 eqv.) was added via syringe at the same temperature and the reaction mixture stirred for 16 h at room temperature. The reaction mixture was cooled to 0 °C and quenched by addition of water (10 mL). The mixture was extracted with Et$_2$O (3 x 10 mL), the combined organic phases were dried *in vacuo*. The resulting yellow oil was taken up in a mixture of hexane/Et$_2$O (8:2 v/v), filtered over a pad SiO$_2$ and freed from solvent *in vacuo* to give the product (662 mg, 4.0 mmol, 80%) as a yellow liquid.

165.62 g/mol

R_f: 0.71 (PE:Et$_2$O 8:2)

m.p.: Ambient temperature.

^{1}H-NMR (400 MHz, CDCl$_3$, δ): 7.59 (dd, J = 0.5 Hz, 1.9 Hz, 1H), 7.23 (d, J = 8.7 Hz, 1H), 7.17 (dd, J = 1.9 Hz, 8.7 Hz, 1H), 7.07 (d, J = 3.1 Hz, 1H), 6.43 (dd, J = 3.1 Hz, 0.5 Hz, 1H), 3.78 (s, 3H).

^{13}C-NMR (101 MHz, CDCl$_3$, δ): 135.3, 130.2, 129.6, 125.2, 121.9, 120.3, 110.3, 100.7, 33.1.
GC-MS (EI): m/z 165.1, 150.1, 128.1.

S-acetyl-BCP-1-thiol (**128**)
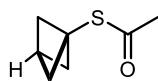
128

Tetrahalide **123** (2.08 g of a 96% purity material [2.00 g pure material], 6.74 mmol, Ark Pharm) was placed in a 50 mL flame-dried assembly of a three-necked RBF with stirring bar, dropping funnel and argon inlet. The starting material was suspended in 3 mL of dry *n*-Pentane, cooled to -84 °C (stirring can become problematic), followed by the addition of MeLi (8.5 mL of a 1.6 M solution in Et$_2$O, 2.02 eqv., Aldrich) under stirring *via* the dropping funnel. The mixture was stirred for 15 min at the same temperature, then the cooling bath was replaced with an ice-water bath and the mixture was stirred for 1.5. The product was then distilled off *in vacuo* using a small distillation bridge (air-cooled) leading to the receiving flask which was cooled to -84 °C.

The ether solution of the propellane intermediate was assayed with quantitative NMR, giving a concentration of 320 mM. A part of the propellane solution (8 mL, 2.56 mmol) was transferred to a Schlenk flask under Ar and then treated with thioacetic acid (180 µL, 2.56 mmol, 1.0 eqv.). The reaction mixture was stirred at RT for 15 min and the remaining ether was carefully distilled off by rotary evaporation. The final product (341 mg, 2.40 mmol, 94%) is a highly volatile colourless liquid with a sharp odour.

142.22 g/mol

m.p.: Ambient temperature.

^{1}H-NMR (400 MHz, CDCl3, δ): 2.73 (s, 1H), 2.19 (s, 3H), 2.13 (s, 6H).

^{13}C-NMR (101 MHz, CDCl3, δ): 196.6, 54.5, 42.0, 31.5, 31.2.
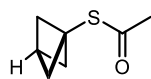
128
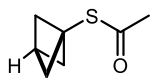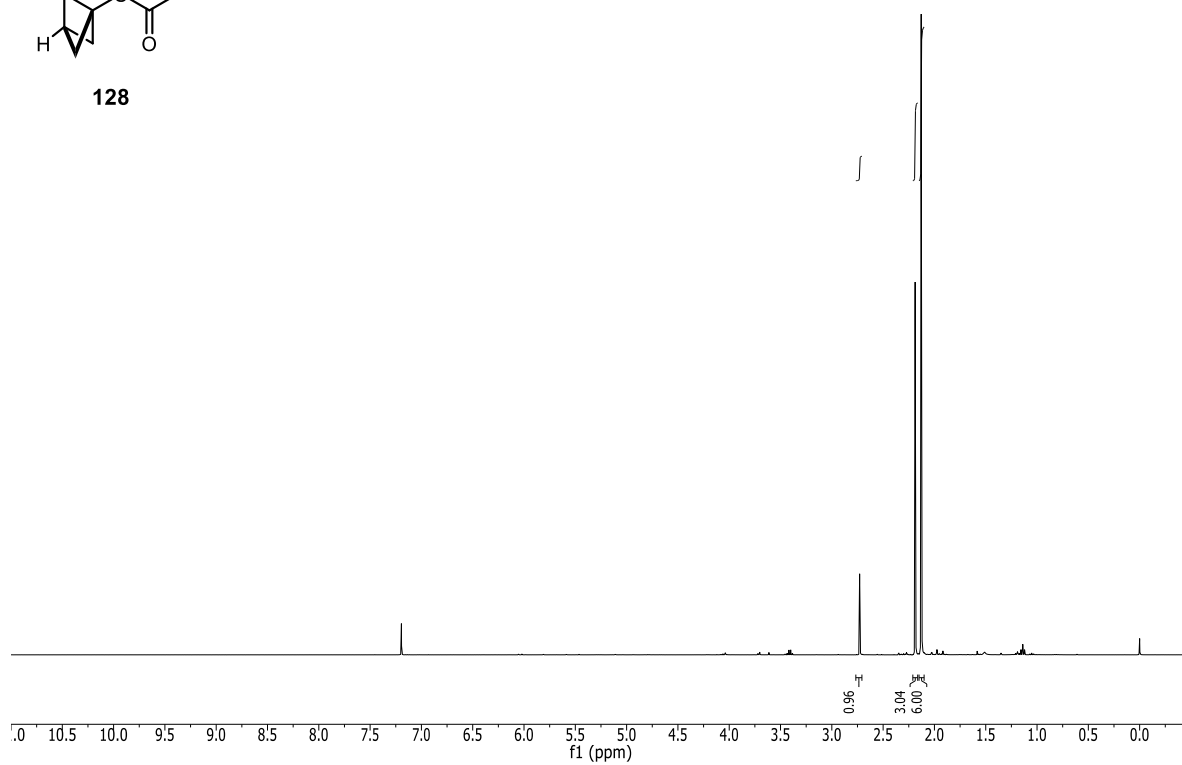
128
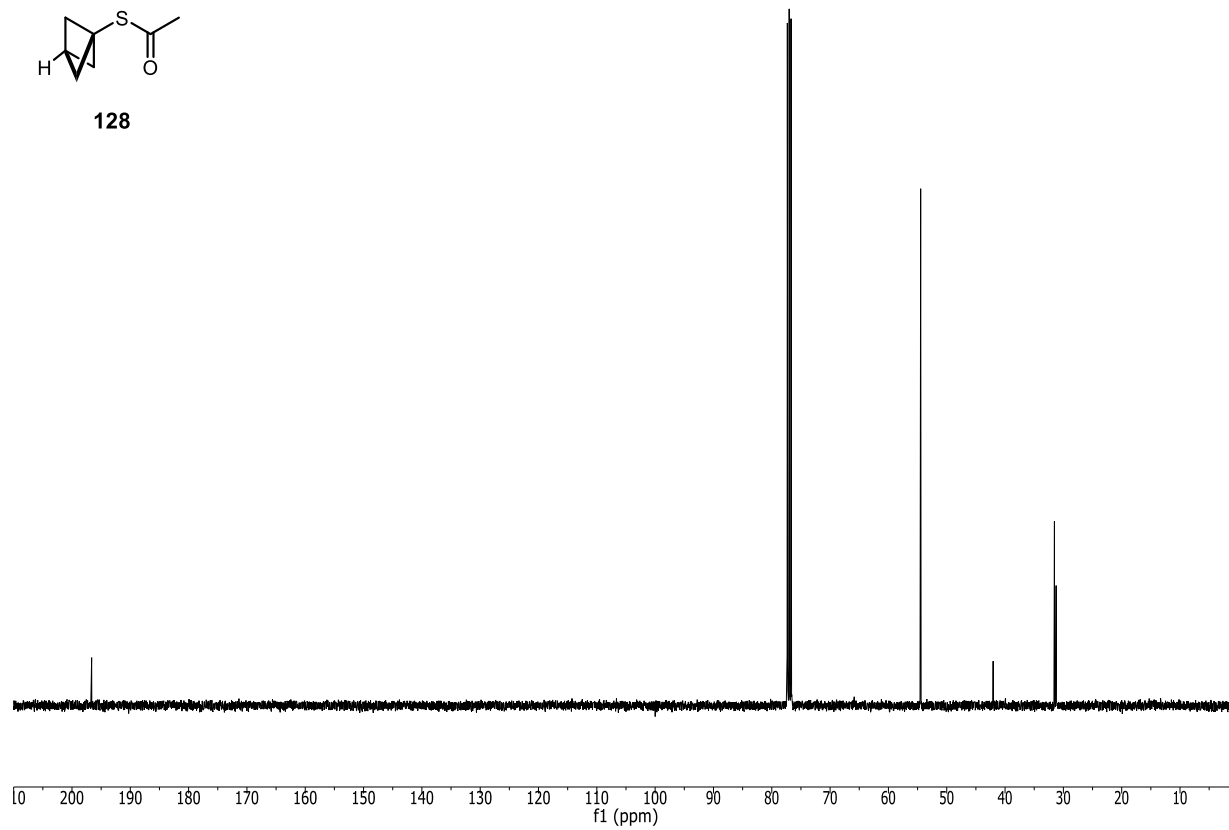
4.4.3.5. Computational details

The calculations were carried out at the B3LYP/6-31G* level of theory using ORCA software.

A typical approach in the literature concerning modeling of homogeneous catalytic species by DFT is to replace transition metal core electrons by an effective potential (termed effective core potential, ECP) as it saves computational time and can reflect relativistic effects, but this was not carried out here since attempted geometry optimizations failed with the LANL2DZ ECP for Ni. Dispersion and solvation interactions were not calculated to save computational effort. Initial geometry optimizations using the PM3 semi-empirical model were carried out starting from manually edited crystal structures (for Ni complexes) or from manually built pre-optimized models. Frequency analysis was carried out after geometry optimization to ensure a local minimum has been found. The obtained structures were visualized with the PYMOL software package.

The modeling results below for complexes **142** – **145** show the respective structural model, followed by atomic coordinates in the xyz format and the total energy in hartrees after corrections obtained from frequency analysis. $ZnCl_2$ and MeSZnCl were modeled similarly, but the results are not shown here explictely for brevity.

Modeling results for complex **142**
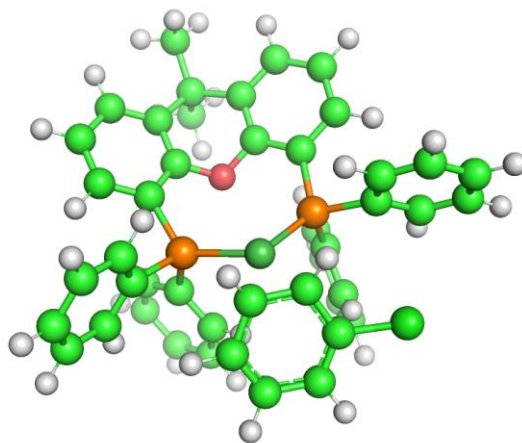
*Supplementary Figure 1: Structural model of complex **142** from the generated xyz file.*

```
Ni       0.430955      -1.033040       0.767956

P       -1.709364      -0.936444       0.220994
```

P	1.613351	0.725088	0.133706
O	−1.080813	1.843683	−0.283682
C	−2.327695	1.784483	0.304213
C	−2.817388	0.508853	0.591558
C	−4.100278	0.440154	1.155991
H	−4.539735	−0.524060	1.384688
C	−4.810204	1.604424	1.450334
H	−5.798612	1.531773	1.895693
C	−4.263134	2.861461	1.184210
H	−4.830913	3.751254	1.436130
C	−3.001293	2.974772	0.594403
C	−2.301433	4.285473	0.209923
C	−0.807571	4.087168	0.504759
C	−0.259138	2.830548	0.222531
C	1.077135	2.484014	0.436540
C	1.916755	3.500808	0.918736
H	2.966064	3.295592	1.093240
C	1.411495	4.768777	1.202497
H	2.076812	5.537398	1.585949
C	0.059477	5.059251	1.008046
H	−0.311904	6.049769	1.250144
C	−2.482758	4.516056	−1.318417
H	−3.545679	4.626256	−1.562503
H	−2.084399	3.677340	−1.896494

H	−1.958595	5.427300	−1.628871
C	−2.882394	5.491353	0.963015
H	−3.944380	5.618158	0.729986
H	−2.382592	6.415463	0.656159
H	−2.776246	5.384195	2.047714
C	−1.954961	−1.151970	−1.600354
C	−0.966993	−1.826397	−2.334162
H	−0.081329	−2.201606	−1.830593
C	−1.108425	−2.016736	−3.709270
H	−0.328909	−2.535384	−4.260437
C	−2.235672	−1.530610	−4.372638
H	−2.341958	−1.671985	−5.445108
C	−3.223665	−0.856294	−3.653201
H	−4.103843	−0.471863	−4.162489
C	−3.085299	−0.669426	−2.277485
H	−3.860957	−0.140498	−1.731869
C	−2.737736	−2.292859	0.948976
C	−2.828615	−2.359109	2.349896
H	−2.336725	−1.600925	2.955327
C	−3.545047	−3.378645	2.973583
H	−3.606203	−3.410855	4.058314
C	−4.176337	−4.360480	2.204755
H	−4.729851	−5.160976	2.688337
C	−4.090306	−4.307132	0.813775

H	−4.579034	−5.066647	0.208634
C	−3.379143	−3.278747	0.188762
H	−3.318628	−3.250639	−0.894279
C	1.924336	0.682580	−1.688305
C	2.546311	−0.457720	−2.226507
H	2.871655	−1.259080	−1.570992
C	2.760993	−0.567103	−3.599889
H	3.253077	−1.451728	−3.996089
C	2.347691	0.452417	−4.460266
H	2.510911	0.364708	−5.531265
C	1.727632	1.586030	−3.935445
H	1.405762	2.387272	−4.595789
C	1.521020	1.703115	−2.559649
H	1.048074	2.597942	−2.168543
C	3.306678	0.833919	0.867023
C	4.471780	1.081790	0.130592
H	4.420809	1.177952	−0.949013
C	5.706190	1.199430	0.772903
H	6.601699	1.383524	0.184834
C	5.791788	1.082604	2.160327
H	6.753755	1.171539	2.658168
C	4.634319	0.850022	2.906347
H	4.690433	0.760618	3.988126
C	3.403982	0.725991	2.263503

H	2.507083	0.545061	2.851961
H	-0.028580	-2.709886	2.517766
C	0.481194	-2.824360	1.558532
C	2.318675	-4.040732	-0.246874
C	1.826887	-2.278528	1.421787
C	0.129296	-3.997526	0.800327
C	0.991688	-4.549832	-0.108503
C	2.709708	-2.985483	0.530960
H	2.307615	-1.807935	2.278234
H	-0.843297	-4.451169	0.964605
H	0.699141	-5.420927	-0.689257
H	3.030743	-4.530680	-0.903142
Cl	4.419495	-2.510889	0.502465

-4463.378363 hartrees

Modeling results for complex **143**
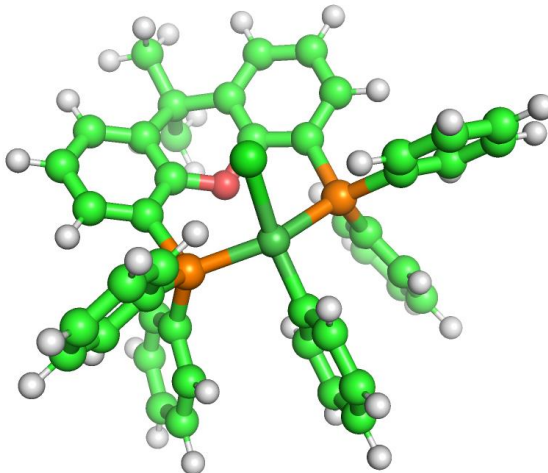
*Supplementary Figure 2: Structural model of complex **143** from the generated xyz file.*

```
Cl     -0.005044      0.718310     -2.557422

Ni     -0.003046     -0.681167     -0.705744

C      -0.008646     -2.358273      0.121026

C      -0.025422     -2.705474      1.478314

C      -0.028990     -4.040989      1.894258

H      -0.042026     -4.270406      2.957853

C      -0.015183     -5.071655      0.954433

H      -0.017841     -6.110945      1.274330

C       0.001995     -4.751526     -0.405459

H       0.013129     -5.543167     -1.151960

C       0.005381     -3.414606     -0.813532

P       2.122274     -0.265998     -0.257210

C       3.442833     -0.765245     -1.443914

C       3.114183     -0.864953     -2.805683

H       2.104881     -0.632929     -3.130003

C       4.083626     -1.236959     -3.737323

H       3.815054     -1.308961     -4.787750
```

C	5.388056	−1.514614	−3.325941
H	6.139997	−1.807550	−4.054079
C	5.723553	−1.416465	−1.974815
H	6.737058	−1.631586	−1.645903
C	4.758282	−1.044401	−1.038086
H	5.030081	−0.981055	0.010474
C	2.759759	−0.835081	1.373167
C	3.071387	−2.194388	1.543277
H	2.951744	−2.885764	0.714684
C	3.521009	−2.669741	2.773547
H	3.759237	−3.723922	2.885249
C	3.647421	−1.800621	3.859482
H	3.993474	−2.173196	4.819983
C	3.321666	−0.453406	3.706100
H	3.412952	0.230330	4.546110
C	2.883699	0.028201	2.470412
H	2.644973	1.081332	2.364605
C	2.279763	1.574921	−0.143453
C	1.185313	2.362240	0.248327
C	1.245240	3.757803	0.339129
C	2.452046	4.375852	−0.000891
H	2.537513	5.456148	0.043884
C	3.557940	3.624065	−0.395725
H	4.486532	4.122919	−0.657858
C	3.472903	2.235744	−0.459823
H	4.331904	1.657498	−0.782851
C	0.008994	4.498529	0.862218
C	0.001745	4.408488	2.415483
H	−0.004560	3.368500	2.755868
H	−0.887609	4.905361	2.819710
H	0.892256	4.896887	2.827706
C	0.015766	5.983131	0.459885

H	0.891967	6.492993	0.872111
H	−0.860350	6.499334	0.864208
H	0.021046	6.109945	−0.627889
O	0.001226	1.715947	0.565310
P	−2.123633	−0.253070	−0.260545
C	−2.273375	1.589435	−0.157656
C	−1.176538	2.370142	0.240195
C	−1.227435	3.766100	0.328265
C	−2.426504	4.391997	−0.024822
H	−2.504856	5.472934	0.017289
C	−3.533205	3.647105	−0.429961
H	−4.455101	4.151910	−0.703688
C	−3.457867	2.257923	−0.489413
H	−4.317337	1.685912	−0.822219
C	−2.770795	−0.806947	1.371573
C	−2.851818	0.054912	2.474097
H	−2.579607	1.100239	2.370695
C	−3.290470	−0.417509	3.713056
H	−3.347888	0.264942	4.557112
C	−3.659861	−1.753584	3.865089
H	−4.005791	−2.118693	4.828498
C	−3.578139	−2.620891	2.773492
H	−3.852108	−3.666496	2.883128
C	−3.128777	−2.154859	1.539556
H	−3.047294	−2.845019	0.705437
C	−3.438694	−0.762646	−1.446966
C	−4.773520	−0.959009	−1.055225
H	−5.062429	−0.822002	−0.017805
C	−5.735971	−1.343543	−1.989368
H	−6.764759	−1.492182	−1.671492
C	−5.377373	−1.541176	−3.323924
H	−6.126841	−1.845153	−4.050029

C	-4.053430	-1.349046	-3.720932
H	-3.766509	-1.499741	-4.758135
C	-3.087431	-0.962054	-2.791494
H	-2.062967	-0.794147	-3.107221
H	0.018719	-3.201975	-1.882718
H	-0.033719	-1.924004	2.233666

-4463.427532 hartrees

Modeling results for complex **144**
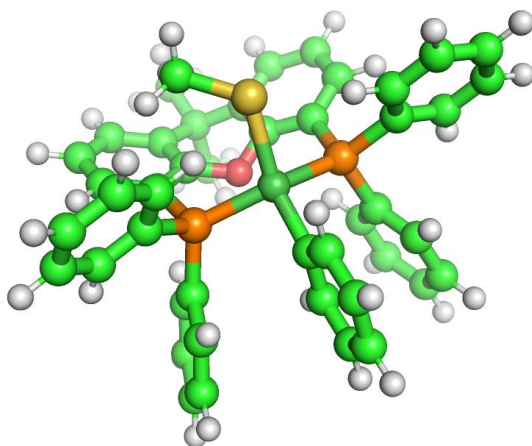
*Supplementary Figure 3: Structural model of complex **144** from the generated xyz file.*

Ni	−0.007356	−0.725372	−0.752634
C	−0.006086	−2.392942	0.140296
C	−0.030374	−2.731007	1.500667
C	−0.032350	−4.062774	1.929003
H	−0.052652	−4.283100	2.994494
C	−0.008039	−5.102549	0.999530
H	−0.009852	−6.138650	1.329887
C	0.019262	−4.794911	−0.362839
H	0.039490	−5.593093	−1.102216
C	0.020243	−3.461566	−0.781959
P	2.064844	−0.271833	−0.186835
C	3.426104	−0.843142	−1.291948

C	3.094013	−1.265744	−2.587993
H	2.056779	−1.219997	−2.913072
C	4.084965	−1.730430	−3.454960
H	3.811120	−2.056197	−4.454870
C	5.415405	−1.781723	−3.039304
H	6.185054	−2.147277	−3.714063
C	5.755650	−1.367509	−1.749278
H	6.789435	−1.409990	−1.416241
C	4.768104	−0.906153	−0.879254
H	5.040582	−0.608323	0.128946
C	2.644131	−0.802137	1.483744
C	3.065026	−2.128244	1.675537
H	3.069231	−2.821001	0.839843
C	3.468792	−2.568706	2.934417
H	3.793339	−3.597743	3.062987
C	3.440459	−1.699262	4.026847
H	3.751604	−2.045540	5.008950
C	3.006884	−0.385647	3.850667
H	2.979032	0.299087	4.694404
C	2.614495	0.061111	2.587368
H	2.294041	1.090596	2.465674
C	2.252134	1.568911	−0.082783
C	1.159331	2.359578	0.306121
C	1.219566	3.757108	0.392728

C	2.425356	4.374903	0.050356
H	2.512445	5.455529	0.092089
C	3.530377	3.619377	-0.342134
H	4.460054	4.116596	-0.603879
C	3.445243	2.230728	-0.401214
H	4.306024	1.653140	-0.720102
C	-0.025279	4.489720	0.905635
C	-0.069758	4.357027	2.455436
H	-0.081426	3.307244	2.763836
H	-0.970638	4.840114	2.850434
H	0.807976	4.836234	2.904139
C	-0.008525	5.982904	0.544578
H	0.859973	6.477987	0.989557
H	-0.893807	6.485183	0.946023
H	0.018780	6.141246	-0.538632
O	-0.028689	1.719431	0.622213
P	-2.100388	-0.258220	-0.260141
C	-2.271822	1.587081	-0.197324
C	-1.194632	2.371299	0.241336
C	-1.245234	3.767679	0.321380
C	-2.423830	4.396302	-0.090811
H	-2.502714	5.477910	-0.059610
C	-3.510403	3.648272	-0.541901
H	-4.418337	4.152076	-0.861207

C	−3.437812	2.257586	−0.585945
H	−4.285815	1.686982	−0.947914
C	−2.678899	−0.750786	1.423143
C	−2.653146	0.134102	2.509403
H	−2.333608	1.161309	2.368649
C	−3.051282	−0.287499	3.779892
H	−3.025831	0.413821	4.609983
C	−3.486818	−1.596860	3.980493
H	−3.801497	−1.923399	4.968214
C	−3.513280	−2.487259	2.904976
H	−3.840150	−3.513031	3.052229
C	−3.103645	−2.071878	1.639552
H	−3.108723	−2.779900	0.816840
C	−3.486101	−0.825900	−1.339821
C	−4.818242	−0.849020	−0.891391
H	−5.054952	−0.529469	0.118846
C	−5.842247	−1.293390	−1.727468
H	−6.866538	−1.306025	−1.364015
C	−5.549548	−1.728566	−3.021777
H	−6.346533	−2.080404	−3.671674
C	−4.230511	−1.714651	−3.474059
H	−3.992999	−2.052391	−4.479116
C	−3.203606	−1.267851	−2.640626
H	−2.184439	−1.253495	−3.010732

H	0.043415	−3.261450	−1.853430
H	−0.046921	−1.945790	2.252433
S	−0.170591	0.375145	−2.744431
C	1.121600	1.589663	−3.229545
H	0.974026	1.810720	−4.291009
H	2.138623	1.211766	−3.090565
H	1.010469	2.520699	−2.667123

-4441.295331 hartrees

Modeling results for complex **145**
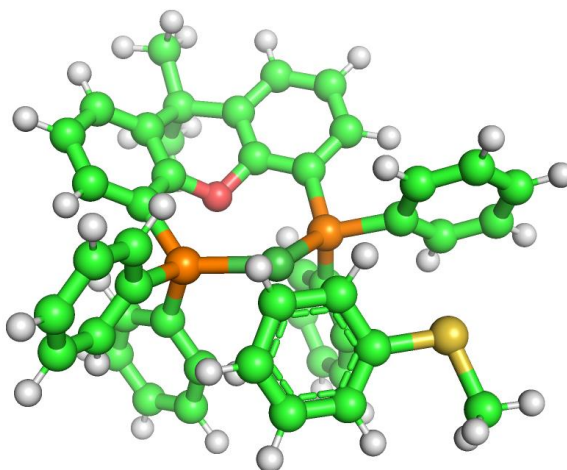
*Supplementary Figure 4: Structural model of complex **145** from the generated xyz file.*

Ni	0.569507	−0.809554	0.792141
P	−1.505209	−1.316112	0.228191
P	1.220747	1.184985	0.118066
O	−1.682377	1.530379	−0.305368
C	−2.858235	1.128906	0.294524
C	−2.973185	−0.232691	0.582815
C	−4.184843	−0.653703	1.151713
H	−4.340162	−1.702261	1.376815
C	−5.185597	0.268889	1.456703
H	−6.112539	−0.074577	1.907675
C	−5.007345	1.628913	1.194702
H	−5.795882	2.326859	1.457437
C	−3.830866	2.087294	0.595860
C	−3.522846	3.542445	0.216508

C	−2.027493	3.761382	0.487677
C	−1.157389	2.703647	0.198645
C	0.225212	2.736916	0.399364
C	0.756393	3.949760	0.867343
H	1.823154	4.045649	1.028923
C	−0.074677	5.031649	1.153913
H	0.358934	5.956258	1.524949
C	−1.456583	4.937168	0.979520
H	−2.084624	5.787186	1.225887
C	−3.788269	3.726944	−1.304891
H	−4.847197	3.554162	−1.529312
H	−3.196082	3.025625	−1.899974
H	−3.527496	4.745798	−1.613163
C	−4.397401	4.537858	0.995060
H	−5.458019	4.368125	0.786147
H	−4.178761	5.565865	0.689483
H	−4.240660	4.457785	2.075989
C	−1.651200	−1.611242	−1.592499
C	−0.528847	−2.103063	−2.277545
H	0.393549	−2.299565	−1.738935
C	−0.587002	−2.347142	−3.649899
H	0.294535	−2.719663	−4.164578
C	−1.762788	−2.098886	−4.359229
H	−1.804474	−2.282358	−5.429806

C	−2.884496	−1.610522	−3.687394
H	−3.805190	−1.414810	−4.231388
C	−2.829821	−1.370808	−2.313640
H	−3.710520	−0.993985	−1.802414
C	−2.136937	−2.897943	0.954742
C	−2.192290	−2.995724	2.355395
H	−1.892765	−2.144745	2.963026
C	−2.629045	−4.165303	2.975117
H	−2.666150	−4.220253	4.060073
C	−3.010081	−5.265859	2.202565
H	−3.342967	−6.181956	2.683332
C	−2.959175	−5.180665	0.811435
H	−3.256130	−6.030760	0.202373
C	−2.530145	−4.003907	0.190837
H	−2.500271	−3.952312	−0.892664
C	1.503675	1.172548	−1.708909
C	2.450655	0.269441	−2.224820
H	3.033285	−0.351110	−1.550291
C	2.658947	0.169896	−3.599975
H	3.400120	−0.528865	−3.979925
C	1.920092	0.959007	−4.484285
H	2.079658	0.876520	−5.556251
C	0.976689	1.854117	−3.981423
H	0.396658	2.474574	−4.659931

C	0.772202	1.963176	−2.604591
H	0.039184	2.671423	−2.234209
C	2.831853	1.792503	0.795614
C	3.831432	2.394135	0.019303
H	3.709193	2.468019	−1.056326
C	4.988232	2.898163	0.616110
H	5.756211	3.356047	−0.002305
C	5.158186	2.818783	1.999086
H	6.059476	3.211622	2.462556
C	4.164510	2.231492	2.784389
H	4.288099	2.165230	3.862160
C	3.012357	1.722393	2.186446
H	2.243299	1.267863	2.806453
H	0.540850	−2.550916	2.550228
C	1.081292	−2.521219	1.600892
C	3.212851	−3.181734	−0.161727
C	2.233931	−1.640761	1.493304
C	1.070517	−3.743650	0.837959
C	2.070623	−4.030663	−0.050629
C	3.324815	−2.064459	0.633921
H	2.533587	−1.071789	2.373719
H	0.251113	−4.441908	0.978009
H	2.038086	−4.945603	−0.638091
H	4.020437	−3.479009	−0.822609

S	4.824703	−1.096985	0.743557
C	6.087834	−2.197894	0.020534
H	6.056694	−3.187241	0.485216
H	7.052004	−1.728617	0.234523
H	5.981826	−2.296698	−1.063808

-4441.281230 hartrees

4.5. References

[1]   E. A. Ilardi, E. Vitaku, J. T. Njardarson, *Journal of Medicinal Chemistry* **2014**, *57*, 2832-2842.

[2]   T. L. Lemke, in *Foye's Principles of Medicinal Chemistry*, Seventh, North American edition ed. (Ed.: D. A. Williams), LWW, **2012**, pp. 1148-1450.

[3]   B. R. Beno, K.-S. Yeung, M. D. Bartberger, L. D. Pennington, N. A. Meanwell, *Journal of Medicinal Chemistry* **2015**, *58*, 4383-4438.

[4]   G. A. Patani, E. J. LaVoie, *Chemical Reviews* **1996**, *96*, 3147-3176.

[5]   J. He, K.-K. Yee, Z. Xu, M. Zeller, A. D. Hunter, S. S.-Y. Chui, C.-M. Che, *Chemistry of Materials* **2011**, *23*, 2940-2947.

[6]   S. Li, L. Ye, W. Zhao, H. Yan, B. Yang, D. Liu, W. Li, H. Ade, J. Hou, *Journal of the American Chemical Society* **2018**, *140*, 7159-7167.

[7]   T. Nakazawa, J. Xu, T. Nishikawa, T. Oda, A. Fujita, K. Ukai, R. E. P. Mangindaan, H. Rotinsulu, H. Kobayashi, M. Namikoshi, *Journal of Natural Products* **2007**, *70*, 439-442.

[8]   T. Tatsuta, M. Hosono, H. Rotinsulu, D. S. Wewengkang, D. A. Sumilat, M. Namikoshi, H. Yamazaki, *Journal of Natural Products* **2017**, *80*, 499-502.

[9]   Y. Shi, Z. Jiang, X. Li, L. Zuo, X. Lei, L. Yu, L. Wu, J. Jiang, B. Hong, *Acta Pharmaceutica Sinica B* **2018**, *8*, 283-294.

[10]   A. P. Kozikowski, M. N. Greco, *Journal of the American Chemical Society* **1980**, *102*, 1165-1166.

[11]   M. S. C. Pedras, Q. H. To, *Phytochemistry* **2015**, *113*, 57-63.

[12]   M. S. C. Pedras, M. Alavi, Q. H. To, *Phytochemistry* **2015**, *118*, 131-138.

[13]   J.-H. Cheng, C. Ramesh, H.-L. Kao, Y.-J. Wang, C.-C. Chan, C.-F. Lee, *The Journal of Organic Chemistry* **2012**, *77*, 10369-10374.

[14]   I. P. Beletskaya, A. V. Cheprakov, *Coordination Chemistry Reviews* **2004**, *248*, 2337-2364.

[15]   A. V. Kalinin, J. F. Bower, P. Riebel, V. Snieckus, *The Journal of Organic Chemistry* **1999**, *64*, 2986-2987.

[16]   a) D. Koziakov, M. Majek, A. Jacobi von Wangelin, *Organic & Biomolecular Chemistry* **2016**, *14*, 11347-11352; b) M. Majek, A. J. von Wangelin, *Chemical Communications* **2013**, *49*, 5507-5509; c) D. Koziakov, M. Majek, A. Jacobi von Wangelin, *European Journal of Organic Chemistry* **2017**, *2017*, 6722-6725.

[17]   Z. Lian, B. N. Bhawal, P. Yu, B. Morandi, *Science* **2017**, *356*, 1059-1063.

[18]   N. Ichiishi, C. A. Malapit, Ł. Woźniak, M. S. Sanford, *Organic Letters* **2018**, *20*, 44-47.

[19]   C. Liu, M. Szostak, *Chemical Communications* **2018**, *54*, 2130-2133.

[20]   H.-J. Xu, Y.-Q. Zhao, T. Feng, Y.-S. Feng, *The Journal of Organic Chemistry* **2012**, *77*, 2878-2884.

[21]   J. C. Vantourout, H. N. Miras, A. Isidro-Llobet, S. Sproules, A. J. B. Watson, *Journal of the American Chemical Society* **2017**, *139*, 4769-4779.

[22]   a) O. Baldovino-Pantaleón, S. Hernández-Ortega, D. Morales-Morales, *Advanced Synthesis & Catalysis* **2006**, *348*, 236-242; b) N. Taniguchi, *The Journal of Organic Chemistry* **2004**, *69*, 6904-6906; c) V. Gómez-Benítez, O. Baldovino-Pantaleón, C. Herrera-Álvarez, R. A. Toscano, D. Morales-Morales, *Tetrahedron Letters* **2006**, *47*, 5059-5062.

[23]   A. García-Domínguez, Z. Li, C. Nevado, *Journal of the American Chemical Society* **2017**, *139*, 6835-6838.

[24]   B. Liu, C.-H. Lim, G. M. Miyake, *Journal of the American Chemical Society* **2017**, *139*, 13616-13619.

[25]   M. Jiang, H. Li, H. Yang, H. Fu, *Angewandte Chemie International Edition* **2017**, *56*, 874-879.

[26]   M. S. Oderinde, M. Frenette, D. W. Robbins, B. Aquila, J. W. Johannes, *Journal of the American Chemical Society* **2016**, *138*, 1760-1763.

[27]   M. Jouffroy, C. B. Kelly, G. A. Molander, *Organic Letters* **2016**, *18*, 876-879.

[28]   B. A. Vara, X. Li, S. Berritt, C. R. Walters, E. J. Petersson, G. A. Molander, *Chemical Science* **2018**, *9*, 336-344.

[29]   K. Masanori, S. Tomiya, M. Toshihiko, *Chemistry Letters* **1978**, *7*, 13-14.

[30]   N. Probst, R. Lartia, O. Théry, M. Alami, E. Defrancq, S. Messaoudi, *Chemistry – A European Journal* **2018**, *24*, 1795-1800.

[31]   K. Masanori, K. Masayuki, M. Toshihiko, *Chemistry Letters* **1983**, *12*, 927-928.

[32]   M. Toshihiko, S. Tomiya, A. Yoriyoshi, S. Jun-ichi, K. Yasuki, K. Masanori, *Bulletin of the Chemical Society of Japan* **1980**, *53*, 1385-1389.

[33]   C. C. Eichman, J. P. Stambuli, *Molecules* **2011**, *16*, 590.

[34]   G. Y. Li, *Angewandte Chemie International Edition* **2001**, *40*, 1513-1516.

[35]   G. Y. Li, G. Zheng, A. F. Noonan, *The Journal of Organic Chemistry* **2001**, *66*, 8677-8681.

[36]   M. Murata, S. L. Buchwald, *Tetrahedron* **2004**, *60*, 7397-7403.

[37]   a) M. A. Fernández-Rodríguez, Q. Shen, J. F. Hartwig, *Chemistry – A European Journal* **2006**, *12*, 7782-7796; b) M. A. Fernández-Rodríguez, Q. Shen, J. F. Hartwig, *Journal of the American Chemical Society* **2006**, *128*, 2180-2181.

[38]   T. Scattolin, E. Senol, G. Yin, Q. Guo, F. Schoenebeck, *Angewandte Chemie International Edition* **2018**, *asap.*

[39]   T. Norris, K. Leeman, *Organic Process Research & Development* **2008**, *12*, 869-876.

[40]   P. D. de Koning, L. Murtagh, J. P. Lawson, R. A. Vonder Embse, S. A. Kunda, W. Kong, *Organic Process Research & Development* **2011**, *15*, 1046-1051.

[41]   B. Chekal, D. Damon, D. LaFrance, K. Leeman, C. Mojica, A. Palm, M. St. Pierre, J. Sieser, K. Sutherland, R. Vaidyanathan, J. Van Alsten, B. Vanderplas, C. Wager, G. Weisenburger, G. Withbroe, S. Yu, *Organic Process Research & Development* **2015**, *19*, 1944-1953.

[42]   H. J. Cristau, B. Chabaud, A. Chêne, H. Christol, *Synthesis* **1981**, *1981*, 892-894.

[43]   G. Yin, I. Kalvet, U. Englert, F. Schoenebeck, *Journal of the American Chemical Society* **2015**, *137*, 4164-4172.

[44]   K. D. Jones, D. J. Power, D. Bierer, K. M. Gericke, S. G. Stewart, *Organic Letters* **2018**, *20*, 208-211.

[45]   X.-B. Xu, J. Liu, J.-J. Zhang, Y.-W. Wang, Y. Peng, *Organic Letters* **2013**, *15*, 550-553.

[46]   V. Percec, J.-Y. Bae, D. H. Hill, *The Journal of Organic Chemistry* **1995**, *60*, 6895-6903.

[47]   P. Guan, C. Cao, Y. Liu, Y. Li, P. He, Q. Chen, G. Liu, Y. Shi, *Tetrahedron Letters* **2012**, *53*, 5987-5992.

[48]   T. Kentaro, *Chemistry Letters* **1987**, *16*, 2221-2224.

[49]   Y. Yatsumonji, O. Okada, A. Tsubouchi, T. Takeda, *Tetrahedron* **2006**, *62*, 9981-9987.

[50]   S. Jammi, P. Barua, L. Rout, P. Saha, T. Punniyamurthy, *Tetrahedron Letters* **2008**, *49*, 1484-1487.

[51]   Y. Zhang, K. C. Ngeow, J. Y. Ying, *Organic Letters* **2007**, *9*, 3495-3498.

[52]   P. Gogoi, S. Hazarika, M. J. Sarma, K. Sarma, P. Barman, *Tetrahedron* **2014**, *70*, 7484-7489.

[53]   A. R. Martin, D. J. Nelson, S. Meiries, A. M. Z. Slawin, S. P. Nolan, *European Journal of Organic Chemistry* **2014**, *2014*, 3127-3131.

[54]   J. Zhang, C. M. Medley, J. A. Krause, H. Guan, *Organometallics* **2010**, *29*, 6393-6401.

[55]   N. P. N. Wellala, H. Guan, *Organic & Biomolecular Chemistry* **2015**, *13*, 10802-10807.

[56]   Y. Q. Cao, Z. Zhang, Y. X. Guo, G. Q. Wu, *Synthetic Communications* **2008**, *38*, 1325-1332.

[57]   M. J. Iglesias, A. Prieto, M. C. Nicasio, *Advanced Synthesis & Catalysis* **2010**, *352*, 1949-1954.

[58]   A. Correa, M. Carril, C. Bolm, *Angewandte Chemie International Edition* **2008**, *47*, 2880-2883.

[59]   J.-R. Wu, C.-H. Lin, C.-F. Lee, *Chemical Communications* **2009**, 4450-4452.

[60]   S. L. Buchwald, C. Bolm, *Angewandte Chemie International Edition* **2009**, *48*, 5586-5587.

[61]   V. P. Reddy, K. Swapna, A. V. Kumar, K. R. Rao, *The Journal of Organic Chemistry* **2009**, *74*, 3189-3191.

[62]   V. P. Reddy, A. V. Kumar, K. Swapna, K. R. Rao, *Organic Letters* **2009**, *11*, 1697-1700.

[63]   Y.-C. Wong, T. T. Jayanth, C.-H. Cheng, *Organic Letters* **2006**, *8*, 5613-5616.

[64]   C. Galli, T. Pau, *Tetrahedron* **1998**, *54*, 2893-2904.
[65]   J. Li, S. G. Ballmer, E. P. Gillis, S. Fujii, M. J. Schmidt, A. M. E. Palazzolo, J. W. Lehmann, G. F. Morehouse, M. D. Burke, *Science* **2015**, *347*, 1221-1226.
[66]   I. Abdiaj, A. Fontana, M. V. Gomez, A. de la Hoz, J. Alcázar, *Angewandte Chemie International Edition* **2018**, *57*, 8473-8477.
[67]   E. R. Welin, C. Le, D. M. Arias-Rotondo, J. K. McCusker, D. W. C. MacMillan, *Science* **2017**, *355*, 380-385.
[68]   E. A. Standley, S. J. Smith, P. Müller, T. F. Jamison, *Organometallics* **2014**, *33*, 2012-2018.
[69]   G. M. Adams, A. S. Weller, *Coordination Chemistry Reviews* **2018**, *355*, 150-172.
[70]   A. Metzger, L. Melzig, C. Despotopoulou, P. Knochel, *Organic Letters* **2009**, *11*, 4228-4231.
[71]   C. A. Fleckenstein, H. Plenio, *Chemical Society Reviews* **2010**, *39*, 694-711.
[72]   M. J. Kamlet, J. L. M. Abboud, M. H. Abraham, R. W. Taft, *The Journal of Organic Chemistry* **1983**, *48*, 2877-2887.
[73]   B. Yang, Z.-X. Wang, *Organic Letters* **2017**, *19*, 6220-6223.
[74]   E. Wenkert, T. W. Ferreira, E. L. Michelotti, *Journal of the Chemical Society, Chemical Communications* **1979**, 637-638.
[75]   M. Mohadjer Beromi, A. Nova, D. Balcells, A. M. Brasacchio, G. W. Brudvig, L. M. Guard, N. Hazari, D. J. Vinyard, *Journal of the American Chemical Society* **2017**, *139*, 922-936.
[76]   C. M. Lavoie, R. McDonald, E. R. Johnson, M. Stradiotto, *Advanced Synthesis & Catalysis* **2017**, *359*, 2972-2980.
[77]   D. S. Wilbur, D. K. Hamlin, M.-K. Chyan, *Bioconjugate Chemistry* **2006**, *17*, 1514-1522.
[78]   A. C. Wotal, D. J. Weix, *Organic Letters* **2012**, *14*, 1476-1479.
[79]   Y. A. Lin, J. M. Chalker, B. G. Davis, *Journal of the American Chemical Society* **2010**, *132*, 16805-16811.
[80]   X.-H. Xu, K. Matsuzaki, N. Shibata, *Chemical Reviews* **2015**, *115*, 731-764.
[81]   S. Mukherjee, T. Patra, F. Glorius, *ACS Catalysis* **2018**, *8*, 5842-5846.
[82]   Y. P. Auberson, C. Brocklehurst, M. Furegati, T. C. Fessard, G. Koch, A. Decker, L. La Vecchia, E. Briard, *ChemMedChem* **2017**, *12*, 590-598.
[83]   A. F. Stepan, C. Subramanyam, I. V. Efremov, J. K. Dutra, T. J. O'Sullivan, K. J. DiRico, W. S. McDonald, A. Won, P. H. Dorff, C. E. Nolan, S. L. Becker, L. R. Pustilnik, D. R. Riddell, G. W. Kauffman, B. L. Kormos, L. Zhang, Y. Lu, S. H. Capetta, M. E. Green, K. Karki, E. Sibley, K. P. Atchison, A. J. Hallgren, C. E. Oborski, A. E. Robshaw, B. Sneed, C. J. O'Donnell, *Journal of Medicinal Chemistry* **2012**, *55*, 3414-3424.
[84]   B. A. Chalmers, H. Xing, S. Houston, C. Clark, S. Ghassabian, A. Kuo, B. Cao, A. Reitsma, C.-E. P. Murray, J. E. Stok, G. M. Boyle, C. J. Pierce, S. W. Littler, D. A. Winkler, P. V. Bernhardt, C. Pasay, J. J. De Voss, J. McCarthy, P. G. Parsons, G. H. Walter, M. T. Smith, H. M. Cooper, S. K. Nilsson, J. Tsanaktsidis, G. P. Savage, C. M. Williams, *Angewandte Chemie International Edition* **2016**, *55*, 3580-3585.
[85]   R. M. Bär, S. Kirschner, M. Nieger, S. Bräse, *Chemistry – A European Journal* **2018**, *24*, 1373-1382.
[86]   F. Dénès, M. Pichowicz, G. Povie, P. Renaud, *Chemical Reviews* **2014**, *114*, 2587-2693.
[87]   J. Belzner, U. Bunz, K. Semmler, G. Szeimies, K. Opitz, A.-D. Schlüter, *Chemische Berichte* **1989**, *122*, 397-398.
[88]   S. Bajo, G. Laidlaw, A. R. Kennedy, S. Sproules, D. J. Nelson, *Organometallics* **2017**, *36*, 1662-1672.
[89]   J. M. Dennis, N. A. White, R. Y. Liu, S. L. Buchwald, *Journal of the American Chemical Society* **2018**, *140*, 4721-4725.
[90]   E. V. Vinogradova, C. Zhang, A. M. Spokoyny, B. L. Pentelute, S. L. Buchwald, *Nature* **2015**, *526*, 687.
[91]   F. Proutiere, F. Schoenebeck, *Angewandte Chemie International Edition* **2011**, *50*, 8192-8195.

[92]   H. Ogawa, H. Minami, T. Ozaki, S. Komagawa, C. Wang, M. Uchiyama, *Chemistry – A European Journal* **2015**, *21*, 13904-13908.
[93]   I. Kalvet, Q. Guo, G. J. Tizzard, F. Schoenebeck, *ACS Catalysis* **2017**, *7*, 2126-2132.
[94]   T. T. Tsou, J. K. Kochi, *Journal of the American Chemical Society* **1979**, *101*, 6319-6332.
[95]   R. Stolley, PhD thesis, University of Utah **2014**.
[96]   E. Alvaro, J. F. Hartwig, *Journal of the American Chemical Society* **2009**, *131*, 7858-7868.
[97]   Y. Takeshi, *Bulletin of the Chemical Society of Japan* **1988**, *61*, 1975-1978.
[98]   H. N. Kagalwala, E. Gottlieb, G. Li, T. Li, R. Jin, S. Bernhard, *Inorganic Chemistry* **2013**, *52*, 9094-9101.
[99]   T. Krüger, B. Krebs, G. Henkel, *Angewandte Chemie International Edition in English* **1989**, *28*, 61-62.
[100]   P. Woodward, L. F. Dahl, E. W. Abel, B. C. Crosse, *Journal of the American Chemical Society* **1965**, *87*, 5251-5253.
[101]   S. Otsuka, *Journal of Organometallic Chemistry* **1980**, *200*, 191-205.
[102]   M.-N. Birkholz, Z. Freixa, P. W. N. M. van Leeuwen, *Chemical Society Reviews* **2009**, *38*, 1099-1118.
[103]   C. M. Lavoie, P. M. MacQueen, N. L. Rotta-Loria, R. S. Sawatzky, A. Borzenko, A. J. Chisholm, B. K. V. Hargreaves, R. McDonald, M. J. Ferguson, M. Stradiotto, *Nature Communications* **2016**, *7*, 11073.
[104]   P. M. MacQueen, J. P. Tassone, C. Diaz, M. Stradiotto, *Journal of the American Chemical Society* **2018**, *140*, 5023-5027.
[105]   a) T. Itoh, T. Matsueda, Y. Shimizu, M. Kanai, *Chemistry – A European Journal* **2015**, *21*, 15955-15959; b) L. Shaw, D. M. U. K. Somisara, R. C. How, N. J. Westwood, P. C. A. Bruijnincx, B. M. Weckhuysen, P. C. J. Kamer, *Catalysis Science & Technology* **2017**, *7*, 619-626.
[106]   E. A. LaPierre, W. E. Piers, C. Gendy, *Organometallics* **2018**.
[107]   D. J. H. Emslie, L. E. Harrington, H. A. Jenkins, C. M. Robertson, J. F. Britten, *Organometallics* **2008**, *27*, 5317-5325.
[108]   J. Magano, S. Monfette, *ACS Catalysis* **2015**, *5*, 3120-3123.
[109]   S. Kozuch, C. Amatore, A. Jutand, S. Shaik, *Organometallics* **2005**, *24*, 2319-2330.

[S1]   a) E. A. Standley, S. J. Smith, P. Müller, T. F. Jamison, *Organometallics* **2014**, *33*, 2012-2018; b) R. S. Sawatzky, M. J. Ferguson, M. Stradiotto, *Synlett* **2017**, *28*, 1586-1591.
[S2]   P. H. Gehrtz, P. Kathe, I. Fleischer, *Chem. - Eur. J.* **2018**, *24*, 8774-8778.
[S3]   B. Yan, L. Liu, S. Huang, Y. Ren, H. Wang, Z. Yao, L. Li, S. Chen, X. Wang, Z. Zhang, *Chem. Commun.* **2017**, *53*, 3637-3640.
[S4]   Z. Demir, E. B. Guven, S. Ozbey, C. Kazak, R. C. Atalay, M. Tuncbilek, *Eur. J. Med. Chem.* **2015**, *89*, 701-720.
[S5]   F. Sandfort, M. J. O'Neill, J. Cornella, L. Wimmer, P. S. Baran, *Angew. Chem., Int. Ed.* **2017**, *56*, 3319-3323.
[S6]   A. Krasovskiy, P. Knochel, *Synthesis* **2006**, *2006*, 0890-0891.
[S7]   H.-J. Xu, Y.-F. Liang, X.-F. Zhou, Y.-S. Feng, *Org. Biomol. Chem.* **2012**, *10*, 2562-2568.
[S8]   J. Xu, T. Wei, J. Xia, Q. Zhang, H. Wu, *Chirality* **2004**, *16*, 341-346.
[S9]   M. Majek, A. J. von Wangelin, *Chem. Commun.* **2013**, *49*, 5507-5509.
[S10]   C. Riccardo, J. Corinna, N. Cristina, *Angew. Chem., Int. Ed.* **2009**, *48*, 8780-8783.
[S11]   M. N. S. Rad, S. Maghsoudi, *RSC Adv.* **2016**, *6*, 70335-70342.
[S12]   C.-K. Chen, Y.-W. Chen, C.-H. Lin, H.-P. Lin, C.-F. Lee, *Chem. Commun.* **2010**, *46*, 282-284.
[S13]   Y. Li, J. Pu, X. Jiang, *Org. Lett.* **2014**, *16*, 2692-2695.
[S14]   T. Itoh, T. Mase, *Org. Lett.* **2004**, *6*, 4587-4590.
[S15]   Y.-C. Wong, T. T. Jayanth, C.-H. Cheng, *Org. Lett.* **2006**, *8*, 5613-5616.

[S16]   X.-B. Xu, J. Liu, J.-J. Zhang, Y.-W. Wang, Y. Peng, *Org. Lett.* **2013**, *15*, 550-553.

[S17]   B. Liu, C.-H. Lim, G. M. Miyake, *J. Am. Chem. Soc.* **2017**, *139*, 13616-13619.

[S18]   W. Erb, M. Albini, J. Rouden, J. Blanchet, *J. Org. Chem.* **2014**, *79*, 10568-10580.

[S19]   B. Lü, C. Fu, S. Ma, *Tetrahedron Letters* **2010**, *51*, 1284-1286.

[S20]   T. Narender, S. Sarkar, K. Rajendar, S. Tiwari, *Org. Lett.* **2011**, *13*, 6140-6143.

[S21]   N. Kataoka, Q. Shelby, J. P. Stambuli, J. F. Hartwig, *J. Org. Chem.* **2002**, *67*, 5553-5566.

[S22]   L. Ackermann, A. R. Kapdi, S. Fenner, C. Kornhaaß, C. Schulzke, *Chem. - Eur. J.* **2011**, *17*, 2965-2971.

[S23]   B.-T. Guan, X.-Y. Lu, Y. Zheng, D.-G. Yu, T. Wu, K.-L. Li, B.-J. Li, Z.-J. Shi, *Org. Lett.* **2010**, *12*, 396-399.

[S24]   M. De Carolis, S. Protti, M. Fagnoni, A. Albini, *Angew. Chem., Int. Ed.* **2005**, *44*, 1232-1236.

[S25]   G. Yin, I. Kalvet, U. Englert, F. Schoenebeck, *J. Am. Chem. Soc.* **2015**, *137*, 4164-4172.

[S26]   J. Masse, *Synthesis* **1977**, *1977*, 341-342.

[S27]   Y. Peng, H. Liu, M. Tang, L. Cai, V. Pike, *Chin. J. Chem.* **2009**, *27*, 1339-1344.

[S28]   L. Horner, E. Winkelmann, K. H. Knapp, W. Ludwig, *Chem. Ber.* **1959**, *92*, 288-292.

5. Summary / Zusammenfassung

The thiophilic interaction between organosulfur compounds and late transition metals can be employed to achieve selective C-S bond formation or activation under mild reaction conditions; an overview of this theme was presented in Chapter 1. Both of these aspects were investigated in this thesis with focus on developing user-friendly synthetic methods with high functional group tolerance.

In Chapter 2, work regarding the Pd-catalyzed hydro(thio)esterification reaction of (mainly) styrenes was presented. In contrast to previously published work, it was possible to conduct carbonylative (thio)esterifications at room temperature at 2.5 bar CO partial pressure in a two-chamber glassware system with N-formylsaccharin as an inexpensive CO surrogate to give selectively products of the 2-arylpropionic acid (thio)ester product class, an underrepresented small molecule building block and NSAID structural motif.

In Chapter 3, a Ni-catalyzed variant of the Fukuyama reaction was developed, which allowed the coupling of LiCl-adducted aryl zinc halides with challenging S-ethyl thioesters to give the corresponding ketones. The low reactivity of organozinc reagents enabled high functional group tolerance, and a variety of polyfunctional ketones could be synthesized, which enable facile downstream chemistry. In contrast to competing Ni-catalyzed Fukuyama coupling methods, relatively low metal loadings (5 mol%), mild conditions (THF, RT) and short reaction times (1.5 h) could be achieved with more economical stoichiometry (1.86 eqv. of the organozinc reagent) than usual. Alkyl-, alkenyl- and alkinyl-zinc reagents however did not show the desired reactivity.

In chapter 4, a Ni-catalyzed Migita reaction was shown, which activates challenging (hetero)aryl chlorides to give aryl thioethers, which have gained importance as structural motifs in non-natural functional molecules such as pharmaceuticals, with relative ease (RT – 60 °C, 15 min – 4 h, 0.5 – 2 mol% catalyst loading, depending on functionality in the substrate). The reaction was based on findings from Chapter 3, where a tandem Fukuyama-Migita reaction was observed. The reaction is unique in the sense that a stoichiometric organozinc reagent fullfils a dual role of reductant and base to generate the thiolate and reduce the Ni precatalyst. In comparison to published work, Ni-catalyzed Migita reactions of various aliphatic thiols are efficiently performed for the first time, but the reactivity of tertiary thiols in this reaction remains sluggish. Thiophenols are also competent coupling partners but require thermal conditions and carefully controlled reagent choice to avoid a competing desulfenylative Kumada coupling.

Die thiophile Wechselwirkung zwischen Organoschwefelverbindungen und späten Übergangsmetallen kann genutzt werden, um selektiv C-S-Bindungs-Bildung oder -Aktivierung zu erreichen; eine Übersicht dieser Thematik findet sich in Kapitel 1. Beide Aspekte wurden in der vorliegenden Arbeit untersucht, wobei der Fokus auf der Entwicklung von anwenderfreundlichen Synthesemethoden mit hoher Funktioneller-Gruppen-Toleranz gelegt wurde.

Arbeiten zur Pd-katalysierten Hydrothioesterifizierungsreaktion von Styrolen wurden in Kapitel 2 präsentiert. Im Gegensatz zu vorher publizierten Arbeiten war es möglich, carbonylierende (Thio-)Esterifizierungen bei Raumtemperatur unter 2.5 bar CO-Partialdruck in einem Zweikammer-Glasdruckgefäß mit *N*-Formylsaccharin als preisgünstiges CO-Surrogat durchzuführen, wobei 2-Arylpropionsäure(thio)ester als Produktklasse erhalten wurden, welche unterrepräsentierte Synthesebausteine und Strukturmotiv in einigen NSAID sind.

Eine Ni-katalysierte Variante der Fukuyama-Reaktion wurde in Kapitel 3 gezeigt, wobei LiCl-Addukte von Arylzinkhaliden mit schwer zu aktivierenden *S*-Ethylthioestern zu den entsprechenden Ketonen gekuppelt werden konnten. Die niedrige Reaktivität von Organozinkverbindungen erlaubte die Darstellung verschiedener polyfunktioneller Ketone, welche wiederum *downstream*-Chemie ermöglichen. Im Vergleich zu konkurrierenden Ni-katalysierten Fukuyama-Reaktionen, waren relative geringe Katalysatorbeladungen (5 mol%), milde Reaktionsbedingnungen (THF, Raumtemperatur) und kurze Reaktionszeiten (1.5 h) möglich, wobei allerdings auch eine ökonomischere Stöchiometrie (1.86 Äqv. des Organozinkreagenzes) als üblich erreicht werden konnte. Bedauerlicherweise zeigten Alkyl- , Alkenyl- und Alkinylzinkverbindungen nicht die gewünschte Reaktivität.

Abschließend wurde in Kapitel 4 eine Ni-katalysierte Migita-Reaktion entwickelt, welche es ermöglicht, herausfordende (Hetero-)Arylchloride mit relativer Leichtigkeit (Raumtemperatur – 60 °C, 15 min – 4 h, 0.5 – 2 mol% Katalysatorbeladung, abhängig von der Funktionalität im Substrat) zu den entsprechenden Arylthioethern zu transformieren, welche als Strukturmotive in verschiedenen nicht-natürlichen funktionalen Verbindungen wie z.B. Pharmazeutika Bedeutung erlangt haben. Die Reaktion wurde basierend auf einer Beobachtung einer Tandem-Fukuyama-Migita-Reaktion aus Kapitel 3 entwickelt. Die entwickelte Reaktion ist einzigartig in dem Sinne, dass das benötigte Organozinkreagenz sowohl die Rolle der stöchiometrischen Base zur Generierung des Thiolats als auch des Reduktionsmittels übernimmt. Im Vergleich zu bereits veröffentlichten Berichten zur Ni-katalysierten Migita-Reaktion war es in dieser Arbeit zum ersten Mal möglich, aliphatische Thiole effizient zu kuppeln, wobei sich tertiäre Thiole aber dennoch als relativ reaktionsträge erwiesen. Thiophenole waren ebenfalls kompetente Kupplungspartner, benötigten aber starke thermische Aktivierung und eine sorgfältige Reagenzauswahl, um eine konkurrierende entschwefelnde Kumada-Kupplung zu vermeiden.

6. Appendix

6.1. List of acronyms

acac	Acetylacetonate	**F-MR**	Fukuyama-Migita reaction
ACS	Acetyl-CoA synthase	**FR**	Fukuyama reaction
APCI	Atmospheric pressure chemical ionization	**GC-FID**	Gas chromatography with Flame ionization detection
ATR	Attenuated total reflection	**GC/MS**	Mass spectrometry-coupled gas chromatography
BBN	9-Bora-bicyclononane	**HPLC**	High performance liquid chromatography
BCP	[1.1.1]bicyclopentane	**HRMS**	High resolution mass spectrometry
BDE	Bond dissociation energy	**HSAB**	Hard/Soft-Acid/Base
BINOL	1,1'-Bi-2-naphthol	**IR**	Infrared spectroscopy
BNPA	BINOL phosphoric acid	**LD$_{50}$**	Median lethal dosis
CFeSP	Corrinoid Iron-Sulfur Protein	**LFSE**	Ligand field stabilization energy
CoA	Coenzyme A	**LRMS**	Low resolution mass spectrometry
cod	1,8-Cyclooctadiene	**Mes**	Mesityl
Cp	Cyclopentadiene	**m.p.**	Melting point
dba	Dibenzylidenacetone	**MR**	Migita reaction
DCM	Dichlormethane	**NMI**	N-Methylimidazole
DCT	Dibenzo[a,e]cyclooctene	**NMP**	N-Methylpyrrolidinone
DFT	Density Functional Theory	**NMR**	Nuclear Magnetic Resonance
DIBALH	Diisobutyl-aluminiumhydride	**NP**	Nanoparticle
DIC	Diisopropylcarbodiimide	***o*Tol**	Ortho-Tolyl
dippf	1,1'-Diisopropylphosphinoferrocene	**ppy**	2-phenylpyridine
DMAP	N,N-Dimethyl-4-aminopyridine	**RBF**	Round bottom flask
DMF	N,N-Dimethylformamide	***R*$_f$**	Retention factor
DMI	1,3-Dimethyl-2-imidazolidinone	**RNA**	Ribonucleic acid
DKR	Dynamic kinetic resolution	**SET**	Single electron transfer
DMSO	Dimethyl sulfoxide	**TBDPS**	*Tert*-butyl-diphenylsilyl
DPEphos	Bis[(2-diphenylphosphino)phenyl] ether	**TBS**	*Tert*-butyl-dimethylsilyl
DPPA	Diphenyl phosphoric acid	**TEMPO**	2,2,6,6-Tetramethylpiperidine N-oxide
dppe	1,2-Diphenylphosphinoethane	**TFP**	Tris(2-furyl)phosphine
dppf	1,1'-Diphenylphosphinoferrocene	**THF**	Tetrahydrofuran
dtbpt	di-tert-butyl(2-(di-tert-butylphosphaneyl)benzyl)phosphane	**TLC**	Thin layer chromatography
ECP	Effective core potential	**TM**	Transition metal
EDA	Electron donor acceptor	**TOF**	Turnover frequency
ESI	Electrospray ionization	**TON**	Turnover number
FDA	Federal drug administration	**Xant**	Xantphos

6.2. Acknowledgements

Ich möchte zunächst Frau Prof. Dr. Ivana Fleischer für die stetige finanzielle und thematische Unterstützung während dieser sehr intensiven Promotionszeit danken. Ich habe die von Ihr gelassenen akademischen Freiheiten sehr genossen. Ihr Arbeitsethos, Humor und konstruktive Herangehensweise waren inspirierend, lehrreich und sorgten immer für eine positive Stimmung im Arbeitskreis.

Ich möchte Herrn Prof. Dr. Martin E. Maier für die Übernahme des Zweitgutachtens danken.

Meinen ehemaligen (Samuel) und derzeitigen Kollegen (Benni, Marlene, Vera, Prasad, Valentin und Regina) möchte ich für die großartige Zeit danken, ob nun die gemeinsamen Feiern in Regensburg/Tübingen und Grillabende mit Ivana oder das offene Ohr für fachliche oder sonstige Fragestellungen. Besonders danken möchte ich Vera Hirschbeck für die effiziente Zusammenarbeit im Themengebiet der Carbonylierungsreaktionen. Ebenso möchte ich Prasad Kathe für die Zusammenarbeit bei der Fukuyama-Reaktion danken – eine erstaunliche Einzelleistung kurz nach dem Start seiner Promotionsarbeiten. Der „neuen Garde" bestehend aus Prasad, Valentin und Regina wünsche ich ganz viel Erfolg beim Erreichen der Forschungsziele. Es erfüllt mich mit Stolz, dass einige meiner Themen weiterbearbeitet werden (auch wenn sich ebenso einiges, wie üblich, als Sackgasse herausstellt).

Mein Dank gilt weiterhin allen Forschungspraktikanten in Regensburg und Tübingen, die mich so tatkräftig unterstützt haben. Besonders den Tübingern Tanno und Laura möchte ich für Ihre Begeisterung und Sorgfalt in meinem letzten Projekt danken. Ich möchte auch dem AK Jacobi für die zeitweilige Seminarheimat in Regensburg und die vielen gemeinsamen Abende danken.

Ebenso möchte ich den unsichtbaren Helden danken, ohne die diese Arbeit nicht möglich wäre: Die Glasbläser, den NMR- und MS-Abteilungen in Regensburg und Tübingen.

Bei meinen Eltern möchte ich mich für die jahrelange Unterstützung bedanken, ohne die ich es sicher nicht geschafft hätte. Die kurzen Heimaturlaube waren für mich besonders schön.

Bei meiner Partnerin Maria möchte ich mich abschließend für den immerwährenden Rückhalt, besonders die Hilfe beim Umzug, und ihre guten Ratschläge bedanken, die mich durch diese anspruchsvolle Zeit geleitet haben.